

Phosphorylation During Ischaemia and Reperfusion of The Heart: A Focus on Protein Phosphatase 2A

by

Charlize White

*Dissertation presented for the degree of
Doctor of Philosophy (Medical Physiology) in the
Faculty of Medicine and Health Sciences at
Stellenbosch University*



Supervisor: Dr Derick van Vuuren

Co-supervisors: Dr Erna Marais and Professor Amanda Lochner

March 2020

By submitting this dissertation electronically, I declare that the entirety of the work contained therein is my own, original work, that I am the sole author thereof (save to the extent explicitly otherwise stated), that reproduction and publication thereof by Stellenbosch University will not infringe any third party rights and that I have not previously in its entirety or in part submitted it for obtaining any qualification.

March 2020

ABSTRACT

Understanding the mechanism and signalling pathways involved in myocardial ischaemia/reperfusion (I/R) injury is a prerequisite for elucidating any novel therapeutic intervention to reduce I/R injury. Historically, protein kinases have been the focus of research on I/R injury while information regarding phosphatases in I/R injury is lacking. Clarifying the role of phosphatases in the cellular response to I/R injury is critical to enhance existing cardioprotective interventions or identify new therapeutic targets.

This study aimed to investigate the effects of protein phosphatase 2A (PP2A, a major phosphatase in the heart) inhibition on the outcomes of I/R and to characterize the phosphoproteome of myocardial tissue exposed to these interventions.

For this study, tissue was generated using the isolated working mouse heart model. Administration of a PP2A inhibitor, okadaic acid (OA; 50 nM), prior to 20 minutes global ischaemia (GI) reduced infarct size ($28 \pm 19\%$) when compared to control ($56 \pm 23\%$; $n=9$; $p < 0.0106$), but did not exert a major effect on functional recovery. Phosphoproteomic analysis conducted on hearts exposed to OA prior to 20 minutes GI followed by 10 minutes reperfusion revealed that 898 proteins and 184 phosphorylated proteins were influenced by PP2A inhibition. Pathway analysis indicated that the major pathways affected by PP2A inhibition were mitochondrial function and oxidative phosphorylation, epithelial adherens signalling and remodelling, and cytoskeletal signalling. Two proteins from the data set, striatin and heat shock protein (HSP) 90 α , were selected for confirmation and further investigation. Mitochondrial respiration was also investigated.

In line with the phosphoproteomic results, OA administration increased the amount of phosphorylated HSP90 α during reperfusion (1.83 ± 0.83 Arbitrary Units (AU) vs 0.69 ± 0.09 AU; $n = 2-4$; $p = 0.0480$) and increased the amount of striatin during reperfusion (1.93 ± 0.84 AU vs 0.80 ± 0.06 AU; $n = 2-4$; $p = 0.0436$). Striatin, but not HSP90 α coimmunoprecipitated with PP2A, indicating that the increased phosphorylation of HSP90 α was an indirect effect of PP2A inhibition. As striatin recruits regulatory proteins into large signalling complexes that mostly include PP2A, co-immunoprecipitation may indicate the presence of these complexes in the heart.

OA was also administered directly to isolated mitochondria, where oxidative phosphorylation analysis was performed polarographically (using a Clark-type electrode). No differences in oxidative phosphorylation or respiratory control ratio were observed. Mitochondria were separated into the outer mitochondrial membrane (OMM) and mitoplast (inner mitochondrial membrane and matrix) using digitonin. Western blot analysis indicated that catalytic and scaffolding subunits of PP2A are probably localized to the OMM, while striatin is located within the mitoplast, a novel finding.

Finally, following an incidental observation, the inhibitory effects of sodium orthovanadate (SOV) on PP2A was investigated. This study is the first to demonstrate that SOV is a weak, competitive inhibitor of PP2A ($IC_{50} \approx 2.2$ mM).

This study is, to our knowledge, the first to use a phosphoproteomic approach to investigate the effects of phosphatase inhibition during myocardial I/R. Our data indicate that PP2A is associated with numerous proteins and processes during I/R, including oxidative phosphorylation and cytoskeletal dynamics.

OPSOMMING

Begrip van die meganisme en seintransduksie-paaië wat betrokke is in miokardiale iskemie/herperfusie (I/H) besering is 'n voorvereiste daarvoor om nuwe terapeutiese ingrepe te ontwikkel om I/H besering te verminder. Histories was meeste van die navorsings-fokus op die rol van kinases in I/H besering, terwyl inligting aangaande fosfatases in hierdie konteks steeds beperk is. Duideliker insig in die rol van fosfatases in die sellulêre reaksie op I/H besering is krities om bestaande kardiobeskerende intervensies te versterk of nuwe ingrepe te identifiseer.

Hierdie studie het ten doel gehad om die effekte van proteïen fosfatase 2A (PP2A, 'n beduidende fosfatase in die hart) inhibisie op die gevolge van I/H te ondersoek, asook om die fosfoproteoom van miokardiale weefsel wat aan hierdie intervensies blootgestel is te ondersoek.

Die geïsoleerde werkende muishart model is gebruik om weefsel voor te berei. Toediening van 'n inhibitor van PP2A, okadaïensuur (OA; 50 nM) onmiddelik voor 20 minute globale iskemie (GI) het infarkt-grootte verminder in vergelyking met kontrole ($28 \pm 19\%$ vs $56 \pm 23\%$; $n=9$; $p < 0.0106$), maar het nie 'n beduidende effek op funksionele herstel gehad nie. Fosfoproteomiese analiese het 898 proteïene en 184 gefosforileerde proteïene geïdentifiseer wat beïnvloed is deur die toediening van OA direk voor 20 minute GI, gevolg deur 10 minute herperfusie. Analise van sellulêre paaië het getoon dat die belangrikste paaië wat beïnvloed word deur PP2A inhibisie betrekking het op mitochondriale funksie en oksidatiewe fosforilasie, epiteel adherens seintransduksie en hermodellering, en sitoskelet seintransduksie. Twee proteïene vanuit die datastel, striatien en hiteskokproteïen (HSP) 90 α , is gekies vir bevestiging en verdere ondersoek. Mitochondriale respirasie is ook ondersoek.

In lyn met die fosfoproteomika resultate het toediening van OA die hoeveelheid gefosforileerde HSP90 α tydens herperfusie verhoog (1.83 ± 0.83 Arbitrêre Eenhede (AE) vs 0.69 ± 0.09 AE; $n = 2-4$; $p = 0.0480$), asook die totale hoeveelheid striatien tydens herperfusie verhoog (1.93 ± 0.84 AE vs 0.80 ± 0.06 AE; $n = 2-4$; $p = 0.0436$). Striatien, maar nie HSP90 α nie, is geko-immunopresipiteer met PP2A wat daarop dui dat die toename in fosforilasie van HSP90 α die gevolg is van 'n indirekte effek van PP2A inhibisie. Striatien werf regulatoriese proteïene na groot seintransduksie-komplekse wat meestal PP2A bevat. Ko-immunopresipitasie van striatien dui dus op die moontlike teenwoordigheid van hierdie komplekse in die hart.

OA is direk toegedien aan geïsoleerde mitochondria waarop polarografiese analiese van oksidatiewe fosforilasie, met behulp van 'n Clark-tipe elektrode, gedoen is. Geen verskille in oksidatiewe fosforilasie of respiratoriese beheer-ratio is waargeneem nie. Mitochondria is verder verdeel in die mitochondriale buitemembraan (MBM) en mitoplast (die mitochondriale binnemembraan en matriks) deur van digitonien gebruik te maak. Western-klad analiese het getoon dat die katalitiese en steier-subeenhede van PP2A waarskynlik in die MBM voorkom, terwyl striatien in 'n nuutvinding in die mitoplast geïdentifiseer is.

Laastens, na aanleiding van 'n toevallige waarneming, is die inhibitoriese effek van natriumorthovanadaat (NOV) op PP2A ondersoek. Hierdie is die eerste studie wat demonstreer dat NOV 'n swak, kompeterende inhibitor van PP2A is ($IC_{50} \approx 2.2 \text{ mM}$).

Na ons kennis, is hierdie studie die eerste om van 'n fosfoproteomiese benadering gebruik te maak om die effekte van fosfatase inhibisie tydens miokardiale I/H te ondersoek. Ons data dui daarop dat PP2A verwant is aan talryke proteïene en prosesse tydens I/H, insluitend oksidatiewe fosforilasie en sitoskelet dinamika.

STATEMENT OF CONTRIBUTION

With regard to this body of work, the nature and scope of all contributions other than my own were as follows:

Contributor	Nature of contribution
Academia Sinica Common Mass Spectrometry Facilities for Proteomics and Protein Modification Analysis	Mass spectrometry and bioinformatics that form part of chapter six.
John Melvin (under the supervision of Charlize White)	Western blot analysis of striatin, HSP90 α , and PKB that form part of chapter seven.
Dr Marguerite Blignaut	Assistance with mitochondrial sub-fractionation and supervision of mitochondrial oxygen consumption studies that form part of chapter eight.
Monique Nieuwenhuizen	Independent blinded pixel quantification of infarct size determination

Acknowledgements

I would like to thank the National Research Foundation, the German Academic Exchange Service (DAAD), and the Harry Crossley Foundation for the funding throughout my PhD that contributed not only to this project, but to developing a young professional. To the Faculty of Medicine and Health Sciences, thank you for the funding that allowed me to visit our collaborators in Taiwan, as well as attend the PSSA.

Dr Derick van Vuuren, you are a remarkable supervisor with extraordinary capacity. You go above and beyond and are willing to get your hands dirty. I appreciate that you always made time for me – I notice when your contributions to my work were done in the early hours of the morning. Thank you for all you have invested in this young scientist and thank you for not being disconnected from my journey as a PhD.

To Professor Amanda Lochner, thank you for scrutinizing every sentence of every chapter. Your feedback is much appreciated and your company during our meetings was very much enjoyed.

Dr Erna Marais, you're a force to be reckoned with, I reckon. Thank you for your valuable insights during our meetings. Also, thank you for showing me the value of a positive attitude.

I would also like to thank Dr's Tzu-Ching Meng and Lucy Yang, and the core facility at Academia Sinica for the phosphoproteomic analysis of my samples and for hosting me during my visits to Taipei. Your country and its culture now have a place in my heart.

John Melvin, I do not exaggerate when I say that I could not have finished on time without your assistance in the lab. Thank you for the blots. Because of your excellence, I never doubted the quality of your work. Thank you for one less thing that I had to stress about.

To Dr Marguerite Blignaut, thank you for assistance with the mitochondrial portion of this work and for availing yourself amidst your busy schedule. The way you formulate protocols under time and resource constraints is a superpower!

To the Division of Medical Physiology, the five years that I have spent here have been wonderful. Thank you for making me part of the family. To everyone in the office, particularly to Danèlle, thank you for your friendship. To Hameer, thank you for your comradery when we were in the Hatchery office. Four years later, I still remember how you encouraged me.

To the friends that I consider as family, thank you for being my community. To list each of your contributions would outnumber the pages of this document. Please know that I am grateful. To Sharne, Kopano, Charie, and Ntando, your encouragement and friendship means the world to me.

To my family - the Nieuwenhuizen's and the White's (and my very involved extended family): thank you for your unconditional love and un-ending support. You probably still don't know what I do, but you championed me all the way to the finish line! Thank you for always encouraging me in everything that I set my mind to. I love you all.

To my dear husband, Paul, thank you for walking this journey with me. Thank you for sharing in my passion and excitement and thank you for believing in me. My victories are yours also.

Finally, I believe that I am made in the image of God, and that the passion I have for science reflects a small part of the passion He has for the intricacies of His creation. Thank you for bringing this work to completion.

“God delights in concealing things; scientists delight in discovering things.”

– *Proverbs 25:2 (The Bible, The Message paraphrase)*

TABLE OF CONTENTS

1	ABSTRACT	I
2	OPSOMMING	III
3	STATEMENT OF CONTRIBUTION	V
4	TABLE OF CONTENTS	VIII
5	LIST OF FIGURES	XIII
6	LIST OF TABLES	XV
7	LIST OF ABBREVIATIONS	XVI
1	CHAPTER ONE - INTRODUCTION	1
1.1	MYOCARDIAL ISCHAEMIA	1
1.1.1	METABOLISM DURING MYOCARDIAL ISCHAEMIA	1
1.1.2	ION HOMEOSTASIS DURING MYOCARDIAL ISCHAEMIA	2
1.1.3	FUNCTIONAL IMPAIRMENT DURING MYOCARDIAL ISCHAEMIA	3
1.1.4	MANAGING AMI	4
1.2	REPERFUSION AND REPERFUSION INJURY	4
1.2.1	REACTIVE OXYGEN SPECIES	7
1.2.2	RESTORATION OF PH	8
1.2.3	CALCIUM	9
1.2.4	MITOCHONDRIAL PERMEABILITY TRANSITION PORE (MPTP)	10
1.2.5	INFLAMMATION	11
1.3	CARDIOPROTECTION	12
1.4	PROTEIN PHOSPHORYLATION	14
1.4.1	PROTEIN PHOSPHORYLATION IN BIOLOGICAL PROCESSES	15
1.5	PHOSPHATASES IN CARDIOPROTECTION	16
1.5.1	PH DOMAIN LEUCINE-RICH REPEAT PROTEIN PHOSPHATASE	16
1.5.2	PHOSPHATASE AND TENSIN HOMOLOGUE DELETED ON CHROMOSOME 10	17
1.5.3	PROTEIN PHOSPHATASE 2C (PP2C) IN MITOCHONDRIA	17
1.5.4	MAPK PHOSPHATASE	18
1.5.5	PROTEIN TYROSINE PHOSPHATASES (PTPs)	18
1.5.6	PROTEIN PHOSPHATASE 2B (PP2B)	19

1.5.7	PROTEIN PHOSPHATASE 1 (PP1) AND PROTEIN PHOSPHATASE 2A (PP2A)	19
1.6	PROTEIN PHOSPHATASE 2A	21
1.6.1	PP2A-C	21
1.6.2	PP2A-A	21
1.6.3	PP2A-B	22
1.7	REGULATION OF PP2A	26
1.7.1	PHOSPHORYLATION	26
1.7.2	METHYLATION	28
1.7.3	OTHER PROTEINS THAT BIND TO PP2A	29
1.8	PP2A REGULATES BIOLOGICAL FUNCTIONS	32
1.8.1	PP2A IN Ca^{2+} HANDLING	32
1.8.2	PP2A IN ION CHANNEL REGULATION	35
1.8.3	PP2A IN CELL DEATH	36
1.9	RATIONALE	39
1.10	AIMS AND OBJECTIVES	41
2	CHAPTER TWO - MATERIALS AND METHODS	42
2.1	MATERIALS	42
2.2	ANIMALS	42
2.2.1	ISOLATED MURINE HEART PERFUSIONS	43
2.2.2	INFARCT SIZE DETERMINATION	45
2.2.3	SAMPLE PREPARATION FOR BIOCHEMICAL ANALYSIS	45
2.2.4	WESTERN BLOT ANALYSIS	46
2.2.5	IMMUNOPRECIPITATION	48
2.2.6	PHOSPHATASE ASSAY	49
2.2.7	STATISTICAL ANALYSES	49
3	CHAPTER THREE - INHIBITOR DOSE DETERMINATION	51
3.1	RATIONALE	51
3.2	METHODS	52
3.2.1	DATA AND STATISTICAL ANALYSIS	53
3.3	RESULTS	54
3.4	DISCUSSION	60
3.5	LIMITATIONS	62

4	<u>CHAPTER FOUR - THE INHIBITORY EFFECTS OF SODIUM ORTHOVANADATE ON PP2A</u>	64
4.1	RATIONALE	64
4.2	METHODS	65
4.2.1	SOV INHIBITION IN PURIFIED ENZYMES	65
4.2.2	SOV INHIBITION IN CARDIAC LYSATES	66
4.2.3	SOV ADMINISTERED IN THE ISOLATED WORKING HEART	68
4.2.4	DATA AND STATISTICAL ANALYSIS	68
4.3	RESULTS	69
4.3.1	SOV INHIBITION IN PURIFIED ENZYMES	69
4.3.2	SOV INHIBITION IN CARDIAC LYSATES	72
4.3.3	SOV INHIBITION IN PERFUSED HEARTS	76
4.4	DISCUSSION	76
4.4.1	THE EFFECTS OF SOV ON PURIFIED ENZYMES	77
4.4.2	THE EFFECTS OF SOV ON LYSATES	77
4.4.3	THE EFFECTS OF SOV ON PERFUSED HEARTS	79
4.4.4	CONCLUSION	79
4.5	LIMITATIONS	80
5	<u>CHAPTER FIVE - THE EFFECT OF PP2A INHIBITION ON INFARCT SIZE AND FUNCTIONAL RECOVERY</u>	82
5.1	RATIONALE	82
5.2	METHODS	83
5.2.1	DATA AND STATISTICAL ANALYSES	84
5.3	RESULTS	84
5.4	DISCUSSION	87
5.5	LIMITATIONS	90
6	<u>CHAPTER SIX - PHOSPHOPROTEOMIC ANALYSIS OF MYOCARDIAL ISCHAEMIA AND REPERFUSION</u>	92
6.1	RATIONALE	92
6.2	METHODS	92
6.2.1	PROTEIN DIGESTION	94
6.2.2	PHOSPHOPEPTIDE ENRICHMENT	94
6.2.3	SHOTGUN PROTEOMIC ANALYSES	94
6.2.4	PROTEIN/PHOSPHOPEPTIDE IDENTIFICATION AND QUANTIFICATION	95

6.2.5	INGENUITY PATHWAY ANALYSIS	96
6.3	RESULTS	96
6.4	DISCUSSION	98
6.4.1	PP2A IN MITOCHONDRIAL FUNCTION AND OXIDATIVE PHOSPHORYLATION	99
6.4.2	PP2A AND THE CYTOSKELETON	101
6.4.3	PP2A AND INTRACELLULAR JUNCTIONS	105
6.4.4	CONCLUSION	107
6.5	LIMITATIONS	108
7	<u>CHAPTER SEVEN - STRIATIN AND HSP90A AS POTENTIAL SUBSTRATES OF PP2A</u>	111
7.1	RATIONAL	111
7.1.1	STRIATIN	111
7.1.2	HEAT SHOCK PROTEIN (HSP) 90A	113
7.1.3	AIMS	114
7.2	METHODS	114
7.2.1	WHOLE CELL LYSATE (NON-FRACTIONATED)	114
7.2.2	IMMUNOPRECIPITATION	115
7.2.3	FRACTIONATION	115
7.2.4	WESTERN BLOT ANALYSIS	116
7.2.5	STATISTICAL ANALYSIS	117
7.3	RESULTS	117
7.3.2	IMMUNOPRECIPITATION	119
7.3.3	FRACTIONATION	120
7.4	DISCUSSION	127
7.4.1	HSP90A	128
7.4.2	STRIATIN	130
7.4.3	PKB/AKT	132
7.4.4	CONCLUSION	133
8	<u>CHAPTER EIGHT - THE EFFECT OF PP2A INHIBITION ON OXIDATIVE PHOSPHORYLATION</u>	134
8.1	RATIONALE	134
8.2	METHODS	135
8.2.1	MITOCHONDRIAL ISOLATION	135
8.2.2	MITOCHONDRIAL OXYGEN CONSUMPTION	136
8.2.3	PHOSPHATASE ASSAY	137

8.2.4	MITOCHONDRIAL SUB-FRACTIONATION WITH DIGITONIN	137
8.2.5	WESTERN BLOT ANALYSIS	138
8.2.6	DATA AND STATISTICAL ANALYSES	138
8.3	RESULTS	139
8.3.1	MITOCHONDRIAL OXYGEN CONSUMPTION	139
8.3.2	PHOSPHATASE ASSAY	140
8.3.3	WESTERN BLOT ANALYSIS	140
8.3.4	MITOCHONDRIAL SUB-FRACTIONATION	141
8.4	DISCUSSION	143
8.5	LIMITATIONS	147
8.6	FUTURE WORK	148
9	<u>CHAPTER NINE - FINAL CONCLUSION</u>	<u>149</u>
10	<u>REFERENCES</u>	<u>153</u>
	<u>ADDENDUM A – INFARCT SIZE DETERMINATION</u>	<u>189</u>
	<u>ADDENDUM B – ADDITIONAL PHOSPHOPROTEOMIC DATA</u>	<u>191</u>
	<u>ADDENDUM C – ADDITIONAL WESTERN BLOT IMAGES</u>	<u>220</u>

LIST OF FIGURES

CHAPTER ONE

Figure 1.1 - PP2A holoenzyme structure	23
Figure 1.2 - PP2A regulates apoptotic proteins	37

CHAPTER TWO

Figure 2.1 - Working mouse heart perfusion apparatus	44
------------------------------------------------------	----

CHAPTER THREE

Figure 3.1 - Perfusion protocol for inhibitor dose determination	52
Figure 3.2 - Confirmation of PP2A immunoprecipitation.	55
Figure 3.3 - Confirmation of the presence of PP2A and the absence of PP1 in immunoprecipitate and matched whole cell supernatant.	56
Figure 3.4 - DIFMU production from PP2A immunoprecipitated from hearts perfused with 10, 50, and 100 nM OA, DMSO, or KHB resuspended in assay buffer.	57
Figure 3.5. – DIFMU production from PP2A immunoprecipitated from hearts perfused with 10, 50, and 100 nM OA, DMSO, or KHB resuspended in 10 mM SOV.	58
Figure 3.6 - DIFMU production from PP2A immunoprecipitated from hearts perfused with 10, 50, and 100 nM OA, DMSO, or KHB resuspended in assay buffer – second experiment.	60

CHAPTER FOUR

Figure 4.1 - Vanadate is a phosphate analogue	64
Figure 4.2 - Experimental design of the effects of inhibitors on total phosphatase activity	67
Figure 4.3 - Perfusion protocol for SOV administration	68
Figure 4.4 - The effect of 10 mM SOV on purified PP2A	70
Figure 4.5 - The effect of 10 mM SOV on purified PTP1 β	70
Figure 4.6 - Calculated IC ₅₀ of SOV inhibition of purified PP2A	71
Figure 4.7 - Kinetic parameters of SOV inhibition	72
Figure 4.8 - The effects of SOV in cardiac lysates determined with different phosphatase inhibitors	73
Figure 4.9 – DIFMU production of immunoprecipitated PP2A from a cardiac lysate treated with assay buffer, 1 mM SOV, or 10 mM SOV.	75
Figure 4.10 - Phosphatase activity from hearts perfused with 1 mM SOV	76

CHAPTER FIVE

Figure 5.1 - Perfusion protocol for IFS determination	83
Figure 5.2 - Coronary flow during drug administration	84
Figure 5.3 - Pre- and post-ischaemic function of hearts perfused with DMSO or OA	85
Figure 5.4 - Post-ischaemic function expressed as a percentage of pre-ischaemic (baseline) function	86

CHAPTER SIX

Figure 6.1 - Perfusion protocol for phosphoproteomic analysis of hearts exposed to ischaemia and reperfusion	93
Figure 6.2 - Volcano plots of total proteins and total phosphoproteins detected by mass spectrometry	96

CHAPTER SEVEN

Figure 7.1 - HSP90 α expression in non-fractionated whole-cell lysate	118
Figure 7.2 - Striatin expression in non-fractionated whole-cell lysate	119
Figure 7.3 - Fold changes of striatin and PKB that has co-immunoprecipitated with PP2A	120
Figure 7.4 - HSP90 α expressed in the cytosolic fraction	121
Figure 7.5 - PKB/Akt expressed in the cytosolic fraction	122
Figure 7.6 - Striatin expressed in the cytosolic fraction	123
Figure 7.7 - PKB/Akt expressed in the membrane fraction	124
Figure 7.8 - HSP90 α expressed in the nuclear fraction	125
Figure 7.9- PKB/Akt expressed in the nuclear fraction	126
Figure 7.10 - Striatin expressed in the nuclear fraction	127

CHAPTER EIGHT

Figure 8.1 - The effects of 50 nM OA on ADP/O, oxidative phosphorylation, and mitochondrial oxygen consumption.	139
Figure 8.2 - The effect of 50 nM OA on mitochondrial phosphatase activity	140
Figure 8.3 - Western blot analysis of mitochondrial complexes in hearts exposed to either DMSO or OA and subjected to ischaemia and/or reperfusion	141
Figure 8.4 - Western blot analysis of the outer mitochondrial membrane and mitoplast fractions obtained after digitonin treatment	143

LIST OF TABLES

CHAPTER ONE

Table 1.1 - Functions of the Bcl-2 family	36
-------------------------------------------	----

CHAPTER TWO

Table 2.1 - Information regarding the antibodies used in this experiment.	48
---------------------------------------------------------------------------	----

CHAPTER THREE

Table 3.1 - Coronary flow of hearts perfused with 10 nM, 50 nM or 100 nM OA, 0.13% DMSO, or KHB.	54
Table 3.2 - Amount of DIFMU produced at t = 120 minutes	56
Table 3.3 - Amount of DIFMU produced at t = 120 minutes in second experiment	59

CHAPTER FOUR

Table 4.1 - A comparison of the reaction rates before and after the addition of 10 μ l inhibitor to lysates pre-treated with either assay buffer, 100 nM OA, 1 mM SOV, or 10 mM SOV.	74
------------------------------------------------------------------------------------------------------------------------------------------------------------------------------------------	----

CHAPTER SIX

Table 6.1 - List of proteins that were differentially expressed or phosphorylated in the 50 nM OA-treated cohort that show a fold change greater than two and a $-\log_{10}$ (p value) greater than 1.3	97
Table 6.2 - List of canonical pathways most affected by PP2A inhibition during myocardial ischaemia and reperfusion that have a p value ≤ 0.0001 .	98
Table 6.3 - Titin phosphosites identified in Mus musculus by phosphoproteomic analysis of hearts exposed to 20 minutes GI and 10 minutes reperfusion	105

LIST OF ABBREVIATIONS

%	Percent
°C	Degrees Celsius
µg	microgram
µl	Microlitre
µm	Micrometre
µM	Micromolar
Å	Angstrom (0.1 nanometre)
ADP	Adenosine diphosphate
ADP/O	The number of ADP molecules utilized per oxygen atom consumed
AMI	Acute myocardial infarction
ANOVA	Analysis of variance
AO	Aortic output
APS	Ammonium persulfate
Asp	Aspartic acid
ATM	Ataxia telangiectasia mutated kinase
ATP	Adenosine triphosphate
AU	Arbitrary units
BCAA	Branched chain amino acid
bpV(phen)	Bispermoxovanadium
BSA	Bovine serum albumin
Ca ²⁺	Calcium
CaCl ₂	Calcium chloride
CaMKII	Calmodulin-dependent kinase II
cat:	Catalogue
Ca _v 1.2	L-type calcium channel
Cgmp	Cyclic guanosine monophosphate
CI	Mitochondrial complex I
CII	Mitochondrial complex II
CIII	Mitochondrial complex III

CIV	Mitochondrial complex IV
cMLCK	Cardiac myosin light chain kinase
CO	Cardiac output
CV	Mitochondrial complex V
Da	Dalton
DAMP	Damage-associated molecular pattern
DDA	Data-dependent acquisition
DiFMU	6,8-difluoro-4-methylumbelliferyl
DiFMUP	6,8-difluoro-4-methylumbelliferyl phosphate
DMSO	Dimethylsulfoxide
DNA	Deoxyribonucleic acid
DSP	Dual specificity phosphatase
EDTA	Ethylenediaminetetraacetic acid
EGTA	Ethyleneglycol-bis(beta-aminoethylether)-N,N'-tetraacetic acid
eNOS	Endothelial nitric oxide synthase
ERK1/2	Extracellular signal-regulated kinase p42/p44
FAM122A	Family with sequence similarity 122A
FKBP12.6	FK 506 binding protein 12.6
FOXO1	Forkhead box 1
g	Gram
GANP	Germinal center-associated nuclear protein
GI	Global ischaemia
GPCR	G-protein coupled receptor
GSK-3 β	Glycogen synthase kinase 3 beta
H ⁺	Hydrogen ion; proton
HCO ₃	Bicarbonate
HEAT	Huntingtin-elongation factor-a subunit-target of rapamycin
HEPES	Hydroxyethyl piperazineethanesulfonic acid
HIV/AIDS	Human immunodeficiency virus/acquired immunodeficiency syndrome
HL-60	Human leukaemia cell line
HSP	Heat shock protein
I/R	Ischaemia/reperfusion
I ₁ ^{PP2A}	Endogenous inhibitor of PP2A 1

I_2^{PP2A}	Endogenous inhibitor of PP2A 2
IC_{50}	Concentration of inhibitor that results in 50% enzyme activity
IFS	Infarct size
IGBP1	Immunoglobulin-binding protein 1; $\alpha 4$
IHD	Ischaemic heart disease
IPA	Ingenuity Pathway Analysis
IPC	Ischaemic preconditioning
K^+	Potassium
KCl	Potassium chloride
kDa	Kilodalton
KE	Potassium chlorideEthylenediaminetetraacetic acid
kg	Kilogram
KH_2PO_4	Monobasic potassium phosphate
KHB	Krebs-Henseleit bicarbonate buffer
K_m	Michaelis constant; the affinity an enzyme has for a substrate
K_{mapp}	Apparent K_m ; K_m in the presence of inhibitors
KO	Knock-out
LCMT1	Leucine carboxyl methyltransferase 1
Leu	Leucine
log	Logarithm
M	Molar
M/S	Mannitol/sucrose
m/z	Mass to charge ratio
mA	Milliampere
MAP	Microtubule associated protein
MAPK	Mitogen activated protein kinase
MAPT	Microtubule associated protein tau
MARCKS	Myristoylated alanine-rich C-kinase substrate
MEK	Mitogen activate protein kinase kinase
mg	Milligram
Mg^{2+}	Magnesium
$MgCl_2$	Magnesium chloride
MI	Myocardial infarction

Mid1	Midline 1
min	Minute
MKP	Mitogen activated protein kinase phosphatase
ml	Milliliter
mm	Millimetre
mM	Millimolar
mmHg	Millimeters mercury
mPTP	Mitochondrial permeability transition pore
mRNA	Messenger ribonucleic acid
MS/MS	Tandem mass spectrometry
msec	Milliseconds
mTOR	Mammalian target of rapamycin
mTORC1	Mammalian target of rapamycin complex 1
MyBP-C	Myosin binding protein C
N2B	N2Bus
Na ⁺	Sodium
NaCl	Sodium chloride (table salt)
NADH	Nicotinamide adenine dinucleotide hydrogen
NaF	Sodium fluoride
nanoLC	Nano-scale liquid chromatography
NAPDH	Nicotinamide adenine dinucleotide phosphate
nAtoms	Nano Atoms
Na _v	Voltage-gated sodium channel
NCX	Sodium calcium exchanger
Ng	nanogram
nM	Nanomolar
nm	Nanometer
nmol	Nanomole
NO	Nitric oxide
OA	Okadaic acid
OMM	Outer mitochondrial membrane
P/T	Ratio of phosphorylated protein to total expressed protein
PBS	Phosphate-buffered saline

PCI	Percutaneous coronary intervention
PEVK	Proline glutamate valine lysine motif
pH	Potential of hydrogen
Phe	Phenylalanine
PHLPP	PH domain leucine-rich repeat protein phosphatase
PI3K	Phosphoinositide 3-kinase
PKA	Protein kinase A
PKB	Protein kinase B
PKC	Protein kinase C
PKG	Protein kinase G
PLB	Phospholamban
PME-1	Protein phosphatase methylesterase
pmol	Picomole
PP1	Protein phosphatase 1
PP2A	Protein phosphatase 2A
PP2A-A	Protein phosphatase 2A subunit A; scaffolding subunit
PP2A-B	Protein phosphatase 2A subunit B; regulatory subunit
PP2A-C	Protein phosphatase 2A subunit C; catalytic subunit
PP2B	Protein phosphatase 2B; calcineurin
PP2C	Protein phosphatase 2C
PP2Cm	Protein phosphatase 2C in mitochondria
PP4	Protein phosphatase 4
PP5	Protein phosphatase 5
PP6	Protein phosphatase 6
ppm	Parts per million
Pro	Proline
PSMF	Phenylmethanesulphonylfluoride
PSP	Serine/threonine phosphatase
PTEN	Phosphatase and tensin homologue
PTP	Protein tyrosine phosphatase
PTP1 β	Protein tyrosine phosphatase 1 beta
PTPA	Phosphotyrosyl phosphatase activator
PVDF	Polyvinylidene fluoride

RCI	Respiratory control index
RIPA	Radioimmunoprecipitation assay
RISK	Reperfusion injury salvage kinase
ROS	Reactive oxygen species
Rpm	Revolutions per minute
RyR	Ryanodine receptor
SAFE	Survival activating factor enhancement
SD	Standard deviation
SDS-PAGE	Sodium dodecyl sulfate polyacrylamide gel electrophoresis
Ser	Serine
SERCA	Sarco-endoplasmic reticulum calcium ATPase
SET	Suvar3-9, enhancer of zeste, trithorax
SG2NA	S/G ₂ nuclear autoantigen
siRNA	Small interfering ribonucleic acid
SIRT3	Sirtuin 3
SOV	Sodium orthovanadate
STAT-3	Signal transducer and activator of transcription 3
STEMI	ST-elevation myocardial infarction
STRIP2	Striatin interacting protein 2
STRIPAK	Striatin-interacting phosphatases and kinases
SV40	Simian virus 40 small-t antigen
t	Time
TBS	Tris-buffered saline
TEMED	Tetramethylethylenediamine
Thr	Threonine
TiO ₂	Titanium dioxide
TIPRL	TOR signalling pathway regulator-like
TNF- α	Tumour necrosis factor alpha
TRIS	Trisaminomethane
TTC	Triphenyltetrazolium chloride
Tyr	Tyrosine
U	Unit
ULK1	Unc-51 like autophagy activating kinase

V	Volt
v/v	Volume per volume
VDAC	Voltage-dependent anion channel
V_{max}	The maximum velocity/rate of reaction
w/v	Weight per volume
WCL	Whole cell lysate
WHO	World Health Organization
x g	Times gravity
α	Alpha
α_4	Alpha four
β	Beta
γ	Gamma
δ	Delta
ϵ	Epsilon

CHAPTER ONE

INTRODUCTION

1.1 MYOCARDIAL ISCHAEMIA

Myocardial ischaemia (MI) is commonly seen in scenarios such as heart transplantation, cardiac surgeries where cardiopulmonary bypass is required, coronary artery disease, and acute myocardial infarction (AMI; heart attack). Although MI from surgical procedures occur in a controlled environment, AMIs can occur anywhere and at any time. Approximately 45% of individuals who experience AMI do not recognize the symptoms and attribute it to a less serious problem (Zhang *et al.*, 2016). A study published in the *Journal of the American Medical Association* (Turkbey *et al.*, 2015) studied individuals with no cardiovascular disease. During a follow-up study 10 years later, the study found that 7.9% of individuals had myocardial scarring - evidence of a mild to moderate myocardial infarction - and approximately 78% of the individuals were unaware of their condition.

MI occurs when there is a reduction of blood flow supplying the heart, usually because of a partial or complete occlusion of the coronary arteries. As a result, the tissue downstream of the occlusion is deprived of oxygen and nutrients and waste products cannot be removed. During ischaemia of a highly metabolic organ such as the heart, the demand for oxygen and nutrients soon exceeds the supply. Since the cardiomyocytes no longer have access to substrates required for normal function, they begin to malfunction. In addition, the cells can no longer efficiently rid themselves of metabolic waste, which begin to rapidly accumulate to toxic levels. Left untreated, cell death ensues and results in a myocardial infarct.

1.1.1 Metabolism during myocardial ischaemia

The heart is heavily dependent on oxygen for metabolism and uses 5% of all the oxygen consumed by the body (Lopaschuk, 2016). The preferred fuel sources for the heart are mostly fatty acids and carbohydrates such as glucose and lactate, etc., which produce a high yield of adenosine triphosphate (ATP) during aerobic conditions and their metabolites feed into the electron transport chain to produce ATP (Lopaschuk *et al.*, 2010). When coronary flow is only partially reduced, as would be the case during mild or moderate ischaemia, fatty acid oxidation still

proceeds but at a lower rate. It is also still coupled to oxidative phosphorylation and produces a significant amount of ATP. However, in severe ischaemia, where minimal coronary flow or total coronary occlusion occurs, the cofactors necessary for fatty acid oxidation are not regenerated by oxidative phosphorylation and fatty acid oxidation ceases (Neely and Morgan, 2003). Under these conditions, ATP production is severely diminished. The rate of ATP production from both fatty acid oxidation and glycolysis is directly proportional to the rate of coronary flow (Neely and Morgan, 2003). Thus, a low coronary flow results in a low rate of ATP production, and during total coronary occlusion, the cardiomyocyte has a very limited capacity to generate ATP through anaerobic glycolysis.

During severe MI, oxygen-dependent metabolism becomes challenging and the cardiomyocyte attempts to compensate by shifting from aerobic to anaerobic respiration and consuming its reserves of high-energy phosphates. The cell begins to transfer phosphates from phosphocreatine to adenosine diphosphate (ADP) in order to create ATP, but these reserves are quickly depleted (Rovetto *et al.*, 1973). Glycogen reserves become the new source of high energy phosphates as they are consumed by anaerobic glycolysis. Since glycolysis can only be coupled to oxidative phosphorylation in aerobic conditions, the products of anaerobic glycolysis, lactate, protons (hydrogen ions; H^+), and inorganic phosphates, begin to accumulate in the ischaemic cardiomyocyte, leading to a reduction in pH. Eventually these metabolites negatively regulate glycolysis to prevent further accumulation of these glycolytic by-products and ATP production ceases (Lopaschuk *et al.*, 2010).

1.1.2 Ion homeostasis during myocardial ischaemia

As ischaemia progresses, anaerobic respiration fails to meet the heart's high demand for ATP. The limited amount of ATP that is produced is largely consumed by the proton-translocating F_1F_0 ATP synthase (complex V of the mitochondrial respiratory chain), which reverses to consume valuable ATP to pump protons into the intermembrane space (Jennings, Reimer and Steenbergen, 1991; Grover *et al.*, 2004). This process is necessary to maintain the mitochondrial membrane potential, but also consumes 35-50% of available ATP (Jennings, Reimer and Steenbergen, 1991). ATP is necessary to maintain ion channels and without it, cellular homeostasis is very quickly disrupted. The result is acidosis originating from the intracellular accumulation of the metabolites of anaerobic respiration, such as lactate, H^+ , creatine, and inorganic phosphates (Hochachka and Mommsen, 1983). To restore the physiological pH, H^+ are extruded out of the cell via the

sodium/hydrogen (Na^+/H^+) exchanger, but Na^+ is simultaneously facilitated into the cardiomyocyte, resulting in an increase in intracellular Na^+ . In addition, the sodium/potassium (Na^+/K^+) ATPase which requires ATP to pump Na^+ out of the cardiomyocyte, ceases to function under ischaemic conditions. The cardiomyocyte attempts to relieve the intracellular accumulation of Na^+ by pumping it out of the cell via the sodium/calcium ($2\text{Na}^+/\text{Ca}^{2+}$) exchanger (NCX), but this only results in an intracellular Ca^{2+} overload, which reduces intracellular enzyme activity. The Ca^{2+} /ATPase pumps cease to function and limits calcium reuptake by the sarcoplasmic reticulum. The increased ion accumulation in the cell causes hyperosmolarity, which results in water influx and cell swelling (Jennings, Reimer and Steenbergen, 1986).

1.1.3 Functional impairment during myocardial ischaemia

Under normal physiological conditions, approximately 60% of ATP produced in the heart is directed towards contractile shortening, and the remaining 40% is utilized in maintaining ion homeostasis (Gibbs, 2017; Suga, 2017). However, under the extreme cellular stress of MI, the cardiomyocyte prioritizes maintenance of ion homeostasis and most available ATP is redirected accordingly. Thus, lower levels of ATP are available for contraction, which will also be inhibited by the increasing acidosis within the cardiomyocyte. Consequently, contractile force rapidly decreases even though the ischaemic tissue receives electric stimuli (Jennings, 2013). As ATP levels continue to fall, ischaemic rigor develops (Bowers, Allshire and Cobbold, 1992). This puts strain on the heart as it can no longer efficiently pump blood to the body. In addition, the myocardium has a limited ability to regenerate tissue (Pfeffer, 1995). Once a significant amount of tissue is irreversibly damaged, it is replaced by connective scar tissue. This scar tissue also has no ability to contract or conduct electrical signals which negatively influences the mechanical properties of the heart (Richardson *et al*, 2015). Decreased left ventricular function, as well as long term risk of ventricular remodelling that leads to heart failure, is directly proportional to the size of the infarct (Richardson *et al.*, 2015).

Infarct size is proportional to the duration of coronary occlusion (Reimer *et al*, 1977) and the rate of coronary flow (Reimer and Jennings, 1979). During ischaemia, irreversible injury first develops in the inner portion of the heart that receives the least amount of coronary flow, the subendocardium. As the ischaemic insult progresses, damage begins to spread from the subendocardium to the epicardium through the full thickness of the ventricular walls (Reimer *et al.*, 1977; Reimer and Jennings, 1979), often referred to as the “wavefront” phenomenon.

1.1.4 Managing AMI

Depending on the cause of infarction, there are three different strategies of intervention for AMI. The first is percutaneous coronary intervention (PCI, also known as angioplasty), a non-surgical procedure where a catheter, equipped with a balloon, is guided through the arteries to the site of occlusion and inflated to widen the occluded artery (Grüntzig *et al*, 1979). The catheter may also be equipped with a stent to maintain the dilation or be used as a drug delivery system (Dehmer and Smith, 2009). The second is administration of a thrombolytic drug, a pharmacological agent that lyses the occlusion (TIMI Study Group, 1985). The last is coronary artery bypass surgery, where another artery from the body is grafted as part of the cardiac circulation but in a manner that bypasses the occluded artery, restoring the circulation to the tissue downstream of the occlusion (Benetti, 1985).

Regardless of the intervention for MI, each has the same intended outcome – restoration of blood flow to the affected tissue, termed reperfusion (Stiermaier *et al.*, 2013). During reperfusion, blood flow to the damaged tissue is re-established, restoring the supply of oxygen and nutrients and allowing removal of accumulated waste metabolites. This is absolutely vital to relieve or greatly reduce the ischaemic insult and salvage the damaged myocardium. However, reperfusion itself is associated with a variety of alterations in the myocardium that result in tissue damage. This phenomenon is known as ischaemia/reperfusion (I/R) injury (Braunwald and Kloner, 1985).

1.2 REPERFUSION AND REPERFUSION INJURY

The histological description of organs undergoing ischaemia and reperfusion shows that reperfusion contributes to a greater amount of injury than that caused by ischaemia alone (Parks and Granger, 2017). However, the amount of tissue damage can be significantly reduced by applying an intervention at the time of reperfusion (Piper, García-Dorado and Ovize, 1998). This has two implications: first, that the injury associated with reperfusion can be minimized and second, that the injury associated with reperfusion is an independent mediator of cardiomyocyte death (Yellon and Hausenloy, 2007). Therefore, reperfusion is a paradox: it is vital to the survival of the ischaemic cell, but simultaneously causes injury that reduces the benefit of reperfusion itself.

Myocardial I/R injury manifests as four types of cardiac dysfunction, namely myocardial stunning, the “no-reflow” phenomenon, reperfusion arrhythmias, and lethal reperfusion injury.

Myocardial stunning is the phenomenon of delayed recovery of contractile function following the restoration of coronary flow, in the absence of tissue damage (Braunwald and Kloner, 1982). It was first described by Heyndrickx and colleagues in 1975 when they showed that canine myocardium exposed to ischaemia did not contract as efficiently after reperfusion as control myocardium (Heyndrickx *et al.*, 1975). The stunned myocardium is viable, but exhibits prolonged dysfunction indicated by a reduction in cardiac output, increased left atrial pressure, and possible tissue hypoperfusion (Sidebotham and Gillham, 2007). The condition itself is temporary, and usually spontaneously resolves within 48-72 hours post ischaemia (Bolli 1992; Grocott *et al.*, 2018) but may be treated with inotropic agents if necessary. Consequently, it is only a major clinical concern when the affected portion of myocardium is large (Piper, García-Dorado and Ovize, 1998). The extent of myocardial stunning is dependent on the duration and severity of the ischaemic insult (Braunwald and Kloner, 1982), as well as cardiac temperature during ischaemia (Engelman, 1994). Oxidative stress and calcium overload (discussed later) are proposed to be the mechanisms of stunning, as they damage myofilaments and render them less responsive to calcium, which results in contractile impairment (Bolli *et al.*, 1989; Bolli, 1992).

“No-reflow” is the failure to achieve uniform reperfusion of the myocardium despite restoration of coronary flow (Kloner, Ganote and Jennings, 1974). “No-reflow” is caused by obstruction of the microvasculature after severe ischaemia and is caused by various factors that may include: damaged capillaries, swollen and irreversibly injured cardiomyocytes, swollen and ruptured endothelial cells that compress the capillaries, vasoconstriction caused by endothelial dysfunction, physical obstruction of the capillary due to endothelial membrane blebbing and leukocyte plugging, and damage caused by reactive oxygen species (Kloner, Ganote and Jennings, 1974; Park and Lucchesi, 1999; Ibáñez *et al.*, 2015). This resultant loss of microvascular integrity prevents arterial blood and pharmacological agents from reaching the ischaemic tissue and thus prevents adequate reperfusion of the ischaemic myocardium, even after the coronary occlusion has been resolved (Kloner, Ganote and Jennings, 1974).

Up to 30% of patients presenting with a particular type of AMI, ST-elevation myocardial infarction (STEMI), experience “no-reflow” (Niccoli *et al.*, 2013) and are at greater risk of developing heart failure and left ventricular remodelling (Morishima *et al.*, 2000). “No-reflow” is evident upon reperfusion and can persist for at least a week (Mewton *et al.*, 2013). In addition, no-reflow has been shown to be an independent predictor of long-term cardiac complications after AMI (Morishima *et al.*, 2000). The “no-reflow” condition can be exacerbated by various factors,

including the presence of microemboli originating from atherosclerotic debris and thrombi generated by PCI. Microvascular obstruction causes irreversible damage and currently no effective therapy exists to prevent microvascular obstruction. Therefore, preservation of the microvasculature is crucial for the recovery of myocardial function.

Rhythm disorders are associated both with ischaemia and reperfusion and are classified as such: ischaemic arrhythmias when associated with coronary occlusion and reperfusion arrhythmias when associated with reperfusion (Adams and Pelter, 2002). Infarct size, duration and severity of ischaemia, rate of reperfusion, as well as the presence of cardiac hypertrophy and/or heart failure, are all associated with the presentation of reperfusion arrhythmias (Matoshvili and Kipshidze, 2014). Approximately 80% of patients treated for MI experience at least one reperfusion arrhythmia incident 48 hours after treatment (Tatli *et al.*, 2013), the most common of which include ventricular premature contractions, ventricular tachycardia, atrial fibrillation, ventricular fibrillation, and accelerated idioventricular rhythm (Tatli *et al.*, 2013). Some arrhythmias are benign and require minimal intervention or usually resolve by themselves, while most are fatal and require urgent treatment (Das and Mishra, 2013).

Lethal reperfusion injury refers specifically to the death of cardiomyocytes as a result of reperfusion, rather than ischaemia (Hausenloy and Yellon, 2013). Although it is difficult to delineate ischaemic and reperfusion injuries, the final size of infarction can be reduced by 40-50% when interventions aimed at preventing reperfusion injury are applied at the onset of reperfusion (Piper, García-Dorado and Ovize, 1998). This would indicate that lethal reperfusion injury can account for up to 50% of the final size of infarction (Hausenloy and Yellon, 2013). Limiting lethal reperfusion injury is necessary to salvage myocardium and currently, no such therapeutic interventions have been standardized.

At the end of ischaemia, the prolonged lack of oxygen and energy substrates for ATP production, combined with the severe accumulation of metabolites associated with anaerobic metabolism compromises cell survival. More specifically, the cardiomyocyte has depleted levels of ATP, an accumulation of inorganic phosphates and lactic acid, has lost ion homeostasis and has increased intracellular Na^+ , Ca^{2+} and H^+ , all of which result in a depolarized membrane potential, cellular swelling, and acidosis. Upon reperfusion, oxygen and substrates for ATP synthesis are restored, resulting in ATP production, while toxic metabolites are also removed from the cell. However, the rapid change in intracellular environment brought on by reperfusion results in several

maladaptive processes that culminate in cell death that is independent of ischaemic cell death. This is termed lethal reperfusion injury and the processes that mediate this are reviewed below.

1.2.1 Reactive oxygen species

Reactive oxygen species (ROS) are oxygen-containing molecules that possess an unpaired electron in their outer orbital (Park and Lucchesi, 1999). ROS are generated by all cells and are important signalling molecules (Truong and Carroll, 2013). Although unstable and highly reactive, their activity is balanced by antioxidant systems within the cell. ROS is generated under normal physiological conditions, and minimal to no ROS is produced during anoxia (Garlick *et al.*, 1987). During cellular stress such as ischaemia, where oxygen is limited, small bursts of ROS are produced (Zhu and Zuo, 2013). During reperfusion, when oxygen is reintroduced, ROS is overproduced and overwhelms the cellular antioxidant systems. ROS interferes with normal cellular signalling (Hausenloy and Yellon, 2013) and reacts with macromolecules such as proteins, membrane lipids, and nucleic acids, damaging them in the process (Park and Lucchesi, 1999).

In the heart, mitochondria are the main source of ROS such as superoxide and hydrogen peroxide. Superoxide is formed by the incomplete reduction of an oxygen molecule when electrons leak in the electron transport chain (Raedschelders, Ansley and Chen, 2012). Superoxide can cause damage by itself, but also acts as a precursor to other damaging free radicals, such as the hydroxyl radical (James *et al.*, 2016). ROS can also be produced by other sources, including xanthine oxidase from endothelial cells, nicotinamide adenine dinucleotide phosphate (NADPH) oxidase from neutrophils, the uncoupled nitric oxide synthase system, uncoupled oxidative phosphorylation, and haemoglobin and myoglobin (in severe injury) (Matsushima, Tsutsui and Sadoshima, 2014; Wu *et al.*, 2018).

During the initial stage of reperfusion, the reintroduction of oxygen results in ATP production by oxidative phosphorylation through the functioning of the electron transport chain (Garcia-Dorado *et al.*, 2014), which re-establishes the mitochondrial membrane potential. This is accompanied by a large burst of ROS (particularly superoxide) which continues for hours after the onset of reperfusion (Halliwell, Lai and Mccay, 1989). The generation of superoxide changes the inter- and intramitochondrial redox environment, which further drives ROS production, a process termed ROS-induced ROS release (Zorov, Juhaszova and Sollott, 2014).

Mitochondrial DNA is especially prone to ROS oxidation, due to its proximity to the electron transport chain (Bliksøen *et al.*, 2015). In addition, lipid peroxidation by ROS destabilizes sarcolemmal and mitochondrial membranes, which results in contractile dysfunction (Verma *et al.*, 2002), mitochondrial swelling (Martindale and Metzger, 2014), and further contributes to Ca^{2+} overload. ROS are also able to stimulate leukocyte activation and trigger the expression of adhesive molecules, which results in leukocyte-endothelial adherence and endothelial swelling (Toyokuni, 1999). This mechanism is partly responsible for microvascular obstruction and the “no-reflow” phenomenon.

Increased oxidative stress during reperfusion results in the uncoupling of nitric oxide synthase, which reduces the production of vascular nitric oxide (NO) and increases superoxide production (Silberman *et al.*, 2010). NO can also react with excess superoxide to form peroxynitrite, which can bind (and thereby damage) proteins, lipids, and DNA. Peroxynitrite formation usually results in the depletion of intracellular antioxidants, inhibition of enzymes including enzymes in the mitochondrial respiratory chain, and reduction of NO bioavailability. NO is a cardioprotective signalling molecule that has antioxidant effects, and its release by endothelial cells promotes vasodilation, inhibition of platelet activation and neutrophil accumulation, as well as modulating cardiac contractile function (Hare and Colucci, 1995; Xie and Wolin, 1996; Ferdinandy and Schulz, 2003).

1.2.2 Restoration of pH

During ischaemia, the cardiomyocyte cannot produce enough ATP by oxidative phosphorylation and switches to anaerobic glycolysis. Most of the ATP produced in glycolysis serves to maintain ion homeostasis. As mentioned previously, the end products of glycolysis, lactate and H^+ , as well as the intracellular accumulation of Na^+ and Ca^{2+} ions, all contribute to decreasing the intracellular pH to below 7. However, acidosis during ischaemia is to an extent cardioprotective (Lemasters *et al.*, 1996). During ischaemia, the increased levels of Ca^{2+} activates Ca^{2+} -dependent cysteine proteases, known as calpains, that degrade various proteins and contribute to the development of contractile dysfunction and cell death (Inserte, Hernando and Garcia-Dorado, 2012). However, acidosis during ischaemia inhibits these enzymes. In addition, acidosis decreases the sensitivity of the contractile proteins to Ca^{2+} (Orchard and Kentish, 2017) and acts directly on the cross bridges (Debold, Beck and Warshaw, 2008), inhibiting cardiomyocyte contractility and protecting the sarcolemma from contraction-induced damage (Jennings, 2013).

Much of the ATP that is generated during ischaemia is used by the F_1F_0 ATP synthase as it functions in reverse to maintain the mitochondrial membrane potential. With the membrane potential intact, the cytosolic accumulated Ca^{2+} can enter the mitochondria through a uniporter causing the opening of the mitochondrial transition permeability pore (mPTP; discussed later). However, the intracellular acidosis prevents this opening until restoration of pH that occurs upon reperfusion (Petronilli *et al.*, 1994; Murphy and Steenbergen, 2008; Halestrap, 2015).

When the myocardium undergoes reperfusion, extracellular H^+ is washed away and transport of intracellular lactate and H^+ is mediated out of the cell by the activation of the lactate/ H^+ symporter, the Na^+/H^+ exchanger and the sodium/bicarbonate (Na^+/HCO_3^-) symporter (Vandenberg, Metcalfe and Grace, 1993). This rapid efflux of H^+ and lactate results in the rapid restoration of physiological pH. This lifts the inhibition of calpains (Inserte, Hernando and Garcia-Dorado, 2012) which leads to plasma membrane rupture, as well as opening of the mPTP (Hausenloy and Yellon, 2003; Murphy and Steenbergen, 2008), which results in cell death. This phenomenon is termed the “pH paradox,” as acidosis appears to be transiently protective during ischaemia, but the rapid restoration of pH required for normal cellular function results in the generation of ROS and opening of the mPTP in the first few minutes of reperfusion, resulting in cell death.

1.2.3 Calcium

Intracellular Ca^{2+} overload begins in ischaemia secondary to the intracellular Na^+ overload and is mediated by the sarcolemmal L-type Ca^{2+} channels. Although reperfusion results in restoration of pH, in the initial stages of reperfusion the cardiomyocyte is still in a state of acidosis and Ca^{2+} and Na^+ overload (Murphy and Steenbergen, 2008). At the onset of reperfusion, there is a transient influx of Ca^{2+} from the extracellular space that exacerbates the intracellular Ca^{2+} overload (Kusuoka *et al.*, 1987; Valverde *et al.*, 2010).

Storage of Ca^{2+} in the myocyte occurs mainly in the sarcoplasmic reticulum, which along with T-tubules, synchronizes excitation-contraction coupling through Ca^{2+} uptake by the sarcoplasmic reticulum Ca^{2+} ATPase (SERCA) and release by ryanodine receptors (Orchard and Brette, 2008). During reperfusion, when intracellular Ca^{2+} is increased and ATPases can function, the sarcoplasmic reticulum's capacity for Ca^{2+} is exceeded and Ca^{2+} is repeatedly released and taken up, resulting in Ca^{2+} oscillations (Siegmund *et al.*, 1997). These oscillations result in myofibrillar

hypercontracture associated with reperfusion (Du Toit and Opie, 1994; Siegmund *et al.*, 1997), which unnecessarily utilizes ATP, and can also contribute to arrhythmias (Murphy and Steenbergen, 2008). Hypercontracture is also partly responsible for the clinical manifestation of myocardial stunning (Piper, García-Dorado and Ovize, 1998).

Much of the ATP that is generated during ischaemia is used by the F_1F_0 ATP synthase as it functions in reverse to maintain the mitochondrial membrane potential. This allows the mitochondria to take up Ca^{2+} through the Ca^{2+} uniporter and results in an increase in mitochondrial calcium during ischaemia (Griffiths *et al.*, 1998). During reperfusion when oxygen can be consumed to maintain the mitochondrial membrane potential, another rise in mitochondrial Ca^{2+} occurs (Griffiths *et al.*, 1998). The rise in mitochondrial Ca^{2+} has detrimental effects such as uncoupling oxidative phosphorylation and inducing mitochondrial swelling, and has been suggested to be a trigger for the opening of the mPTP (García-Rivas *et al.*, 2005).

1.2.4 Mitochondrial permeability transition pore (mPTP)

Permeability transition refers to the increasing permeability of the inner mitochondrial membrane for small solutes (<1.5 kDa) (Halestrap, 2009). It is well accepted that permeability transition is largely facilitated by the mPTP, a large conductive pore located on the inner mitochondrial membrane. Despite extensive research, the exact composition of the mPTP is not known, although it is suggested the pore is modulated by the binding of cyclophilin D in the matrix of the mitochondrion (Tanveer *et al.*, 1996) which in turn favours mPTP opening. It has also been suggested that pore formation occurs as a result of Ca^{2+} -dependent transformation of F_1F_0 ATP synthases, which form channels in the inner mitochondrial membrane (Giorgio *et al.*, 2017). Although little is known about the mPTP structure, the effects of mPTP opening and pharmacological inhibition thereof has been well-documented.

Prolonged opening of the pore is linked to mitochondrial dysfunction, as it results in mitochondrial membrane depolarization resulting in the uncoupling of oxidative phosphorylation and cessation of ATP synthesis (Hausenloy *et al.*, 2004; Heusch, Boengler and Schulz, 2010; Bernardi and Di Lisa, 2015). The pore also facilitates the release of mitochondrial Ca^{2+} , and the increased colloidal osmotic pressure results in swelling of the matrix compartment (Halestrap *et al.*, 1998; Bernardi, 2017). Eventually the outer mitochondrial membrane will rupture, resulting in the release of cytochrome c and pro-apoptotic proteins (Halestrap, 2009).

Many of the components of reperfusion injury such as restoration of pH, ROS and oxidative stress, as well as Ca²⁺ overload, appear to converge on the mitochondria by acting as stimuli for the opening of the mPTP (Griffiths and Halestrap, 2015). Transient opening of the pore is essential for cardioprotection (Hausenloy *et al.*, 2004), as it reduces matrix calcium load and induces ROS release (Zorov, Juhaszova and Sollott, 2014) which may have a role in signalling. However, permanent opening of the pore serves as an end-effector of lethal reperfusion injury culminating in cell death. It therefore presents a very promising target for therapeutic intervention to reduce reperfusion injury.

1.2.5 Inflammation

Ischaemia severely compromises the sarcolemma of affected cells, and the rupture of the sarcolemma is associated with necrosis (Jennings *et al.*, 1960; Reimer and Jennings, 1979; Jennings, Reimer and Steenbergen, 1986), dispersing the cellular contents into the extracellular space. These molecules are termed damage-associated molecular patterns (DAMPs), as they act as endogenous signals that bind to pattern-recognition receptors (such as toll-like receptors), thereby activating the immune system and producing a potent inflammatory response (Chen and Nuñez, 2010; Vénéreau, Ceriotti and Bianchi, 2015; Roh and Sohn, 2018). During ischaemia, neutrophils from the border of the infarct slowly infiltrate the ischaemic area (Reimer, Murry and Richard, 1989). Without reperfusion, neutrophils are restricted to the border zone and very few neutrophils successfully migrate to the centre of the infarct (Vinten-Johansen, 2004). Within the first few hours of reperfusion, neutrophil accumulation and infiltration is accelerated, peaking at 24 hours (Vinten-Johansen, 2004) and persisting for days.

Myocardial infarct healing and post-infarct remodelling are dependent on neutrophils and other inflammatory processes for the removal of necrotic cells and debris, angiogenesis, and reconstruction of the extracellular matrix (Polverini, 2011; Frangogiannis, 2012; Fujii, Wang and Nagai, 2014; Ramos *et al.*, 2018). However, neutrophils generate large quantities of ROS and release proteases, both which theoretically could exacerbate vascular and myocardial tissue damage (Reimer, Murry and Richard, 1989). It is not yet clear whether inflammation contributes to lethal reperfusion injury, as all forms of reperfusion injury can be observed in a neutrophil-free environment, and thus are independent of neutrophil action (Baxter, 2002). Additionally, increasing evidence suggests that neutrophils regulate reparative processes within the myocardium (Puhl and Steffens, 2019).

I/R injury is a multifaceted consequence to the rapid changes in the intracellular environment brought on by reperfusion. Yet, reperfusion is essential for survival of the myocardium. One of the most important aspects of treating AMI is to minimize the total ischaemic time by reducing the time between the onset of symptoms and treatment, as increased ischaemic time is associated with greater myocardial tissue damage (Reimer and Jennings, 1979; Khalid, Jneid and Denktas, 2017). Since the original description of ischaemic preconditioning, the improved and standardized treatment of coronary syndromes has reduced overall morbidity and mortality associated with cardiovascular disease. Despite this, ischaemic heart disease still remains the leading cause of death and long-term morbidity, globally (Shah *et al.*, 2018). Thus, cardioprotective strategies to minimize reperfusion injury is potentially the ideal treatment for MI, but the translation of these interventions into clinical practice is the next frontier for scientists and clinicians.

1.3 CARDIOPROTECTION

Interventions to reduce I/R injury have been studied in the laboratory setting for the past three decades. In 1986, Murry and co-workers (Murry, Jennings and Reimer, 1986) showed that brief episodes of ischaemia and reperfusion administered before a major ischaemic insult resulted in a 25% reduction in infarct size. This was termed ischaemic preconditioning (IPC) and its discovery revealed that the heart has the innate ability to protect itself against ischaemic damage. In 1993, researchers showed that brief episodes of I/R in one vascular bed protected remote, virgin myocardium from subsequent ischaemia, a phenomenon termed remote ischaemic conditioning (Przyklenk *et al.*, 1993). Three years later, Gho and co-workers reported that ischaemic preconditioning in other organs and tissues, such as limb skeletal muscle, could also confer protection on the heart during ischaemia (Gho *et al.*, 1996). In 2003, researchers reported that very brief episodes of I/R after a major ischaemic insult, at the onset of reperfusion (Zhao *et al.*, 2003), conferred a significant degree of cardioprotection (although less than that of IPC). The application of this intervention, called ischaemic postconditioning, within reperfusion following ischaemia makes it particularly attractive in terms of clinical application.

Both pre- and postconditioning reduce I/R injury by activating intracellular signalling pathways (Yellon and Opie, 2006) and interestingly, both manoeuvres share the same mechanisms. During ischaemia, molecules such as adenosine (Liu *et al.*, 1991), catecholamines (Schomig, 1990), opioids (Schultz *et al.*, 2017), and bradykinin (Noda *et al.*, 1993) are released by

cardiomyocytes and endothelial cells in response to a decrease in the oxygen supply/demand ratio, followed by reperfusion. These molecules bind to their respective receptors and activate different downstream signalling pathways.

The most extensively studied signalling pathway in IPC is phosphatidylinositol 3-kinase (PI3K) and its downstream target- Akt/ protein kinase B (PKB) (Solenkova *et al.*, 2005). Signalling through PI3K-Akt stimulates the production of NO through the phosphorylation (and consequent activation) of endothelial nitric oxide synthase (eNOS). NO then stimulates guanylyl cyclase, increasing the levels of cyclic guanosine monophosphate (cGMP) which in turn, activates protein kinase G (PKG) (Cohen *et al.*, 2001; Physiol *et al.*, 2013). PKG phosphorylates the mitochondrial ATP-dependent K⁺ channels, opening them and mediating a burst of ROS, which activates other downstream mediators of IPC such as protein kinase C (PKC) and extracellular signal-regulated kinase p42/p44 (ERK1/2). Together the PI3K/Akt/ERK signalling pathways are termed the “reperfusion injury salvage kinases” or RISK pathway (Hausenloy and Yellon, 2004). The RISK pathway appears to converge on glycogen synthase kinase 3 β (GSK-3 β) and its inactivation by phosphorylation which consequently prevents mPTP opening (Juhászova *et al.*, 2004).

Another pathway which has been implicated in cardioprotection is the survival activating factor enhancement (SAFE) pathway that is activated by tumour necrosis factor alpha (TNF- α) and results in the activation of transcription factor signal transducer and activator of transcription-3 (STAT-3) (Lacerda *et al.*, 2009). Both RISK and SAFE complexes appear to terminate on the mitochondria, specifically by preventing the opening of the mPTP.

Although pre- and postconditioning elicit the most potent cardioprotection, they require several episodes of ischaemia and reperfusion and in a clinical setting, requires manipulation of the atherosclerotic lesion, which could result in microembolization (Heusch, 2013). Alternatively, cardioprotection can be elicited by pharmacologically activating key mediators of the RISK or SAFE signalling complexes, initiating the protective downstream effects of these pathways. In addition, many proteins that do not form part of the RISK or SAFE pathway can also be targeted to promote cell survival although these are not covered in this review. Numerous proteins such as PKC, Akt/PKB, ERK 1/2, GSK3- β , apoptotic proteins (BAD, BAX, BIM, p53 and caspases), and various proteins regulating the mPTP, are regulated by phosphorylation, which is a dynamic process mediated by kinases and phosphatases.

1.4 PROTEIN PHOSPHORYLATION

Protein phosphorylation is an important regulatory mechanism of protein function in response to extracellular stimuli. Although molecules such as lipids and sugars can also be modified by phosphorylation, this review will focus primarily on proteins, as they mediate most intracellular signalling, particularly in the context of ischaemia, reperfusion, and cardioprotection. During protein phosphorylation, a phosphate group is covalently bound to a target protein. This changes the substrate specificity, subcellular location, or reactivity of the target protein, allowing it to execute a function that the unphosphorylated molecule could not (Beltrao *et al.*, 2013).

Of the 21,000 proteins encoded by the human genome, more than 60% of these proteins are confirmed to be phosphorylated. Kinexus PhosphoNET reports over 200,000 known human phosphorylation sites, of which over 177,000 have been experimentally confirmed, and predicts another 760,000 additional sites that are likely to be phosphorylated (Kinexus Bioinformatics Corporation, 2017). In addition, it lists the average number of phosphorylation sites per protein as 42.6. Therefore, each protein has multiple phosphorylation sites that are used to regulate its function. Proteins can be phosphorylated on amino acid residues serine, threonine, and tyrosine. 86.4% of phosphorylation takes place on serine residues, while 11.8% and 1.8% of phosphorylation occurs on threonine and tyrosine residues, respectively (Olsen *et al.*, 2006). Phosphorylation is mediated by a class of enzymes known as the kinases that are classified according to their amino acid residue targets. Serine/threonine kinases mediate phosphorylation on serine and threonine residues, tyrosine kinases mediate phosphorylation on tyrosine residues, and dual-specificity kinases can act on all three residues.

Phosphorylation can also be reversed by removal of the phosphate group. This process, termed dephosphorylation, is governed by a class of enzymes known as the phosphatases. Like the kinases, they are also named after the residues they act on, serine/threonine phosphatases (PSPs), tyrosine phosphatases (PTPs), and dual-specificity phosphatases (DSPs) that act on all three residues. Once a protein is dephosphorylated, it regains its original function and cellular localization prior to phosphorylation. The action of phosphatases complements the activity of the kinases and together, they act as a molecular switch that controls protein function. The phosphorylation state of a given protein, and by extension its functionality, is therefore strictly regulated by the balance between kinase and phosphatase activity.

There are 518 kinases (Manning *et al.*, 2002) and 137 phosphatases encoded within the human genome. Although the number of kinase genes are disproportionately higher than that of their

phosphatase counterparts, phosphatases compensate for fewer genes with higher protein abundance (Smoly *et al.*, 2017) and a large variety of subunits. Phosphatases may exist as monomers or multimeric complexes made up of various subunits. In addition, each subunit may have multiple isoforms that can complex with other subunits in many combinations to form different variants of the same enzyme. These variants have different substrate specificities and cellular locations (Seshacharyulu *et al.*, 2013), allowing the same phosphatase to act on a broad range of protein targets. Normal phosphatase activity is critical to maintain proper protein function.

Phosphorylation can affect a protein's function in almost every conceivable way. The addition or removal of a negatively charged phosphate group promotes a conformational change in the target protein and changes its stability, as well as kinetic and dynamic properties (Farrar *et al.*, 1990), such as its affinity for substrates or its enzyme activity. Phosphorylation can act as a molecular switch that either activates or deactivates a protein, such as glycogen phosphorylase b, which is converted to the active glycogen phosphorylase a upon phosphorylation (Krebs and Fischer, 2003), or glycogen synthase, which is inactivated by phosphorylation (Soderling *et al.*, 1979). Phosphorylation may also change a protein's cellular localization. As an example, p38 mitogen-activated protein kinase (MAPK) is imported into the nucleus once it is phosphorylated and requires dephosphorylation to be exported from the nucleus (Gong *et al.*, 2010). Additionally, phosphorylation promotes protein-protein interactions, which may be necessary for biological effect. An example of this is the association of phospholamban with SERCA, which inhibits Ca^{2+} uptake by the sarcoplasmic reticulum. When phospholamban is phosphorylated by protein kinase A (PKA), it can no longer associate with SERCA which in turn results in an increase in Ca^{2+} uptake (Hagemann and Xiao, 2002). As a last example, phosphorylation can mark a protein for destruction. This is illustrated by the phosphorylation of p53 which frees it from a ubiquitination ligase and results in its ubiquitination and subsequent proteosomal degradation (Lavin and Gueven, 2006; Rider *et al.*, 2009).

1.4.1 Protein phosphorylation in biological processes

Phosphorylation is required for normal biological function and is a key regulatory mechanism in many biological processes. Reversible phosphorylation is most evident in the production and recycling of ATP, as it requires the transfer of phosphate groups, and is vital in processes such as DNA replication (Boulikas, 1994), cell proliferation (Minella *et al.*, 2008), and cell death (Niemi and

Mackeigan, 2012; Dondelinger, Vandenabeele and Bertrand, 2016). It is therefore not surprising that abnormal kinase or phosphatase activity can result in various diseases (Cohen, 2001). In fact, altered phosphorylation is one of the hallmarks of cardiovascular diseases (Luo and Anderson, 2013).

As stated previously, protein phosphorylation represents a major mediator of signalling during ischaemia and reperfusion and may be manipulated (through conditioning or pharmacological agents) to protect the myocardium. Much research has focused on the kinases that mediate protection (such as the mediators of RISK) as they activate various signalling pathways. However, these signalling pathways are also regulated by phosphatases, an aspect of signalling in cardioprotection that has historically been overlooked.

1.5 PHOSPHATASES IN CARDIOPROTECTION

Phosphatases were traditionally viewed as passive housekeeping enzymes that maintain a ubiquitous degree of dephosphorylation within the cell, “deactivating” signals after dynamic kinase action. However, research into phosphatases demonstrated that they are much more dynamic than initially proposed and do not always serve to deactivate proteins. Historically, research on phosphatases, even basic expression in normal physiology, has been limited, possibly due to the limited methodology available for measuring phosphatase activity. As such, little information of the participation of protein phosphatases in I/R exist, but what is known is briefly summarized below.

1.5.1 PH domain leucine-rich repeat protein phosphatase

PH domain leucine-rich repeat protein phosphatase (PHLPP) is related to protein phosphatase 2C (PP2C) and has two specific isoforms, PHLPP-1 and PHLPP-2 (Gao, Furnari and Newton, 2005; Brognard *et al.*, 2007). These isoforms dephosphorylate the same Ser473 residue on Akt/PKB, but on different Akt/PKB isoforms (Gao, Furnari and Newton, 2005; Brognard *et al.*, 2007). Hypoxia downregulates both PHLPP1 and PHLPP2 expression (Wen *et al.*, 2013). In reperfusion following ischaemia, downregulation of PHLPP1 enhances Akt-mediated protection (Miyamoto, Murphy and Brown, 2008).

A recent study by Xing and colleagues identified PHLPP-1 as a negative regulator of insulin signalling, and that insulin, in turn, regulates PHLPP-1 by indirectly mediating its degradation by

ubiquitin (2016). The same study showed that PHLPP-1 expression increases with age, and that insulin administration decreased PHLPP1 expression in young rat hearts, but not in aged animals. PHLPP-1 deletion reduces infarct size by 45% in mouse hearts (Miyamoto *et al.*, 2010), and PHLPP-1 downregulation following insulin administration is cardioprotective in young animals (Xing *et al.*, 2016). Conversely, upregulated expression of PHLPP-1 promotes apoptosis and exacerbates I/R injury (Xing *et al.*, 2016).

1.5.2 Phosphatase and tensin homologue deleted on chromosome 10

Phosphatase and tensin homologue deleted on chromosome 10 (PTEN) is a tumour suppressor (Li *et al.*, 1997) that negatively regulates the PI3K/Akt pathway (Hlobilková *et al.*, 2003). Phosphorylation of PTEN and Akt/PKB increases after brain ischaemia (Choi *et al.*, 2005). The phosphorylation, and subsequent inactivation, of PTEN may be an endogenous protective mechanism to prevent tissue damage, as its activity inhibits anti-apoptotic signals (Choi *et al.*, 2005). Cardiac-specific knockout of PTEN increased recovery of left ventricular developed pressure and reduced myocardial infarct size following 30 minutes global ischaemia (Ruan *et al.*, 2009).

Downregulation of PTEN can also improve PI3k/Akt signalling that is impaired in pathological conditions such as diabetes (Wijesekara *et al.*, 2005; Jiang, 2007). For example, knockout of PTEN protected mice from high fat diet-induced insulin resistance and diabetes and improved insulin sensitivity (Wijesekara *et al.*, 2005).

1.5.3 Protein Phosphatase 2C (PP2C) in mitochondria

Lu and co-workers identified a novel phosphatase located exclusively in the mitochondrial matrix. This phosphatase contained a serine/threonine domain common to the PP2C family and a mitochondrial targeting sequence and was thus named protein phosphatase 2C in mitochondria (PP2Cm, Lu *et al.*, 2007). PP2Cm is highly expressed in tissue with a high metabolic activity, such as the brain and heart, and loss of its expression is associated with the progression of pathological remodelling in the heart (Lu *et al.*, 2007). Mitochondrial assays indicate that PP2Cm inactivation does not affect oxygen consumption, mitochondrial matrix volumes after repeated ADP challenges, or the recovery of mitochondrial membrane potential, indicating that it does not affect mitochondrial respiration (Lu and Wang, 2008). However, PP2Cm is important in

maintaining the mPTP in a closed conformation and the loss of PP2Cm facilitates the opening of the mPTP in response to calcium overload (Lu *et al.*, 2007). PP2Cm is therefore essential for cell survival and normal development.

PP2Cm is also a regulator of branched chain amino acid (BCAA) metabolism (Lu *et al.*, 2009). BCAAs directly inhibit glycolytic enzymes and promote fatty acid oxidation, rendering BCAA catabolism critical for efficient glucose metabolism. PP2Cm deletion results in an increase in circulating and tissue BCAAs, including the heart, and increases the heart's vulnerability to ischaemic insult (Li *et al.*, 2017). Since PP2Cm has important roles in BCAA catabolism and stabilizing the mPTP, loss of function or inhibition may exacerbate I/R injury.

1.5.4 MAPK Phosphatase

MAPK phosphatases (MKPs) are dual-specificity phosphatases that dephosphorylate and inactivate MAPKs. *Ex vivo* rodent heart perfusions show that activation of MKP-1 by administration of dexamethasone either intraperitoneally or directly to the circulating perfusate, either before ischaemia or at the onset of reperfusion, reduced infarct size and increased functional recovery (Fan *et al.*, 2009). These effects were associated with increased expression of MKP-1 and a reduction in p38 MAPK activity, indicated by decreased p38 MAPK phosphorylation. Overexpression of MKP-1 in mice resulted in protection from I/R injury associated with the inhibition of p38 MAPK phosphorylation and upregulation of Bcl-2 (Kaiser *et al.*, 2004). Thus, MKPs illustrate that phosphatase activity is not always associated with detrimental effects.

1.5.5 Protein tyrosine phosphatases (PTPs)

Inhibition of PTPs by vanadium compounds has been shown to protect the heart from I/R injury (Takada, 2004). PTP inhibition resulted in an increased phosphorylation of Akt/PKB, glycogen synthase kinase-3 β and Bad, and inhibited caspase-3 activation induced by ischaemia (Takada, 2004). Studies with bis(maltolato)oxovanadium administered just before the onset of reperfusion indicate that the compound reduces infarct size in a concentration-dependent manner and this reduction in infarct size is comparable to that induced by pre-ischaemic drug administration (Liem, 2004). The cardioprotection conferred by bis(maltolato)oxovanadium was abolished with the administration of a tyrosine kinase inhibitor as well as a K⁺ATPase inhibitor, indicating that during reperfusion PTPs play a role in regulating cardiac K⁺ ion channels (Liem, 2004).

1.5.6 Protein Phosphatase 2B (PP2B)

Much of the involvement of protein phosphatase 2B (PP2B, also known as calcineurin) in I/R injury has been studied in cerebral ischaemia, although a few studies documenting PP2B involvement in myocardial I/R injury do exist. Weinbrenner and colleagues showed that inhibition of PP2B by either cyclosporine A or FK-506 administered during early ischaemia protected the heart from ischaemic damage (1998). Cyclosporine A has been shown to mediate cardioprotection through inhibition of the opening of the mPTP, and it may be the likely mechanism of cardioprotection, rather than PP2B inhibition. However, studies of PP2B in the brain using PP2B specific inhibitors indicate that PP2B inhibition reduces neuronal cell death following cerebral ischaemia (Drake *et al.*, 1996; Bochelen, Rudin and Sauter, 1999).

1.5.7 Protein phosphatase 1 (PP1) and protein phosphatase 2A (PP2A)

Protein phosphatase 1 (PP1) and protein phosphatase 2A (PP2A), along with PP2B are the major serine/threonine phosphatases in myocardial tissue. Due to the lack of specific inhibitors for PP1, its inhibition is often studied in conjunction with PP2A inhibition (as PP2A is inhibited by several non-specific inhibitors at concentrations much lower than that required for PP1 inhibition). Administration of calyculin A at concentrations that inhibit both phosphatases 75 minutes after simulated ischaemia protected isolated rabbit cardiomyocytes against ischaemic damage in a concentration-dependent manner (Armstrong *et al.*, 1998). The inhibition of PP1 and PP2A mimics IPC, but these phosphatases are not inhibited by IPC, indicating that they do not play a direct role in mediating IPC (Weinbrenner, Baines, *et al.*, 1998).

A study by Fenton and colleagues showed that IPC is less effective in aged myocardium and 55% of aged animals could not be protected by IPC (2005). Administration of a PP2A inhibitor, okadaic acid (OA), at the onset of reperfusion increased the percentage of viable tissue in the young animals. PP2A activity was increased after ischaemia in both the young and old animals, but the increase in PP2A activity was more pronounced in the aged animals (Fenton, Dickson and Dobson, 2005).

Van Vuuren showed that at 10 minutes global ischaemia, methylated PP2A accumulates in the nucleus and progressively translocated to the cytosol (2014). OA administered at a PP2A-specific dose prior to ischaemia resulted in an increase in the phosphorylation of Akt/PKB, ERK 1/2 and glycogen synthase kinase 3 β (GSK-3 β) and reduced infarct size, while the administration of a PP2A

activator, FTY720, decreased the phosphorylation of GSK-3 β , p38 MAPK and Akt/PKB and increased infarct size when compared to control (Van Vuuren, 2014). Taken together, this indicates that PP2A activation during ischaemia favours cell death, although not all studies with PP2A inhibitors reported a significant reduction in infarct size (Fan *et al.*, 2010). Inhibition of PP1 and PP2A appears to be beneficial during ischaemia and reperfusion, but it is unclear how much protection is attributed to PP1 alone.

From this, one might assume that inhibition of PP2A will favour cell survival. However, increased PP2A activity is not always associated with adverse outcomes and decreased PP2A activity is not always associated with better outcomes. A recent study utilizing a rat model of chronic kidney disease demonstrated that this condition increases myocardial infarct size during ischaemia and reperfusion by downregulating myocardial B55 α , an important regulatory subunit of PP2A (Tobisawa *et al.*, 2017). Based on other findings of PP2A in myocardial ischaemia/reperfusion injury, one might expect that a decrease in PP2A expression in the heart will favour cell survival during infarction, but this is contrary to what was observed by Tobisawa and co-workers. They reported that downregulation of PP2A-B55 α resulted in an increase in infarct size due to insufficient Akt/PKB activation. The primary phosphorylation site responsible for Akt/PKB activation, Ser473, has been reported to be phosphorylated under conditions of PP2A inhibition. However, Tobisawa and colleagues demonstrated that another residue on Akt/PKB, Thr308, needs to be dephosphorylated for proper phosphorylation of Ser473 (2017). As PP2A is responsible for this dephosphorylation, downregulation of PP2A-B55 α resulted in poor activation of Akt/PKB and increased infarct size. Thus, it is not the mere activity of PP2A that contributes to cell death, but rather its action on specific targets that determine cellular outcomes.

To summarize, phosphatase inhibition would appear to favour cell survival by enhancing phosphorylation of kinases such as PKB/Akt and preventing apoptosis, but not all phosphatase inhibition is associated with cell survival (such as MKPs and PP2Cm). As stated above, the action of various phosphatases on specific targets determine cellular outcomes, rather than phosphatase activity in general. The identities of many phosphatase substrates are not yet known, and it is critical to identify these targets to better understand the role of phosphatases in pathologies such as ischaemia and reperfusion. To address this, the remainder of this review will focus on PP2A, a phosphatase responsible for the majority of dephosphorylation events in the myocardium.

1.6 PROTEIN PHOSPHATASE 2A

PP2A is a serine/threonine phosphatase that, along with PP1 and PP2B, catalyses approximately 90% of all dephosphorylation events that occur in cardiac tissue (Cohen, 2002). PP2A is a complex holoenzyme composed of three subunits: the structural/scaffolding subunit (PP2A-A), regulatory subunit (PP2A-B), and catalytic subunit (PP2A-C) (DeGrande *et al.*, 2013). Both A and C subunits have two isoforms and the B subunit has four families of isoforms. The binding of the different isoforms, along with proteins that interact with the holoenzyme, results in a multitude of potential holoenzyme combinations. The various holoenzymes reflect the diverse temporal, spatial, and substrate specificity characteristics of PP2A. The isoforms of each subunit are briefly discussed below.

1.6.1 PP2A-C

The 36-38 kDa C subunit (PP2A-C) is responsible for PP2A enzymatic activity. PP2A-C exists in two isoforms, α and β , both of which are ubiquitously expressed (Janssens and Goris, 2001) and are also present in the human heart (Lüss *et al.*, 2000). Although both isoforms consist of 309 amino acids and share 97% sequence similarity (Hemmings *et al.*, 1990), they are not equally expressed in tissue nor do they possess a redundant function. PP2A-C α knockout in mice is embryonically lethal at day 6.5 demonstrating a critical role for this isoform as well as the inability of PP2A-C β to compensate for PP2A-C α loss of function (Götz *et al.*, 1998). Isoform α is expressed predominantly in the plasma membrane while isoform β is expressed in the cytoplasm and nucleus (Khew-Goodall and Hemmings, 1988). In addition, PP2A-C α is more abundantly expressed in tissue than PP2A-C β due to its strong gene promotor activity and rate of mRNA turnover (Khew-Goodall and Hemmings, 1988; Seshacharyulu *et al.*, 2013).

1.6.2 PP2A-A

The structural, or scaffolding subunit (PP2A-A; also known as PR65) is a 65 kDa protein composed of 15 tandem repeats of a 39 amino acid sequence known as the HEAT (huntingtin - elongation - A subunit – TOR) motif. The scaffold is an elongated, horseshoe-shaped structure that facilitates the binding of PP2A-C, as well as other proteins, to itself (Cho and Xu, 2007). Together with PP2A-C, PP2A-A forms a dimer known as the core dimer (AC dimer, or core enzyme). PP2A-A not only

functions as a scaffold in this context, but also improves substrate peptide binding thereby influencing substrate specificity (Price and Mumby, 2000).

Like PP2A-C, PP2A-A also has two distinct isoforms, α and β , that are both found in the cytoplasm (Zhou *et al.*, 2003). Although they share 86% sequence similarity and are ubiquitously expressed (Hemmings *et al.*, 1990) the A α isoform is expressed in approximately 90% of PP2A assemblies and accounts for 0.1% of total cell protein (Seshacharyulu *et al.*, 2013). A α also displays a stronger binding affinity for B and C subunits than A β (Zhou *et al.*, 2003).

On its own, the core dimer functions within the cellular environment and accounts for one-third of the total PP2A in the cell (Kremmer *et al.*, 1997). Research suggests that PP2A-A may also play a role in substrate interaction, possibly through a conformation change in PP2A-C upon binding, or by directly interacting with the substrate (Price and Mumby, 2000). Therefore, the core dimer has a substrate specificity that is different from the holoenzyme and likewise, responds differently to inhibitors and stimulators (Kamibayashi *et al.*, 1994; Price and Mumby, 2000). The core dimer may also serve as reservoir of enzyme that upon stimulus, can readily bind to different B subunits (Kremmer *et al.*, 1997).

1.6.3 PP2A-B

There are four families of regulatory subunits: B (PR55/B55), B' (PR61/B56), B'' (PR72) and B''' (striatin) (the numbers represent the approximate molecular weight of the relevant subunit in kDa). 15 genes produce more than 26 different splice variants and despite binding to similar sequences on PP2A-A, the families of subunits have no genetic sequence similarity themselves (Zolnierowicz *et al.*, 1994). Each of these families have multiple isoforms: B $\alpha - \delta$, B' $\alpha - \epsilon$, and B'' $\alpha - \gamma$; which yields approximately 15 different regulatory subunits able to bind to the core dimer. As PP2A-A and PP2A-C each have two isoforms, the combination of the different isoforms within the A, B, and C subunits produce a minimum of 75 enzymatically active subpopulations of the PP2A holoenzyme (Janssens and Goris, 2001). Since the A and C subunits are expressed uniformly and the B subunits are differentially expressed in tissue-specific and even subcellular-specific manners, the B subunits mediate the cellular localization and specificity of PP2A (Janssens and Goris, 2001). Figure 1.1 shows the holoenzyme structure.

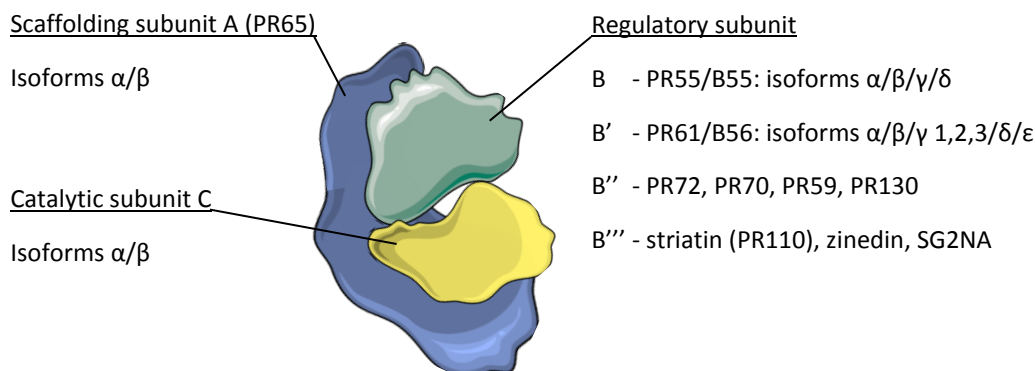


Figure 1.1 - PP2A holoenzyme structure

The scaffolding (A), regulatory (B), and catalytic (C) subunits, with alternative names and isoforms, that make up the PP2A holoenzyme.

Image created with smart.servier.com

1.6.3.1 B family (PR55/B55)

The 55 kDa subunit has four isoforms (α , β , γ , δ) that are expressed in a tissue-specific manner (Mayer *et al.*, 1991; Zolnierowicz *et al.*, 1994). These isoforms are differentially expressed in tissues and even in different regions within a tissue or in specific areas within the cell. For example, studies in rodents indicate that B55 β and γ are almost exclusively expressed in the brain, but B55 β expression is low in the cerebellum whilst B55 γ expression is high in the hindbrain (Strack *et al.*, 1998). In terms of intracellular distribution, B55 α and B55 β are located in the cytosol and B55 γ is located in the cytoskeletal fraction (Strack *et al.*, 1998; Janssens and Goris, 2001). Recent studies have also confirmed the presence of both B55 α and B55 β in the human heart (DeGrande *et al.*, 2013). In addition, expression of B family isoforms may also vary during developmental stages (Strack *et al.*, 1998).

B55 has been shown to be essential for cytoskeletal dynamics, nuclear translocation (Turowski *et al.*, 2013), and cell division, as it regulates entry into and exit from mitosis (Mochida *et al.*, 2009; Schmitz *et al.*, 2010; Hégarat *et al.*, 2014; Cundell *et al.*, 2016). A PP2A-B55 trimer is also responsible for breakdown of spindles during mitosis and reassembly of the nuclear envelope, decondensed chromatin, and the Golgi apparatus (Schmitz *et al.*, 2010). A recent study of the PP2A-B55 interactome identified several proteins that were previously not known to bind to B55 (Wang *et al.*, 2018). These proteins are involved in processes such as cell division, cytoskeletal components, DNA replication and repair, Golgi dynamics, mitochondrial function, and intracellular signalling (Wang *et al.*, 2018).

1.6.3.2 B' family (PR61/B56)

The B56 subunit is the predominant regulatory subunit in cardiac PP2A (Tehrani, Mumby and Kamibayashi, 1996). It has five different isoforms (α , β , γ , δ , and ϵ) that have different subcellular localizations, and all five isoforms have been identified in the human heart (DeGrande *et al.*, 2013). α , β , δ , and ϵ isoforms are expressed in the cytoplasm. Additionally, δ is also expressed in the nucleus, along with γ 1 and γ 3 (McCright *et al.*, 1996; Tehrani, Mumby and Kamibayashi, 1996; Ito *et al.*, 2000).

B56 subunits appear to have an important role in regulating cytoskeletal structure. B56 α binds to ankyrin-B, an adapter protein required for normal subcellular localization of the Na⁺/Ca²⁺ exchanger, Na⁺/K⁺ ATPase, and inositol 1,4,5-trisphosphate receptor (Bhasin *et al.*, 2007). B56 γ 1 interacts with paxillin, another adapter protein expressed at focal adhesions. It therefore targets PP2A to focal adhesions, where it regulates cell motility through cytoskeletal organization (Ito *et al.*, 2000). B56 α and β are involved in the dephosphorylation of the microtubule-associated protein tau and abnormal PP2A activity may be implicated in the progression of Alzheimer's disease (Sontag *et al.*, 1999). In addition, increased expression of the α , β , and ϵ isoforms are associated with both ischaemic and non-ischaemic heart failure (DeGrande *et al.*, 2013).

A characteristic unique to the B' isoforms (except B56 γ) is that they can be regulated by phosphorylation. PP2A activity can be increased upon the phosphorylation of B' δ on Ser566 by PKA (Ahn *et al.*, 2007). PP2A activity can also be inhibited by PKC-dependent phosphorylation of B56 α on serine residue 41 (Kirchhefer *et al.*, 2014).

1.6.3.3 B'' family (PR72)

The B'' family has five members, PR130, PR72, PR70, PR59 and G5PR. PR72 and PR130 appear to be splice variants of the same gene (Hendrix *et al.*, 1993) and both are expressed in the human heart (DeGrande *et al.*, 2013). Both isoforms have an identical C-terminus, but PR130 has a 665 amino acid sequence in its N-terminal region that is replaced with a 44 amino acid sequence present in PR72. This difference accounts for the tissue-specific distribution of these isoforms; PR130 has a ubiquitous distribution in tissues, while PR72 is exclusively expressed in heart and skeletal muscle (Hendrix *et al.*, 1993).

PR72 contains two Ca^{2+} binding sites formed by small helix–loop–helix motifs, known as EF-hands (Janssens *et al.*, 2003) that are also present in other calcium sensor proteins such as calmodulin, troponin C, and S100. These EF-hands bind calcium with differing affinities. The integrity of EF2 is required for the subunit to bind with the scaffold subunit and target PR72 to the nucleus, while the integrity of EF1 is required for PP2A-PR72 to alter the cell cycle (Janssens *et al.*, 2003). After Ca^{2+} binds to the loop, it changes the conformation of the EF-hands and exposes a hydrophobic protein-binding surface that allows the B'' subunits to bind to and regulate secondary proteins (Zhang, Tanaka and Ikura, 1995). The function of skeletal and cardiac muscle is largely dependent on Ca^{2+} and since PR72 is exclusively expressed in these tissues, its sensitivity to Ca^{2+} may mediate a link between Ca^{2+} signalling and phosphorylation.

G5PR is the newest proposed member of the B'' subunit family (Kono *et al.*, 2002). G5PR was identified as a germinal center-associated nuclear protein (GANP)-associated molecule by yeast two-hybrid screening (Abe *et al.*, 2000; Janssens *et al.*, 2003). Like PR130 and PR72, it also contains EF-hands. It is able to associate with both protein phosphatase 5 (PP5) and the PP2A core dimer, and studies in knockout mice suggest that G5PR is necessary to inhibit activation induced cell death in B cells (Xing *et al.*, 2005).

Little is known about PR59 and PR70, especially in the context of the heart. PR59 is a mouse-specific subunit with no human orthologue that has been identified yet. It interacts with retinoblastoma-like p107 protein and when overexpressed, results in G1/S arrest of cell cycle progression (Voorhoeve, Hijmans and Bernards, 1999). PR70 also has an EF-motif that is dependent on Ca^{2+} levels to regulate its binding to the core dimer and subsequent activity (Eichhorn, Creighton and Bernards, 2009). It binds to tumour suppressor retinoblastoma protein and facilitates its dephosphorylation (Magenta *et al.*, 2008).

1.6.3.4 B''' family

The B''' family is made up of striatin (PR110), S/G₂ nuclear autoantigen (SG2NA), and zinedin. Striatin and SG2NA are related proteins that both contain WD40 repeats (short, structural motifs that often end in a tryptophan-aspartic acid dipeptide) and form stable complexes with the PP2A core dimer (Moreno *et al.*, 2000). All three proteins bind to calmodulin in a Ca^{2+} -dependent manner (Castets *et al.*, 2000; Moreno *et al.*, 2000). Although the B''' family is ubiquitously expressed, they are highly expressed in the central and peripheral nervous systems (Hwang and Pallas, 2014).

Striatin is expressed in cardiomyocytes and is more abundant in the atria than in the ventricles (Nader *et al.*, 2017). Striatin regulates contraction, as overexpression of striatin results in an increase in the rate of spontaneous contraction of cultured cardiomyocytes, and knockdown of striatin reduced rate of contraction (Nader *et al.*, 2017). Heterozygous deletion of striatin in mice resulted in elevated heart rate, reduced ejection fraction, and reduced systolic function (Frangogiannis, 2012; Rostron *et al.*, 2017), as well as enhanced vasoconstriction and decreased vascular relaxation (Garza *et al.*, 2015). Striatin has also been associated with salt sensitivity hypertension, and may regulate vascular function through modulation of endothelial NO-cGMP (Garza *et al.*, 2015).

Striatin can form large signalling complexes with phosphatases and kinases known as striatin-interacting phosphatase and kinase (STRIPAK) complexes, all containing the PP2A core dimer (Moreno *et al.*, 2000). STRIPAK complexes regulate many biological processes, mediate signalling pathways, and have also been linked to various diseases. As the biological roles of STRIPAK complexes is beyond the scope of this review, the reader is directed to a comprehensive review on the subject by Hwang and Pallas (2014).

1.7 REGULATION OF PP2A

PP2A can be regulated by post-translational modification, autoregulation, subunit diversity (as discussed above), and protein interaction. PP2A-C contains a unique motif, Thr304-Pro-Asp-Tyr-Phe-Leu309, in the C-terminal tail that is located at the interface between the other subunits (Xu *et al.*, 2006; Cho and Xu, 2007). Although PP2A is responsible for the post-translational modification of multiple proteins, it too is subject to regulation through post-translational modification, specifically phosphorylation and methylation of this particular motif on PP2A-C. As discussed above, the B' subunit family can also be regulated by phosphorylation, thus changing the substrate specificity and cellular location of the PP2A holoenzyme.

1.7.1 Phosphorylation

PP2A-C can be phosphorylated by epidermal growth factor, as well as insulin receptor and nonreceptor kinases, such as oncogenic p60^{v-src}, lymphocyte-specific p56^{lck}, and Src (Chen, Martin and Brautigam, 1992). This phosphorylation occurs on a tyrosine residue, Tyr307, in the C-terminal

of PP2A-C (Chen, Martin and Brautigan, 1992) and results in inhibition of PP2A by two separate mechanisms. First, it restricts the binding capability of the B' subunit to the core dimer by binding to the free hydrogen on the tyrosine residue of PP2A-C and preventing its interaction with a valine residue in the peptide backbone of the B' subunit (PR61/B56) (Cho and Xu, 2007; Longin *et al.*, 2007). In addition, phosphorylation of Tyr307 could prevent another post-translational modification, methylation of a leucine residue, Leu309, and thus influence the assembly of the holoenzyme (Ogris, Gibson and Pallas, 1997; Longin *et al.*, 2007; Nunbhakdi-Craig *et al.*, 2007). Consequently, when a cell experiences an increase in tyrosine phosphorylation (such as in response to epidermal growth factor or insulin), PP2A is subsequently inactivated for a short time. This allows a signal to pass from cellular surface receptors to the intracellular downstream effectors, thus mediating intracellular changes (Janssens and Goris, 2001). Overexpression of a tyrosine phosphatase such as PTP1 β , decreases the level of phosphorylated Tyr307, enhancing PP2A activity (Shimizu *et al.*, 2003).

In the initial studies of PP2A regulation by tyrosine phosphorylation, researchers observed that PP2A phosphorylation by a tyrosine kinase was enhanced in the presence of a PP2A inhibitor (Chen, Martin and Brautigan, 1992). This behaviour was characteristic of auto-dephosphorylation, indicating that PP2A is able to catalyse the removal of a phosphate group on one of its own residues, but also implying that PP2A has tyrosine phosphatase activity (Chen, Martin and Brautigan, 1992), which in fact can be measured *in vitro* (Chernoff *et al.*, 1983). PP2A's PTP activity is lower than that of a true tyrosine phosphatase, such as PTP1 β , but still contributes to the total cellular PTP activity (Cayla *et al.*, 1990). In addition, PP2A has fewer tyrosyl substrates than a true PTP (Agostinis *et al.*, 1996). PP2A's auto-dephosphorylation capacity is a function of its PTP activity and may ensure that PP2A activity is only transiently inhibited during tyrosine kinases signalling.

PP2A-C has also been shown to be phosphorylated *in vitro* on a threonine residue, Thr304, by autophosphorylation-activated protein kinase (Guo and Damuni, 1993). This phosphorylation leads to the loss of PP2A activity, which can also be recovered upon auto-dephosphorylation (Guo and Damuni, 1993). However, the purpose of PP2A inactivation by threonine phosphorylation is still not known (Janssens and Goris, 2001).

1.7.2 Methylation

Although PP2A methylation is documented in literature, how it contributes to regulation of PP2A is poorly understood. However, what is known regarding the function of methylation is briefly summarized below.

The leucine residue in the C-terminal tail of PP2A-C, Leu309, can be methylated, although it is not known whether methylation has a direct effect on the catalytic subunit activity of PP2A. Past studies have shown conflicting results where methylation results in a moderate increase in PP2A activity (Favre *et al.*, 1994), no change in PP2A activity (Ogris, Gibson and Pallas, 1997), and a decrease in PP2A activity (Zhu *et al.*, 1997). However, it is most likely that methylation of the catalytic subunit affects PP2A activity by influencing B subunit binding, which in turn, influences catalytic activity and substrate specificity (Bryant, Westphal and Wadzinski, 1999; Ikehara *et al.*, 2007). Interestingly, a larger fraction of PP2A holoenzymes are carboxymethylated than in the core dimer (Bryant, Westphal and Wadzinski, 1999).

Carboxymethylation of PP2A-C appears to regulate the holoenzyme assembly as it increases the affinity of the core dimer to bind to certain regulatory subunits (Cho and Xu, 2007; Longin *et al.*, 2007; Nunbhakdi-Craig *et al.*, 2007). Methylation of the catalytic subunit neutralizes the charge repulsion of the negatively charged regions at the interface of the regulatory and scaffolding subunits and thus promotes B' subunit (PR61/B56) binding (Cho and Xu, 2007). Certain B subunits require PP2A-C to be methylated before binding, while other subunits bind regardless of the catalytic methylation status (Bryant, Westphal and Wadzinski, 1999; Longin *et al.*, 2007; Nunbhakdi-Craig *et al.*, 2007). Both the B' (PR61/B56) and the B'' (PR72) subunits bind methylated and demethylated core dimers with similar affinity, but PR55 α almost exclusively assemble with methylated core dimers (Ogris, Gibson and Pallas, 1997; Bryant, Westphal and Wadzinski, 1999; Longin *et al.*, 2007). Methylation may possibly contribute to the regulation of PP2A activity (Hombauer *et al.*, 2007) by ensuring that only active catalytic subunits can be integrated into the holoenzyme complex and simultaneously preventing the formation of inactive trimeric holoenzymes (Sents *et al.*, 2013). This may explain the observation that carboxymethylation is seen more frequently in holoenzymes than in core dimers (Bryant, Westphal and Wadzinski, 1999).

Carboxymethylation is catalysed by leucine carboxyl methyltransferase 1 (LCMT1) (Lee and Stock, 1993; De Baere *et al.*, 1999). Methylation can also be reversed, and this is catalysed by protein phosphatase methylesterase (PME-1) (Lee *et al.*, 2002). LCMT1 is localized in the cytoplasm, Golgi

region, and late endosomes, while PME-1 is predominantly expressed in the nucleus (Longin *et al.*, 2008). The restriction of these enzymes to their respective subcellular locations prevents an unnecessary cycling of methylation and demethylation events. Consistent with the function of these enzymes, methylated PP2A is found in abundance in the cytoplasm, while demethylated PP2A is found in the nucleus (Longin *et al.*, 2008). LCMT1 deficiency results in apoptosis (Lee *et al.*, 2002; Longin *et al.*, 2007), while LCMT1 (Lee *et al.*, 2002) and PME-1 (Ortega-Gutiérrez *et al.*, 2008) knockout mice have lethal phenotypes, indicating the importance of these enzymes in the maintenance of normal PP2A function.

1.7.3 Other proteins that bind to PP2A

There are also several proteins that are not classified as regulatory subunits that can bind to the core dimer or holoenzyme. These include phosphotyrosyl phosphatase activator (PTPA), alpha 4 ($\alpha 4$), PME-1, TOR signalling pathway regulator-like (TIPRL), simian vacuolating virus 40 (SV40), as well as endogenous and exogenous inhibitors. These proteins serve to activate or inhibit PP2A, reduce or enhance PP2A degradation, or change PP2A's substrate specificity or cellular localization. Thus, they are important regulators of PP2A and what is known regarding their functions are discussed below.

1.7.3.1 *Phosphotyrosyl phosphatase activator (PTPA)*

PP2A's PTP activity can be induced or activated by PTPA (Cayla *et al.*, 1990). Structural analysis of PTPA show that it acts as a chaperone to facilitate PP2A activation (Guo *et al.*, 2014) in a magnesium (Mg^{2+}) and ATP-dependent manner (Cayla *et al.*, 1990). Upregulation of PTPA results in increased PTP1 β expression and activity, and knockdown of PTP1 β by siRNA abolished PTPA-induced PP2A activation (Luo *et al.*, 2013). This suggests that PTPA may regulate PP2A activity through PTP1 β -mediated dephosphorylation of Tyr307.

PP2A's PTP activity (regulated independently of serine/threonine phosphatase activity) is necessary for proper functioning of PP2A serine/threonine phosphatase activity. (Fellner *et al.*, 2003). PTPA induces a conformation change in the PP2A-C by functioning as a peptidyl-prolyl cis/trans isomerase targeting Pro190, and resulting in an active catalytic subunit with the correct substrate specificity for serine and threonine, rather than tyrosine residues (Fellner *et al.*, 2003; Jordens *et al.*, 2006). Genetic upregulation of PTPA has been shown to increase the

methylation of PP2A-C, resulting in increased catalytic activity (Luo *et al.*, 2013). In yeast, deletion of PTPA is associated with a conformational change of the catalytic subunit that reduces PP2A's serine/threonine phosphatase activity and increases its tyrosine phosphatase activity (Fellner *et al.*, 2003). This conformational change also reduced enzyme stability and increased its dependence on metal ions.

1.7.3.2 Protein phosphatase methyltransferase (PME-1)

As stated above, PME-1 mediates the demethylation of the catalytic subunit. However, PME-1 can also bind to the core dimer with high affinity (Ogris *et al.*, 1999) thereby inactivating PP2A-C by covalently binding directly to the active site and evicting the manganese ions required for PP2A's phosphatase activity (Xing *et al.*, 2008). This facilitates a long-term, stable interaction with an inactive core dimer which can coprecipitate with PME-1 (Longin *et al.*, 2004). This may serve to prevent unregulated over-activity until a substrate-recognizing B subunit binds and the holoenzyme is completely assembled (Kaur and Westermarck, 2016). Inactive PP2A that has complexed with PME-1 can be reactivated by PTPA that facilitates a conformation change in the catalytic subunit, rendering it active (Longin *et al.*, 2004).

1.7.3.3 $\alpha 4$

$\alpha 4$ (also known as immunoglobulin- α -binding protein 1, IGBP1) can bind directly to the catalytic subunit of PP2A and form a stable complex (Murata, Wu and Brautigan, 2002). When $\alpha 4$ binds to the catalytic subunit, it displaces the A and B-type subunits and reduces PP2A activity (McConnell *et al.*, 2010). However, the effects of this binding are numerous and ambiguous, as the functional role of $\alpha 4$ has not been fully elucidated. Several functions of $\alpha 4$ have been proposed.

$\alpha 4$ may also function similarly to B subunits in that it acts as a substrate-targeting subunit (Prickett and Brautigan, 2007) that can bind potential substrates through its flexible C-terminal domain (Sents *et al.*, 2013). Substrates of $\alpha 4$ /PP2A-C include MEK3, p53, c-Jun, ATM, mTOR, and various DNA repair proteins (Prickett and Brautigan, 2007)

$\alpha 4$ can simultaneously bind PP2A-C and Midline 1 (Mid1), a putative E3 ubiquitin ligase that is thought to facilitate the polyubiquitination and subsequent degradation of PP2A-C (Trockenbacher *et al.*, 2001). Originally it was thought that $\alpha 4$ targets PP2A-C for degradation, but further investigation into the ubiquitination of the PP2A-C/ $\alpha 4$ /Mid1 complex revealed that

ubiquitination actually serves to protect PP2A-C from degradation (McConnell *et al.*, 2010). $\alpha 4$ is monoubiquitinated in the cell and contains a unique ubiquitin-interacting motif that interacts with the ubiquitin group, thereby “capping” it and preventing polyubiquitination (McConnell *et al.*, 2010). This model may explain how $\alpha 4$ protects PP2A-C from degradation (Kong *et al.*, 2009). In this regard, $\alpha 4$ also serves as a scaffolding protein for PP2A-C and Mid1 and the binding of both PP2A-C and Mid1 are required for $\alpha 4$ to exert its protective effects.

PP2A $\alpha 4$ is critical to PP2A stability, and its deletion results in a progressive loss of PP2A, PP2C, protein phosphatase 4 (PP4), and protein phosphatase 6 (PP6) activity, as well as loss of the PP2A-A subunit (Kong *et al.*, 2009). Under conditions of cellular stress such as DNA damage, heat shock, or starvation, PP2A holoenzymes become unstable and PP2A activity decreases. When $\alpha 4$ is overexpressed, PP2A activity recovers faster after exposure to cellular stressors. Kong and colleagues suggest that $\alpha 4$ may bind to the catalytic subunit, protecting it from degradation until it can reintegrate into a holoenzyme that mediates cellular survival (2009). $\alpha 4$ may therefore serve as a modulator of PP2A stability in response to the cellular environment (Sents *et al.*, 2013).

1.7.3.4 TOR signalling pathway regulator-like (TIPRL)

$\alpha 4$ can simultaneously bind PP2A-C and another protein, TIPRL, thereby forming a rapamycin-insensitive complex (McConnell *et al.*, 2007; Smetana and Zanchin, 2007). TIPRL selectively binds unmethylated PP2A in a manner that inactivates PP2A (Wu *et al.*, 2017). This complex possesses no PP2A activity and plays an important role in mTOR signalling (Smetana and Zanchin, 2007) and ATM-mediated control of DNA replication and repair (McConnell *et al.*, 2007). TIPRL also binds to PP2A-A in a unique manner that enables it to bind disease-associated mutant PP2A, thereby reducing the holoenzyme assembly and subsequent inactivation of mutant PP2A (Wu *et al.*, 2017).

1.7.3.5 Simian vacuolating virus 40 (SV40)

PP2A-C is also a target of the small t-antigen of two DNA viruses, SV40 and polyoma virus. SV40 binds to PP2A-A, displacing PP2A-B in the process and thereby disrupting the substrate specificity and cellular localization conferred by the B subunit. This reduces PP2A's affinity for multiple substrates, but also stimulates cell proliferation through the MAPK pathway (Sontag *et al.*, 1993). SV40 has proven to be a useful tool for studying malignancies in human tissue (Yu, Boyapati and Rundell, 2001).

1.7.3.6 I_1^{PP2A} and I_2^{PP2A}

Endogenous inhibitors of PP2A 1 and 2 (I_1^{PP2A} and I_2^{PP2A}) are two inhibitors of PP2A that are able to bind the holoenzyme, the core dimer, and PP2A-C, by binding to PP2A-C in a non-competitive manner (Katayose *et al.*, 2000). Cloning studies identified I_1^{PP2A} as PHAP-I, a protein involved in proliferation, and I_2^{PP2A} was identified as SET, a protein associated with various malignancies. Both inhibitors complex with PP2A and limit its tumour suppressor function.

1.7.3.7 Family with sequence similarity 122A (FAM122A)

Recently, a new endogenous inhibitor of PP2A was identified, namely family with sequence similarity 122A (FAM122A; Fan *et al.*, 2016). FAM122A is able to interact with PP2A-A α and B55 α subunits directly and this results in inhibition of PP2A activity. FAM122A promotes polyubiquitination and subsequent degradation of PP2A-C. Overexpression of FAM122A enhances cell proliferation, while silencing of FAM122A inhibits cell growth (Fan *et al.*, 2016). The physiological and pathological significance of FAM122A is yet to be determined.

1.8 PP2A REGULATES BIOLOGICAL FUNCTIONS

PP2A is an important regulator of the cell cycle and functions as both a tumour suppressor and tumour promotor, depending on the specific holoenzyme and target substrate (for an interesting review on the topic, see Kiely and Kiely, 2015). PP2A regulates several processes such as metabolism, cell death, DNA repair, cytoskeletal dynamics, and the stress response. The role of PP2A in processes related to the heart and I/R injury are discussed below.

1.8.1 PP2A in Ca²⁺ handling

Contraction of heart muscle is regulated by changes in the intracellular concentration of Ca²⁺. When the sarcolemma is depolarized in response to an action potential, the voltage-dependent L-type calcium channels open and release a small amount of Ca²⁺ into the dyadic space. The increased concentration of Ca²⁺ opens the ryanodine receptors (RyRs), releasing a large amount of calcium from the sarcoplasmic reticulum in a process termed calcium-induced calcium release (Fabiato, 2017). The intracellular Ca²⁺ concentration rapidly increases to a level required for optimal binding to troponin C of the troponin/tropomyosin complex, in turn activating the

myofilaments that initiate the cross-bridge cycling that produces muscle contraction. For relaxation (and subsequent ventricular refilling) to occur, intracellular Ca^{2+} must be removed by closing the RyRs, and either pumping Ca^{2+} back into the sarcoplasmic reticulum by SERCA or out of the cell by the $\text{Na}^+/\text{Ca}^{2+}$ exchanger (Eisner *et al.*, 2017).

PP2A is closely associated with several proteins involved in contraction: connexin 43 (Ai and Pogwizd, 2005), the $\text{Na}^+/\text{Ca}^{2+}$ exchanger (Schulze *et al.*, 2003), L-type Ca^{2+} channels (Davare, Horne and Hell, 2000), RyR (Marx *et al.*, 2000), phospholamban (Macdougall, Jones and Cohen, 1991), troponin I (Mumby *et al.*, 1987), and myosin light chain 2 (Mumby *et al.*, 1987). It is therefore not surprising that phosphatase inhibition is associated with increased Ca^{2+} currents and regulates excitation-contraction coupling in cardiac tissue (DuBell *et al.*, 2002).

1.8.1.1 L-type Ca^{2+} channels

L-type Ca^{2+} channels ($\text{Cav}1.2$) can be phosphorylated by PKA (De Jongh *et al.*, 1996), which increases the channel activity in response to β -adrenergic stimulation (Bean, Nowycky and Tsien, 1984). Phosphorylation of the α -subunit of $\text{Cav}1.2$ can occur on Ser 1928 and 1866, mediated by PKA (Lemke *et al.*, 2008) and Ser1512 and Ser1570 mediated by Ca^{2+} /calmodulin-dependent protein kinase II (CaMKII) (Lee *et al.*, 2006; Blaich *et al.*, 2010). Of these, Ser1928 appears to have an essential role in $\text{Cav}1.2$ regulation (Lemke *et al.*, 2008). Although both PP1 and PP2A can dephosphorylate Ser1928, PP2A, along with PKA forms a macromolecular signalling complex with these channels that is independent of the phosphorylation status of the channel (Davare, Horne and Hell, 2000). PP2A is located next to Ser1928, the main PKA binding site in the complex, and this proximity may mediate fast and localized signalling (Hall *et al.*, 2006). Immunoprecipitation of the channel complex from rat brain results in coprecipitation of PP2A, and 80% of channels were complexed with PP2A (Davare, Horne and Hell, 2000). Targeting to the $\text{Cav}1.2$ is achieved through the B56 regulatory subunit of PP2A.

1.8.1.2 Ryanodine receptors (RyRs)

RyRs are macromolecular channel complexes regulated by kinases (particularly PKA and CaMKII) and phosphatases (PP1 and PP2A) that closely associate with the complex (Marx *et al.*, 2000). A regulatory subunit, a cytosolic FK 506 binding protein 12.6 (FKBP12.6) facilitates closing of the channel and stabilizes its closed conformation (Marx *et al.*, 2000). Upon β -adrenergic stimulation, phosphorylation of the RyR dissociates FKBP12.6 and opens the channel. Phosphorylation can

occur on three different residues: Ser2808, mediated by PKA (Wehrens *et al.*, 2004) and possibly CaMKII (Rodriguez, Bhogal and Colyer, 2003), Ser2814 mediated by CaMKII (Wehrens *et al.*, 2004), and Ser2030 mediated by PKA (Xiao *et al.*, 2005). Closing the channel requires dephosphorylation by either PP1, which can dephosphorylate Ser2808 and S2814, or PP2A, which can only dephosphorylate Ser2814 (Huke and Bers, 2008).

RyR phosphorylation is increased in heart failure, despite down regulation of β -adrenergic receptors. This may be attributed to reduced amounts of PP1 and PP2A. Heart failure reduces the expression of the ryanodine receptor itself, FKBP12.6, PP1 and PP2A, while increasing the expression of CaMKII (Ai *et al.*, 2005). Pharmacological inhibition of PP2A, as well as overexpression of a specific microRNA results in hyperphosphorylation of RyR2 at Ser2814, which promotes diastolic Ca^{2+} release events (Terentyev *et al.*, 2009; Belevych *et al.*, 2011) and may lead to impaired contractility (as intracellular Ca^{2+} is required to be high in systole and low in diastole for proper contractile functioning).

1.8.1.3 Phospholamban (PLB)

PLB is a negative regulator of SERCA. This inhibition is removed by PKA phosphorylation at Ser16 and by CaMKII at Thr17 and results in the removal of intracellular Ca^{2+} during relaxation. PP1 is the major phosphatase regulating PLB and can catalyse dephosphorylation on both Ser16 and Thr17 (Macdougall, Jones and Cohen, 1991). However, PP2A does mediate approximately 30% of PLB dephosphorylation, particularly on Thr17 (Macdougall, Jones and Cohen, 1991). The subunit B56, has been shown to target PP2A dephosphorylation of Ser16 of PLB.

1.8.1.4 Connexin 43

Connexins are transmembrane proteins present at gap junctions and in the mitochondria (Boengler *et al.*, 2005). Connexin 43 is phosphorylated predominantly on serine residues, and to a small extent on threonine and tyrosine residues. Similar to the ryanodine receptor and L-type calcium channels, it may also form complexes with kinases, PP1, PP2A, and other regulatory proteins (Ai and Pogwizd, 2005). Connexin 43 exists mainly in the phosphorylated state in the heart. Dephosphorylation of connexin 43 is suggested to be mediated by both PP1 and PP2A based on the phosphorylation sites on connexin 43 as well as the colocalization of PP1 and PP2A with connexin 43 (Ai and Pogwizd, 2005).

Connexins can polymerize and form a hemichannel that, together with a hemichannel from a neighbouring cell, form a gap junction. Gap junctions have been shown to play a role in infarct propagation and uncoupling the connexin hemichannels reduces infarct size (Totzeck *et al.*, 2008). Connexin 43 is dephosphorylated during ischaemia, and although the amount of PP2A is increased during ischaemia, it does not mediate connexin 43 dephosphorylation during ischaemia (Totzeck *et al.*, 2008). Interestingly, dephosphorylation of Connexin 43 during ischaemia is due to low ATP levels rather than hypoxia (Turner *et al.*, 2004). In addition, the levels of PP2A that colocalize with connexin 43 and thus dephosphorylate connexin 43, increases in heart failure (Ai and Pogwizd, 2005).

1.8.2 PP2A in ion channel regulation

A study done in alveolar epithelial cells demonstrated that when cells were stimulated with G-protein coupled-receptor (GPCR) agonists, Na⁺/K⁺-ATPase was recruited by exocytosis to the cell membrane (Lecuona *et al.*, 2006). The same stimulus also resulted in a rapid translocation of PP2A from the cytosol to the membrane fraction where PP2A can dephosphorylate the ser18 residue of the Na⁺/K⁺-ATPase α 1 subunit, maintaining the Na⁺/K⁺-ATPase within the membrane (Lecuona *et al.*, 2006); Kimura *et al.*, 2011; Hua *et al.*, 2018). When PP2A activity is suppressed, Na⁺/K⁺-ATPase becomes phosphorylated and results in a loss of membrane Na⁺/K⁺-ATPase (Hua *et al.*, 2018).

PP2A-B56 α is also indispensable for the regulation of voltage-gated sodium channels (Nav). Knockout of B56 α resulted in decreased sensitivity to adrenergic stimuli, altered cardiomyocyte excitability, and surprisingly, reduced CaMKII-dependent phosphorylation of Nav1.5 (El Refaey *et al.*, 2019). PP2A-B56 α is localized at the intercalated disc with Nav1.5, CaMKII, as well as ankyrin-G and β IV spectrin (El Refaey *et al.*, 2019).

In the heart, the Na⁺/Ca²⁺ exchanger exists in a macromolecular complex with kinases such as PKA and PKC, PKA-anchoring protein, as well as PP1 and PP2A (Schulze *et al.*, 2003). The precise mechanisms of how the Na⁺/Ca²⁺ exchanger is regulated is still a matter of controversy (Ruknudin *et al.*, 2007; Wanichawan *et al.*, 2011), but these complexes of kinases and phosphatases may ensure rapid phosphorylation and dephosphorylation that is necessary for the proper functioning of these channels and exchangers.

1.8.3 PP2A in cell death

Apoptosis, or programmed cell death, is a process whereby the cell regulates its own death. It is a tightly regulated process, and dysregulation of apoptosis results in cancers, autoimmune diseases, and neurodegenerative disorders. The Bcl-2 family contains pro- and anti-apoptotic proteins that regulate cell death by either promoting or inhibiting apoptosis (see Table 1.1; Adams and Cory, 2001). Apoptosis is regulated by various post-translational modifications, including phosphorylation, and PP2A has been shown to be critical in the regulation of especially Bcl-2 proteins. The role of PP2A as it regulates certain apoptotic proteins is illustrated in Figure 1.2.

Table 1.1 - Functions of the Bcl-2 family

Protein	Phospho-site	Pro or anti apoptotic	Function	References
Bcl-2	Thr56	Anti	Increased protein stability	Breitschopf <i>et al.</i> , 2000
	Thr69	Anti	Decreased p53 binding	Basu, DuBois and Haldar, 2006; Deng <i>et al.</i> , 1998
	Ser70	Pro or anti	Decreased p53 binding	Basu, DuBois and Haldar, 2006
	Thr74	Anti	Increased protein stability	Breitschopf <i>et al.</i> , 2000
	Ser87	Anti	Decreased p53 binding	Basu, DuBois and Haldar, 2006
Bak	Tyr108	Anti		Fox <i>et al.</i> , 2010
Bad	Ser75	Pro	14-3-3 Sequestration	Datta <i>et al.</i> , 1997
	Ser99	Pro	14-3-3 Sequestration	Datta <i>et al.</i> , 1997
	Ser118	Pro	Disrupts Bad/Bcl _{XL} interaction	Virdee, Parone and Tolkovsky, 2000
Bid	Thr59	Anti	Proximal to caspase 8 cleavage site	Esposti <i>et al.</i> , 2003
	Ser64	Anti	Proximal to caspase 8 cleavage site	Esposti <i>et al.</i> , 2003
Bcl _{XL}	Ser64	Pro	Disrupts Bcl _{XL} /Bax interaction	Kharbanda <i>et al.</i> , 2000
	Thr115	Pro		Kharbanda <i>et al.</i> , 2000
Bax	Ser60	Pro	Induces mitochondrial localization	Arokium <i>et al.</i> , 2007
	Ser163	Pro	Facilitates mitochondrial localization	Linseman <i>et al.</i> , 2004
	Ser184	Pro	Decreases mitochondrial localization	Gardai <i>et al.</i> , 2004
	Ser112	Pro	14-3-3 Sequestration	Zha <i>et al.</i> , 1996
	Ser136	Pro	14-3-3 Sequestration	Zha <i>et al.</i> , 1996

Table adapted from Niemi and MacKeigan, 2012

Bcl-2 is a potent anti-apoptotic protein that is regulated by phosphorylation of its Ser70 residue (Deng *et al.*, 1998). Its apoptosis-suppressing activity is abolished by dephosphorylation mediated by PP2A (Deng *et al.*, 1998). Studies have shown that PP2A also regulates Bcl-2 levels, and dephosphorylation protects Bcl-2 from proteosomal degradation, as cells treated with a PP2A inhibitor, okadaic acid, resulted in the selective degradation of the phosphorylated Bcl-2 population (Lin *et al.*, 2006). However, it is possible that degradation of Bcl-2 is dependent on other unknown factors in addition to phosphorylation (Lin *et al.*, 2006).

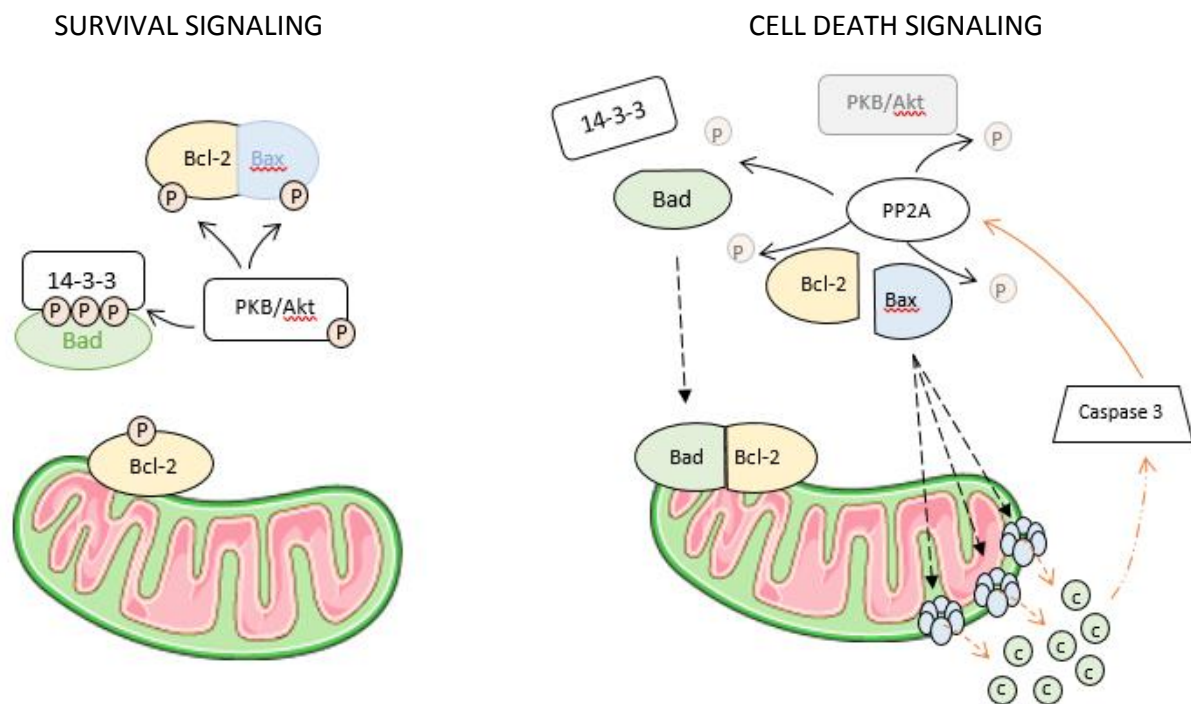


Figure 1.2 - PP2A regulates apoptotic proteins

During cell survival signalling, kinases (such as PKB/Akt) phosphorylates Bad, resulting in the association of Bad with 14-3-3. Consequently, Bad/14-3-3 is sequestered in the cytoplasm. When Bcl-2 is phosphorylated, it associates with Bax in the cytoplasm, preventing the translocation of Bax to the mitochondria. During cell death, PP2A dephosphorylates PKB/Akt, Bcl-2, Bax, and Bad. Bad dissociates from 14-3-3 and heterodimerizes with Bcl-2, inhibiting Bcl-2's anti-apoptotic function. Bax translocates to the mitochondria where it forms oligomeric pores, facilitating the release of cytochrome c. Caspase 3 is activated either intrinsically downstream of cytochrome c release or extrinsically through activation of the death receptor, whereafter it cleaves PP2A, allowing PP2A to associate with PKB/Akt, facilitating its dephosphorylation.

Bad and Bax are two pro-apoptotic proteins that form part of the Bcl-2 family. During survival signalling, Bad is phosphorylated by Akt/PKB on either Ser112 or Ser136 which mediates the binding of Bad to 14-3-3 which, in turn sequesters it in the cytoplasm (Zha *et al.*, 1996). Bad/14-3-3 is unable to translocate to the mitochondrial membrane and heterodimerize with Bcl-2, thereby preventing apoptosis. PP2A is a critical regulator of Bad as it can dephosphorylate Bad on

Ser112, resulting in apoptosis (Chiang *et al.*, 2003). Bax is predominantly found in the cytoplasm where it is heterodimerized to an anti-apoptotic Bcl-2 protein. When the cell is exposed to an apoptotic stimulus, Bax translocates to the mitochondria where it forms oligomeric pores in the mitochondrial outer membrane, facilitating mitochondrial depolarization and cytochrome c release (Gardai *et al.*, 2004). Dephosphorylation of Bax by PP2A can disrupt the Bax/Bcl-2 heterodimer in the cytoplasm, releasing Bax and activating apoptosis (Xin and Deng, 2006).

Caspase 3 is one of the executioner caspases that is a downstream effector of apoptosis (Orth *et al.*, 1996). Once activated, it cleaves and inactivates key enzymes involved in DNA repair and is responsible for some of the morphological characteristics of apoptosis, such as chromatin condensation and DNA fragmentation (Porter and Jänicke, 1999). One target of caspase 3 cleavage is PP2A-A, and cleavage results in an increased association of PP2A with Akt/PKB, facilitating its dephosphorylation and initiating apoptosis (Santoro *et al.*, 2016; Zhou *et al.*, 2017)(Santoro *et al.*, 2016). Removal of the scaffolding subunit also alters the catalytic subunit's affinity towards other substrates, such as $\alpha 4$ (Chung *et al.*, 1999; Kong *et al.*, 2009) and some unknown pro-apoptotic proteins (Santoro *et al.*, 2016). Thus, PP2A not only functions upstream in apoptotic signalling, but also downstream of caspases.

PP2A dephosphorylates FOXO1 (forkhead box O1), a transcription factor that regulates the cell cycle and apoptosis. When FOXO is phosphorylated by Akt/PKB in response to survival factors (such as insulin-like growth factor), its transcriptional activity ceases and it is exported from the nucleus (Rena *et al.*, 2015). However, when FOXO1 is dephosphorylated, it results in the transcription of pro-apoptotic proteins, such as Bim (Yan *et al.*, 2008).

Not much is known about PP2A's involvement in autophagy. Autophagy is activated when the mammalian target of rapamycin (mTOR) complex-1 (mTORC1) is inhibited. Recently it was demonstrated that PP2A-B55 α is activated upon starvation and dephosphorylates ULK1 (a substrate for mTORC1), a critical step in autophagy induction (Wong *et al.*, 2015). PP2A B55 α has also been shown to associate with Beclin 1, a scaffold protein that assembles autophagy stimulators and suppressors (Fujiwara *et al.*, 2016). PP2A-B55 α complexes with Beclin 1 under normal physiological conditions, and dissociates from Beclin-1 under starved conditions, enabling phosphorylation of Beclin 1 (Fujiwara *et al.*, 2016). Interestingly, Beclin 1 is a point of convergence for autophagy and apoptosis, as Bcl-2 (anti-apoptotic protein) interacts with Beclin 1 to inhibit autophagy (Pattingre *et al.*, 2005). Switching from apoptosis to autophagy thereby serves as an

alternative to cell death, if autophagy can be maintained at a level that is compatible with cell survival.

1.9 RATIONALE

In 2016, ischaemic heart disease (IHD) ranked first on the top five leading causes of death worldwide. The total number of IHD-related deaths in 2016 alone was 9.48 million, an increase of 19% from 2006 (Naghavi *et al.*, 2017). Although IHD has remained the leading cause of morbidity and mortality in high- and middle-income countries since 1990, most IHD-related deaths in 2016 occurred in middle- and low-income countries, an extremely alarming statistic (Naghavi *et al.*, 2017). In addition, the WHO reports that in 2016, more deaths in low-income countries were attributed to IHD than to HIV/AIDS, malaria, stroke, or tuberculosis (World Health Organization, 2018).

The prevalence of IHD in sub-Saharan Africa is also increasing, most probably from the cumulative effects of the increasing prevalence of risk factors for IHD, as well as the poor management of those risk factors. Sub-Saharan Africa has seen an increase in the prevalence of hyperlipidaemia and hypertension, as well as a lack of awareness of hyperlipidaemia and hypertension and their respective treatments, an increase in the prevalence of obesity (29%), one of the highest alcohol consumption rates in the world, increased tobacco usage (particularly in adolescents), dyslipidaemia, and the adoption of a more “Westernized” lifestyle and diet (Onen, 2013; Keates *et al.*, 2017). Consequently, these countries are faced with another new burden of disease, non-communicable diseases, which add to the existing burden of HIV/AIDS, tuberculosis, malaria, and injury.

Although HIV/AIDS remains the leading cause of death in South Africa, IHD was the second leading cause of death in 2017 (compared to fourth in 2007), ranking above diseases such as tuberculosis and lower respiratory infections (Naghavi *et al.*, 2017). In addition, the distribution of anti-retroviral therapy and the reduction in opportunistic infections has improved survival of HIV-infected individuals. As a result, sub-Saharan Africa has one of the largest populations of individuals living with HIV (UNAIDS, 2018). Most deaths among the HIV-infected population is now due to non-communicable diseases, especially cardiovascular disease. Recent studies in developed countries (Shah *et al.*, 2018) as well as in South Africa (Becker *et al.*, 2010) have shown

a link between the development of cardiovascular disease and HIV infection. These studies show that people living with HIV are twice as likely to develop cardiovascular disease, even in the absence of traditional cardiovascular risk factors (Becker *et al.*, 2010). Therefore, new therapeutic strategies are desperately needed to reduce the burden of disease, especially in developing nations such as South Africa.

As previously stated, reperfusion injury can induce myocardial injury independent of ischaemic injury and can account for as much as 50% of the final size of infarction. Limiting I/R injury is therefore necessary to salvage myocardium and currently, no such therapeutic intervention has yet translated into clinical practice. Thus, understanding how ischaemia and reperfusion affect the heart, as well as the mechanism of I/R injury and the signalling pathways involved, is a prerequisite for elucidating any novel therapeutic intervention to reduce I/R injury. Currently, none of the laboratory-tested interventions for reducing I/R injury have successfully been translated from the basic laboratory into clinical practice. Part of this challenge is the current gap in knowledge regarding the cellular response to I/R and the mechanisms associated with cardioprotection.

Historically, most research related to I/R injury has focussed on the role of protein kinases and their potential as therapeutic targets. Phosphoproteomic data show that up to one third of all phosphorylation events are reversible (Olsen *et al.*, 2006) and yet very little research on the functional roles of protein phosphatases exist. Although both kinases and phosphatases mediate the phosphorylation state of a protein, phosphatases have a greater influence on the duration of protein phosphorylation and by extension, the magnitude of the effects elicited by signalling pathways (Hornberg *et al.*, 2004). Phosphatases may therefore present as a target for cardioprotection to enhance the efficacy of existing cardioprotective interventions, but more information clarifying the role of phosphatases, particularly in ischaemia and reperfusion, is needed before this can be pursued. In light of the many important roles that PP2A has in the cell, as well as the pathologies that arise due to abnormal PP2A activity, PP2A must have an important role in I/R. Identifying the substrates of PP2A is a crucial step not only in understanding PP2A-related pathologies, but also understanding how PP2A responds to conditions such as ischaemia and reperfusion.

1.10 AIMS AND OBJECTIVES

Therefore, this study seeks to contribute to the limited information regarding the role of protein phosphatases, particularly PP2A, in the context of ischaemia and reperfusion of the heart by identifying proteins that were previously not known to be targets of PP2A. For this reason, a model free from pathologies was selected and no cardioprotective interventions (such as pre- or postconditioning) were utilized.

The hypothesis of this study is that PP2A negatively regulates protein phosphorylation, specifically in sustained ischaemia and subsequent reperfusion, thereby contributing to injury, and inhibition of PP2A will favour survival. The question is, which substrates are specifically involved in this context? Thus, the central aim of this study is to describe the participation of PP2A in the phosphorylation events surrounding myocardial ischaemia and reperfusion using the isolated working mouse heart model. To achieve this, we will pursue the following specific aims:

- 1.) To characterize the phosphoproteome of myocardial tissue obtained from hearts subjected to ischaemia and reperfusion.
- 2.) To investigate the effects of PP2A inhibition on the outcomes of I/R in terms of infarct size and functional recovery. Although the effects of PP2A inhibition on IFS has been described, there is no consensus as to whether PP2A inhibition is cardioprotective.
- 3.) Once the effect of PP2A inhibition has been confirmed, the next aim will be to identify proteins that are not known to be substrates of PP2A by the phosphoproteomic analysis of myocardial tissue exposed to ischaemia and reperfusion in the presence or absence of a PP2A inhibitor, okadaic acid. Proteins which are dephosphorylated during ischaemia and/or reperfusion, but show increased phosphorylation when okadaic acid was administered, will be selected for further study. This knowledge will contribute to the mechanism by which PP2A inhibition influences cell fate.
- 4.) Once these proteins have been selected, to describe how the expression or phosphorylation state of these proteins (identified in aim 3) changes during ischaemia and reperfusion, and if inhibition of PP2A influences their phosphorylation state or expression. To confirm whether these proteins are substrates for PP2A, western blot analysis will be conducted on hearts exposed to ischaemia and reperfusion either in the presence or absence of a PP2A inhibitor, okadaic acid. Co-immunoprecipitation experiments will also be conducted to determine whether PP2A has a direct interaction or forms a complex with these proteins.

CHAPTER TWO

MATERIALS AND METHODS

This chapter gives general information pertaining to the experimental methods and techniques used in this study. Specific details regarding each technique or adaptations to a given protocol, as well as the experimental approach are described in the relevant chapters.

2.1 MATERIALS

Carbogen gas (95% oxygen/5% carbon) was obtained from Afrox (South Africa), heparin sodium Fresenius (1000 U/ml) was obtained from a local pharmacy, sodium pentobarbital (Eutha-naze) was obtained from Bayer, the EnzChek[®] Phosphate Assay Kit (E6646) and the PageRuler[™] Pre-stained Protein Ladder (26617) used in western blotting were obtained from Thermo Fisher Scientific (USA). Western blot reagents were purchased from BioRad (Lasec, South Africa), Immobilon[®]-P PVDF membrane from EMD Millipore (Merck; IPVH00010), and 96-well plates from SPL Life Sciences (30496). Unless otherwise indicated, all western blot antibodies were obtained from Cell Signalling Technology Inc. (USA). All other reagents and chemicals (purified enzymes, okadaic acid, sodium orthovanadate, protease inhibitors) were purchased from Sigma-Aldrich-Merck, except where indicated otherwise, and further information is provided in the relevant chapters.

2.2 ANIMALS

All experimental protocols (SU-ACUD14-00054) involving animals were approved by Stellenbosch University's Research Ethics Committee: Animal Care and Use. Experiments were conducted in accordance with the accepted standards for the use of animals in research as reflected in the South African National Standards 10386: 2008.

C57BL/6 mice were housed at the Central Research Facility (Stellenbosch University) in a temperature-controlled environment with a 12-hour light/dark cycle. Mice were fed normal chow and had free access to food and water until the time of experimentation. Adult male mice (25-30

g) were injected intraperitoneally with 100 μ l phosphate buffered saline (PBS) containing 100 U of heparin to prevent thrombosis in the microvasculature of the heart. Five minutes post heparin administration, the mouse was anaesthetized by intraperitoneal injection of 100 μ l PBS containing 3 mg of sodium pentobarbital (Eutha-naze; 100 mg/kg). Fresh heparin and sodium pentobarbital dilutions were prepared daily. Animals were handled by an animal laboratory technologist registered with the South African Veterinary Council (AL17/15891).

2.2.1 Isolated murine heart perfusions

Once a deep anaesthesia had been confirmed, as determined by the absence of both the pedal pain withdrawal reflex and ocular reflex, the heart was rapidly excised, rinsed in warm, modified Krebs-Henseleit bicarbonate buffer (KHB; 118.5 mM NaCl; 25 mM NaHCO₃; 4.7 mM KCl; 1.2 mM KH₂PO₄; 1.2 mM MgCl₂; 2.5 mM CaCl₂; 11 mM glucose) to facilitate the expulsion of excess blood in the heart, and transferred to a petri dish containing ice-cold KHB to limit ischaemic injury. The heart was trimmed of excess lung and vascular tissue and the aorta was cannulated with a 19-gauge blunted, metal needle. The needle containing the cannulated heart was transferred to the perfusion apparatus where retrograde perfusion commenced with warm KHB. After the heart recommenced normal contraction, the pulmonary vein was also cannulated with a curved metal cannula, which would deliver KHB into the left atrium (and subsequently, the left ventricle) during antegrade perfusion, stimulating ventricular contraction. Double-walled perfusion glassware was connected to a circulating water bath to maintain the temperature of circulating KHB at 36.5 °C, and the ambient temperature around the heart was maintained at 36.5 °C by a double-walled chamber that surrounded the mounted heart. Temperature was monitored by a temperature probe placed as close as possible to the mounted heart.

Once the heart was fully cannulated, it was stabilized in retrograde mode at a constant pressure of approximately 75 mmHg using non-recirculating KHB gassed with 95% oxygen/5% carbon dioxide at 37 °C. No pacing was applied, and hearts were allowed to beat spontaneously. After the heart had stabilized, retrograde perfusion was changed to antegrade perfusion (work heart mode with a preload of 12.5 mmHg), where KHB entered the left atrium through the cannulated pulmonary vein, emptied into the left ventricle, and was expelled through the aorta against an afterload of 50 mmHg (Aasum *et al.*, 2002; du Toit *et al.*, 2007; Figure 2.1). Thereafter, the heart was once again perfused in retrograde mode with KHB containing drug (where applicable). For

studies utilizing ischaemia and reperfusion, hearts were subjected to global ischaemia (GI), which is accomplished by ceasing all perfusion to the heart, and reperfusion (where applicable), which is initiated by the re-establishment of retrograde perfusion.

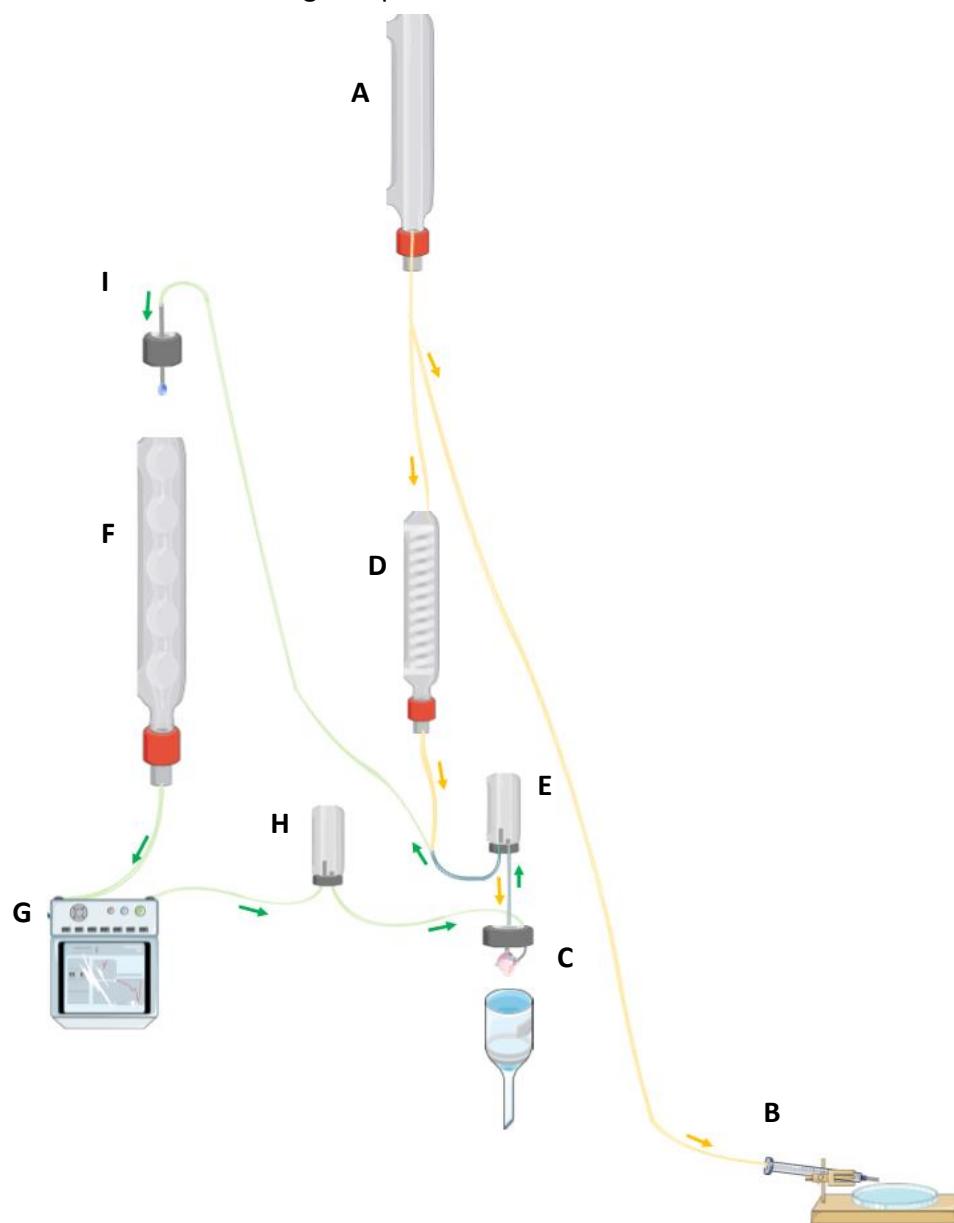


Figure 2.1 - Working mouse heart perfusion apparatus

Perfusate flows from the retrograde (Langendorff) reservoir (A) to the mounting dish (B) where heart is mounted in ice-cold KHB. The mounted heart is transferred to the perfusion apparatus (C) and the pulmonary vein cannulated. KHB flows from the retrograde reservoir through double-walled glassware (D), to a bubble trap (E), and finally to the heart through the aorta. Direction of flow in the retrograde line is indicated by yellow arrows. During antegrade mode (work heart), KHB flows from the antegrade reservoir (F) to the pump (G), through another bubble trap (H), and to the heart through the pulmonary vein. KHB enters the left ventricle and is pumped out of the heart through the aorta, up the aortic line (I), where aortic output is measured. Direction of flow in the antegrade line is indicated by green arrows. Direction of flow is maintained by taps (not shown).

KHB = Krebs Henseleit buffer

Image created with smart.servier.com

Coronary flow and aortic output (in antegrade mode only) were measured by timed collection of coronary and aortic effluents at five-minute intervals during stabilization, work heart, as well as drug administration, and expressed as volume flow per minute. Functional parameters such as systolic pressure and heart rate, were measured by a pressure transducer (Biopac Systems Inc., USA) in the aortic perfusion line that was connected to a computer (AcqKnowledge, Biopac Systems Inc.). Prior to each experiment, baseline pressure (zero) was established to reflect the retrograde pressure of approximately 75 mmHg. Hearts that had an aortic output less than 4 ml/min were excluded from analysis. With the exception of hearts used for infarct size analysis, all hearts were freeze clamped immediately after experimentation and stored in liquid nitrogen (-196 °C).

2.2.2 Infarct size determination

For experiments where infarct size was the endpoint, hearts were subjected to 20 minutes global ischaemia followed by 60 minutes reperfusion. The hearts were then immediately frozen at -20 °C after experimentation. Once frozen, the hearts were sliced into six sections with an approximate thickness of one millimetre, and incubated in phosphate buffer (pH 7.4) containing 1% w/v triphenyltetrazolium chloride (TTC; Sigma Aldrich, cat: T8877) for 10 minutes at 36 °C. TTC reacts with active dehydrogenases in viable tissue to form a brick-red precipitate that is absent in infarcted tissue (Lindsey *et al.*, 2018). This reaction is then terminated by fixing the heart slices in 10% v/v formaldehyde solution overnight at 4 °C, which also increases the contrast between the red (viable) and pale (infarcted) tissue. Consistent and accurate visual determination of infarcted and viable tissue is difficult due to the small size of the murine heart. Thus, the slices were placed between two glass plates, scanned at a high resolution, and the image enlarged on Paint.net © (dotPDN LLC, 2018). Using this software, the background of the image was removed, leaving only an image of the heart slices. The images were then uploaded onto Image J (W, Rasband; National Institute of Health, USA) by an individual who was not associated with this study and was blinded to the identity of the heart slices. The area of infarct was estimated visually to determine the number of pixels in the infarcted tissue, which was then expressed as a percentage of total pixels.

2.2.3 Sample preparation for biochemical analysis

One-half of a mouse heart was pulverized in a stainless-steel mortar cooled in liquid nitrogen. The pulverized tissue was added to lysis buffer containing 150 mM NaCl, 5 mM HEPES, 5% glycerol, 10

μ l protease inhibitor per 10 ml lysis buffer, 0.1% 2-mercaptoethanol, 1 mM ethylenediaminetetraacetic acid (EDTA), 50 μ g/ml phenylmethane sulfonyl fluoride (PMSF) and 0.16 mg/ml benzamidine. Phosphatase inhibitors were included in lysis buffers used for western blotting but excluded from lysis buffers where phosphatase activity assays were conducted. Stainless steel beads (1.6 mm) were added to each sample, and the samples homogenized using the Bullet blender (Next Advance, Inc.) and left to rest at 4 °C for 20 minutes. This was followed by centrifugation at 12,074 x g at 4 °C for 20 minutes, where after the supernatants were collected. The protein content of each sample was determined by the Bradford technique (Bradford, 1976), and the individual samples diluted with lysis buffer to a uniform protein concentration. Samples were then used for either Western blotting, immunoprecipitation, or phosphatase assays.

2.2.4 Western blot analysis

For western blot analysis, 3x Laemmli buffer (2.5 M glycerol, 10% SDS, 1.275 mM bromophenol blue, 15% β - mercaptoethanol, 0.189 M trisaminomethane adjusted to pH 6.8 with hydrochloric acid; TRIS-HCl) was added to samples after which the samples were boiled for five minutes and stored at - 80 °C. Prior to separation, the samples were again boiled for five minutes and briefly centrifuged for 15 seconds. Protein separation was achieved by sodium dodecyl sulfate polyacrylamide gel electrophoresis (SDS-PAGE) using either hand-cast mini gels (4% and 12% acrylamide in the stack and running gel, respectively) in a Bio-Rad Mini PROTEAN II system, or Criterion [™] TGX Stain-Free gels (4-20% acrylamide, Bio-Rad; cat: 5678095) in a Bio-Rad MIDI system (Bio-Rad Laboratories, Inc., USA). Where hand-cast running gels were used, the 12.5% resolving gels were prepared with acrylamide (Sigma-Aldrich Merck), 0.375 M TRIS-HCl (pH 8.8), 1% SDS, 0.05% ammonium persulfate (APS), and 0.2% tetramethylethylenediamine (TEMED), while the stacking gels (4% acrylamide) were prepared with 0.126 M TRIS-HCl (pH 6.8), 1% SDS, 0.05% APS and 0.2% TEMED. Additionally, the running gels contained 0.5% 2,2,2 Trichloroethanol (Stainfree; Sigma-Aldrich, cat: 8086100100), which reacts with tryptophan groups under ultraviolet light to produce fluorescence that can be measured with a 300 nm transilluminator (Ladner *et al.*, 2004). This negates an additional staining step to visualize proteins. PageRuler [™] Pre-stained Protein Ladder was used as a protein marker.

The gels were subjected to electrophoresis at 100 V and 200 mA for 10 minutes to separate the proteins in the stacking gel and then at 200 V and 200 mA for one hour to separate the proteins

in the running gel. The running buffer used for gel electrophoresis contained 25 mM TRIS, 192 mM glycine, and 3.5 mM SDS. Once proteins were separated, the Stainfree gel was activated for a minute on the ChemiDoc imaging system and an image of the gel was stored by the ChemiDoc software (Bio-Rad Laboratories, Inc., USA).

Following this, proteins from the gel were transferred to a polyvinylidene fluoride (PVDF) membrane using a tank electro-transfer system. Transfer was performed at 200 V and 200 mA on ice for one hour using transfer buffer that contained 25 mM TRIS, 192 mM glycine, and 20% methanol. The membranes were visualized on the ChemiDoc imaging system for total loaded proteins and an image of this was saved on the ChemiDoc imaging software for later normalization. The membranes were then placed in Tris buffered saline (TBS; 20 mM TRIS-HCl at pH 7.6, 137 mM NaCl) containing 0.1% Tween-20 (TBS-Tween) and 5% fat-free milk and gently agitated for 1.5 hours to block available binding sites and prevent non-specific antibody binding.

After blocking, the membranes were washed with three changes of TBS-Tween buffer, followed by a five-minute wash. This cycle was repeated three times. The membranes were then incubated overnight at 4 °C with the relevant primary antibody (Table 2.1) and washed thoroughly as described above. Following this, the membranes were incubated at room temperature with a goat anti-rabbit horseradish-peroxidase conjugated secondary antibody (Cell Signalling Technology; cat: 7060S), unless otherwise indicated. This was done under constant, gentle agitation for an hour at room temperature and washed as described above. Thereafter, the membrane was incubated in Clarity™ Western ECL Blotting Substrate (Bio-Rad Laboratories Inc.; cat: 1705061) for five minutes and visualized on the ChemiDoc imaging system.

The membrane image of total protein loaded onto the gel and transferred to the membrane was used to normalize for unequal protein loading. Each lane was automatically selected by the ImageLab 5.0 software and manually adjusted to include as much of the lane as possible, accounting for protein diffusion out of the lane area and lane curvature. The software calculated the pixel intensity for the entire selected area in each lane and normalized it to the first sample lane. Thereafter, the bands in the final blot are compared to the total protein loaded in its corresponding lane. This corrects for unequal protein loading and negates the use of a loading control. The normalized pixel intensities for each protein band were exported to an Excel Spreadsheet (Microsoft, USA) and the fold-changes expressed relative to the average of the

control samples. Where phosphorylation was measured, it was expressed as a ratio to the total protein. Data were then exported to GraphPad© Prism (GraphPad Software Inc., San Diego, CA) for statistical analyses.

Table 2.1 - Information regarding the antibodies used in this experiment.

Antibody	Size (kDa)	Dilution	Product no:	Supplier
Total VDAC	32	1:1000	4866	Cell Signalling Technology
Total SIRT3	28	1:1000	5490	Cell Signalling Technology
Total PP2A-A	60	1:1000	2041	Cell Signalling Technology
Total PP2A-C	36/38	1:1000	2038	Cell Signalling Technology
PP2A-C (immunoprecipitation)	N/A	1:10	sc-6110	Santa Cruz Biotechnology
Total PP1	38	1:1000	2582S	Cell Signalling Technology
Total PKB	60	1:1000	4691	Cell Signalling Technology
Phospho-PKB (Ser473)	60	1:1000	4060	Cell Signalling Technology
Total HSP90α	90	1:1000	8165S	Cell Signalling Technology
Phospho-HSP90α (Thr5/7)	90	1:1000	3488	Cell Signalling Technology
Total Striatin	110	1:500	HPA017286	Sigma Aldrich
Total OXPHOS Rodent WB	C I-20 kDa	1:1000	ab110413	Abcam
Antibody Cocktail	C II-30kDa			
	C III-48 kDa			
	C IV-40 kDa			
	C V-55 kDa			

CI = complex I; CII = complex II; CIII = complex III; CIV = complex IV; CV = complex V

2.2.5 Immunoprecipitation

Before immunoprecipitation, samples were diluted to equal protein concentrations. The lysates were then precleared by the addition of A/G agarose beads (Sigma Aldrich; cat: 11719408001) and mixed by gentle agitation for an hour at 4 °C. Following this the samples were centrifuged at 12,074 x g at 4 °C for 45 seconds and the supernatant removed and incubated with a PP2A antibody (Santa Cruz Biotechnology Inc.; sc-6110) overnight at 4 °C, and then with 50 µl A/G agarose beads. The antibody-bead complex was recovered by centrifuging the sample (12,074 x g at 4 °C for 45 seconds) and removing the supernatant. The antibody-bead complex was washed

by adding PP2A activity assay buffer (500 mM HEPES buffer at pH 7.4, 50 mM MgCl₂, 0.002% 2-mercaptoethanol, 0.5 mg/ml bovine serum albumin ;BSA), centrifuging the sample (12,074 x g at 4 °C for 45 seconds), and removing the supernatant. This was repeated three times before the sample was resuspended in assay buffer. Care was taken to ensure that each sample contained equal volumes of assay buffer.

2.2.6 Phosphatase assay

General phosphatase activity in the lysate and PP2A-specific activity (using immunoprecipitated samples) was measured using the the EnzChek[®] Phosphatase Assay Kit according to the manufacturer's protocol (Molecular Probes Inc, 2004). Using this kit, phosphatase activity is measured by the dephosphorylation of a non-fluorescent substrate, 6,8-difluoro-4-methylumbelliferyl phosphate (DIFMUP), where removal of its phosphatase group produces a fluorescent product, 6,8-difluoro-4-methylumbelliferyl (DIFMU). The amount of fluorescence produced within the sample is therefore directly proportional to phosphatase activity.

Briefly, 50 µl of each sample and 50 µl of DIFMUP were added to a flat-bottom, black, 96-well microplate. Since any phosphatase can dephosphorylate the DIFMUP substrate, specific inhibitors must be utilized to distinguish between different phosphatases in crude tissue lysates. Where additional inhibitors were used, the protocol was adapted to ensure the final reaction volume was 100 µl and the concentration of components was the same as specified in the manufacturer's protocol. The plates were incubated at 37.5 °C in a FLUOstar Optima microplate reader (BMG Labtech, Germany) for the duration the experiment. Fluorescence was measured at 355/460 nm excitation/emission at 5-minute intervals, for 120 minutes, unless otherwise indicated. Wells containing only assay buffer and DIFMUP served as a background measurement (blank). Phosphatase activity is expressed in amount of DIFMU produced that was calculated from a standard curve of DIFMU (0 – 100 µM) that was included in each experiment. Unless otherwise stated, all samples contained an equal amount of protein.

2.2.7 Statistical analyses

Statistical analyses of experiments are addressed in each chapter. GraphPad[®] Prism (GraphPad Software Inc., San Diego, CA) was used for all analysis. A p-value equal to or less than 0.05 was

considered significant, and unless otherwise indicated, all data are expressed as mean \pm standard deviation (SD).

CHAPTER THREE

INHIBITOR DOSE DETERMINATION

3.1 RATIONALE

Pharmacological inhibition of an enzyme is a useful tool for determining the function of an enzyme, particularly in an acute setting. In the past, pharmacological inhibition of PP2A has been utilized to determine the targets of PP2A dephosphorylation, as well as the effects of acute PP2A inhibition. However, although there are numerous phosphatase inhibitors available, there are currently no exogenous inhibitors that specifically inhibit PP2A without inhibiting other phosphatases, particularly PP1. For this study okadaic acid (OA) was utilized, as it is very well described and commonly used. OA is a polyether fatty acid first isolated from marine sponges (Tachibana *et al.*, 1981). In a cell-free system, OA is a potent inhibitor of PP2A and PP4 ($IC_{50} = 0.5-1$ nM; Cohen, Klumpp and Schelling, 1989; Ishihara *et al.*, 1989) and at higher concentrations inhibits PP1 ($IC_{50} = 15-50$ nM; Ishihara *et al.*, 1989) and other minor phosphatases such as PP3, PP5, and PP6. Currently, it is not possible to distinguish PP2A and PP4 activity using exogenous inhibitors, but at a low concentration, OA can selectively inhibit PP2A/PP4 without significantly affecting PP1 activity. Although the function of PP4 is not fully understood, it plays a role in DNA damage repair, mitosis, and cell proliferation (Mourtada-Maarabouni and Williams, 2008), but seems to contribute relatively little to total phosphatase activity, when compared to PP2A or PP1. Since PP1 and PP2A are responsible for over 90% of dephosphorylation events in the heart, distinction between these major phosphatases were the focus of the experimentation, rather than delineating PP2A and PP4 activity.

Due to its hydrophobicity, OA is able to penetrate the cell membrane (Namboodiripad and Jennings, 2017), but transverses the membrane with difficulty and accumulates slowly within the cell (Herzig and Neumann, 2000; Swingle, Ni and Honkanen, 2007). Thus, the amount of OA in the perfusate of an isolated heart may not be the amount of OA that is available in the intracellular environment. In addition, the reported inhibitory concentrations were determined in cell culture and in cell-free systems. These concentrations may not be sufficient to inhibit PP2A in cardiac tissue, as cardiac tissue contains a large amount of PP2A (Khew-Goodall and Hemmings, 1988), which further necessitates the use of a higher concentration of inhibitor.

Therefore, the purpose of these experiments was to determine the optimal concentration of OA dissolved in perfusate that would result in sufficient inhibition of PP2A *ex vivo*, while having a minimal effect on the activity of PP1.

3.2 METHODS

To determine the optimal concentration of OA for use in isolated heart perfusions, hearts were perfused with either KHB (control) or KHB containing either 100 nM, 50 nM, or 10 nM OA, or 0.13% DMSO (vehicle control). Hearts were stabilized in retrograde mode for 15 minutes, perfused in antegrade mode for 15 minutes where the hearts were allowed to function, and then again perfused in retrograde mode for 20 minutes where drug, vehicle, or KHB was administered (Figure 3.1). After experimentation, the hearts were freeze clamped and stored in liquid nitrogen until further use.

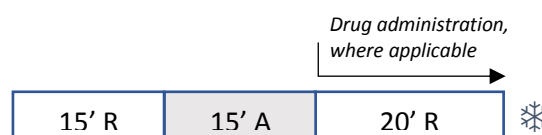


Figure 3.1 - Perfusion protocol for inhibitor dose determination

Hearts were perfused in retrograde mode for 15 minutes, in antegrade mode for 15 minutes to determine function, and again in retrograde mode for 20 minutes, during which time OA, DMSO, or KHB was administered. R = retrograde perfusion, A = antegrade perfusion, ❄ = freeze clamping.

One-half of each heart sample was pulverized in a stainless-steel mortar cooled in liquid nitrogen. The powdered tissue was added to 400 µl lysis buffer and the protein concentration determined using the Bradford technique (Bradford, 1976). The samples were then adjusted to 550 µg in 550 µl of lysis buffer and PP2A was immunoprecipitated from each of the samples by adding 50 µl PP2A-Agarose bead complex (Protein A/G PLUS-Agarose Immunoprecipitation Reagent, Santa Cruz; sc-80665 AC). The antibody/bead complex (pellet) was recovered by centrifuging the sample and removing the supernatant, which was stored at – 80 °C for western blot confirmation of immunoprecipitation. After washing the antibody/bead complex, the antibody/bead complex was resuspended in 500 µl assay buffer. Each sample was divided into three aliquots: two 200 µl samples for the phosphatase assay, and a 100 µl sample for Western blotting. The two assay samples were centrifuged and resuspended in 200 µl containing either assay buffer or assay buffer containing 10 mM sodium orthovanadate (SOV). SOV was used as a negative control of inhibition, as it is considered to be a specific and exclusive inhibitor of tyrosine phosphatases and is not expected to have an effect on serine/threonine phosphatases, such as PP2A.

50 µl of the 200 µl sample (either in the presence or absence of SOV) were loaded in duplicate into a 96-well microplate (SPL Life Sciences, Korea) so that each well contained 50 µl of sample and 50 µl of DiFMUP. The plates were incubated at 37.5 °C and phosphatase activity was measured by the generation of the DiFMUP substrate, 6,8-difluoro-4-methylumbelliferyl (DiFMU). Fluorescence was measured at 355/460 nm excitation/emission at 5-minute intervals, for 120 minutes.

For confirmation of immunoprecipitation, samples reserved for western blot analysis were centrifuged, the supernatant removed, and the antibody/bead complex resuspended in 80 µl 1x Laemmli buffer (10 % glycerol, 3% SDS, 0.425 mM bromophenol blue, 5% β- mercaptoethanol, 63 mM TRIS-HCl (pH 6.8)). 15 µl of each sample (containing approximately 15 µg protein) was loaded onto a Criterion™ TGX Stain-Free gel (4-20% acrylamide, Bio-Rad). To confirm the presence of PP2A and absence of PP1 in the immunoprecipitated samples, western blot analysis was performed on one immunoprecipitated sample from each cohort, its corresponding supernatant (removed when the antibody/bead/PP2A was recovered) and an additional. The supernatants were prepared for western blotting by removing 60 µl from each sample and adding 30 µl of 3x Laemmli buffer. 10 µl of each immunoprecipitation and supernatant samples (containing approximately 10 µg protein) were loaded onto a hand-cast mini gel. The membranes were then exposed to either a PP2A (Cell Signalling Technology; cat: 2038) or PP1 (Cell Signalling Technology; cat: 2582S) primary antibody.

3.2.1 Data and statistical analysis

Data were exported to an Excel spreadsheet (Microsoft, USA) where the measured fluorescence was corrected for background fluorescence by subtracting the amount of fluorescence generated by wells containing only assay buffer and DiFMUP. To compare the coronary flows of hearts perfused with different inhibitors, as well as the amount of PP2A present in each immunoprecipitated sample, a one-way analysis of variance (ANOVA) with a Bonferroni multiple comparison test was conducted in GraphPad© Prism. For comparisons of enzyme activity, a two-way ANOVA with a Dunnett's *post-hoc* test was utilized. A p-value equal to or less than 0.05 was considered significant. Data are expressed as mean ± SD.

3.3 RESULTS

Coronary flow from hearts perfused with differing concentrations of OA or 0.13% DMSO was not significantly different when compared to control (Table 3.1). Western blot analysis confirmed the presence of PP2A in each of the immunoprecipitated samples and there were no significant differences in the amount of PP2A between cohorts (Figure 3.2). When comparing immunoprecipitated PP2A samples with their corresponding whole cell supernatants, PP2A was present in both the immunoprecipitate and supernatant, although a large amount of PP2A remained in the supernatant (Figure 3.3 A). Much non-specific binding was observed with the PP1 antibody, but bands were only observed in the whole cell supernatant, confirming the absence of PP1 in the immunoprecipitate (Figure 3.3 B).

Table 3.1 - Coronary flow of hearts perfused with 10 nM, 50 nM or 100 nM OA, 0.13% DMSO, or KHB. There were no significant differences in coronary flow during retrograde perfusion or during drug administration between each of the cohorts.

	Coronary flow during retrograde perfusion (ml/min)	Coronary flow during drug administration (ml/min)
KHB (control)	0.97 ± 0.18	0.58 ± 0.22
0.13% DMSO (vehicle control)	0.82 ± 0.23	0.98 ± 0.58
10 nM OA	1.23 ± 0.37	0.85 ± 0.44
50 nM OA	1.19 ± 0.21	0.60 ± 0.11
100 nM OA	1.34 ± 0.29	0.40 ± 0.16

Data analysed by one-way ANOVA with Bonferroni post-hoc and expressed as mean ± SD. n = 3-4.

KHB = Krebs Henseleit solution, DMSO = dimethylsulfoxide, OA = okadaic acid

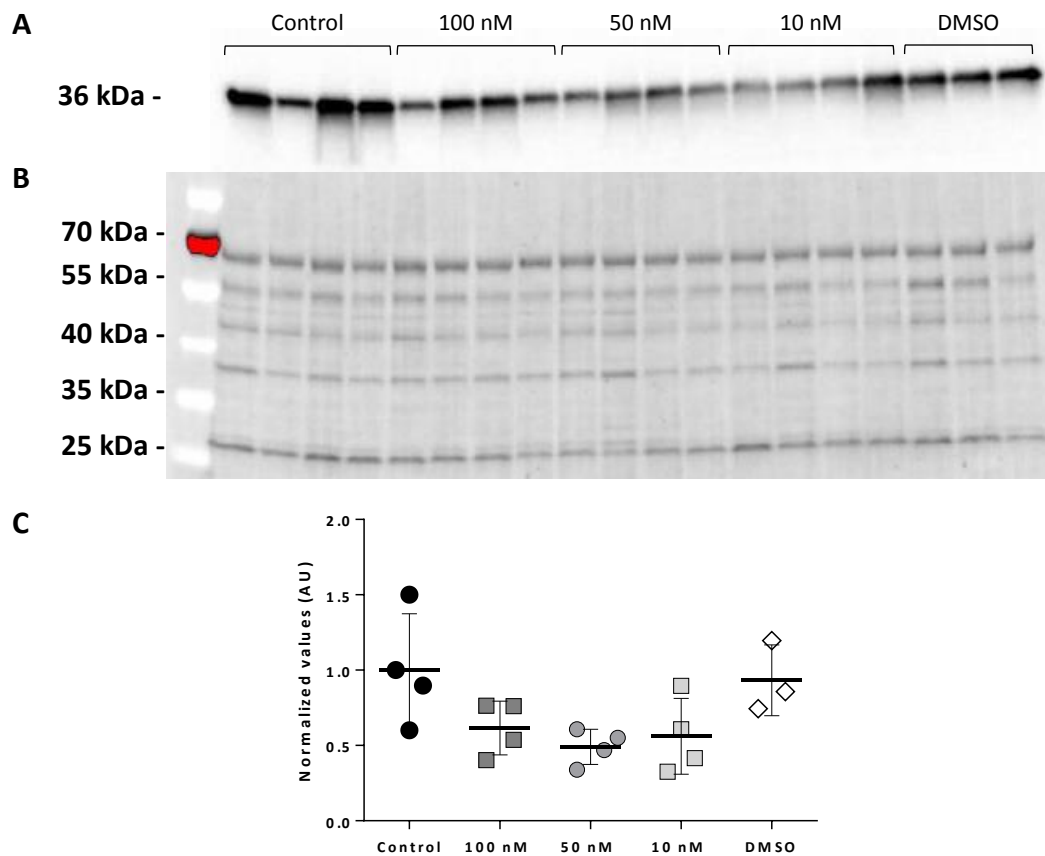


Figure 3.2 - Confirmation of PP2A immunoprecipitation.

Western blotting confirmed the presence of PP2A in the recovered antibody-bead complex by using a PP2A-C primary antibody (A). (B) shows the total protein transferred from the SDS gel onto the membrane, indicating the presence of other proteins bound to PP2A during immunoprecipitation. (C) No significant differences in amount of recovered PP2A was found between samples between cohorts (Bonferroni post hoc test; $n = 3-4$).

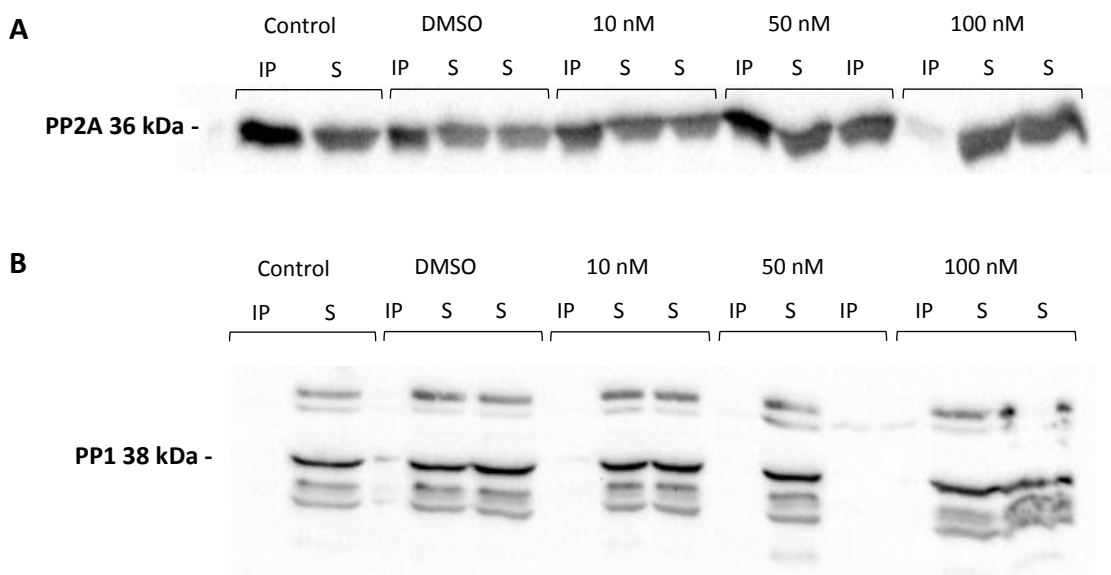


Figure 3.3 - Confirmation of the presence of PP2A and the absence of PP1 in immunoprecipitate and matched whole cell supernatant.

Immunoprecipitated PP2A samples alongside their matched whole cell supernatant and another supernatant from the same cohort were loaded onto a gel and probed with a PP2A-C primary antibody (A) or PP1 primary antibody (B). PP2A was present in both immunoprecipitated samples and supernatants, while PP1 was only present in the supernatants.

With regards to the enzyme activity assay, no significant differences in total DIFMU production was seen in the 50 nM and DMSO treated cohorts when compared to control after 120 minutes of incubation with the DiFMUP substrate (Table 3.2; Figure 3.4). A significant reduction in total DIFMU production was seen in the 100 nM cohort when compared to control and increased DIFMU production was observed in the 10 nM treated cohort after 120 minutes (Figure 3.4). Interestingly, the DIFMU production of the replicates that were resuspended in KHB containing 10 mM SOV was significantly reduced in all cohorts when compared to control samples resuspended in KHB alone ($p < 0.001$; Figure 3.5).

Table 3.2 - Amount of DIFMU produced at t = 120 minutes

Activity of PP2A immunoprecipitated from hearts perfused with either 10 nM, 50 nM or 100 nM OA, KHB, or 0.13% DMSO was measured over 120 minutes. Only 100 nM OA administration reduced DIFMU production when compared to control. Increased DIFMU production was observed in the 10 nM OA cohort when compared to control.

	Amount of DIFMU (nmol) at t = 120 minutes	significance
KHB (control)	0.85 ± 0.15	-
0.13% DMSO (vehicle)	0.87 ± 0.06	p = 0.9955
10 nM OA	1.01 ± 0.03	p = 0.0077
50 nM OA	0.72 ± 0.21	p = 0.3889
100 nM OA	0.50 ± 0.09	p = 0.0002

Data analysed by two-way ANOVA with Dunnett's post-hoc and expressed as mean ± SD, 3-4 hearts per group, where each heart sample was assayed in duplicate.

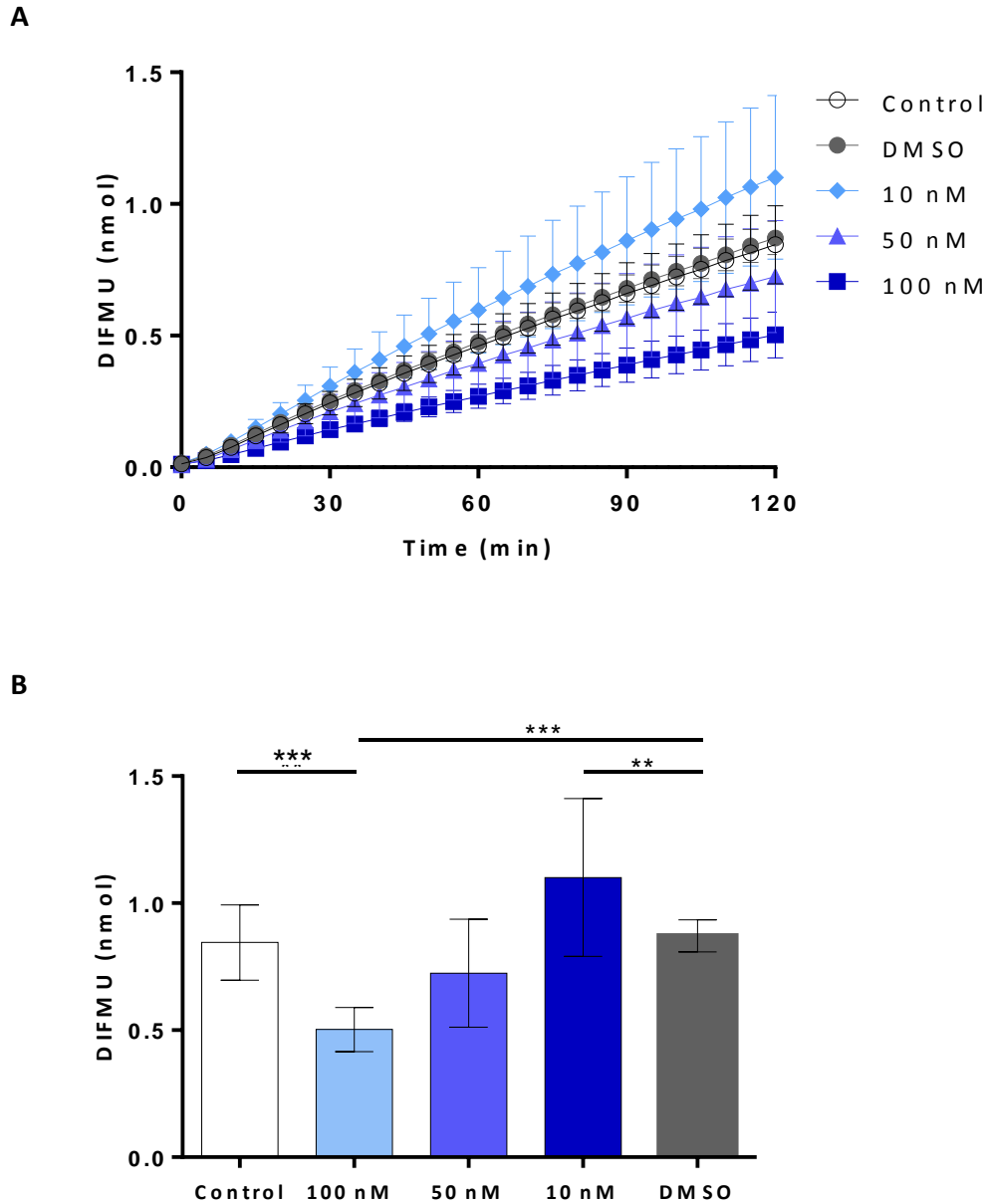


Figure 3.4 - DIFMU production from PP2A immunoprecipitated from hearts perfused with 10, 50, and 100 nM OA, DMSO, or KHB resuspended in assay buffer.

PP2A was immunoprecipitated from hearts which were perfused with either 10 nM, 50 nM, 100 nM, 0.13% DMSO (vehicle), or KHB (control). Perfusion with 100 nM significantly reduced DIFMU production over time (A) when compared to control or ($p < 0.0002$) DMSO ($p < 0.0002$). At the end of experimentation (B), increased DIFMU production was seen in the 10 nM group when compared to DMSO ($p < 0.008$). Data expressed as mean \pm SD nmol DIFMU produced over time. Cohorts contained 3-4 hearts and each heart was assayed in duplicate.

** $p < 0.01$

*** $p < 0.001$

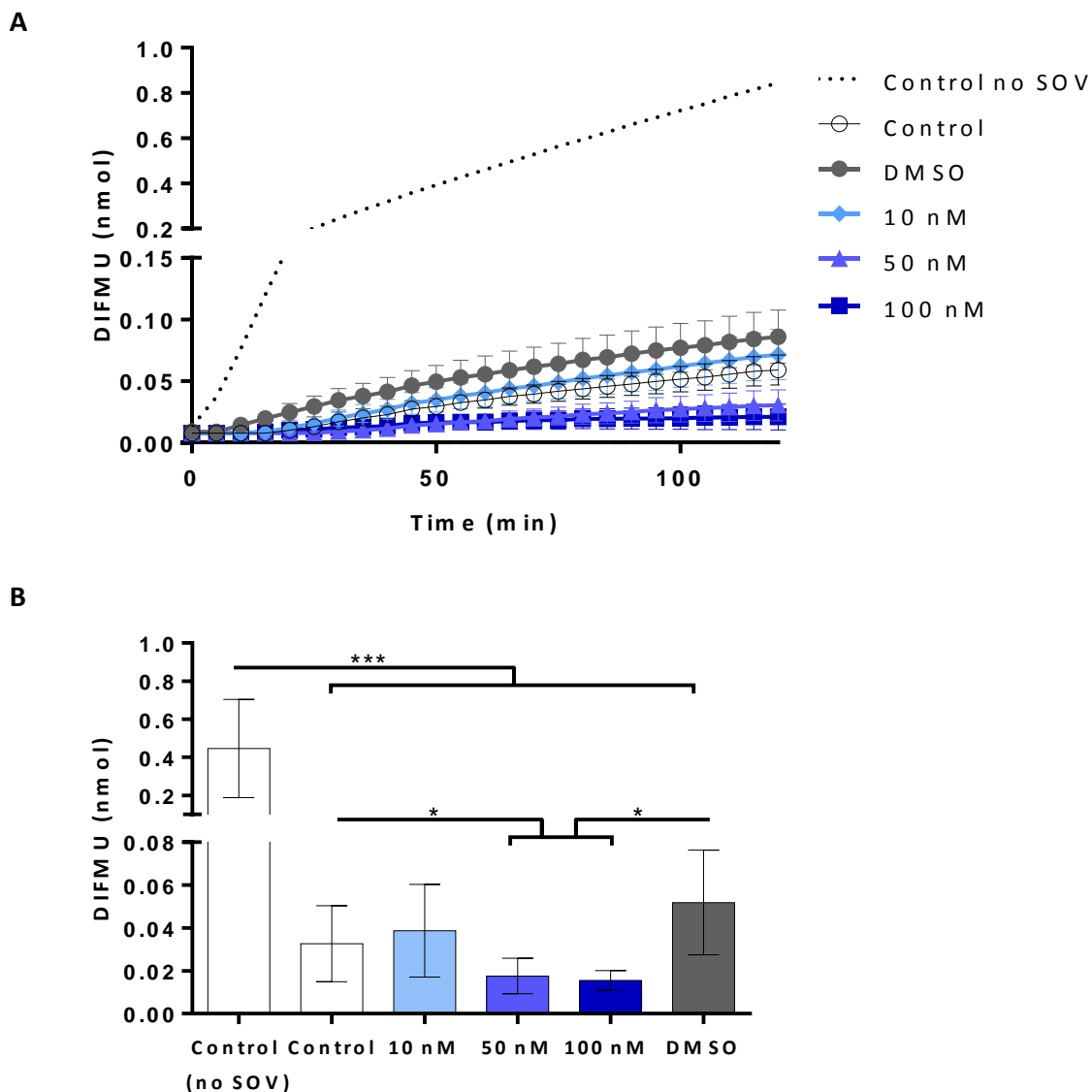


Figure 3.5. – DIFMU production from PP2A immunoprecipitated from hearts perfused with 10, 50, and 100 nM OA, DMSO, or KHB resuspended in 10 mM SOV.

Immunoprecipitated PP2A activity was significantly reduced when the antibody/bead complex was resuspended in 10 mM SOV when compared to PP2A activity resuspended in assay buffer (“Control no SOV,” $p < 0.0001$; graphed for comparative purposes; two-way ANOVA with a Bonferroni post hoc test). DIFMU production over time (A) and at the end of experimentation (B) are shown. DIFMU production after 100 nM and 50 nM OA administration was significantly reduced in the presence of SOV when compared to control and DMSO in the presence of SOV ($p < 0.05$). Data expressed as mean \pm SD over time (two-way ANOVA with a Bonferroni post hoc test). Cohorts contained 3-4 hearts and each heart was assayed in duplicate.

* $p < 0.05$
*** $p < 0.001$

Due to the variation observed in the enzyme activity assay after immunoprecipitation, the experiment was repeated with the remaining frozen tissue in the same manner as described above, except no groups were resuspended in 10 mM SOV. In the second experiment, the duration of the assay was increased to 180 minutes, but for comparative purposes, DIFMU production at $t = 120$ was used for data analysis (Table 3.1). In the second experiment, the 50 nM, 100 nM, and DMSO cohorts had significantly lower DIFMU production from $t = 90$ minutes until the end of experimentation when compared to control (Figure 3.6). Therefore, all groups were compared to DMSO. The control cohort had a significantly higher DIFMU production than DMSO ($p = 0.0068$) and the 50 nM cohort had a significantly lower DIFMU production than DMSO ($p = 0.0416$). Although the amount of DIFMU produced in the 100 nM cohort was not significantly different than that produced in the 50 nM cohort, it was not significantly lower than DIFMU produced by the DMSO cohort.

Table 3.3 - Amount of DIFMU produced at $t = 120$ minutes in second experiment
DIFMU production in hearts perfused with either 10 nM, 50 nM or 100 nM OA, KHB, or 0.13% DMSO was measured over 120 minutes. All groups, including the DMSO vehicle, had significantly decreased DIFMU production when compared to control at $t = 120$ minutes, thus all groups were compared to DMSO. Only 50 nM OA administration resulted in reduced DIFMU production.

	Amount of DIFMU (nmol) at $t = 120$ minutes	significance
KHB (control)	2.43 ± 0.13	$p = 0.0068$
0.13% DMSO (vehicle)	2.14 ± 0.22	-
10 nM OA	2.28 ± 0.49	$p = 0.7197$
50 nM OA	1.91 ± 0.33	$p = 0.0416$
100 nM OA	1.97 ± 0.42	$p = 0.2056$

Data analysed by two-way ANOVA with Dunnett's post-hoc and expressed as mean \pm SD. $n = 3-4$ hearts per group, where each heart sample was assayed in duplicate.

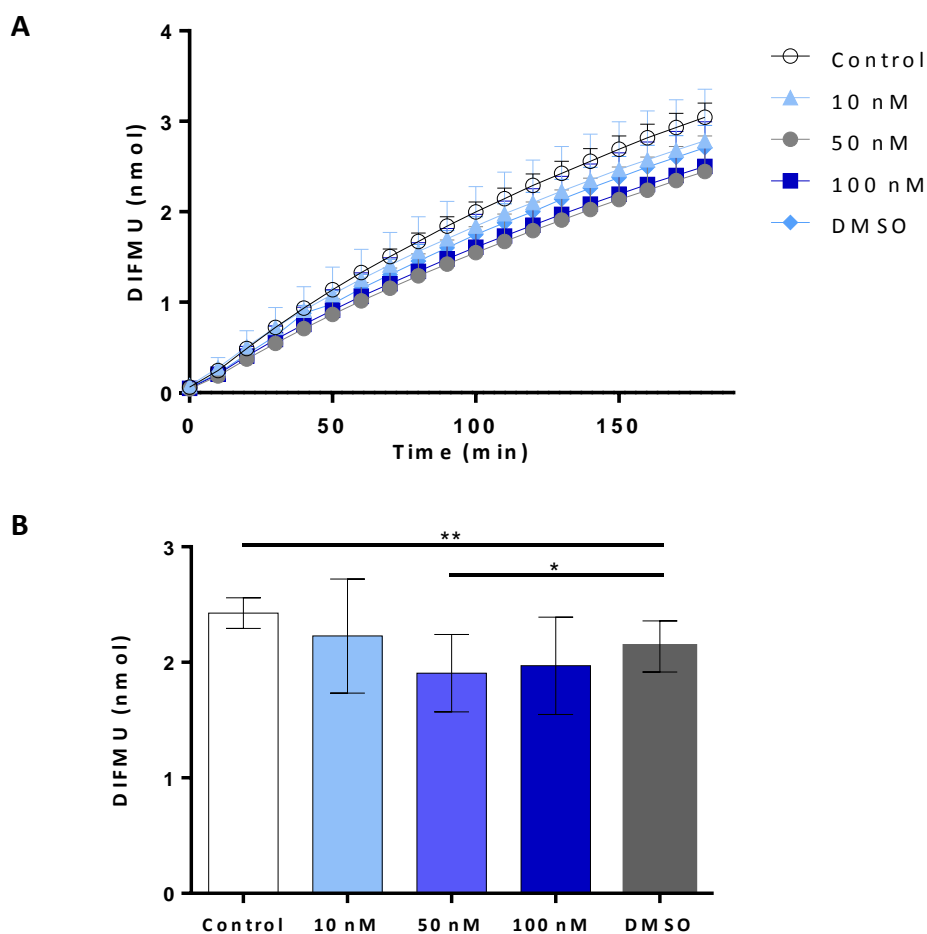


Figure 3.6 - DIFMU production from PP2A immunoprecipitated from hearts perfused with 10, 50, and 100 nM OA, DMSO, or KHB resuspended in assay buffer – second experiment.

PP2A was immunoprecipitated from hearts which were perfused with either 10 nM, 50 nM, 100 nM, 0.13% DMSO, or KHB (control; $n = 3-4$). DIFMU production over time (A) in the 50 nM, 100 nM, and DMSO cohorts were significantly lower when compared to control at $t = 90$ minutes ($p < 0.05$). At the end of experimentation (B), only the 50 nM cohort had significantly lower DIFMU production when compared to DMSO ($p < 0.05$). Each sample was assayed in duplicate. Data expressed as mean \pm SD of groups over time.

* $p < 0.05$

** $p < 0.01$

3.4 DISCUSSION

The aim of these experiments was to determine the optimal concentration of OA to administer *ex vivo* that would result in PP2A inhibition (measured *in vitro*). Enzyme activity was measured by the amount of DIFMU produced. In the first enzyme activity assay, only hearts perfused with 100 nM OA had significantly decreased DIFMU production when compared to control (0.50 ± 0.087 nmol vs. 0.85 ± 0.15 nmol DIFMU). In the repeated assay, both 50 nM and 100 nM OA, as well as the DMSO cohort had decreased DIFMU production when compared to control. Accordingly, all

cohorts were compared to DMSO. Although 50 nM and 100 nM administration resulted in a comparable amount of DIFMU production (1.91 ± 0.33 nmol and 1.97 ± 0.42 nmol, respectively) only 50 nM resulted in significantly lower DIFMU production when compared to DMSO.

Much variation between the technical repeats of the cohorts (0.1 – 0.5 nmol DIFMU), as well as variation between the first and second (repeated) experiments were observed, despite the use of the same heart tissue, antibody, bead, enzyme assay kit, and detection protocol. The variation could possibly be attributed to pipetting errors during the washing and recovery of the antibody-bead complexes, and/or inconsistent loading of antibody-bead complexes into the 96-well plate. Hearts perfused with 10 nM OA displayed an increase in DIFMU production in the first experiment, which might also be attributed to inconsistent loading.

To determine the concentration of inhibitor to use for future experimentation, both 100 nM and 50 nM were considered, as they both resulted in the reduction of PP2A activity. Although this is substantially higher than the IC_{50} for PP2A (0.1 – 1 nM), studies using the isolated heart system have reported using values between 10 nM and 100 nM (Weinbrenner, Baines, *et al.*, 1998; Fenton, Dickson and Dobson, 2005; Fan *et al.*, 2010; Sariahmetoglu *et al.*, 2012; Van Vuuren, 2014). As stated previously, OA is extremely hydrophobic and able to penetrate the cell membrane, but may also accumulate within the cell membrane (Herzig and Neumann, 2000; Swingle, Ni and Honkanen, 2007). Thus, the amount of OA in the perfusate does not reflect the final intracellular concentration of OA nor the *in vitro* IC_{50} values for PP2A and PP1. Although 100 nM OA will result in inhibition of PP2A, using concentrations of inhibitor that are higher than necessary may result in the inhibition of PP1. As there are no simple methods of selectively determining PP1 activity, there would be uncertainty regarding the possible interference of PP1 inhibition, especially since PP1 and PP2A share some downstream targets. To minimize the possibility of PP1 inhibition, the lowest concentration of OA that reduces PP2A activity must be used. Our results indicate that both 50 nM and 100 nM OA inhibit PP2A. As reports in literature indicate that 100 nM OA inhibits PP1 (Fenton, Dickson and Dobson, 2005), 50 nM OA was selected for further experimentation.

An unexpected result of this experiment was the inhibition of enzyme activity by SOV. This may indicate that enzyme activity was due to a large amount of contaminating tyrosine phosphatases, although it is unlikely, as the PP2A antibody used would have had to non-specifically bind a large and diverse population of tyrosine phosphatases. Alternatively, SOV is a phosphate analogue and acts as a reversible, competitive, inhibitor of protein tyrosine phosphatases (PTPs) (Crans *et al.*,

2004). It is commonly added in lysis buffers, along with protease inhibitors and other phosphatase inhibitors, such as sodium fluoride (NaF, a serine/threonine phosphatase inhibitor). This is done to preserve the intracellular phosphorylation state of the cellular environment. Although the effects of SOV on PP2A activity are poorly documented, SOV is assumed to be ineffective at inhibiting PP2A, as PP2A has been described in literature as the most “vanadate-resistant” phosphatase (Alessi *et al.*, 1995). This rationale was the basis for the selection of SOV as a negative control of inhibition. However, significant and unexpected enzyme inhibition by SOV was observed, contrary to existing literature.

As a phosphate analogue, SOV should theoretically fit within the active site of PP2A (like its phosphate targets), and depending on the strength of its binding, interfere with enzyme activity. SOV is also a competitive inhibitor (Crans *et al.*, 2004) and increasing the concentration of inhibitor would yield greater inhibition. This effect would be more pronounced in a purified setting, such as immunoprecipitation. SOV is known to be specific to PTPs at low concentrations but may become less specific to PTPs at higher concentrations and result in the inhibition of other phosphatases.

What remains to be investigated is whether the inhibition of PP2A by SOV observed in this experiment also occurs in a cellular system and not just in a purified setting, at which concentration this inhibition occurs, the type of inhibition, and whether this is physiologically relevant. This will be the focus of chapter four.

3.5 LIMITATIONS

A major limitation of this experiment is the lack of methods to measure specific phosphatase activity. Currently, there are a few methods to determine phosphatase activity *in vitro* by using either radiolabelled substrates, or non-protein substrates in colorimetric and fluorescence assays. The EnzChek® Phosphatase Assay Kit used in this study is a fluorescence-based phosphatase assay, which has several advantages. First, fluorescence-based assays have a greater sensitivity and lower limits of detection than colorimetric assays, requiring less enzyme and substrate (Wegner *et al.*, 2007). Second, the amount of time required to prepare the substrate is significantly less than that required in radioactive assays. Lastly, the DIFMUP substrate is non-specific and can be dephosphorylated by any phosphatase at a neutral pH, unlike 4-methylumbelliferyl phosphate assays that require an alkaline environment (ThermoScientific,

2004). However, this presents a problem when attempting to measure specific phosphatase activity (such as PP2A) within cardiac tissue that contains a diversity of phosphatases. There are no synthetic substrates available that are specific to PP2A, nor are there sufficiently specific phosphatase inhibitors that inhibit PP2A without influencing PP1 or PP4. Like okadaic acid, most inhibitors are relatively selective for certain phosphatases, but this is dependent on the concentration of inhibitor used and becomes limiting in an *ex vivo* setting. Thus, to purify PP2A, immunoprecipitation was utilized in the experiment. However, when the immunoprecipitated samples were compared to their corresponding whole cell lysate supernatant, it was evident that not all PP2A was immunoprecipitated from the samples. In addition, the amount of PP2A present in the immunoprecipitate was not consistent between samples, which may have contributed to the variation observed in the enzyme activity assay (Figure 3.3).

Finally, the observed variation may also, in part, be due to differences in coronary flow of hearts during administration of the drug. The amount of OA in the intracellular environment is dependent on the amount of perfusate that reaches the heart. Although, non-significant when compared to control, coronary flow varied within cohorts and is also a factor that influences the amount of OA available to inhibit PP2A.

CHAPTER FOUR

THE INHIBITORY EFFECTS OF SODIUM ORTHOVANADATE ON PP2A

4.1 RATIONALE

In chapter three, 10 mM sodium orthovanadate (SOV) added to immunoprecipitated PP2A resulted in significant inhibition of PP2A, a phosphatase reported to be resistant to inhibition by vanadium compounds (Alessi *et al.*, 1995).

SOV is considered a phosphate analogue (Figure 4.1), as it has a similar structure to that of an inorganic phosphate and functions as a transition state

analogue for the phosphatase-catalysed reaction (Guan and Dixon, 1991). SOV complexes with the cysteine residue located within the active site of PTPs and forms a thiol-vanadyl ester bond that resembles the thiol-phosphate bond that forms during a dephosphorylation reaction (Huyer *et al.*, 1997). In this manner, SOV acts as a competitive inhibitor of PTPs. Other vanadium compounds, such as pervanadate, can act as irreversible inhibitors by oxidizing the cysteine residue (Huyer *et al.*, 1997).

Phosphatases are divided into four classes based on sequence homology of their catalytic domains. Alkaline phosphatases possess a serine residue and its hydroxyl group forms a covalent bond with the target phosphate group. Acid phosphatases and some protein phosphatases contain a histidine residue and its imidazole group forms the covalent bond with the phosphate groups. PTPs contain a cysteine residue that forms a thiol bond with the phosphate group, and serine/threonine phosphatases contain metal ions in the active site that facilitate the hydrolysis of the phosphate group (Barford, Das and Egloff, 1998). Based on the structure of the active site, different classes of phosphatases will interact with vanadium compounds in different manners, which may account for the variation in the degree of inhibition by vanadium compounds (Crans *et al.*, 2004).

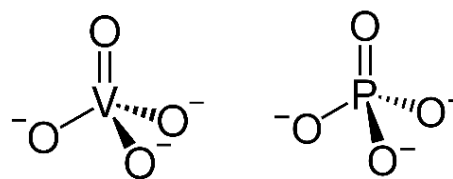


Figure 4.1 - Vanadate is a phosphate analogue

Vanadate (left) has a similar structure to a phosphate molecule (right) and binds to the active site of tyrosine phosphatases.

Images: commons.wikimedia.org

As a phosphate analogue, SOV should theoretically fit within the active site of PP2A. However, as PP2A does not possess a cysteine residue in its active site, the degree of inhibition observed would most likely be less pronounced than that of PTPs. As an extensive literature search did not provide clear evidence of SOV's effect on PP2A the aim of this chapter is therefore to confirm the data presented in chapter three that SOV is able to inhibit PP2A. Furthermore, we set out to determine at what concentration this inhibition is observed, the enzyme kinetics thereof, and whether this is likely to be seen in an *in vivo* setting.

4.2 METHODS

4.2.1 SOV inhibition in purified enzymes

SOV was prepared according to the method described by Gordon (1991) where the solution was adjusted to pH 10.0 (the solution turns yellow) and boiled until clear. The solution was cooled, and the process repeated until the solution was clear at pH 10.0. To determine whether the inhibition observed in chapter three could be reproduced, SOV was administered at the same concentration, 10 mM, to commercially obtained purified PP2A (Sigma Aldrich; cat: P6993). A purified tyrosine phosphatase, PTP1 β (Sigma Aldrich; cat: SRP0213), was also utilized as it is a known target of SOV. PP2A and PTP1 β were diluted to a final concentration of 0.5 U/ml and 200 ng/ml, respectively, as determined by optimization experiments (data not shown). Enzymes were treated with either 10 mM SOV, 50 nM OA, 2 μ M bisperoxovanadium(phen) (bpV (phen); Sigma Aldrich; cat: SML0889), or assay buffer. OA served as a positive control of PP2A inhibition, while bpV (phen) (a vanadium compound used as an inhibitor of PTP1 β) served as a positive control of PTP1 β inhibition. Enzyme activity was measured using the The EnzChek[®] Phosphatase Assay Kit, with an adaptation to the manufacturer's protocol (Molecular Probes Inc, 2004) in which 50 μ l of enzyme, 25 μ l of inhibitor (OA, SOV, or bpV(phen)), and 25 μ l of DIFMUP were added to a 96-well microplate. Enzyme activity in the presence of an inhibitor was compared to enzyme activity in the untreated controls (assay buffer). Fluorescence was measured at five-minute intervals for 120 minutes.

Once inhibition was confirmed, another fluorescence-based activity assay was conducted to determine enzyme kinetics. To determine the degree of inhibition, PP2A at a final concentration of 0.5 U/ml in each well was exposed to varying concentrations of SOV (0.625 – 10 mM) and 100 μ M of substrate (DIPMUP; see chapter two). The Michaelis–Menten constant (K_m) and maximum

velocity (V_{\max}) were determined under different substrate concentrations (25 - 200 μM) in the presence of PP2A (0.25 U/ml) and either 0.5 mM, 1 mM, or 5 mM SOV, or assay buffer (control). Fluorescence was measured at 10-minute intervals for 180 minutes.

4.2.2 SOV inhibition in cardiac lysates

Since competitive inhibition can be overcome by the addition of substrate, the aim of the next set of experiments was to determine whether inhibition of PP2A by SOV is still seen in an environment where other substrates are present, such as a whole cell lysate. However, measuring specific phosphatase activity is impossible without the use of inhibitors to distinguish between different phosphatases and purifying the PP2A may not provide an accurate representation of the environment within the whole cell lysate. Therefore, two experiments were conducted to assess whether SOV interacts with PP2A in the whole cell lysate and whether this affects PP2A activity.

In the first set of experiments, cardiac lysates were prepared from a previously frozen perfused control sample that did not receive any drug or undergo ischaemia or reperfusion. The sample was divided into four groups, each containing four samples (assayed in duplicate). Each group was treated with either assay buffer (control), 100 nM OA, 1 mM SOV, or 10 mM SOV. Enzyme activity was measured using the EnzChek[®] Phosphatase Assay Kit according to the manufacturer's protocol, in which 50 μl of each sample and 50 μl of DIFMUP were added to a 96-well microplate. Fluorescence was measured continuously at 10-minute intervals for three hours and at $t = 60$ minutes, 10 μl of additional inhibitor (100 nM OA, 1 mM SOV, or 10 mM SOV) or assay buffer was added to each of the four samples in each group (Figure 4.2). If SOV inhibits PP2A in lysates, then addition of a PP2A inhibitor (OA) should not result in a further reduction of product formation or enzyme velocity, as PP2A would already be inhibited by SOV. Inhibitor was also added at the same concentration already present in the lysates (such as 1 mM SOV added to 1 mM SOV pre-treated lysates, or 100 nM OA added to 100 nM OA pre-treated lysates) to maintain the same concentration of inhibitor during the change in volume. To reduce the number of variables in this experiment, the amount of enzyme and substrate were not replenished.

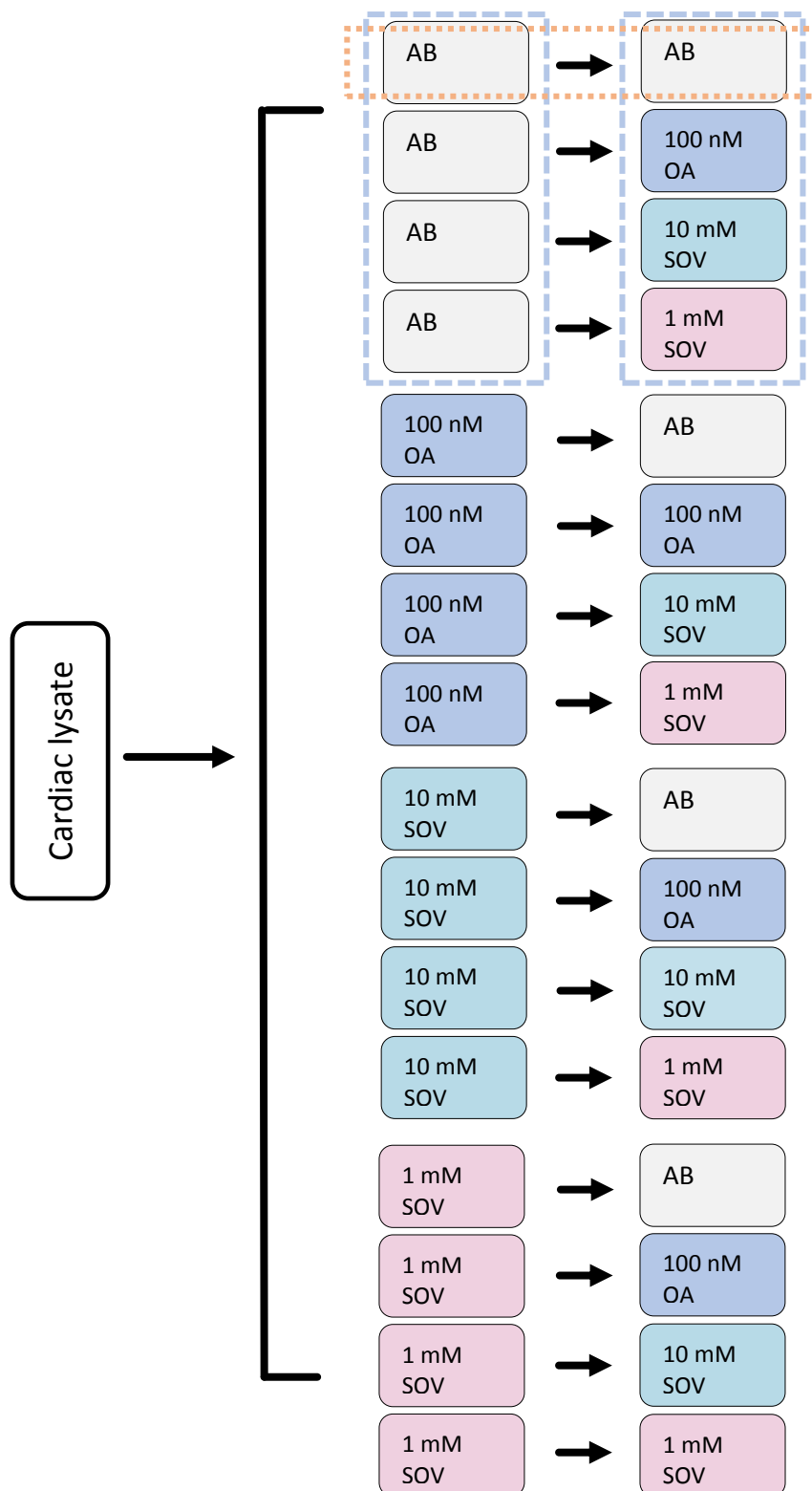


Figure 4.2 - Experimental design of the effects of inhibitors on total phosphatase activity

A cardiac sample ($n = 1$) was divided into four groups containing four samples each and treated with either assay buffer (AB), 100 nM OA, 10 mM SOV, or 1 mM SOV. Enzyme activity was measured every 10 minutes. At $t = 60$ minutes, additional inhibitor or assay buffer was added to each of the samples and measurements continued for another 120 minutes. Dashed boxes indicate the different statistical comparisons that were performed: Rates before (and after) the addition of inhibitor for all samples in a group were compared (blue), and the change in rate after the addition of inhibitor was compared for each sample (orange). Assay was conducted in duplicate. AB = assay buffer, OA = okadaic acid, SOV = sodium orthovanadate

In the second experiment, PP2A was immunoprecipitated from lysates treated with either 1 mM SOV, 10 mM SOV, or assay buffer (control). This would also give an indication of the strength of this interaction if SOV co-immunoprecipitates with PP2A. Enzyme activity was measured using the EnzChek® Phosphatase Assay Kit according to the manufacturer's protocol. Measurements were taken at 10-minute intervals for 180 minutes.

4.2.3 SOV administered in the isolated working heart

To determine whether SOV administered *ex vivo* could influence PP2A *in vitro*, mouse hearts (n = 3 per group) were perfused with SOV or KHB (control) for 20 minutes following a 15-minute retrograde and 15-minute antegrade perfusion (Figure 4.3). A concentration of 1 mM SOV was selected, as our data indicated that SOV inhibits PP2A at this concentration, and it is in the range of concentrations used previously in literature (Donthi, Huisamen and Lochner, 2000). Hearts were immediately freeze-clamped and stored in liquid nitrogen. Lysates were prepared from frozen tissue as described in chapter two. The protein concentration of all samples was adjusted to 1.5 µg/µl and an aliquot of each sample was used to measure total phosphatase activity. The remaining 200 µl of samples were incubated overnight at 4 °C with 20 µl PP2A immunoprecipitation antibody (Santa Cruz Biotechnology Inc.; cat: sc-6110), and then again incubated for three hours at 4 °C with Agarose A bead. Phosphatase activity in both the IP and total lysates was measured using the EnzChek® Phosphatase Assay Kit according to the manufacturer's protocol. Measurements were taken at 10-minute intervals for 180 minutes.

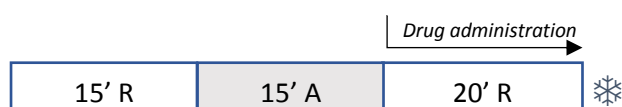


Figure 4.3 - Perfusion protocol for SOV administration

Hearts were perfused in retrograde mode for 15 minutes, in antegrade mode for 15 minutes to determine function, and again in retrograde mode for 20 minutes, where 1 mM SOV was administered. The hearts were then freeze clamped for further experimentation. n = 3 hearts per cohort.

R = retrograde perfusion, A = antegrade perfusion, ❄ = freeze clamping.

4.2.4 Data and statistical analysis

Data were exported to an Excel spreadsheet (Microsoft, USA) where the measured fluorescence was corrected for background fluorescence by subtracting the amount of fluorescence generated

by wells containing only assay buffer and DiFMUP. For experiments in lysates where additional inhibitor was added to each sample, DIFMU production before the addition was calculated from a linear curve generated from the standard that was included on the microplate. DIFMU production after additional inhibitor was calculated from the same standard to which 10 μ l of assay buffer was added in order to account for the change in volume. Data were then exported to GraphPad® Prism.

To determine the IC_{50} , the percentage remaining activity of PP2A was plotted against the log transformed concentration of inhibitor (SOV). Enzyme velocity (pmol DIFMU/min) and substrate concentration (μ M) data were fit to the Michaelis-Menten equation using the nonlinear least squares function. K_m and V_{max} were determined by the best fitted model (as determined by GraphPad® Prism). The inhibition profile was determined by a Lineweaver Burk (double reciprocal) plot of $1/V_{max}$ against $1/K_m$.

All experiments were analysed in GraphPad® Prism. For experiments where lysates were pre-treated with inhibitors and then received additional inhibitor, the rate before and after the addition was compared for each sample by using a paired Student's T-test, and the rates before and after were compared to all other samples in each group using a two-way ANOVA with a Bonferroni multiple comparison test. A p-value equal to or less than 0.05 was considered significant. Unless otherwise indicated, data are expressed as mean \pm SD.

4.3 RESULTS

4.3.1 SOV inhibition in purified enzymes

10 mM SOV administered to 0.5 U/ml PP2A resulted in significant reduction in DIFMU production when compared to control (31.04 ± 0.24 pmol vs 249.72 ± 21.61 pmol DIFMU at 120 minutes, $p < 0.0001$; Figure 4.4). As expected, 10 mM SOV administered to 200 ng/ml PTP1 β resulted in decreased DIFMU production when compared to control (101.64 ± 0.24 pmol vs $1,113.45 \pm 29.31$ pmol DIFMU produced at 120 minutes, $p < 0.0001$; Figure 4.5). DIFMU production decreased with increasing concentrations of SOV and the IC_{50} value was calculated to be approximately 2.2 mM (Figure 4.6).

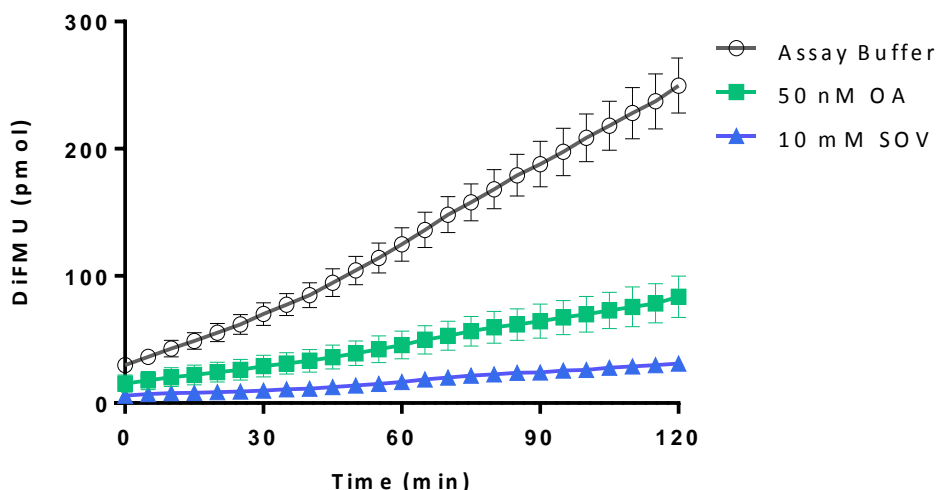


Figure 4.4 - The effect of 10 mM SOV on purified PP2A

DIFMU production was significantly reduced in the 10 mM SOV cohort when compared to that of the assay buffer (control) cohort ($p < 0.0001$). 50 nM OA served as a positive control of PP2A inhibition and significantly reduced DIFMU production ($p < 0.0001$). Data are expressed as mean \pm SD of two technical repeats over time. OA = okadaic acid, SOV = sodium orthovanadate

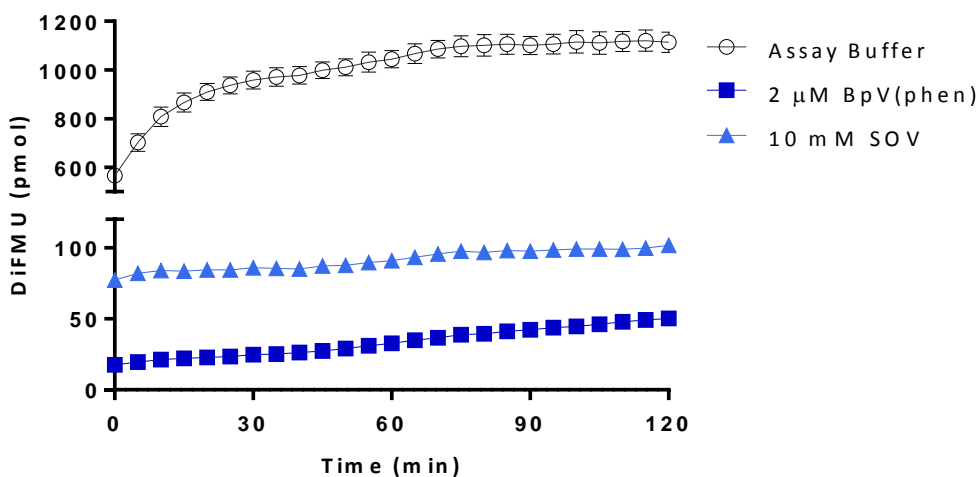


Figure 4.5 - The effect of 10 mM SOV on purified PTP1B

PTP1B activity was reduced in the presence of both 10 mM SOV and 2 μM BpV(phen), vanadium compounds that are known inhibitors of tyrosine phosphatases. Data are expressed as mean \pm SD of two technical repeats. BpV(phen) = bisperoxovanadium, SOV = sodium orthovanadate

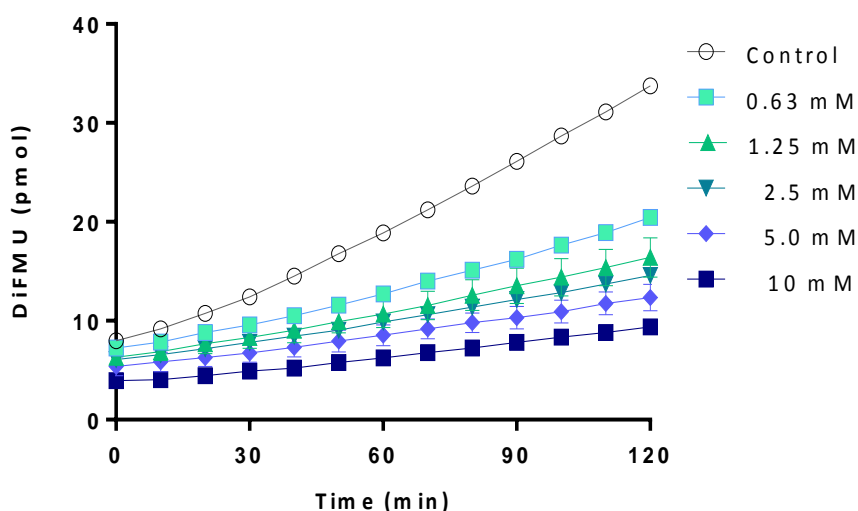


Figure 4.6- Activity of purified PP2A in the presence of increasing concentrations of SOV
 PP2A activity decreases with increasing concentrations of SOV. Significant inhibition was observed for all concentrations of SOV when compared to PP2A activity in the presence of assay buffer (control) ($p < 0.0001$). Data are expressed as mean \pm SD of two technical repeats.
 SOV = sodium orthovanadate

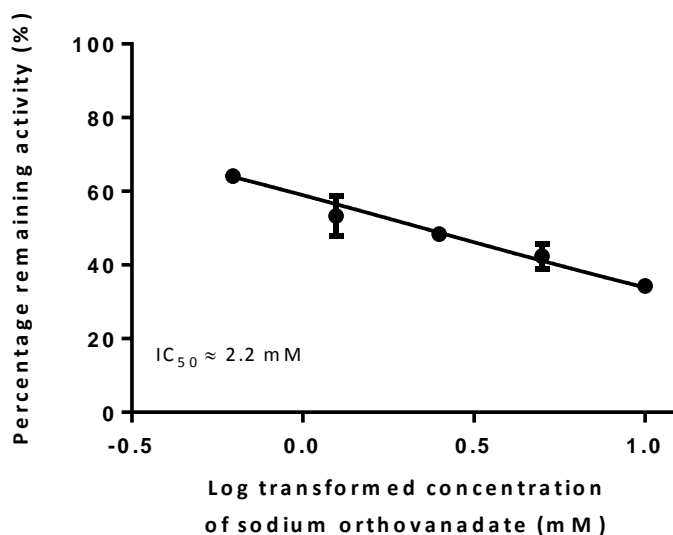


Figure 4.6 - Calculated IC_{50} of SOV inhibition of purified PP2A
 0.25 U/ml PP2A was incubated at increasing concentrations of SOV (0.625 – 10 mM) for 120 minutes. 2.2 mM SOV resulted in a 50% reduction in enzyme activity. Data are expressed as mean \pm SD of two technical repeats
 SOV = sodium orthovanadate

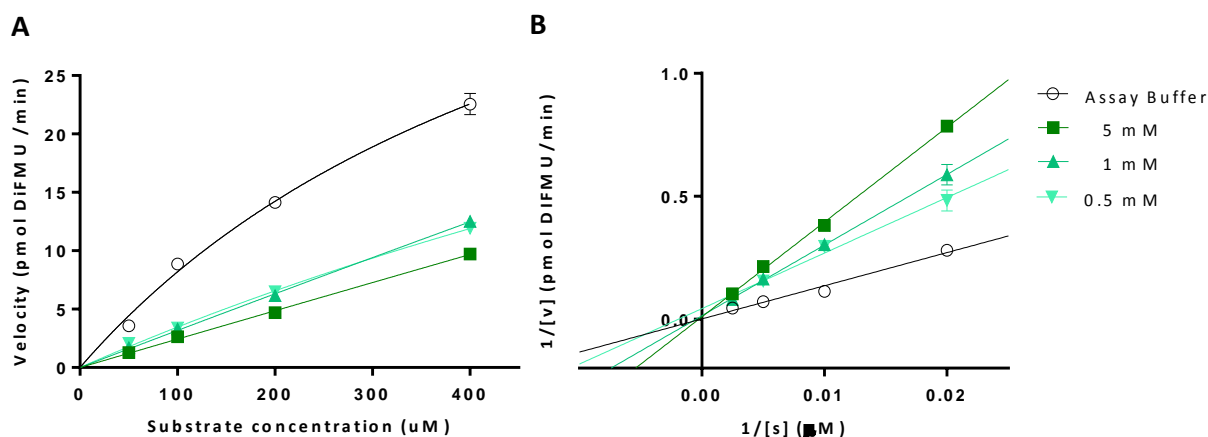


Figure 4.7 - Kinetic parameters of SOV inhibition

(A) shows PP2A enzyme activity in the presence and absence of inhibitors fitted to the Michaelis-Menten model. The K_m for PP2A was calculated to be $624.9 \mu\text{M}$ in the absence of inhibitors, indicating that PP2A possesses weak affinity for the DIFMUP substrate. The K_{mapp} appears to increase to $1,236 \mu\text{M}$ in the presence of 0.5 mM SOV, to $5,975 \mu\text{M}$ in the presence of 1 mM SOV, and to $6,544 \mu\text{M}$ in the presence of 5 mM SOV. V_{max} was calculated to be $59.55 \text{ pmol DIFMU/min}$ in the absence of inhibitors and could not be reliably calculated for PP2A activity in the presence of inhibitors. The mode of inhibition as determined by the Lineweaver-Burk plot matches that of competitive inhibition. Data are expressed as mean \pm SD. $n = 2$, including two technical repeats.

SOV = sodium orthovanadate

The K_m for the control reaction was calculated to be $624.9 \mu\text{M}$, indicating that PP2A possesses weak affinity for the DIFMUP substrate. The K_{mapp} (apparent K_m ; K_m in the presence of an inhibitor) increased with increasing concentration of inhibitor: $1,236 \mu\text{M}$ in the presence of 0.5 mM SOV, $5,975 \mu\text{M}$ in the presence of 1 mM SOV, and $6,544 \mu\text{M}$ in the presence of 5 mM SOV, indicating that PP2A has even less affinity for the DIFMUP substrate in the presence of SOV (Figure 4.8 A). V_{max} was calculated to be $59.55 \text{ pmol DIFMU/min}$ for the control reaction and was difficult to estimate for PP2A in the presence of inhibitors. An increase in K_{mapp} is consistent with competitive inhibition. When the data was transformed into a Lineweaver-Burk plot, the inhibition profile of increasing concentrations of SOV on PP2A activity matched that of competitive inhibitors (Figure 4.7 B).

4.3.2 SOV inhibition in cardiac lysates

Graphs of enzyme activity for lysates pre-treated with various inhibitors and then treated with additional inhibitors are shown in Figure 4.8. A comparison of rates before and after the addition of inhibitor to each sample is summarized in Table 4.1 **Error! Reference source not found.**

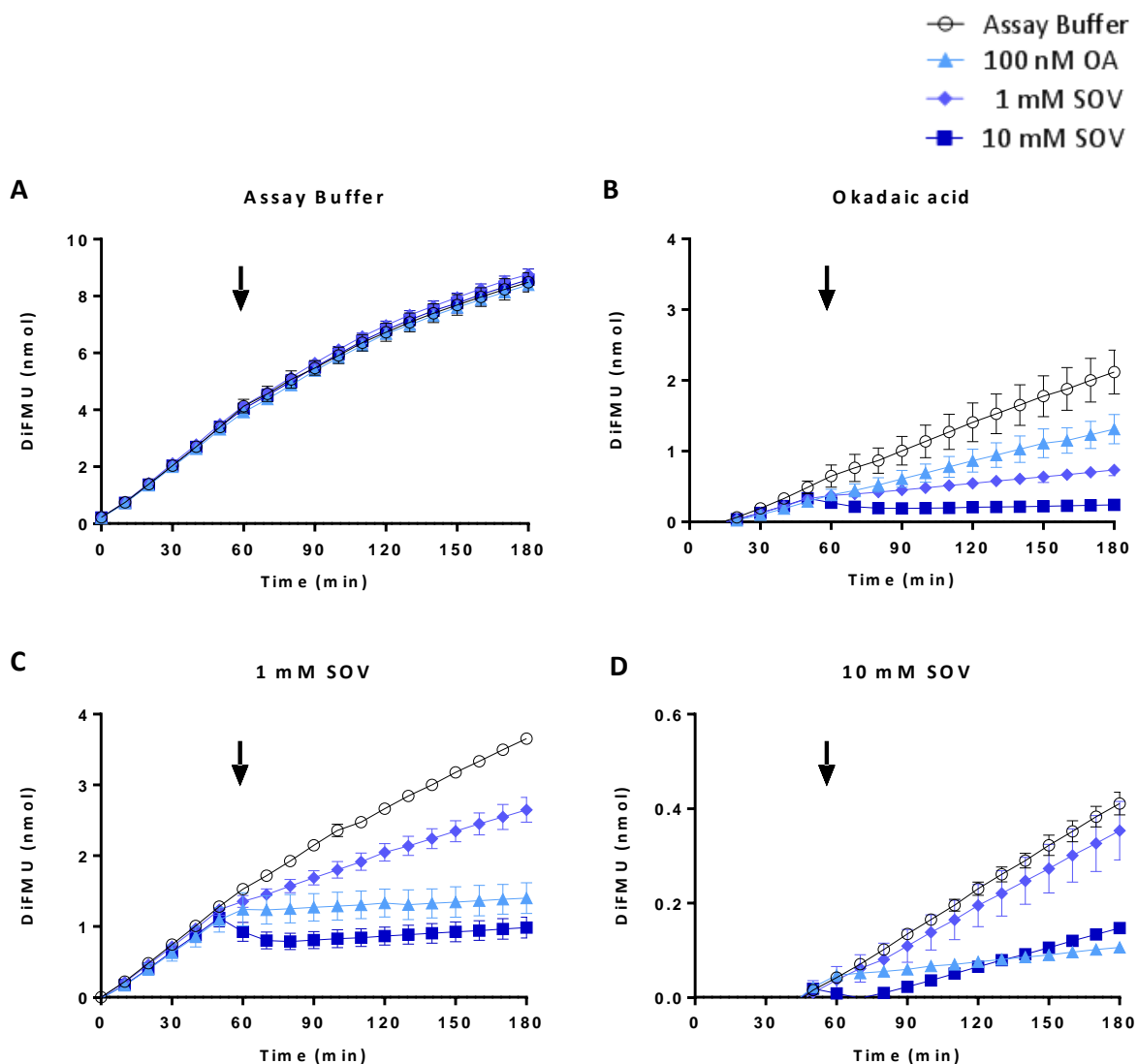


Figure 4.8 - The effects of SOV in cardiac lysates determined with different phosphatase inhibitors

A cardiac lysate ($n = 1$) was divided and treated with either assay buffer (control), 100 nM OA, 1 mM SOV, or 10 mM SOV. Phosphatase activity was measured every 10 minutes for 180 minutes. At $t = 60$ minutes, additional inhibitor was added to the wells, as indicated by the arrows. DIFMU production was the same for all samples within the same pre-treatment group. (A) shows lysates pre-treated with assay buffer that received inhibitors at $t = 60$ minutes. Although the addition of inhibitors (and assay buffer) decreased DIFMU production, the reduction in product formation was not different between the inhibitor samples. In the OA pre-treated group (B), the addition of 1 mM or 10 mM SOV reduced DIFMU production when compared to the addition of assay buffer, although the production of DIFMU did not differ before and after additional OA. In the 1 mM SOV pretreated group (C), the addition of inhibitors and assay buffer reduced DIFMU production, although the reduction in DIFMU production was significantly greater than that observed in the assay buffer group ($p < 0.001$). 100 nM OA and 10 mM SOV significantly reduced DIFMU production when compared to DIFMU production in the presence of 1 mM SOV ($p < 0.0001$). DIFMU production in the presence of 100 nM OA did not differ from the DIFMU production in the presence of 10 mM SOV ($p > 0.9999$). DIFMU production was not affected by the addition of inhibitors in the 10 mM SOV-treated groups (D). Data are expressed as mean \pm SD of two technical repeats over time. OA = okadaic acid, SOV = sodium orthovanadate

Table 4.1 - A comparison of the reaction rates before and after the addition of 10 μ l inhibitor to lysates pre-treated with either assay buffer, 100 nM OA, 1 mM SOV, or 10 mM SOV.

Rate before additional inhibitor (pmol DIFMU/min)	Inhibitor	Rate after additional inhibitor (pmol DIFMU/min)	p value
<i>Lysates pre-treated with assay buffer</i>			
31.77 \pm 1.06	Assay buffer	17.49 \pm 0.63	< 0.0001
32.77 \pm 0.19	1 mM SOV	18.58 \pm 0.49	< 0.0001
31.95 \pm 1.42	10 mM SOV	18.26 \pm 0.82	< 0.0001
31.10 \pm 0.49	100 nM OA	17.98 \pm 0.34	< 0.0001
<i>Lysates pre-treated with 100 nM OA</i>			
4.00 \pm 3.56	Assay buffer	3.93 \pm 3.44	> 0.9999
4.35 \pm 0.47	1 mM SOV	1.44 \pm 0.03	= 0.0302
4.35 \pm 0.48	10 mM SOV	0	< 0.0001
4.02 \pm 0.58	100 nM OA	3.74 \pm 0.53	> 0.9999
<i>Lysates pre-treated with 1 mM SOV</i>			
12.08 \pm 0.59	Assay buffer	8.55 \pm 0.37	< 0.0042
12.39 \pm 0.67	1 mM SOV	5.20 \pm 0.45	< 0.0001
11.41 \pm 1.16	10 mM SOV	0.24 \pm 0.07	< 0.0001
11.13 \pm 1.38	100 nM OA	0.64 \pm 0.19	< 0.0001
<i>Lysates pre-treated with 10 mM SOV</i>			
1.68 \pm 0.07	Assay Buffer	1.48 \pm 0.09	> 0.9999
1.64 \pm 0.16	1 mM SOV	1.27 \pm 0.15	> 0.9999
1.73 \pm 0.08	10 mM SOV	0.56 \pm 0.03	> 0.9999
1.71 \pm 0.02	100 nM OA	0.24 \pm 0.02	> 0.9999

For all pre-treated groups, the initial reaction velocity of each sample did not differ from those in the same pre-treatment group ($p > 0.9999$). For lysates that were pre-treated with assay buffer, the addition of inhibitor (including assay buffer) reduced enzyme velocity (Figure 4.8A; Figure 4.8 - The effects of SOV in cardiac lysates determined with different phosphatase inhibitors $p < 0.0001$). However, neither 100 nM OA, 1 mM SOV, or 10 mM SOV reduced enzyme rate when compared to assay buffer ($p > 0.9999$), indicating that the decrease in fluorescence was due to other factors, such as substrate depletion and product accumulation.

In the 100 nM OA pre-treated group, (Figure 4.8B). The addition of assay buffer at $t = 60$ minutes did not change the enzyme velocity, while the addition of SOV (1 mM SOV and 10 mM SOV) reduced the enzyme velocity when compared to the addition of assay buffer ($p < 0.0302$ for 1 mM SOV; $p = 0.0001$ for 10 mM SOV). The addition of 100 nM OA did not have any effect on enzyme velocity. Thus, both concentrations of SOV resulted in additional phosphatase inhibition, while the administration of OA to OA pre-treated lysates did not result in any additional inhibition.

In the 1 mM SOV pretreated group, the addition of inhibitors and assay buffer reduced the enzyme velocity (Figure 4.8C; $p < 0.0001$). However, the enzyme velocity was significantly reduced in the presence of inhibitors when compared to that of assay buffer ($p < 0.0001$). In addition, enzyme velocity in the presence of either 100 nM OA or 10 mM SOV was significantly reduced when compared to enzyme velocity in the presence of 1 mM SOV ($p < 0.0001$). Enzyme velocity in the presence of 100 nM OA did not differ from the enzyme velocity in the presence of 10 mM SOV ($p > 0.9999$).

For the 10 mM SOV pre-treated set of lysates, the addition of an inhibitor did not influence enzyme velocity, nor did the type of inhibitor influence enzyme velocity (Figure 4.8D; $p > 0.9999$).

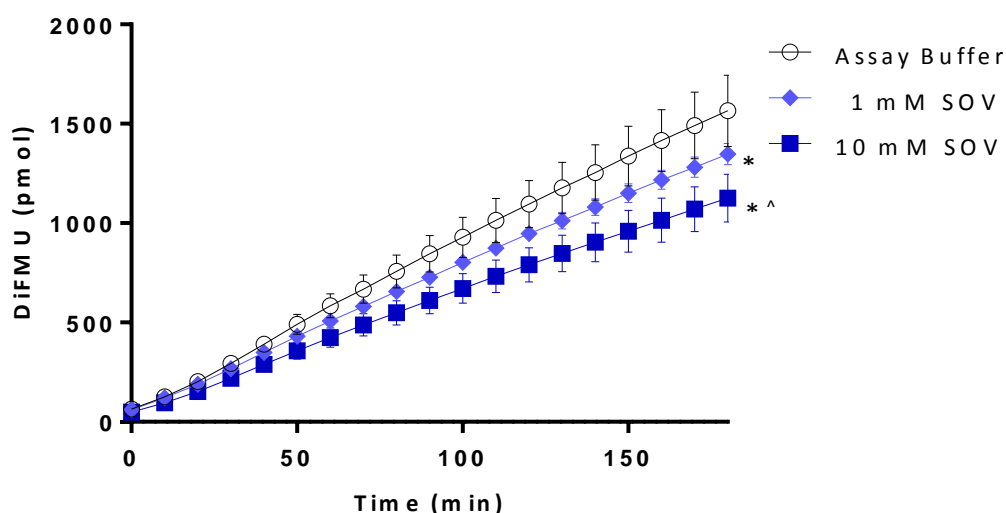


Figure 4.9 – DIFMU production of immunoprecipitated PP2A from a cardiac lysate treated with assay buffer, 1 mM SOV, or 10 mM SOV.

A cardiac lysate ($n = 1$) was divided and treated with either assay buffer (control), 1 mM SOV or 10 mM SOV. PP2A was immunoprecipitated from each sample and DIFMU production measured. At $t = 90$ minutes, DIFMU production was decreased in the 1 mM SOV ($p < 0.0474$) and 10 mM SOV groups ($p < 0.0001$) when compared to control. DIFMU production in the 10 mM group was also significantly decreased when compared to the 1 mM SOV group ($p < 0.0494$). Data are expressed as mean \pm SD of five technical repeats.

* = significant when compared to assay buffer

^ = significant when compared to 1 mM SOV

SOV = sodium orthovanadate

In the final experiment done in cardiac lysates, lysates were pre-treated with assay buffer (control), 1 mM SOV, or 10 mM SOV. PP2A was immunoprecipitated from the pre-treated lysates and enzyme activity was measured (Figure 4.9). From $t = 90$ minutes, PP2A activity was reduced

in both SOV pre-treatment groups when compared to control ($p < 0.0474$ for 1 mM SOV; $p < 0.0001$ for 10 mM SOV), and greater inhibition was seen in the 10 mM SOV treated group when compared to the 1 mM SOV group ($p < 0.0494$). A more pronounced decrease in enzyme activity was observed at the end of experimentation when compared to control ($p < 0.0001$ for both groups).

4.3.3 SOV inhibition in perfused hearts

In hearts perfused with 1 mM SOV or KHB, there were no differences in total phosphatase activity measured in lysates prepared from these hearts (Figure 4.10). In the assay measuring total phosphatase activity, enzyme activity could only be measured for 60 minutes, as the amount of fluorescence generated was similar to that of the 100 μ M standard used to determine the amount of DIFMU produced.

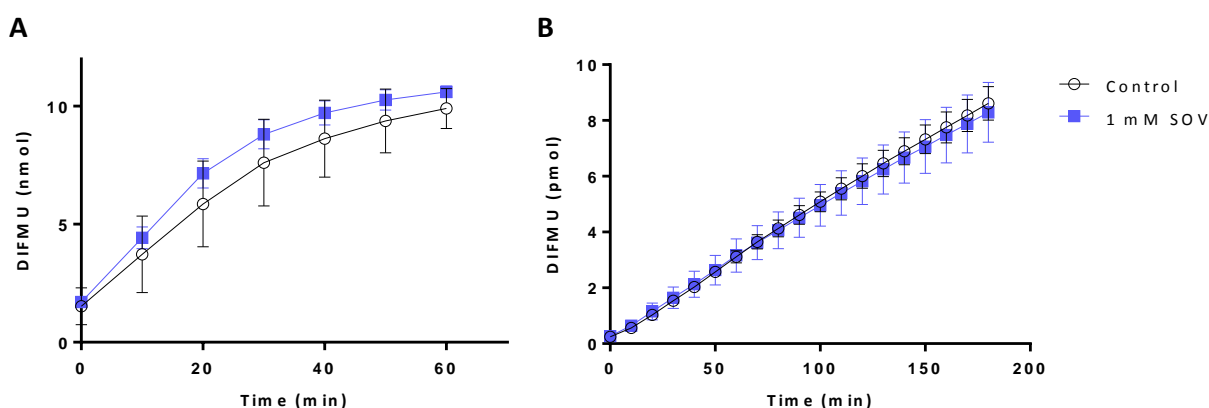


Figure 4.10 - Phosphatase activity from hearts perfused with 1 mM SOV

Hearts were perfused with either 1 mM SOV or KHB (control) for 20 minutes. 1 mM SOV did not have any effect on total phosphatase activity (A). When PP2A was immunoprecipitated from these samples, no differences in PP2A activity between the 1 mM SOV and KHB groups were observed (B). Data are expressed as mean \pm SD of quadruplicate wells; $n = 3$.

SOV = sodium orthovanadate

4.4 DISCUSSION

The aim of this set of experiments was to determine whether SOV is able to inhibit PP2A, to describe the inhibition, and to determine whether this is likely to be seen in tissue homogenates (as many researchers use SOV in lysate preparation) and an *in vivo* setting.

4.4.1 The effects of SOV on purified enzymes

For experiments conducted in purified enzymes, SOV was able to inhibit PP2A in a concentration-dependent manner. The IC_{50} value for SOV's effect on PP2A was calculated to be 2.2 mM (Figure 4.6), which is substantially higher than that associated with the inhibition of PTP's such as PTP1 β (0.02 – 1 μ M; Zhang *et al.*, 2015). This indicates that SOV is a weak inhibitor of PP2A.

The K_m data obtained would indicate that in order to achieve an optimal reaction speed, PP2A requires a relatively large concentration of DIFMUP substrate (625 μ M; Figure 4.7) when compared to other substrates of PP2A, such as phosphorylated atrial natriuretic peptide ($K_m = 42 \mu$ M; Dautzenberger, G, Muller and Richter, 1993). Thus, PP2A's dephosphorylation of DIFMUP proceeds at a slower rate than natural substrates of PP2A, which may explain why the maximum concentration of purified PP2A (as determined by optimization assays) was required for experimentation when compared to the lower enzyme concentration of PTP1 β necessary to produce a similar reaction rate (data not shown). Measuring PP2A activity with natural substrates is possible and may have given a better approximation of the kinetic parameters but requires the phosphorylation of a natural substrate with radiolabelled phosphates as a prerequisite to the experiment. This process is extremely tedious and logistically challenging.

Increasing the concentration of SOV resulted in increasing K_{mapp} values (Figure 4.7), indicating that at higher concentrations of SOV, DIFMUP dephosphorylation takes place at an even slower rate. The V_{max} for PP2A in the presence of inhibitors could not be calculated with certainty as the reaction rate proceeded too slowly. Thus, no conclusion could be drawn about how V_{max} was affected by the presence of SOV. However, when the data obtained from the Michaelis-Menten experiments were transformed into a Lineweaver-Burk plot, the $1/V_{max}$ (y-intercept) remained relatively unchanged, and the $1/K_m$ increased, which is consistent with the action of a competitive inhibitor (Figure 4.7). Therefore, it can be concluded that SOV functions as a competitive inhibitor of PP2A, which is consistent with its action on PTPs (Huyer *et al.*, 1997; Crans *et al.*, 2004).

4.4.2 The effects of SOV on lysates

The effect of SOV on phosphatase activity within tissue lysates was difficult to measure, as it required additional inhibitors to distinguish between the different phosphatases. In this particular experiment, lysates were pre-treated with either 1 mM SOV, 10 mM SOV, 100 nM OA, or assay buffer (control), and enzyme activity was measured continuously (Figure 4.8). Wells were then

treated at 60 minutes with additional inhibitor and enzyme activity was measured for another 120 minutes to determine which phosphatase families were affected by the additional inhibitor. In the group pre-treated with assay buffer, the addition of inhibitors significantly reduces enzyme rate in all samples, but the reduction was similar to the reduction in enzyme rate of the samples where assay buffer (instead of inhibitor) was added (Figure 4.8 A). The enzyme reaction proceeded without restriction resulting in significantly more product formation at $t = 50$ minutes (≈ 4 nmol) when compared the inhibitor pre-treated groups (≈ 0.1 - 0.8 nmol). This reaction for this group of samples may possibly have begun approaching plateau, where most substrate had already been converted to product, and the addition of inhibitors had no effect on the amount of fluorescence already produced. In addition, the decreasing amounts of substrate coupled with the increased fluorescence may have masked the effects of the inhibitors in that the inhibitor is acting on enzyme that already has decreasing amounts of substrate.

Although the concentrations of the additional inhibitor were calculated with a final volume of 110 μ l in mind, no additional substrate and enzyme was added together with the inhibitor addition. Therefore, the addition of assay buffer would reduce the concentration of both enzyme and substrate, resulting in a decreased rate of reaction. Interestingly, a further reduction in enzyme activity due to inhibitors was only observed when the lysates were already pre-treated with an inhibitor.

Addition of SOV (1 and 10 mM) reduced enzyme activity in the 100 nM OA pre-treated groups, indicating that phosphatases in addition to PP2A and PP1 were inhibited (Figure 4.8B). This was expected, as OA is specific to PP1, PP2A, and PP4, while SOV is a known PTP inhibitor (Crans *et al.*, 2004). The inhibition by SOV was also concentration dependent – at low concentrations it reduced phosphatase activity, but at higher concentrations, almost all phosphatase activity within the lysate ceased. This may indicate that SOV inhibits other major phosphatases such as PP1, although this cannot be confirmed with the data generated in this experiment. However, a previous study has shown that SOV inhibits PP2B (calcineurin), and unlike PP2A that requires high concentrations of SOV, PP2B is inhibited at micromolar concentrations (Fukunaga *et al.*, 2002). When lysates were pre-treated with 1 mM SOV, addition of 100 nM OA reduced enzyme activity which is expected, as OA and SOV inhibit different populations of phosphatases (Figure 4.8C). However, OA administration had no effect on phosphatase activity when lysates were treated with 10 mM SOV, indicating that PP2A may already be maximally inhibited (Figure 4.8D). In addition, when PP2A was immunoprecipitated from lysates that were treated with differing concentrations of

SOV, concentration-dependent inhibition was observed, despite the several wash steps required during immunoprecipitation (Figure 4.9). This indicates that SOV interacts with PP2A within tissue homogenates and binds tight enough to co-immunoprecipitate with PP2A. Taken together, the data suggest that SOV inhibits PP2A in lysates at concentrations commonly used in standard lysis buffer.

4.4.3 The effects of SOV on perfused hearts

Perfusions with 1 mM SOV had no effect on phosphatase activity, which was unexpected (Figure 4.10). One millimolar is significantly higher than concentrations used in previous studies using the isolated perfused heart that reported using 1 - 4 μ M (Matsubara *et al.*, 1995; Takeda *et al.*, 2003). However, it is difficult to determine whether 1 mM SOV would elicit an effect in an experiment that is free of any perturbations or stimuli of phosphatase activity: SOV was administered for 20 minutes after a stabilization period, where the heart was not subject to ischaemia, and the animal was free from pathologies. In the absence of phosphatase inhibition, phosphorylated PKB/Akt or GLUT 4 translocation could have been measured (Donthi, Huisamen and Lochner, 2000) to determine whether 1 mM SOV elicited a cellular effect that did not include phosphatase inhibition, or whether the concentration used in this study was too low.

4.4.4 Conclusion

To our knowledge, this study is the first to demonstrate that SOV is a weak, competitive inhibitor of PP2A. No other studies describing the effects of SOV on the kinetic parameters of PP2A, the inhibition of immunoprecipitated PP2A, or the effects of SOV in the isolated, perfused, rodent heart, were found during an extensive search of existing literature.

SOV is able to inhibit PP2A, but at concentrations much higher than that required for inhibition of PTPs. It is not clear whether this inhibition will be/has been observed in an *in vivo* setting, as it is dependent on the concentration of inhibitor used and this study was not able to confirm the efficacy of 1 mM SOV in eliciting a cellular response. Lower concentrations of SOV are commonly reported in literature, but few studies have reported using millimolar concentrations of SOV (Tsiani, Abdullah and Fantus, 1997; Donthi, Huisamen and Lochner, 2000). If SOV exerts its action through phosphatase inhibition at these concentrations, the effect of SOV is most likely a result of pan-phosphatase inhibition, rather than specific PTP inhibition. In addition, these results show

that the use of 1 mM SOV in standard lysis buffer results in the inhibition of PP2A while another study showed that PP2B is inhibited by even lower concentrations of SOV (Morioka *et al.*, 1998). For researchers interested in preserving the phosphorylation status of their sample, using millimolar concentrations of SOV is of no concern. However, this becomes problematic for studies on serine/threonine phosphatases where SOV is used to obtain samples free from PTP activity, or studies that used SOV under the assumption that it selectively inhibits PTPs. Thus, using lower (micromolar) concentrations of SOV may result in PTP inhibition while leaving PP2A unaffected, but will still inhibit PP2B activity.

Lastly, this study was only able to investigate SOV which is a competitive, reversible inhibitor of PTPs. However, other vanadium compounds, such as pervanadate, are irreversible inhibitors of PTP's, as they oxidize the cysteine residue in the active site (Huyer *et al.*, 1997). PP2A does not possess a cysteine residue in its catalytic site, and may be unaffected (or in the least, not irreversibly inhibited) by these compounds. However, due to time constraints, this could not be determined in this current study.

4.5 LIMITATIONS

A limitation of this study that cannot be overlooked is the small sample size. Except for the K_m and V_{max} determination that had a samples size of two, the experiments in purified enzymes and cardiac lysates were conducted on one sample with two-five technical replicates. Numerous optimization experiments were conducted with purified enzymes to determine the optimal enzyme and inhibitor concentrations, limiting the amount of purified enzyme to use in subsequent experiments. For experiments in cardiac lysates, a large sample size was not possible due to limited amounts of untreated tissue. It must be noted that SOV's effect on PP2A was initially observed in a samples size of four, with two technical replicates.

As stated previously, the EnzChek® Phosphatase Assay Kit is the most convenient phosphatase activity assay that is available (alternatives are discussed in chapter three; see "Limitations"), but the kinetic experiments conducted in this study indicate that PP2A possesses a weak affinity for the DIFMUP substrate. Given these results, it is likely that repeating these experiments using an alternative phosphatase assay may yield different results.

The *ex vivo* perfusions with SOV did not affect *in vitro* phosphatase activity. It is possible that SOV exerts effects other than phosphatase inhibition (such as GLUT4 translocation) which could have been measured.

As mentioned previously, there are no specific inhibitors available to distinguish between different phosphatases or different phosphatase families. At most, the inhibitors that are available are selective for certain phosphatases at different concentrations (for example, PP2A should be inhibited by 5 nM OA, leaving PP1 unaffected). Consequently, any experiment that aims to determine specific phosphatase activity within a sample containing multiple phosphatases must make use of various inhibitors.

CHAPTER FIVE

THE EFFECT OF PP2A INHIBITION ON INFARCT SIZE AND FUNCTIONAL RECOVERY

5.1 RATIONALE

In chapter three, we concluded that 50 nM OA administered to the heart during *ex vivo* perfusion was sufficient to inhibit PP2A activity (measured *in vitro*). Although the signalling associated with PP2A inhibition will be investigated in chapter six, it is important to first establish whether PP2A inhibition has any effect on the outcomes of myocardial I/R injury, especially since there is little consensus in literature regarding the effects of PP2A inhibition on cell survival (Weinbrenner, Baines, *et al.*, 1998; Fenton, Dickson and Dobson, 2005; Fan *et al.*, 2010; Van Vuuren, 2014). This chapter will therefore focus on the impact of PP2A inhibition on the outcome of I/R injury.

As discussed in chapter one, cell death occurs not only as a result of ischaemia, but also as a result of reperfusion, where reperfusion can account for 40-50% of the final size of infarction (Piper, García-Dorado and Ovize, 1998). It is therefore necessary to ensure that during the *ex vivo* heart perfusion protocol, the duration of reperfusion is sufficient for the complete development of infarction. Previous studies in a mouse model of I/R found 20 minutes global ischaemia (GI) and 30 minutes reperfusion to be adequate for infarct development (Xi, Hess and Kukreja, 1998; A. Khan *et al.*, 2006; Du Toit *et al.*, 2007), while other researchers employed 35 minutes ischaemia and 60 minutes reperfusion (Valls-Lacalle *et al.*, 2016). A recent study has shown increased infarction with longer duration of both ischaemia and reperfusion (Rossello *et al.*, 2016). As functional recovery was an endpoint for this study, the duration of GI needed to be long enough to result in an acceptable range of infarction (40-60%), but not so severe as to result in complete loss of function due to massive cell death or extensive stunning. The GI time was therefore set at 20 minutes with a longer reperfusion period of 60 minutes. Since DMSO may have a potential effect on enzyme activity (as hinted at in chapter three), the concentration of DMSO used to dissolve OA was reduced from 0.13% to 0.002% to minimize any effect attributed to the vehicle. Therefore, using the isolated working mouse heart model, we set out to determine the effect of PP2A inhibition on I/R injury as defined in terms of infarct size (IFS) and functional recovery.

5.2 METHODS

To determine the effect of PP2A inhibition on IFS and functional recovery, hearts were stabilized in retrograde mode for 15 minutes and perfused for 15 minutes in antegrade mode (working heart mode) to determine baseline (pre-ischaemic) function. 50 nM OA or 0.002% DMSO (vehicle control) was administered for 20 minutes in retrograde mode before 20 minutes of no-flow GI. The hearts were reperfused for a total of 60 minutes: 15 minutes in retrograde, 15 minutes in antegrade mode (as post-ischaemic function parameters can only be measured in antegrade mode), and 30 minutes in retrograde mode (Figure 5.1). Coronary flow and aortic output (during perfusion in antegrade mode) were measured by timed collection of coronary and aortic effluents at five-minute intervals during stabilization and reperfusion and expressed as volume flow per minute. Functional parameters such as systolic and diastolic pressure and heart rate, were measured by a pressure transducer (Biopac Systems Inc., USA) inserted in the aortic perfusion line and connected to a computer (AcqKnowledge, Biopac Systems Inc.). Each cohort contained 9 animals.



Figure 5.1 - Perfusion protocol for IFS determination

Hearts were perfused in retrograde mode for 15 minutes, in antegrade mode for 15 minutes to determine function, and again in retrograde mode for 20 minutes, during which time OA (50 nM) or vehicle control (0.002% DMSO) was administered. The hearts were then subjected to 20 minutes GI followed by 30 minutes reperfusion. $n = 9$.

R = retrograde perfusion, A = antegrade perfusion, GI = global ischaemia

At the end of 60 minutes reperfusion, hearts were immediately stored at -20°C and once frozen, sliced into one-millimetre thick sections, and incubated in phosphate buffer (pH 7.4) containing 1% w/v triphenyltetrazolium chloride (TTC) for 15 minutes at 36°C . The heart slices were then fixed in 10% v/v formaldehyde solution overnight at 4°C . The slices were placed between two glass plates, scanned at a high resolution, and enlarged on Paint.net © (dotPDN LLC, 2018). Using this software, the background of the image was removed, leaving only an image of the heart slices. The images were then uploaded onto Image J (W, Rasband; National Institute of Health, USA) by an individual who was not associated with this study and was blinded to the identity of the heart slices. The area of infarct was estimated visually to determine the number of pixels in the infarcted tissue, which was then expressed as a percentage of total pixels (see addendum A).

5.2.1 Data and statistical analyses

Functional data and IFS data were compiled in Microsoft Excel (Microsoft, USA). Thereafter, data were analysed in GraphPad® Prism 6.0. Coronary flow, cardiac output (CO; the sum of coronary flow and aortic output), aortic output (AO), heart rate, and systolic and diastolic pressures after ischaemia were expressed as a percentage of function prior to ischaemia. Data are expressed as mean \pm standard deviation, unless otherwise stated. A two-tailed, paired Student's T-test was used to compare pre- and post-ischaemic functions within cohorts. A two-tailed, unpaired Student's T-test was used to compare post-ischaemic functions and infarct size between cohorts. A p-value equal to or less than 0.05 was considered significant.

5.3 RESULTS

Coronary flow during drug administration did not differ between hearts perfused with OA (1.06 ± 0.34 ml/min) and that of hearts perfused with the vehicle control (1.12 ± 0.13 ml/min; Figure 5.2). In both cohorts, post-ischaemic cardiac output, aortic output, and systolic pressure were significantly decreased as compared to pre-ischaemic functions (Figure 5.3). Pre-ischaemic heart rate was not different to post-ischaemic heart rate for both cohorts. Ischaemia reduced CO, AO, and systolic pressure, and OA administration was not able to rescue, coronary flow, AO or systolic and diastolic pressures. Post-ischaemic CO in the OA cohort was significantly better when compared to DMSO ($p = 0.0412$; Figure 5.3), indicating a degree of protection. However, when these values were expressed as a percentage of pre-ischaemic function, they were non-significant (Figure 5.4A). OA administration resulted in a significant reduction in infarct size ($28 \pm 19\%$) when compared to DMSO ($56 \pm 23\%$, $n=9$; $p = 0.0106$; Figure 5.4E).

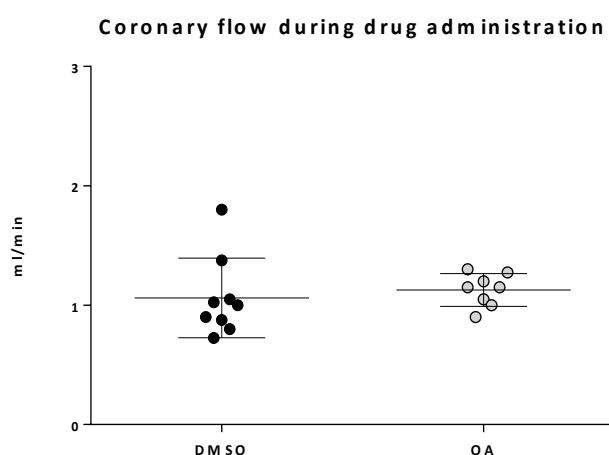


Figure 5.2 - Coronary flow during drug administration

Coronary flow was measured at five-minute intervals for the duration of drug administration. OA had no effect on coronary flow. Data are expressed as mean \pm SD ml/min. $n=9$.

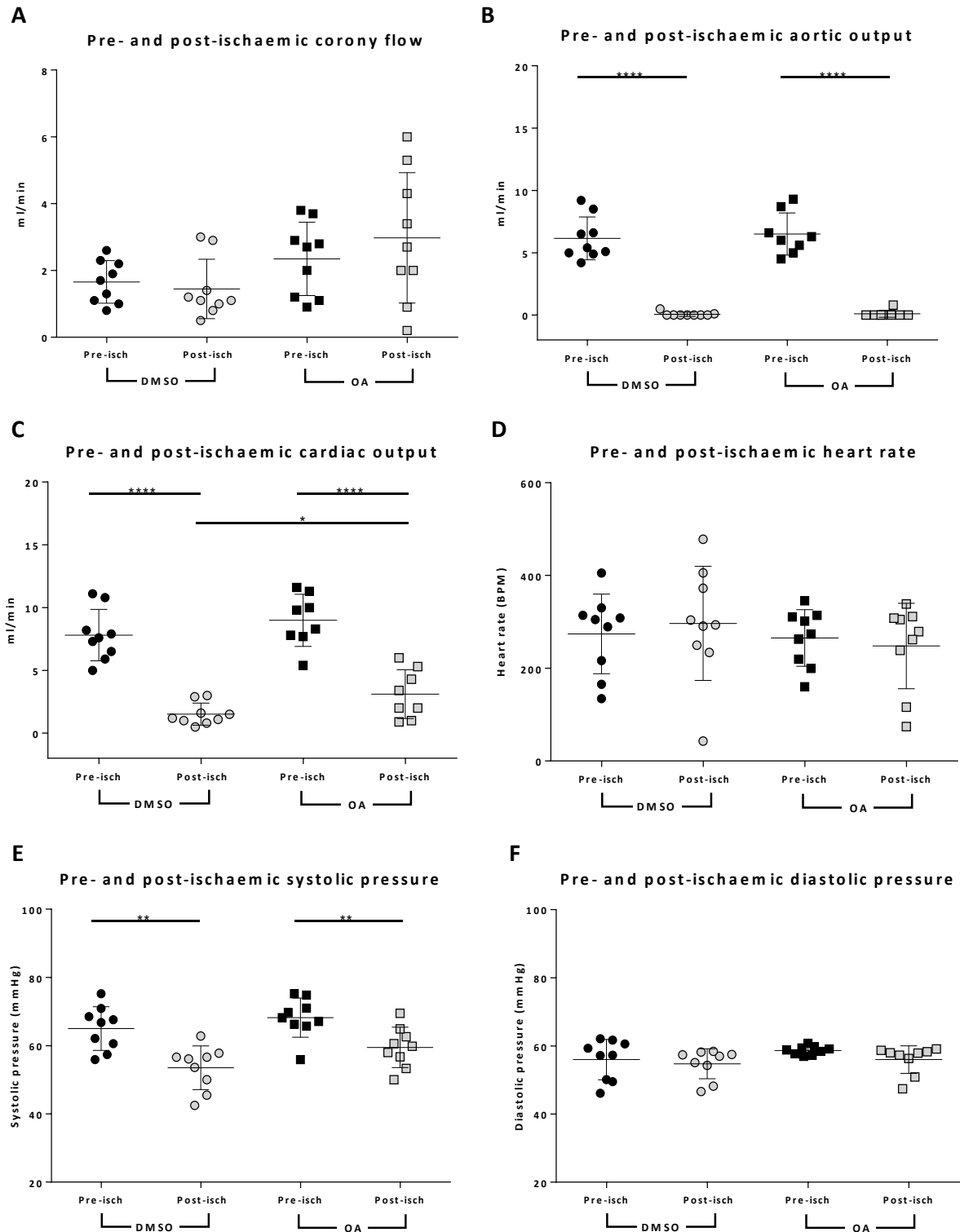


Figure 5.3 - Pre- and post-ischaemic function of hearts perfused with DMSO or OA

Coronary flow, cardiac output (aortic output and coronary flow combined), aortic output, systolic and diastolic pressure, and heart rate were measured before and after 20 minutes GI. Aortic output (B), cardiac output (C), and systolic pressure (E) were significantly decreased in both cohorts after GI ($p < 0.05$). No change in coronary flow (A), heart rate (D) or diastolic pressure (F) was observed after ischaemia when compared to control for both cohorts. OA administration improved total cardiac output ($p = 0.0412$) but not coronary flow or aortic output and had no effect on systolic and diastolic pressures and heart rate. Pressure and heart rate data were obtained by a pressure transducer connected into the aortic line. Data are expressed as mean \pm SD, $n = 9$.

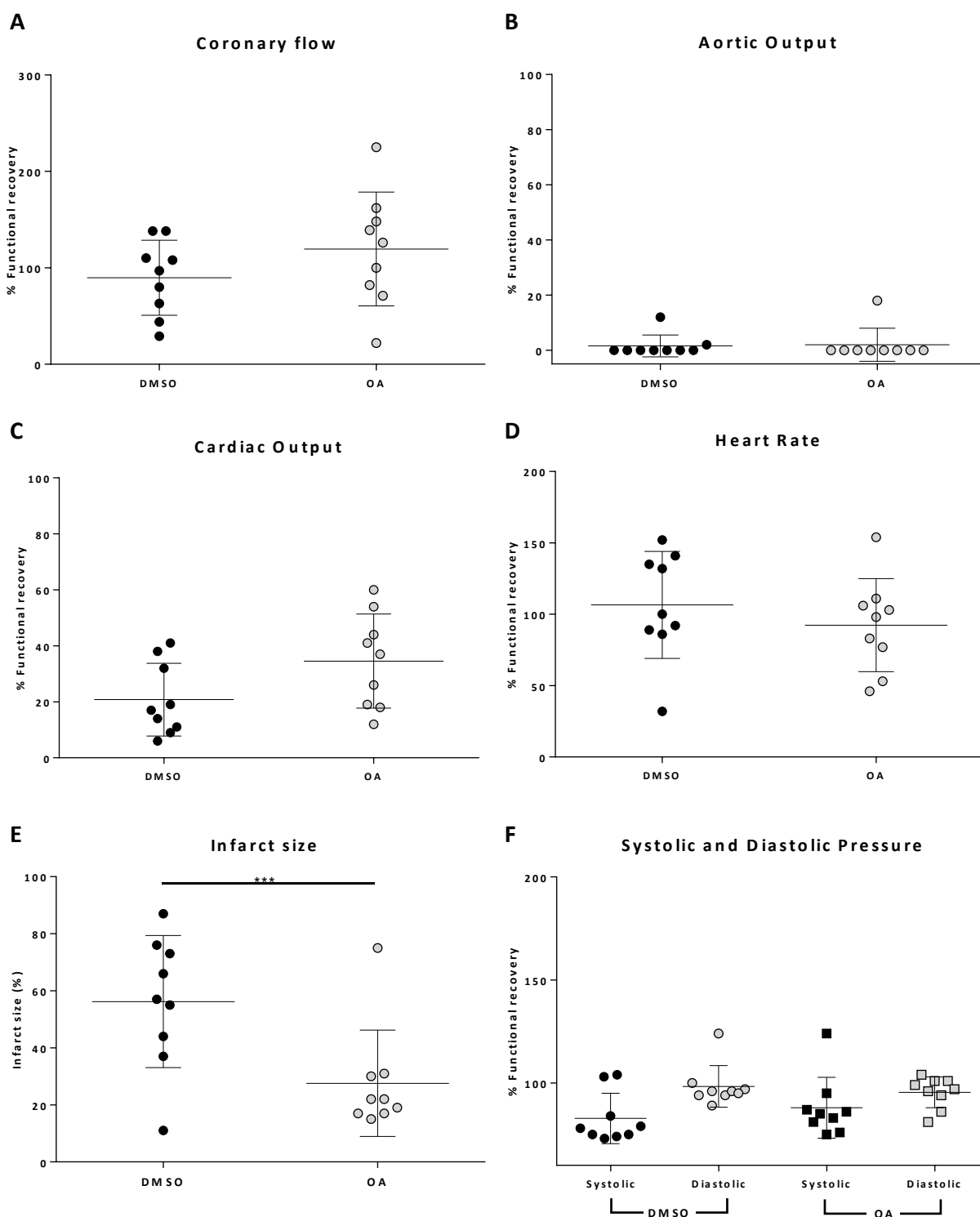


Figure 5.4 - Post-ischaemic function expressed as a percentage of pre-ischaemic (baseline) function

Hearts were exposed to 50 nM OA or 0.002% DMSO for 20 minutes prior to 20 minutes GI. OA administration resulted in a significant reduction in infarct size (E; unpaired Student's T-test, $p = 0.0106$; $n=9$), but did not rescue coronary flow (A), aortic output (B), cardiac output (C), heart rate (D) or systolic and diastolic pressure (F). Pressure and heart rate data were obtained by a pressure transducer connected into the aortic line. Data are expressed as mean \pm SD.

5.4 DISCUSSION

Having established that 50 nM OA administered to the heart during *ex vivo* perfusion was sufficient to inhibit PP2A activity, the purpose of this set of experiments was to determine whether PP2A inhibition has any effect on the outcomes of I/R injury, as the few studies from existing literature report contradictory results.

Although the effects of OA/PP2A inhibition has been studied in various models such as cardiomyocytes (Weinbrenner, Baines, *et al.*, 1998), and the isolated rabbit (Weinbrenner, Liu, *et al.*, 1998) and rat (Fenton, Dickson and Dobson, 2005; Fan *et al.*, 2010; Van Vuuren, 2014) heart, this study is the first to assess the effects of OA administration in the mouse model. In addition, this study is one of the few that utilized the *ex vivo* working heart technique in the mouse to assess function.

The endpoints of this study were functional recovery and IFS. As such, the duration of GI needed to be sufficient to result in an acceptable range of infarction, without resulting in complete loss of function due to cell death and severe stunning. The average IFS for hearts receiving only DMSO (vehicle control) was 60%, which is within an acceptable range for studies with the same endpoint, as a sufficient IFS is necessary to measure whether a given drug or intervention is effective at reducing IFS (Du Toit *et al.*, 2007; Van Vuuren, 2014; Espach, 2017; Lindsey *et al.*, 2018). Additionally, a reduction in IFS cannot be measured accurately if IFS is too small.

20-minute OA administration prior to 20 minutes ischaemia resulted in a significant increase in CO relative to vehicle control (although this was not accompanied by an increase in either coronary flow or aortic output in the OA cohort when compared to control). However, the increase in CO was not significant when expressed as a percentage of pre-ischaemic function and compared to the degree of recovery of the vehicle control. OA had no effect on coronary flow, aortic output, systolic and diastolic pressures, or heart rate. Interestingly, ischaemia had no effect on heart rate, indicating that the decrease in function was due to a failure to generate contractile force, possibly due to stunning. OA administration, did however, reduce infarct size when compared to DMSO ($28 \pm 19\%$ vs $56 \pm 23\%$; $p = 0.0106$; Figure 5.4E). These results are in agreement with similar studies on the effects of PP2A inhibition on IFS in the isolated perfused rat (van Vuuren, 2014) and rabbit (Weinbrenner, Baines, *et al.*, 1998) models. However, as mentioned, both Fenton *et al.* (2005) and Fan *et al.* (2010) report that PP2A inhibition does not reduce IFS.

In 2005, Fenton and co-workers performed a set of experiments to determine whether phosphatase inhibition enhanced preconditioning and would result in reduced IFS. For this, they used both young (3-4 months) and aged (21-22 months) rats, and using the isolated heart perfusion technique, subjected hearts to two five-minute cycles of IPC. In the first set of experiments, 100 nM OA was administered during IPC. In the second set of experiments, OA was administered during IPC and during the first 10 minutes of reperfusion. In the last set of experiments, OA was administered during both IPC and reperfusion. The hearts were subject to 45 minutes GI (for IPC protocols) or 30 minutes GI (for non-IPC protocols), followed by three hours reperfusion. When 100 nM OA was administered during IPC alone or during both IPC and reperfusion, IFS was significantly reduced in the aged heart when compared to untreated controls. However, in non-preconditioned young hearts, 100 nM OA administration prior to ischaemia did not result in any change in IFS when compared to control, but a small, significant reduction in IFS was observed when OA was administered during reperfusion alone.

Unlike the study performed by Fenton and co-workers, this present study observed a significant reduction in IFS when OA was administered prior to ischaemia. When comparing the two studies, many differences in study design become evident, some of which may account for the conflicting outcomes. First, the duration of ischaemia and reperfusion was shorter in this study (20 minutes GI and 60 minutes reperfusion) when compared to that of Fenton and co-workers (30 minutes GI and 180 minutes reperfusion). Despite this difference, both GI and reperfusion times resulted in a similar size of infarction in the control hearts ($56 \pm 23\%$, mean \pm SD; vs $57 \pm 5\%$, mean \pm standard error). Shorter durations of ischaemia results in reversible injury, and as the duration of ischaemia increases, so does the amount of irreversibly injured cardiomyocytes (Jennings *et al.*, 1960). Therefore, a shorter duration of ischaemia would result in fewer irreversibly injured cardiomyocytes, which may have been salvaged by PP2A inhibition prior to ischaemia (as was observed in this study), while a longer duration of ischaemia did not salvage the affected tissue, as was reported in the study by Fenton and co-workers.

The second difference in study design is the concentration of inhibitor used and duration of administration. Fenton and co-workers made use of 100 nM OA administered for 25 minutes prior to ischaemia while this study used 50 nM OA administered for 20 minutes prior to ischaemia. Although the concentration of OA used in this study was substantially less than that in the Fenton study, it was experimentally determined to be effective (in chapter three) and was therefore used in subsequent experiments. That being said, both dosages were effective at reducing IFS in their

respective studies (Fenton *et al.* showed that OA administration during IPC reduced IFS in aged heart when compared to IPC alone, and reduced IFS in young heart when administered during reperfusion), even though the pre-ischaemic administration of OA did not reduce IFS in the absence of IPC in either young or aged animals in the Fenton study. In the Fan study (2010), 7.5 nM OA was administered for 10 minutes prior to ischaemia and did not elicit any effect.

Another key difference between these studies is the selection of animal model and sample size. Although this study used a mouse model while the Fenton study used a rat model, similar studies using rats (and rabbits) have also shown conflicting data – van Vuuren (2014) showed that 10 nM OA administered for 10 min prior to ischaemia resulted in approximately 15% reduction in infarct size, while Fan and co-workers (2010) reported no effect on IFS with 7.5 nM OA administration. This study also made use of a much larger sample size (n=9) than the Fenton study (n=4). In our experience, this is an important shortcoming: although, IFS determination is a reliable and relevant endpoint in assessing the potential of various agents to reduce infarction, the technique itself has a degree of variation which necessitates the use of a relatively large sample size. Thus, caution should be exhibited when interpreting results obtained from studies with smaller sample sizes, particularly in IFS determination.

Fan and co-workers (2010) also reported that OA administration did not reduce IFS in an isolated rat heart model: 7.5 nM OA was administered for 10 minutes prior to 35 minutes regional ischaemia and the authors observed no changes in IFS when compared to control. However, it is possible that 7.5 nM OA was not sufficient to exert any effect on PP2A, especially as the selection of 7.5 nM OA was based on IC₅₀ values reported in literature that would result in PP2A-specific inhibition, rather than a concentration that was experimentally determined to be effective.

Although 50 nM OA significantly reduced IFS, it had little effect on functional recovery (heart rate, aortic output, and systolic and diastolic pressures). Although it might be intuitive that a reduction in IFS should be associated with functional recovery, many previous studies have also reported reductions in IFS that are independent of functional recovery (Cohen, Yang and Downey, 1999; Ford *et al.*, 2001; Lochner, Genade and Moolman, 2003; Van Vuuren, 2014). IFS determination is conducted using TTC, which reacts with dehydrogenases in viable tissue to distinguish between viable and necrotic tissue (Fishbein *et al.*, 1981). IFS determination is a measure of the extent of cell death, and as stated in chapter one, PP2A has been implicated in various stages of cell death (both apoptosis and necrosis). It is therefore not surprising that inhibition of PP2A results in a decrease in the amount of cell death, causing a reduction in IFS. Functional recovery, however, is

influenced by all forms of reperfusion injury, namely the “no reflow” phenomenon, stunning, arrhythmias, and lethal reperfusion injury.

Lochner and colleagues (2003) demonstrated that the mode of perfusion influences recovery after ischaemia; hearts that were perfused in retrograde (Langendorff) mode recovered better than hearts perfused in working heart (antegrade) mode. Hearts perfused in retrograde, although stable, do not perform any work, while hearts perfused in antegrade must work against an afterload of 50 mmHg. Thus, perfusion in antegrade mode requires more energy than in the retrograde preparation, which is associated with an increased consumption of oxygen and energy-providing substrates (Chain, Mansford and Opie, 1969; Taegtmeyer, Hems and Krebs, 1980). As ATP levels at the end of ischaemia are largely depleted (Neely *et al.*, 1973), energy production during reperfusion may not adequately meet the demand required for mechanical function against an afterload of 50 mmHg. Thus, the lack of functional recovery after ischaemia may in part, be due to inadequate energy production, which was not influenced by a phosphatase inhibitor.

In conclusion, this study shows that PP2A inhibition immediately prior to sustained ischaemia favours cell survival, as OA administration effectively reduced IFS and increased cardiac output, without affecting any other functional parameters. However, the manner by which PP2A inhibition affects intracellular processes resulting in cell survival without affecting function is not fully understood. To begin addressing this question, we employed a phosphoproteomic approach to determine how various proteins are affected by PP2A inhibition and this is covered in chapter six.

5.5 LIMITATIONS

In our current setup, functional parameters (such as heart rate and pressures) can only be measured during antegrade perfusion (working heart), but antegrade perfusion cannot be sustained for the entire 60 minutes of reperfusion. There are two reasons for this. First, optimization studies (data not shown) performed in our laboratory have shown that prior to ischaemia, baseline function declines in work heart mode after approximately 30 minutes. In an injured heart, function deteriorates even more rapidly as the injured heart struggles to sustain work. Second, when using a recirculating system for antegrade perfusion, drug should only be

administered in retrograde mode, where the risk of drug recirculation is minimal. Thus, working heart mode was employed before and after ischaemia to determine function.

CHAPTER SIX

PHOSPHOPROTEOMIC ANALYSIS OF MYOCARDIAL ISCHAEMIA AND REPERFUSION

6.1 RATIONALE

In the previous chapter, it was determined that OA administration reduces IFS, while failing to exert any additional effects on functional parameters. Although it has been established that PP2A inhibition prior to myocardial ischaemia enhances the phosphorylation of PKB/Akt, ERK 1/2, and GSK-3 β at reperfusion (Van Vuuren, 2014), very little information exists regarding the intracellular targets of PP2A in the context of I/R injury. Therefore, we employed a phosphoproteomic approach to further investigate the effect of PP2A inhibition during myocardial ischaemia and reperfusion.

Sample preparation and mass spectrometry data were acquired in collaboration with Drs Tzu-Ching Meng and Lucy Yang of The Institute for Biological Chemistry at Academia Sinica, and the Academia Sinica Common Mass Spectrometry Facilities for Proteomics and Protein Modification Analysis, located at the Institute of Biological Chemistry, Academia Sinica, in Taipei, Taiwan. The work is supported by the Academia Sinica Core Facility and Innovative Instrument Project (AS-CFII-108-107).

6.2 METHODS

In chapter three, 50 nM OA was selected as the optimal concentration of inhibitor to dissolve in the perfusate. Therefore, to determine the phosphoproteomic profile of hearts exposed to ischaemia and reperfusion, hearts were perfused with either untreated KHB, 0.002% DMSO (vehicle control) or 50 nM OA. During the stabilization period, hearts were perfused for 15 minutes in retrograde mode, 15 minutes in antegrade mode, followed by administration of 50 nM OA for 20 minutes in retrograde mode. Thereafter hearts were exposed to 20 minutes ischaemia, and where applicable, hearts were reperfused in retrograde mode (Figure 6.1). 10 minutes reperfusion was selected for this study (rather than the 60 minutes used for IFS determination) as early reperfusion has been shown to be a critical period in the development of I/R injury and

the best opportunity for clinical intervention. Hearts in the control cohort received no drug during retrograde mode and normal retrograde perfusion was given instead of ischaemia.

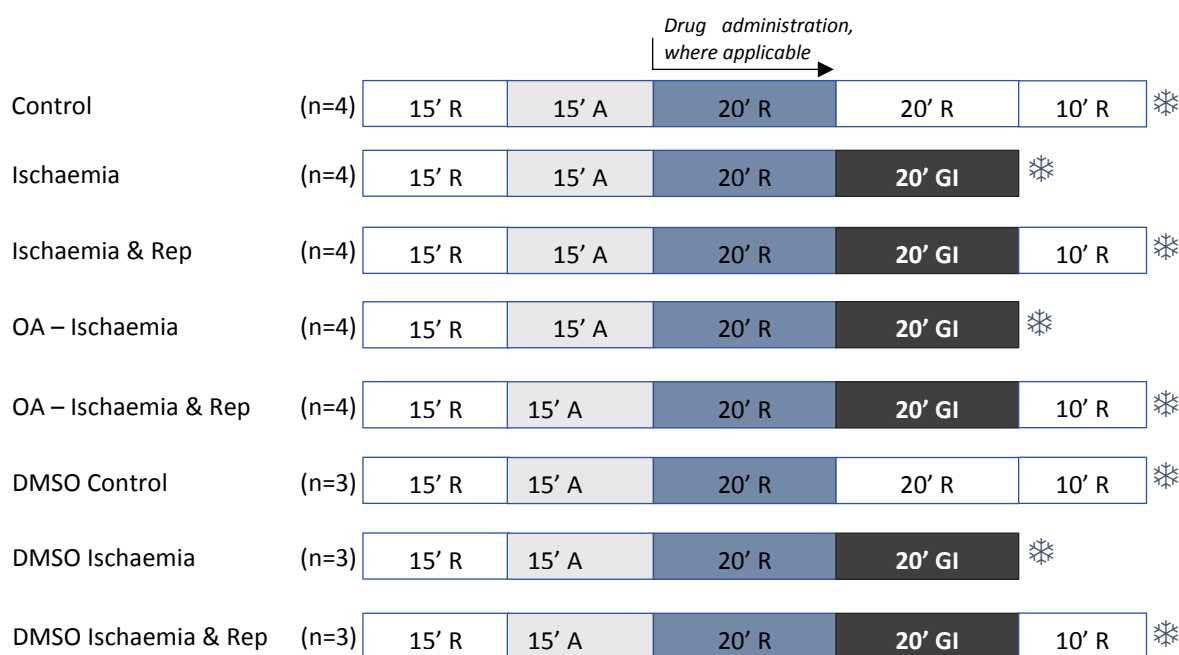


Figure 6.1 - Perfusion protocol for phosphoproteomic analysis of hearts exposed to ischaemia and reperfusion

Hearts were perfused in retrograde mode for 15 minutes, in antegrade mode for 15 minutes to determine function, and again in retrograde mode for 20 minutes, during which time KHB (control), OA (50 nM), or vehicle control (0.002% DMSO) was administered. The hearts were then subjected to 20 minutes GI and 10 minutes reperfusion. $n = 3-4$.

R = retrograde perfusion, A = antegrade perfusion/working heart, GI = global ischaemia

KHB = Krebs Henseleit bicarbonate buffer

At the completion of the perfusion experiment, hearts were freeze-clamped and stored in liquid nitrogen until further use. One-half of each heart was pulverized using a cooled mortar and pestle and added to a radioimmunoprecipitation assay (RIPA) buffer containing 1 mM EDTA, 10 mM sodium fluoride (NaF), 2 mM SOV, 50 μ l of protease inhibitor and 10 mM sodium pyrophosphate. The samples were then homogenized using the Bullet blender (Next Advance, Inc.), followed by centrifugation at 12,074 x g at 4 °C for 20 minutes, where after the protein content of the supernatant of each sample was determined by the Bradford technique (Bradford, 1976). For each sample, a volume corresponding to 1,500 μ g protein was aliquoted into cryovials, frozen in liquid nitrogen, and shipped on dry ice to our collaborators at Academia Sinica in Taipei, Taiwan. The sample shipment took approximately five days and were stored at -80 °C upon arrival.

Due to certain factors beyond our control, only two cohorts, DMSO-treated I/R (n= 1) and OA-treated I/R (n = 3), were analysed by mass spectrometry and compared. The limitations of this are addressed in the relevant section.

6.2.1 Protein digestion

Each sample was diluted with urea (8 M) to a final volume of 380 μ l. 10 μ l dithioerythritol (78 mM) in 8 M urea was added to each sample and then incubated for an hour at 37 °C. Following this, the samples were alkylated by the addition of 10 μ l iodoacetamide (400 mM) and left in a dark room for an hour at room temperature. The samples were then loaded into a 30 kDa Amicon centrifugal filter (Millipore) and centrifuged at 14,000 x g for 15 minutes. 400 μ l urea (8 M) was added to the samples, followed by centrifugation at 14,000 x g for 15 minutes (repeated five times) to remove the detergents. Next, the samples were digested with Lys-C protease (Pierce™, ThermoFisher Scientific) for three hours, followed by an overnight trypsin digestion at 37 °C. The digestion was quenched by adding 10% formic acid to a final concentration of 0.1%. An aliquot of each sample was used for global proteome analysis and another aliquot was used for phosphopeptide enrichment.

6.2.2 Phosphopeptide enrichment

The Titansphere™ Phospho-TiO MP kit (GL Sciences Inc., Japan) was used for phosphopeptide enrichment according to the manufacturer's protocol. All samples including total proteome, phosphopeptide enrichment, and enrichment flow-through were dried in a vacuum concentrator and then desalted using Zip-tips (C18 resin, Millipore). The resulting phosphopeptides were concentrated in a vacuum concentrator before subsequent nano-scale liquid chromatography (nanoLC) tandem mass spectrometry (MS/MS) analysis.

6.2.3 Shotgun proteomic analyses

NanoLC- MS/MS analysis was performed on an EASY-nLC™ 1200 system equipped with a Nanospray Flex™ ion source (Thermo Fisher Scientific, Bremen, Germany) and coupled to a Thermo Orbitrap Fusion™ Lumos™ mass spectrometer (Thermo Fisher Scientific) operated in data dependent acquisition (DDA) mode. Samples were loaded onto a 75 μ m x 250 mm PepMap C18 column (Thermo Fisher Scientific) packed with 2 μ m particles with a pore width of 100 Å. Peptide

elution was achieved by applying a mixture of Solvent A (0.1% formic acid in water) and Solvent B (80% acetonitrile with 0.1% formic acid). Separation was achieved in 120 minutes using a gradient from 5 % to 45 % solvent B at a flow rate of 300 nl/min.

For DDA, survey scans of peptide precursors from 350 to 1600 m/z were acquired at 240,000 resolution (at 400 m/z) with target automatic gain control value of 2×10^5 . Tandem MS was performed by isolation window at 0.7 Da with the quadrupole, higher energy collisional dissociation fragmentation with normalized collision energy of 30, and rapid scan MS analysis in the ion trap. Only precursors with a charge state of 2^+ to 6^+ were sampled for a second in-tandem mass analysis (MS2). For MS2, target automatic gain control value was set to 1×10^4 and the maximum injection time was 35 msec. The dynamic exclusion duration was set to 15 seconds with a 10 ppm tolerance around the selected precursor and its isotopes. The instrument was run in top speed mode with 3 second cycles and monoisotopic precursor selection was enabled. All samples (total proteins and phosphoproteins) had two technical replicates.

6.2.4 Protein/phosphopeptide identification and quantification

Raw files from Orbitrap Fusion™ mass spectrometry were analysed using Thermo Proteome Discoverer™ (version 2.3, Thermo Scientific). Using the database search engine Mascot 2.6, MS2 spectral data were searched against the Swissprot database for *Mus musculus* to determine peptide identities. The following search parameters were employed: tryptic digestion with up to two missed cleavages, carbamido-methylation of cysteines as fixed modifications, methionine oxidation, deamidation of asparagine and glutamine residues, serine, threonine, and tyrosine phosphorylation, and protein N-terminal acetylation were variable modifications, a minimum of seven amino acids per peptide, precursor mass tolerance was 10 ppm and 0.6 Da for the fragment ions.

Peptide spectral matches were validated using Percolator in Proteome Discoverer™ based on q -values at a 1% false discovery rate. The site localization score for phosphorylation was computed using ptmRS in Proteome Discoverer™ and a score greater than 75% was considered as a valid phosphosite. Only the leading proteins which had the highest peptide coverage among the members of a protein family and had at least two peptides and one unique peptide were reported. To adjust for protein loading error, the precursor peak area was extracted as peptide abundance and normalized to the total abundance of all peptides in a sample file.

Protein abundance was calculated based on the three most abundant peptides. Protein ratios from TiO₂ flow-through proteome quantitation were used to adjust the ratios for phosphopeptides to account for the change in total protein expression. Mass spectrometry data will be uploaded to a proteomics repository at a later stage. The identified proteins are listed in Addendum B.

6.2.5 Ingenuity Pathway Analysis

Ingenuity Pathway Analysis (IPA; Qiagen, Redwood City, USA), a web-based computational platform designed for system biology, was used to further analyse the data by conducting a biological function enrichment analysis to identify pathways that are significantly represented by the proteins identified in this study. The data were analysed using a Fisher's exact test and a p-value of 0.05 was considered statistically significant.

6.3 RESULTS

Proteomic analysis of myocardial tissue that was subjected to 20 minutes ischaemia and 10 minutes reperfusion after receiving either DMSO (vehicle control) or 50 nM OA resulted in a total of 1841 proteins and 684 phosphorylated proteins that were significantly expressed or phosphorylated ($p \leq 0.05$) in myocardial tissue exposed to ischaemia and reperfusion. Of these,

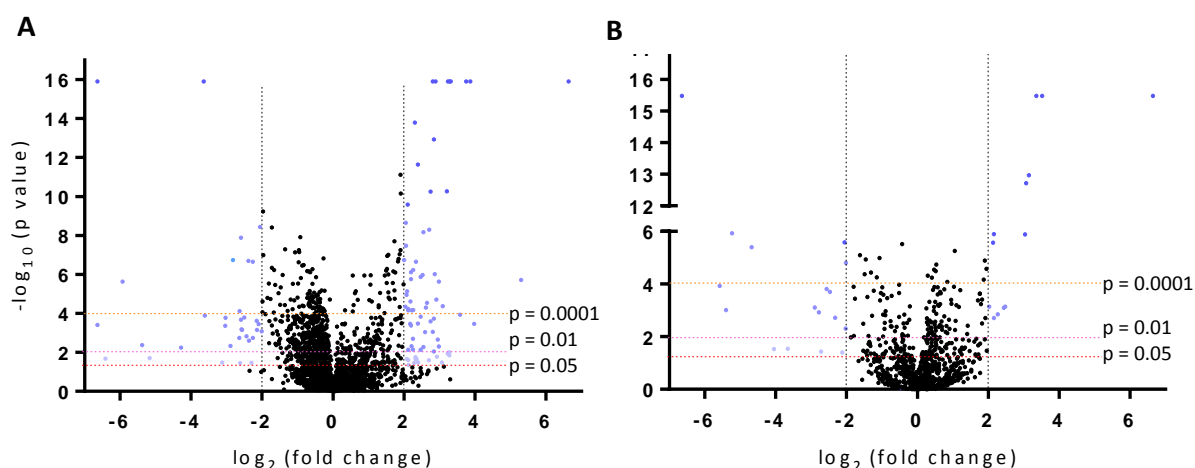


Figure 6.2 - Volcano plots of total proteins and total phosphoproteins detected by mass spectrometry
Hearts perfused with 50 nM OA prior to 20 minutes ischaemia and 10 minutes reperfusion were analysed by mass spectrometry where total proteins (A) and phosphorylated proteins (B) were identified. For each protein, the $-\log_{10}$ p value was plotted against the \log_2 fold change to create a volcano plot. Proteins with a two-fold increase (positive values) or decrease in abundance (negative values), and a p value ≤ 0.05 were highlighted in blue. P values of 0.05, 0.01 and 0.0001 are indicated on plots.

898 proteins were differentially expressed, and 184 proteins were differentially phosphorylated in the OA-treated cohort. For each protein, the p-value was transformed by $-\log_{10}$ so that smaller p-values are graphed as larger values. These were plotted against the \log_2 transformed abundance ratio to create a volcano plot, which is shown in Figure 6.2. Proteins that showed at least two-fold increase or decrease in expression (differentially expressed; above 2 and below -2 on the x-axis) and achieved statistical significance (above 1.3 on the y-axis) were highlighted in blue. The extensive list of proteins identified in this study that were differentially expressed in the OA I/R cohort when compared to the DMSO (vehicle) I/R cohort can be found in Addendum B (Table B.1). Proteins in the OA-treated cohort that showed either a two-fold increase or decrease in phosphorylation (differentially phosphorylated; fold change greater than 2 or less than -2, respectively) and achieved statistical significance of 0.05 ($-\log_{10}$ p value = 1.3) when compared to the DMSO-treated cohort are listed in Table 6.1 and highlighted in blue in Figure 6.2B.

Table 6.1 - List of proteins that were differentially expressed or phosphorylated in the 50 nM OA-treated cohort that show a fold change greater than two and a $-\log_{10}$ (p value) greater than 1.3

Accession no:	Description	Proteome		Phosphoproteome	
		Fold change	$-\log_{10}$ (p value)	Fold change	$-\log_{10}$ (p value)
Q9DCX2	ATP synthase subunit d, mitochondrial	-0.29	1.41	6.64	15.48
P45481	CREB-binding protein			6.64	15.48
P07901	Heat shock protein 90 α	-0.42	3.09	6.64	15.48
P27546	Microtubule-associated protein 4			6.64	15.48
Q3UIZ8	Myosin light chain kinase 3	-0.5	2.35	6.64	15.48
P26645	Myristoylated alanine-rich C-kinase substrate			6.64	15.48
O09130	NFATC2-interacting protein			6.64	15.48
Q3UQS8	RNA-binding protein 20			6.64	15.48
O55106	Striatin	-6.64	15.91	6.64	15.48
Q8CHW4	Translation initiation factor eIF-2B subunit ϵ			6.64	15.48
O70373	Xin actin-binding repeat-containing protein 1			6.64	15.48
P61014	Cardiac phospholamban			3.52	15.48
O70468	Myosin-binding protein C, cardiac-type			3.36	15.48
Q7TQ48	Sarcalumenin	-0.24	2.80	3.04	5.89
O88492	Perilipin-4			2.48	3.14
Q99MS7	EH domain-binding protein 1-like protein			2.44	3.10
A2ASS6	Titin			2.27	2.85
Q9ET78	Junctophilin-2			2.16	5.90
Q3UIL6	Pleckstrin homology domain-containing family A member 7			2.16	2.71
P159017	Bcl-2-like protein 13			2.13	5.58
P10637	Microtubule-associated protein tau			2.12	6.02
Q4QQM4	Tumor protein p53-inducible protein 11			2.02	3.15

Biological function enrichment analysis was conducted using IPA to identify pathways that are significantly represented by the proteins identified in this study. The full list of canonical pathways associated with PP2A inhibition during myocardial ischaemia and reperfusion are listed in Table B.2 in Addendum B. The pathways that displayed a p-value of ≤ 0.0001 ($-\log_{10}$ p value ≥ 4 in the table) are listed below in Table 6.2.

Table 6.2 - List of canonical pathways most affected by PP2A inhibition during myocardial ischaemia and reperfusion that have a p value ≤ 0.0001 .

Pathway	Proteome $-\log_{10}$ (p value)	Phosphoproteome $-\log_{10}$ (p value)
Mitochondrial dysfunction	9.67	1.14
Oxidative phosphorylation	9.80	0.61
Remodelling of adherens junctions	8.03	1.86
Adherens junction signalling	7.85	1.24
Actin cytoskeleton signalling	4.71	2.50
Sirtuin signalling pathway	6.72	0.27
Integrin linked kinase signalling	4.85	1.84
RhoGDI signalling	5.35	1.11
Protein kinase A signalling	1.29	4.12
Tight junction signalling	4.18	1.16
Caveolar-mediated endocytosis signalling	4.83	0
Vasodilation	4.39	0
Regulation of Actin-based Motility by Rho	4.08	0

6.4 DISCUSSION

The aim of the study was to identify proteins that are not known to be substrates of PP2A in the context of myocardial ischaemia and reperfusion. For this we conducted a phosphoproteomic analysis of myocardial tissue that received 50 nM OA prior to ischaemia and reperfusion to determine the effect of PP2A inhibition on the cellular response to I/R stress. 1841 proteins and 684 phosphorylated proteins were identified in the analysis, of which 898 proteins were differentially expressed and 184 proteins were differentially phosphorylated under conditions of PP2A inhibition (listed in Addendum B). IPA determined that the major canonical pathways affected were mitochondrial dysfunction, oxidative phosphorylation, regulation and remodelling of adherens junctions, as well as cytoskeletal signalling. Thus, the discussion that follows concerns the function of phosphorylated proteins listed in Table 6.1 (differentially expressed in the OA-cohort) as they pertain to either mitochondrial function, oxidative phosphorylation, cytoskeletal

signalling, or adherens junction signalling. Where possible, what is known regarding the protein's role in I/R injury or as a substrate of PP2A is discussed.

6.4.1 PP2A in mitochondrial function and oxidative phosphorylation

Although many of the differentially expressed phosphorylated proteins in the dataset either form part of the cytoskeleton or regulate the cytoskeleton, a large proportion of proteins affected by PP2A inhibition prior to 20 minutes ischaemia and 10 minutes reperfusion have a role in mitochondrial dysfunction and oxidative phosphorylation. Mitochondria predominantly function to generate ATP, but also generate and metabolize ROS, participate in apoptosis, and regulate intracellular calcium (Brand and Nicholls, 2011). Although it is difficult to define mitochondrial dysfunction, abnormality in any of these functions could be considered as such.

Of the proteins listed in Table B.1, 44 are subunits of the electron transport chain complexes, eight are subunits from enzymes that form part of the Krebs cycle, and eight are subunits of enzymes that form part of glycolysis. Certain subunits that make up complexes II and III of the electron transport chain (succinate dehydrogenase and cytochrome *bc₁* complex, respectively) showed a slight decrease in abundance when compared to the DMSO-treated cohort, and certain subunits in complexes IV and V (cytochrome c oxidase and F₁F₀ ATP synthase, respectively) showed an increase in abundance when compared to the DMSO-treated cohort. Complex I (NADH dehydrogenase) showed a slight decrease in most, but not all proteins when compared to the DMSO-treated cohort, but several subunits displayed an increase in abundance. For example, alpha subcomplex subunit 3 was increased by a factor of 2, iron-sulfur protein 3 was increased by a factor of 1.5, while the other proteins and subunits affected were decreased by a factor of 0.2-1, and iron-sulfur protein 6 was decreased by a factor of 1.97. This would indicate that the subunits of complex I are not collectively modulated. Only certain proteins within the complexes appear to be affected by PP2A inhibition, but changes in individual subunits can alter the levels of assembly of the complexes, an observation that has also been reported in other phosphoproteomic studies (Zhang, Pan and Hutchins, 2002; Højlund *et al.*, 2003), including one investigating the proteomic changes associated with myocardial preconditioning (Arrell *et al.*, 2006). Ischaemia suppresses activity of all complexes in a time-dependent manner (Leistner *et al.*, 2019), although complex I appears to be most susceptible (Paradies *et al.*, 2004). Inhibition of global complex activity is also associated with cell death (Wolvetang *et al.*, 1994), although a reduction in oxidative phosphorylation efficiency is associated with decreased ROS production

(Cadenas, 2018). It cannot be assumed that increased protein abundance associated with the complexes would be associated with increased complex activity and consequently, decreased cell death. However, the phosphorylation of Bcl-2-like proteins identified in this study (Table 6.1) suggests that the majority of cardiomyocytes were protected against apoptosis under the conditions studied. Whether this is related to oxidative phosphorylation cannot be established with the current data, but it appears that the reduction in oxidative phosphorylation and phosphorylation of Bcl-2-like proteins may serve to protect the cardiomyocytes from cell death.

50 nM OA administration appears to increase the abundance of selected proteins associated with complexes IV and V, and to an extent, complex I. Previous studies utilizing an anti-anginal drug, ranolazine, showed increased complex I activity and increased proteins associated with complex I compared to untreated hearts exposed to I/R (Gadicherla *et al.*, 2012). This was associated with improved cardiac function after I/R. Thus, the IFS-reducing effects of OA may, in part, be due to the increased abundance of mitochondrial proteins associated with complexes I, IV and V, although whether this is associated with increased complex activity could not be established.

Subunit d of complex V was the only subunit that was phosphorylated and present in high abundance (fold change of 6.64; $p < 0.0001$). Subunit d forms part of the F_0 subcomplex, but not much is known about its specific function or how phosphorylation affects its function (Long, Yang and Yang, 2015). Studies in *Drosophila* show that knock-down of subunit d is associated with increased resistance to oxidative stress, reduced protein damage and aggregation, and reduced phosphorylation of S6K (ribosomal protein s6 kinase), as well as ERK in TOR and MAPK signalling, respectively (Sun *et al.*, 2014). Phosphorylation of another subunit, the β subunit (not reported in this study) has been documented in type two diabetes mellitus (Højlund *et al.*, 2003), uptake of iron into mitochondria from iron-overloaded heart (Min *et al.*, 2013), and in myocardial preconditioning (Arrell *et al.*, 2006). Therefore, phosphorylation of the d subunit may potentially form part of a stress response. However, it is unclear whether phosphorylation is associated with increased or decreased complex V activity, although our results show increased abundance of complex V proteins which may indicate increased complex V activity (but this cannot be confirmed with the available data). Phosphorylation may also play a role in complex assembly (Reinders *et al.*, 2007), which would be necessary when complex V proteins are upregulated.

Sustained ischaemia suppresses activity of the mitochondrial complexes, particularly complex I (Paradies *et al.*, 2004; Leistner *et al.*, 2019). Our results reflect early reperfusion (10 minutes) and indicate an increase in the abundance of certain proteins associated with complexes I, IV, and V,

indicating that OA-mediated cardioprotection may involve partial or accelerated recovery of the mitochondrial complexes. Based on literature we speculate that phosphorylation of subunit d of complex V might be part of the response to stress. Taken together, the results suggest that PP2A suppresses the mitochondrial complexes during I/R.

However, further experimentation is needed to confirm these results. Whether the increase in complex subunit abundance correlates with subunit (and possibly complex) upregulation can be confirmed with western blotting, although investigating each subunit individually is not possible at this stage. Commercial OXPHOS kits that contain antibodies for subunits from each complex are available but contain only one subunit from each complex as an indicator of complex protein expression. Alternatively, complex activity can be determined using isolated mitochondria and measuring respiratory control. These experiments could give an indication of whether the increased protein abundance observed during PP2A inhibition prior to myocardial ischaemia and reperfusion correlates with complex upregulation, and whether complex upregulation results in increased respiration (rather than a compensatory mechanism). These experiments will be addressed in chapter eight.

6.4.2 PP2A and the cytoskeleton

The cytoskeleton is a dynamic scaffold composed of three main types of protein: microfilaments (actin polymers), microtubules (composed of tubulin), and intermediate filaments (Hein *et al.*, 2000). The cytoskeleton provides structural integrity, mediates biomechanical signalling, and organizes the organelles within a cell (Sequeira *et al.*, 2014). The cytoskeleton and its accessory proteins can be regulated by phosphorylation and in this regard, PP2A has been shown to be a key regulator of the cytoskeleton.

Cytoskeletal integrity is vital for proper cellular function and disruption or depolymerization of the cytoskeleton results in cell death (Kim *et al.*, 2002). Interestingly, both PP2A activation (Meng *et al.*, 2011; Li *et al.*, 2012) and PP2A inhibition (Usui *et al.*, 1999; Plácido *et al.*, 2017) results in cytoskeleton depolymerization, although only when inhibitors were administered for more than three hours (Usui *et al.*, 1999; Plácido *et al.*, 2017). As information regarding PP2A's contribution to cytoskeletal maintenance is well-established, the reader is directed to a review by Hoffman and colleagues (2017) for more information. However, information regarding the role of PP2A in the maintenance of the cytoskeleton in ischaemia/reperfusion (myocardial or otherwise), is

lacking. Thus, the role of the phosphorylated cytoskeletal proteins listed in Table 6.1 will be discussed below, and where possible, information regarding PP2A's regulation of that protein will be provided.

6.4.2.1 *Microtubule associated protein tau*

Microtubule associated protein tau (MAPT) promotes microtubule assembly and stabilization in neuronal cells (Sotiropoulos *et al.*, 2017). Most information regarding MAPT relates to various tau pathologies such as Alzheimer's disease, where hyperphosphorylated tau aggregates to form abnormal protein deposits in the brain (Sontag *et al.*, 1999). PP2A is responsible for the dephosphorylation of MAPT (Sontag *et al.*, 1996) and PP2A dysfunction is linked to Alzheimer's disease (Sontag and Sontag, 2014). Recently MAPT was identified in cardiac tissue, and KO of MAPT in mice increased systolic blood pressure and hypertrophy of the heart that worsened with age (Betrie *et al.*, 2017). Phosphorylated MAPT was abundantly expressed (fold change = 6.64) in the OA-treated cohort and PP2A is a known regulator of MAPT dephosphorylation in the brain (Martin *et al.*, 2013), but the function of phosphorylated cardiac MAPT or whether this is regulated by PP2A inhibition has not been documented.

6.4.2.2 *Microtubule associated protein 4*

Our results show that phosphorylated microtubule associated protein (MAP) 4 was abundantly expressed (fold change = 6.64) in hearts exposed to 50 nM OA prior to myocardial I/R. A recent study has shown that phosphorylated MAP4 is not only associated with mitochondrial dysfunction in myocardial ischaemia, but that phosphorylated MAP4 actually drives pathological cardiac remodelling (Li *et al.*, 2018). During hypoxia, MAP4 becomes phosphorylated, dissociates from microtubules, and translocates from the cytosol to the mitochondria (Hu *et al.*, 2014). This is regulated through p38 MAPK and results in the opening of the mPTP and subsequent apoptosis. Interestingly, a recent proteomic study determined that subunit 1 of mitochondrial complex 1 may be a target of phosphorylated MAP4 (Li *et al.*, 2019).

6.4.2.3 *Myosin light chain kinase 3*

Myosin light chain kinase 3 (cardiac myosin light chain kinase; cMLCK) is responsible for the phosphorylation of the regulatory myosin light chain that results in actomyosin contraction (Rigor *et al.*, 2013). Whether cMLCK activity is beneficial appears to be tissue-specific as increased

actomyosin contraction improves ventricular tissue contractility (Gao *et al.*, 2014) but contributes to hyperpermeability in endothelial cells (Rigor *et al.*, 2013). In cardiac tissue, cMLCK activity appears to be beneficial as mutations in cMLCK is associated with dilated cardiomyopathy (Tobita *et al.*, 2017) and upregulation of cMLCK expression several days after myocardial infarction improves cardiac function (Gu *et al.*, 2010). Additionally, cMLCK has been shown to be degraded by matrix-metalloproteinase 2 in response to I/R (Gao *et al.*, 2014).

cMLCK activity is regulated by phosphorylation by either PKA, PKC, CaMKII, or a tyrosine kinase (Hashimoto and Soderling, 1990; Goekeler *et al.*, 2000), where phosphorylation results in cMLCK activity except in the case of PKA, where phosphorylation results in inhibition of cMLCK. Although an increase in phosphorylated cMLCK was identified in our dataset, the limited information on its phosphosites (not shown) makes it impossible to determine whether cMLCK was active in this dataset. OA administration does result in reduced IFS, although it had little effect on functional recovery. In addition, PKA signalling was pronounced in OA treated hearts (Table 6.2), which in that case, would favour inhibition of cMLCK.

6.4.2.4 *Myristoylated, alanine-rich C kinase substrate (MARCKS)*

MARCKS is a filamentous cytoskeletal protein that functions in actin crosslinking, regulates focal adhesion kinase (Heidkamp *et al.*, 2007) and is a potential convergence point of calcium–calmodulin and PKC signal transduction pathways in the regulation of the actin cytoskeleton (Hartwig *et al.*, 1992). MARCKS is inhibited under basal conditions by PKC (Heidkamp *et al.*, 2007) and dephosphorylated by PP2A (Tanabe *et al.*, 2012). How phosphorylation changes its function is not fully understood.

6.4.2.5 *Myosin-binding protein C*

Myosin-binding protein C (MyBP-C) is a myofibrillar protein important for normal myocardial contractility and stability (Decker *et al.*, 2012). MyBP-C has been shown to be dephosphorylated during ischaemia, which results in its degradation into an N-terminal 40 kDa fragment that is released into the circulation upon reperfusion (Govindan *et al.*, 2012). This fragment has been shown to disturb contractility (Govindan *et al.*, 2012) and may be partly responsible for stunning (Decker *et al.*, 2012). Phosphorylated MyBP-C has been shown to be cardioprotective (Sadayappan *et al.*, 2006) and a high abundance of phosphorylated MyBP-C was reported in our

dataset, indicating that the cardioprotective effect elicited by OA may in part be mediated by this protein.

6.4.2.6 *Titin*

Titin is an extremely large protein that forms a continuous filament network in the sarcomeres of striated muscle (Hamdani, Herwig and Linke, 2017). Titin has an elastic spring-like characteristic that generates “passive tension,” that determines the stiffness of the cardiomyocytes and contributes to the total stiffness of the myocardial wall (Linke, 2008). Cardiac titin contains two unique sequences, the ‘N2B’ element (‘N2Bus’) and the ‘PEVK’ segment (26–28 residue motifs rich in proline, glutamate, valine and lysine) that can be phosphorylated by different kinases (Hamdani, Herwig and Linke, 2017). The PEVK region is predominantly phosphorylated by PKC α and phosphorylation at this site increases passive tension (Hidalgo *et al.*, 2009; Hudson *et al.*, 2010; Hamdani, Franssen, *et al.*, 2013). Phosphorylation on the N2B element is mediated by PKA, PKG, ERK 2 and CaMKII δ and results in decreased stiffness (Yamasaki *et al.*, 2002; Krüger *et al.*, 2009; Perkin *et al.*, 2015). Myocardial stiffness associated with titin phosphorylation has been reported in diastolic dysfunction due to heart failure (Hudson *et al.*, 2011; Hamdani, Franssen, *et al.*, 2013; Hamdani, Krysiak, *et al.*, 2013; Mohamed *et al.*, 2016), hypertension (Kovács *et al.*, 2016), and myocardial ischaemia (Kötter *et al.*, 2016).

This study identified 44 titin phosphosites (Table 6.3), four of which have not been identified in literature according to PhosphoSitePlus® (Hornbeck *et al.*, 2015; <https://www.phosphosite.org/uniprotAccAction?id=A2ASS6>). PP2A administration did result in the phosphorylation of two unknown serine residues, however, the four novel phosphorylation sites were present in both DMSO and OA-treated cohorts, indicating that they were not a result of OA-treatment/PP2A inhibition. Dephosphorylation of titin is known to be accomplished by PP5 (Krysiak *et al.*, 2018), and the role of PP1 and PP2A in this process has not been confirmed.

Table 6.3 - Titin phosphosites identified in *Mus musculus* by phosphoproteomic analysis of hearts exposed to 20 minutes GI and 10 minutes reperfusion

Site	Previous identification of the phosphosite	Site	Previous identification of the phosphosite	Site	Previous identification of the phosphosite
S262	1,6,9	T12869	1,6,9	T33962	8
S264	1,2,6,9	S12871	1,2,6,9	S33963	1,21
T266	1,2,6,9	S12884	1-6,9-14	S34107	1,6
S301	1,2	S13780	1	S34112	15
S307	1	S21152	1,9	S34113	1
T812	1,2	S21895	1,9	S34451	1,9
S1415	1,2	S29997	1	S34464	1,2,3,6
S1424	1,2	T33859	1,2	S34470	1,2,9
S1429	1,2	T33859	1,2,6	S34476	1,2,6,9
S1434	1,2	S33861	1,2,6	S34488	1,2,9
S1439	1,2	Y33864	1	S34571	-
S2078	1,9	S33875	1,2	S34573	16
S2080	1,2,6,7,9	S33880	1,2	S34778	1
S3743	-	S33918	-	S35128	1,9
S9144	1,2,6,7,9	S33923	-		

1 - (Lundby *et al.*, 2013); 2 - (Mertins *et al.*, 2014); 3 - (Hudson *et al.*, 2011); 4 - (Hudson *et al.*, 2010); 5 - (Hidalgo *et al.*, 2009); 6 - (Zanivan *et al.*, 2008); 7 - (Villén *et al.*, 2007); 8 - (Stokes *et al.*, 2012); 9 - (Hamdani, Krysiak, *et al.*, 2013); 10 - (Kötter *et al.*, 2016); 11 - (Mohamed *et al.*, 2016); 12 - (Hamdani, Franssen, *et al.*, 2013); 13 - (Kovács *et al.*, 2016); 14 - (Hutchinson *et al.*, 2015); 15 - (Guo *et al.*, 2008); 16 - (Huttlin *et al.*, 2010)

6.4.3 PP2A and intracellular junctions

Cardiomyocytes are connected to each other by intercalated discs which are composed of gap junctions and adherens junctions. Gap junctions allow for direct communication between adjacent cells, while adherens junctions function in cell-to-cell adhesion (Tansey *et al.*, 2006). Disruption of intercalated discs have been implicated in ischaemic and hypertrophic cardiomyopathy, atrial fibrillation, and congestive heart failure (Peters *et al.*, 1993; Zuppinger, Eppenberger-Eberhardt and Eppenberger, 2000; Kostetskii *et al.*, 2005). The contribution of PP2A to the regulation and maintenance of intracellular junctions has been extensively described and will therefore not be covered (for this, the reader is directed to a review by McCole, 2013). Certain phosphorylated proteins identified in this study that are related to junction signalling are discussed below.

6.4.3.1 Striatin

As stated in chapter one, striatin is a regulatory subunit of PP2A (Castets *et al.*, 2000). However, it was first identified in neurons, where it is proposed to function as a scaffolding protein that interacts with mediators of vesicular trafficking (Castets *et al.*, 1996). In addition, striatin also

forms part of adherens junctions at the intercalated discs in cardiac tissue (Hwang and Pallas, 2014; Franke *et al.*, 2015). Striatin deficiency has been associated with salt sensitivity hypertension, enhanced vasoconstriction, and decreased vascular relaxation (Garza *et al.*, 2015). Interestingly, striatin is also necessary for the membrane estrogen receptor signalling that results in the cardioprotective effects of estrogen (Bernelot Moens *et al.*, 2012).

As a subunit of PP2A, striatin targets PP2A to microtubules and its downregulation results in hyperphosphorylation, and subsequent depolymerization of MAP2 (Kaźmierczak-Barańska *et al.*, 2015). In addition, striatin mutations are associated with dilated cardiomyopathy in boxer dogs (Meurs *et al.*, 2013). Several phosphoproteomic studies have identified phosphorylated striatin from various tissues (Ballif *et al.*, 2004; Munton *et al.*, 2007; Villén *et al.*, 2007; Trinidad *et al.*, 2008) and a high abundance of phosphorylated striatin was identified in our dataset. The function of phosphorylated striatin has however yet to be defined.

6.4.3.2 *Xin-actin binding repeat-containing protein 1*

Xin-proteins are striated muscle-specific proteins that are localized at the intercalated discs of cardiac tissue and belong to the family of adhesion, anchoring, and binding proteins (Wang *et al.*, 2014). Xin proteins are barely detectable in healthy tissue (Sinn *et al.*, 2002; Hawke *et al.*, 2007), but are upregulated in response to tissue damage, indicating that it may form part of remodelling and repair of damaged muscle (Hawke *et al.*, 2007; Nilsson *et al.*, 2013). Deletion of Xin in a murine model results in late-onset cardiomyopathy with conduction defects (Wang *et al.*, 2014). Quantitative phosphoproteomic analysis of the pressure-overload murine heart (induced by transverse aortic constriction) confirmed the rapid and transient phosphorylation of Xin shortly after aortic banding (Chang *et al.*, 2013), which may contribute to Xin's function during muscle damage. Therefore, the increase in phosphorylated Xin-protein reported in this study may possibly contribute to tissue repair.

6.4.3.3 *Junctophilin-2*

Junctophilin-2 is cardiac structural protein that is critical in the formation of junctional membrane complexes necessary for excitation-contraction coupling (Beavers *et al.*, 2014). Junctophilin-2 expression is decreased in myocardial ischaemia and hypertrophy (Wagner *et al.*, 2012) and mutations in junctophilin-2 has been documented in hypertrophic cardiomyopathy (Landstrom *et al.*, 2007; Matsushita *et al.*, 2007). Upregulation of junctophilin-2 prevents endoplasmic reticulum

stress in response to hypoxia/reoxygenation (simulated I/R) in H9c2 cells and prevents apoptosis by blocking Ca^{2+} leakage from ryanodine receptors (Zijun Su, 2017). Mutated junctophilin-2 that cannot be phosphorylated has been associated with altered intracellular Ca^{2+} handling, possibly through the compromised ability to bind to ryanodine receptors (Woo *et al.*, 2010). In this current study, phosphorylated junctophilin-2 was increased in abundance, indicating that PP2A could be a regulator of junctophilin-2 and this interaction could be part of the cardioprotective mechanism of OA. However, further research is needed to confirm and elaborate on these possibilities.

6.4.4 Conclusion

This study assessed the phosphoproteome of myocardial tissue that was exposed to 50 nM OA prior to 20 minutes GI and 10 minutes reperfusion. Pathway analysis demonstrated that the most affected pathways represented by the affected proteins were oxidative phosphorylation and mitochondrial function, cytoskeletal remodelling, and junction signalling. As such, what is known about the phosphorylated proteins in these pathways were discussed although the function of many of these proteins have not been confirmed in myocardial I/R. Clearly there are many proteins and pathways that remain to be investigated in the pathophysiology of I/R and in cardioprotection.

Several proteins that are known targets of PP2A, such as MAPT and MARCKS, were phosphorylated during PP2A inhibition, confirming the effect of OA administration. In addition, proteins that are known to be phosphorylated during I/R, such as MyBP-C and Xin-protein were also observed. In addition, the phosphorylation status of certain proteins would suggest that PP2A-inhibition during I/R is cardioprotective: phosphorylated MyBP-C is known to be cardioprotective, Xin-protein functions in tissue repair, and MAP4 phosphorylation is necessary for cardiac remodelling.

It is interesting to note that the well-known survival kinases were not included in the lists of differentially expressed proteins, possibly because their expression is increased in I/R, regardless of drug treatment. However, PI3K-Akt signalling was a pathway listed in Table B.2, indicating that PP2A inhibition may enhance PKB/Akt phosphorylation (which has been confirmed elsewhere; Fan *et al.*, 2010; Van Vuuren, 2014).

Various cardioprotective interventions that activate survival signalling appear to converge on the mitochondria. It is therefore not surprising that oxidative phosphorylation and more broadly, mitochondrial function were most affected. Cytoskeletal disorganization has also been implicated

in various pathological states, and the phosphorylation of the proteins identified in this study has paradoxically been associated with both cardioprotection and cell death, as discussed above. The aim of this study was to determine the intracellular response (in the context of PP2A inhibition) during ischaemia and reperfusion and the results indicate that PP2A regulates many different cellular pathways.

The results of the study give an indication of how much is still to be discovered regarding the function of PP2A. We have identified several potential substrates of PP2A, although the experiments that are required to confirm this, fall outside the scope of this study. We are also the first to document that MAPT is phosphorylated in cardiac tissue that received a PP2A inhibitor prior to ischaemia and reperfusion, but the function of phosphorylated cardiac MAPT is not known. Lastly, four phosphosites of cardiac titin were identified, which to our knowledge, has not been documented before.

In view of these results, two potentially interesting proteins were selected for further analysis. The chapters that follow will investigate the role of striatin and heat shock protein 90 α (chapter seven) in the response to ischaemia and reperfusion -- both in the presence and absence of OA. We will also describe the interaction of PP2A with these proteins. Lastly, to elaborate on some of the data presented here, the effects of PP2A inhibition on oxidative phosphorylation will be investigated using isolated mitochondria, and this will be described in chapter eight.

6.5 LIMITATIONS

The results of this study were severely limited due to unexpected factors involved in the shipment of samples from Cape Town, South Africa, to Taipei, Taiwan. These factors included extended storage of frozen lysates, prolonged duration of shipping, samples storage at different temperatures during initial storage, shipment, and subsequent storage upon receipt of the samples. In addition, samples were subjected to at least one freeze/thaw cycle before being processed for mass spectrometry.

Cardiac tissue was prepared in lysis buffer in preparation for shipment, but due to problems with the shipment and import license, the lysates were frozen in liquid nitrogen where they were kept until shipment approximately one month later. Once the samples arrived in Taiwan (approximately five days after leaving Cape Town), they were frozen away in storage. The samples were thawed for western blot analysis, which confirmed that various proteins, such as Akt/PKB,

were still phosphorylated in I/R samples (data not shown). One sample from each cohort were prepared for mass spectrometry and analysed one month after arriving in Taiwan due to availability of the mass spectrometer. At this point (and after a volume of sample was used for blotting), it was determined that there was not sufficient protein in each of the samples for optimal technical repeats. The remainder of the I/R cohorts were analysed 10 months after the first analysis (11 months after shipment).

For the best yield during phosphopeptide enrichment, 400 µg protein is required per sample. However, despite the 1200 µg of protein per sample lysate prepared in our laboratory, only a maximum of 200 µg protein could be extracted from each sample during sample preparation in Taiwan. As this is the minimal requirement for analysis, only three samples from the OA I/R cohort and two samples from the DMSO I/R cohort were analysed. In addition, the limited volume only allowed for two technical repeats. Although it is difficult to determine why such a pronounced decrease in protein yield was observed, the following reasons are put forth as possible factors that may contribute to protein loss. First, the volume of lysates used for western blot analysis contributed to the amount of protein removed from the sample. Second, the method of protein determination (such as the Bradford or Lowry) has shown to yield different results for the same sample (Mæhre *et al.*, 2018), and the same amount of protein may be determined differently between the two different laboratories. Spectrophotometric protein determination methods (such as the Bradford method) are often affected by interfering substances, such as detergents, and could thus overestimate the protein content. Third, freeze/thaw cycles and extended periods of storage have been shown to affect sample integrity. Freeze/thaw cycles also result in evaporation and consequently concentrate the amount of salt and detergent in a sample (which has been shown to interfere with protein determination). Fourth, proteins can adhere to surfaces of polypropylene tubes, contributing to protein loss.

The aim of this study was to characterize the phosphoproteome of myocardial tissue obtained from hearts subjected to ischaemia and reperfusion. Due to the size of the mouse heart, global ischaemia rather than regional ischaemia was used to achieve a greater and more homogenous population of infarcted tissue for analysis. Although in the globally ischaemic model, the entire heart become ischaemic, the viability of cardiomyocytes differs based on their location in the heart. This results in tissue injury that ranges in severity, rather than a uniform population of cardiomyocytes that have the approximately the same extent of injury. This may complicate data analysis, as comparison of two different cohorts does not yield binary results (dead vs alive) but

is rather an indication of viability (more or less viable). In addition, although we were able to analyse hearts from the OA and DMSO (vehicle) I/R cohorts with mass spectrometry, we were not able to do so with the control, ischaemia, I/R, DMSO ischaemia, and OA ischaemia cohorts for a comprehensive comparison.

CHAPTER SEVEN

STRIATIN AND HSP90A AS POTENTIAL SUBSTRATES OF PP2A

7.1 RATIONAL

In the previous chapter, phosphoproteomic analysis of myocardial tissue exposed to 50 nM OA (or 0.002% DMSO as a vehicle control) and subjected to 20 minutes GI and 10 minutes reperfusion yielded a total of 1841 proteins and 684 phosphorylated proteins. The pathways most influenced by an inhibition of PP2A immediately prior to I/R related to mitochondrial function, cytoskeletal signalling, and adherens junction signalling. Two proteins from the data set were selected for further analysis based on the following criteria: (i) the proteins had to be differentially expressed as well as (ii) undergo a change in phosphorylation in the OA-treated group, and (iii) the phosphorylated protein must have at least a two-fold increased expression. These changes had to be statistically significant since a high degree of certainty was required in the identification of these proteins. 41 proteins fit these criteria and a brief literature search was conducted to determine the function of each protein, whether the proteins had any reported or possible association with PP2A, as well as any known roles in I/R. From this set of data, two scaffolding proteins, striatin and heat shock protein (HSP) 90 α were selected.

7.1.1 Striatin

Striatin is a scaffolding protein that mediates vesicular trafficking (Moreno *et al.*, 2000), regulates cell adhesion (Lahav-Ariel *et al.*, 2019), and functions as a regulatory subunit of PP2A (Castets *et al.*, 2000). Striatin has been reported to be localized in both the cytosolic and membrane fractions of atrial and ventricular cardiomyocytes (Gaillard *et al.*, 2001; Huret, 2011; Nader *et al.*, 2017). It has no intrinsic catalytic activity, but can function as a scaffolding protein that recruits kinases and phosphatases to form large signalling complexes called STRIPAK (striatin-interacting phosphatase and kinase) complexes (Goudreault *et al.*, 2009). STRIPAK complexes contain a member of the striatin family (striatin, zinedin, or SG2NA), and interestingly, almost always contains the AC dimer of PP2A (Moreno *et al.*, 2000). Other proteins that have been reported in STRIPAK complexes include germinal-center kinase III proteins such as Mst3, Mst4, and Ysk-1,

striatin-interacting proteins 1/2, sarcolemmal associated membrane proteins, and misshapen-like kinase 1 (Goudreault *et al.*, 2009).

Many STRIPAK proteins are phosphorylated, and this phosphorylation is enhanced when cells are treated with OA (Moreno, Lane and Pallas, 2001). This would indicate that one of the functions of the complex is to hold PP2A in close proximity to kinases which in turn regulate various functions (Rostron *et al.*, 2017). This was validated by Gordon and coworkers who demonstrated that point mutations in striatin reduce PP2A binding and results in hyperphosphorylation and activation of Mst3 (2011).

Although research on the function of striatin in the heart is scarce, the few studies investigating the role of striatin in the cardiovascular system have shown its importance for normal cardiovascular function. Global striatin knockout in mice is embryonically lethal, but knockdown results in viable and fertile mice that develop cardiomyopathies (Rostron *et al.*, 2017). Striatin modulates endothelial NO-cGMP, and striatin deficiency is associated with salt sensitivity hypertension, enhanced vasoconstriction, and decreased vascular relaxation (Garza *et al.*, 2015). Studies in mice indicate that dietary sodium restriction results in increased striatin expression in the heart and aorta in response to aldosterone (Pojoga *et al.*, 2012). Striatin mutations are associated with ventricular systolic dysfunction, dilatation and tachyarrhythmias, and sudden death in boxer dogs (Meurs *et al.*, 2013). Striatin also regulates cardiomyocyte contraction rate: overexpression of striatin causes a twofold increase in the rate of spontaneous contraction while knockdown of striatin reduces contraction rate (Nader *et al.*, 2017). Striatin is also partly responsible for the non-genomic steroid activation of downstream signalling, as it acts as a scaffold to target the estrogen receptor, PP2A and eNOS, to the cell membrane, and disruption of this complex prevents the phosphorylation of MAPK, PKB/Akt, and eNOS by estrogen (Lu *et al.*, 2004; Bernelot Moens *et al.*, 2012). Thus, striatin's function as a scaffold is necessary for the signalling that results in the cardioprotective effects of estrogen (Bernelot Moens *et al.*, 2012).

Phosphoproteomic analysis revealed a high abundance of phosphorylated striatin in the OA-treated I/R cohort (see chapter six). Various high-throughput analyses have identified various phosphorylation sites on striatin, with Ser137, Thr145, Ser227, Ser245, Ser259 being the most commonly reported (Hornbeck *et al.*, 2015). However, none of these sites has been confirmed or evaluated using methods other than mass spectrometry. As such, the role of phosphorylated striatin remains unknown.

7.1.2 Heat shock protein (HSP) 90 α

HSP90 α belongs to the HSP90 family of molecular chaperones. HSP90 α is ubiquitously expressed in the cytoplasm of all tissues but is less abundant than the HSP90 β isoform. However, it is highly inducible upon cellular stress (Hoter, El-Sabban and Naim, 2018). As a chaperone, HSP90 α promotes the proper folding of newly synthesized or incorrectly folded proteins, thereby decreasing the aggregation of mis-folded proteins (Subbarao Sreedhar *et al.*, 2004). Additionally, it also facilitates degradation of damaged or misfolded proteins that cannot be salvaged and stabilizes proteins during cellular stress. HSP90 also functions in the maturation of various signalling proteins such as steroid receptors and kinases (Schmidt and Perlmutter, 2005).

The cytoskeleton is also regulated by HSP90. HSP90 binds to actin filaments when the intracellular environment is depleted of ATP (Fostinis *et al.*, 1992). It also protects tubulin (Weis *et al.*, 2010) and myosin (Etard, Roostalu and Strähle, 2008) from heat denaturation.

Most research regarding HSP90 does not distinguish between the α and β isoforms, as they have a similar structure and function. However, each isoform has a distinct and non-redundant function in response to stress. In studies on wound healing (another type of hypoxic environment), it was reported that HSP90 β functioned to stabilize cell surface receptors, while HSP90 α promoted cell motility that resulted in wound closure (Jayaprakash *et al.*, 2015). However, both isoforms have been shown to be cardioprotective. Both HSP90 α and β promote eNOS activity by facilitating the simultaneous phosphorylation of Ser1177 by PKB/Akt and dephosphorylation of Thr495 by PP2B (Kupatt *et al.*, 2004; Barrera-Chimal *et al.*, 2014). HSP90 also delivers proteins, including PKC ϵ , to the mitochondria, through HSP90's interaction with mitochondrial import proteins (Young, Hoogenraad and Hartl, 2003; Budas *et al.*, 2010). The translocation of PKC ϵ to the mitochondria is also an integral part of HSP90's cardioprotective function.

HSP90 is regulated by phosphorylation by ATM kinase (Elaimy *et al.*, 2016) and dephosphorylation by PP5. However, PP5 is only responsible for dephosphorylation of two of the ten known phosphosites that regulate HSP90's conformation (Soroka *et al.*, 2012). Although most studies refer to the pan population of HSP90, the α and β isoforms have distinctly different functions and may therefore be regulated differently. As the phosphoproteomic results of this study indicate increased abundance of phosphorylated HSP90 α after the administration of a PP2A inhibitor, PP2A could be a potential regulator of HSP90 α .

7.1.3 Aims

The overarching aim of this chapter was to confirm our phosphoproteomic data and specifically determine the effects of PP2A inhibition prior to ischaemia and reperfusion on these proteins. Unfortunately, no commercial anti-phospho-striatin antibody was available to investigate the effects of PP2A inhibition on the phosphorylation of striatin. However, total striatin antibodies were available and these were used in experimentation. Immunoprecipitation of PP2A was also used as a tool to provide insight into whether the selected proteins have a direct interaction with PP2A. PKB/Akt was also investigated, as it is a client protein of HSP90 and *in vitro* studies showed that it is catalytically active when complexed with HSP90 (Basso *et al.*, 2002). It is postulated that HSP90 complex formation with PKB/Akt facilitates kinase activation by preventing both dephosphorylation and degradation of PKB/Akt that results in apoptosis (Sato, Fujita and Tsuruo, 2000). PP2A inhibition prior to ischaemia has previously been shown to enhance PKB/Akt phosphorylation (Van Vuuren, 2014), but how this might relate to HSP90 α phosphorylation and interaction with PP2A has not yet been reported.

7.2 METHODS

Hearts were perfused using the same protocol specified in chapter six for the phosphoproteomic analysis (Figure 6.2). Hearts were perfused for 15 minutes in retrograde mode, 15 minutes in antegrade mode, followed by either 50 nM OA or 0.002% DMSO administration for 20 minutes in retrograde mode. Thereafter hearts were exposed to 20 minutes ischaemia, and where applicable hearts were reperfused for 10 minutes in retrograde mode. Appropriate vehicle cohorts were used (as described in chapter six) and hearts in the control cohort received normal retrograde perfusion instead of ischaemia. At the completion of the perfusion experiment, hearts were freeze-clamped and stored in liquid nitrogen until further use.

7.2.1 Whole cell lysate (non-fractionated)

Approximately one-quarter of each mouse heart was used to prepare whole cell lysates using a lysis buffer containing 1 mM EDTA, 20 mM TRIS-HCl, 1 mM EGTA, 150 mM NaCl, 2.5 mM tetra-Na pyrophosphate, 1 mM β -glycerophosphate, 1 mM SOV, 50 μ g/ml PMSF, 1% Triton-X-100, and 50 μ l of protease inhibitor. The samples were then homogenized using the Bullet blender (Next Advance, Inc.), left on ice for 20 minutes, and then centrifuged at 1,000 x g at 4 °C for 20 minutes.

However, as the tissue had been used for other experiments, four of the 20 original samples contained very little tissue and had to be excluded from analysis. For the remaining samples, stainless steel beads (1.6 mm) were added to each sample, the samples homogenized using the Bullet blender (Next Advance, Inc.) and left to rest at 4 °C for 20 minutes. This was followed by centrifugation at 12,074 x g at 4 °C for 20 minutes and collection of the supernatant. To preserve sample volume, protein concentration was determined using the Direct Detect® Infrared Spectrometer (Merck Millipore), which requires only 2 µl of sample and determines protein concentration within one minute. Although protein determination with this method is more accurate than the traditional Bradford assay, it can be costly and was only used in this study for samples of small volume.

7.2.2 Immunoprecipitation

Approximately one-quarter of a mouse heart was used to prepare whole cell lysates using the same lysis buffer as described previously in chapter two, except for the exclusion of phosphatase inhibitors. Stainless steel beads (1.6 mm) were added to each sample, and the samples homogenized using the Bullet blender (Next Advance, Inc.) and left to rest at 4 °C for 20 minutes, followed by centrifugation at 12,074 x g at 4 °C for 20 minutes where after the supernatant was collected. The protein content was determined by the Bradford technique and all samples were diluted to 600 µg in 500 µl (1.2 µg/ul). 50 µl of PP2A antibody (Santa Cruz Biotechnology Inc.; sc-6110) was added to each sample and left overnight at 4 °C. 50 µl A/G agarose beads (Sigma Aldrich; cat: 11719408001) was then added to each sample, and gently agitated at 4 °C for three hours. The antibody-bead complex was recovered by centrifuging the sample (12,074 x g at 4 °C for 45 seconds) and removing the supernatant. The antibody-bead complex was then washed by adding lysis buffer, centrifuging the sample (12,074 x g at 4 °C for 45 seconds), and removing the supernatant. This was repeated three times before the sample (antibody-bead complex) was resuspended in lysis buffer containing Laemmli buffer and stored at – 80 °C for further western blot analysis.

7.2.3 Fractionation

Myocardial tissue was separated into cytosolic, nuclear, and membrane fraction (where the membrane fraction contained plasma, mitochondrial, nuclear, Golgi, and endoplasmic reticulum). Differential centrifugation was used to split myocardial fractions using a protocol previously described in our laboratory (Marais *et al.*, 2005). One-half of each heart was pulverized using a

cooled mortar and pestle and added to the same lysis buffer described above, but without Triton X-100. The samples were then homogenized using the Bullet blender (Next Advance, Inc.) left on ice for 20 minutes, and then centrifuged at 1,000 x g at 4 °C for 10 minutes.

The supernatant was removed from the pellet, placed into a clean tube, and centrifuged at 100,000 x g for 60 minutes. The resulting pellet contained the crude membrane fraction and was resuspended in 600 µl lysis buffer containing 1% Triton X-100 by adding zirconium oxide beads (0.5 mm) and using the Bullet Blender (Next Advance, Inc.). The supernatant on the other hand, contained the cytosolic fraction. Both fractions were immediately stored at – 80 °C.

The pellet from the initial centrifugation was resuspended in 300 µl lysis buffer containing 1% Triton X-100, by homogenizing it in the Bullet Blender (1.5 mm stainless steel beads; Next Advance, Inc.). It was subsequently left on ice for 10 minutes and then centrifuged at 12,074 x g at 4 °C for 30 minutes. The supernatant from this spin contained the nuclear fraction and was stored at – 80 °C. The protein content of all samples in all fractions was determined by the Bradford technique.

7.2.4 Western blot analysis

For both the different fractions, as well as whole cell preparations, individual samples were diluted with lysis buffer to a uniform protein concentration and 3x Laemmli buffer was added to samples (0.78 µg/µl for the membrane fraction, 2 µg/µl for the cytosolic and nuclear fractions, 1.67 µg/µl for the WCL). 20 µl of each whole cell lysate was immediately stored for western blot analysis of mitochondrial complexes (chapter eight), and the remainder of the samples were boiled for five minutes and stored at - 80 °C. Western blot analysis was conducted as described in chapter two. The membranes were incubated overnight at 4 °C with either PKB (phospho or total), HSP90α (phospho or total), or total striatin and washed thoroughly as described previously. Following this the membranes were incubated at room temperature with a goat anti-rabbit horseradish-peroxidase conjugated secondary antibody (Cell Signalling Technology; cat: 7060S) under constant, gentle agitation for an hour at room temperature and washed as described above. Thereafter, the membrane was incubated in Clarity™ Western ECL Blotting Substrate (Bio-Rad Laboratories Inc.; cat: 1705061) for five minutes and visualized on the ChemiDoc imaging system.

7.2.5 Statistical analysis

Western blot protein bands were normalized to total protein loaded onto the membrane using ImageLab 5.0 software (see chapter two for full description). Images of the total protein loaded on the membranes can be found in Addendum C. Data were exported to an Excel spreadsheet where fold changes and phosphorylated/total protein ratio (P/T) were calculated. Data were then analysed in GraphPad© Prism where a one-way ANOVA with a Holm-Sidak *post-hoc* test was performed, as specific groups were compared (Control vs ischaemia; ischaemia vs, I/R; effect of OA on ischaemia and reperfusion). All data are expressed as mean \pm SD and a p-value equal to or less than 0.05 was considered significant.

7.3 RESULTS

7.3.1.1 *Whole cell lysate (non-fractionated)*

Whole cell lysates (WCL) were prepared from mouse hearts exposed to I/R in the presence and absence of OA. However, as the tissue had also been used for other experiments, four samples (one each from the DMSO ischaemia and I/R cohorts, and two samples from the OA ischaemia cohort) either had no remaining tissue or too little tissue to be used for analysis. Total HSP90 α expression in the OA ischaemia cohort was increased when compared to the DMSO ischaemia cohort ($p = 0.0107$) and the control cohort ($p = 0.0268$; Figure 7.1A). An increase in absolute phosphorylation was observed in the OA-treated I/R cohort when compared to its DMSO counterpart ($p = 0.0480$; Figure 7.1B). However, no differences in P/T were observed (Figure 7.1),

probably due to the very large variation in certain cohorts, or to the fact that the increase in total protein and phosphorylation followed the same pattern.

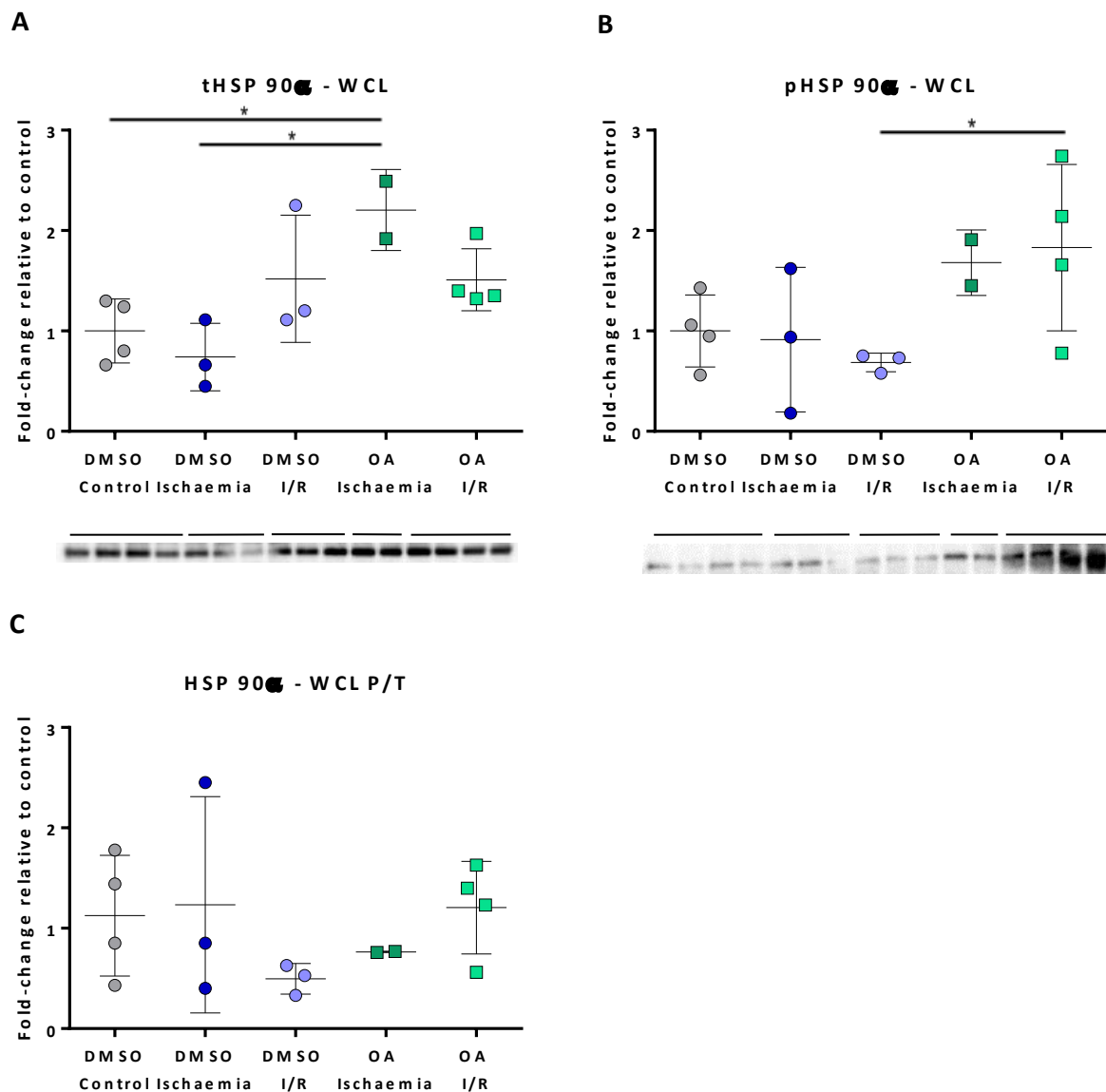


Figure 7.1 - HSP90 α expression in non-fractionated whole-cell lysate

Western blot analysis of HSP90 α in a whole cell lysate revealed increased protein expression in the OA-ischaemia cohort (A) when compared to the DMSO-ischaemia cohort ($p = 0.0107$) and the control cohort ($p = 0.268$). An increase in phosphorylation (B) was observed in the OA-treated I/R cohort was significantly higher than that of its DMSO-treated counterpart ($p = 0.0480$). No differences in P/T (C) was observed. $n = 2-4$

* $p < 0.05$

P/T = ratio of phosphorylated to total protein

WCL = whole cell lysate

Western blot data generated for the analysis of PKB/Akt (particularly phosphorylated PKB/Akt) resulted in a lot of non-specific binding, making analysis challenging. Unfortunately, due to time constraints, the analysis of PKB/Akt in the WCL was excluded from this study.

An increase in striatin expression was observed in the OA-treated I/R cohort when compared to its DMSO counterpart ($p = 0.0436$; Figure 7.2).

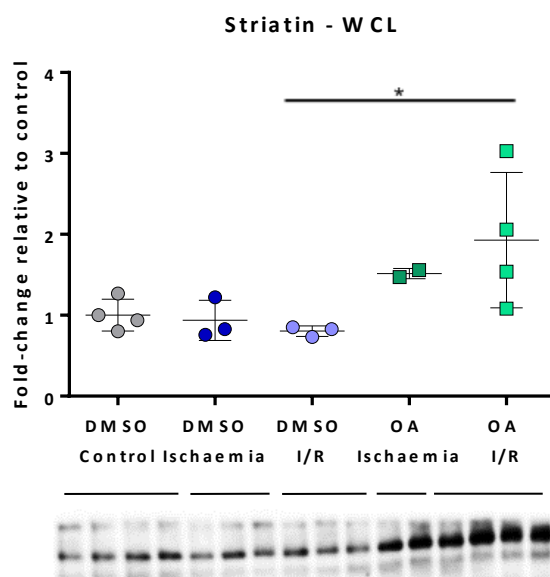


Figure 7.2 - Striatin expression in non-fractionated whole-cell lysate

Western blot analysis of striatin in the whole cell lysate revealed an increase in expression in the OA-treated I/R cohort when compared to its DMSO counterpart ($p = 0.0436$). $n = 2-4$

7.3.2 Immunoprecipitation

As the lysis buffer used to prepare myocardial tissue for immunoprecipitation was void of phosphatase inhibitors, only total protein antibodies were used for western blot investigation. Western blot analysis of immunoprecipitated PP2A revealed that striatin co-precipitates with PP2A (Figure 7.3A), which is not surprising, as striatin is a known regulatory subunit of PP2A and the AC dimer is an integral component of STRIPAK complexes. The experimental interventions under investigation did not influence the degree of association between striatin and PP2A. PKB/Akt was also found to co-precipitate with PP2A, but this was not consistent across samples, and no trend between cohorts was observed. HSP90 α did not co-precipitate with PP2A (data not shown).

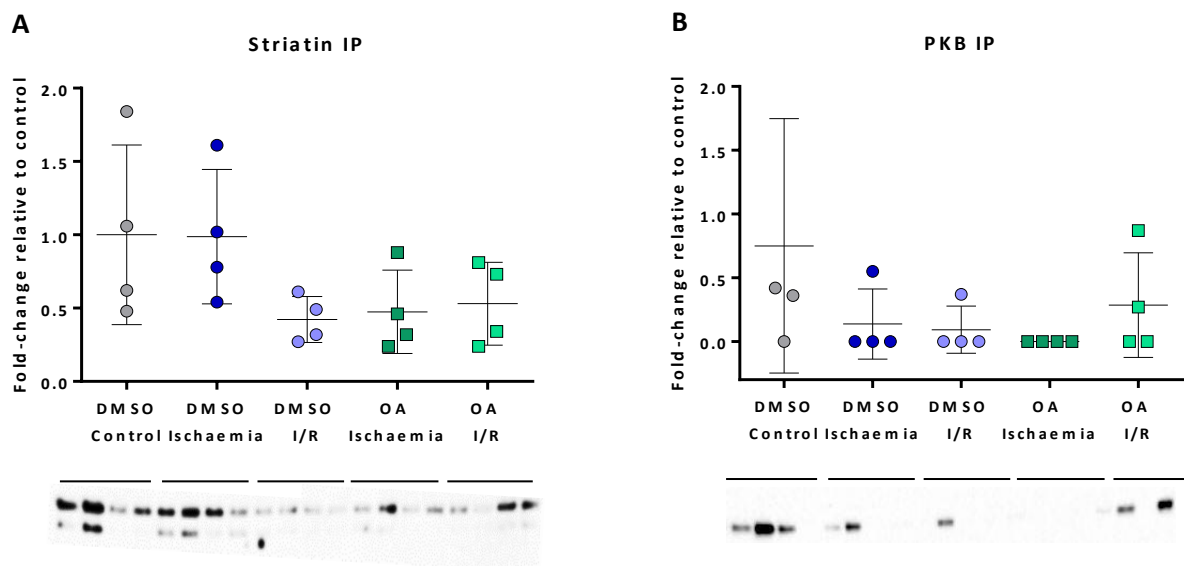


Figure 7.3 - Fold changes of striatin and PKB that has co-immunoprecipitated with PP2A

PP2A was immunoprecipitated from hearts perfused with 0.002% DMSO (vehicle) or 50 nM OA and exposed to 20 minutes GI, or 20 minutes GI and 10 minutes reperfusion. Striatin was identified in the immunoprecipitate (A). PKB/Akt co-precipitation was identified in some samples (B), but this was inconsistent with no observed trend among cohorts. $n = 4$.

7.3.3 Fractionation

7.3.3.1 Cytosolic fraction

HSP90 α was present in the cytosol and expression did not differ between cohorts (Figure 7.4A). Phosphorylated HSP90 α yielded two protein bands (Figure 7.4B **Figure 7.3**), one at 95 kDa (top band; 1) and another at approximately 90 kDa (bottom band; 2). Phosphorylation of HSP90 α did not differ between cohorts, and did not result in different P/T between cohorts (Figure 7.4C).

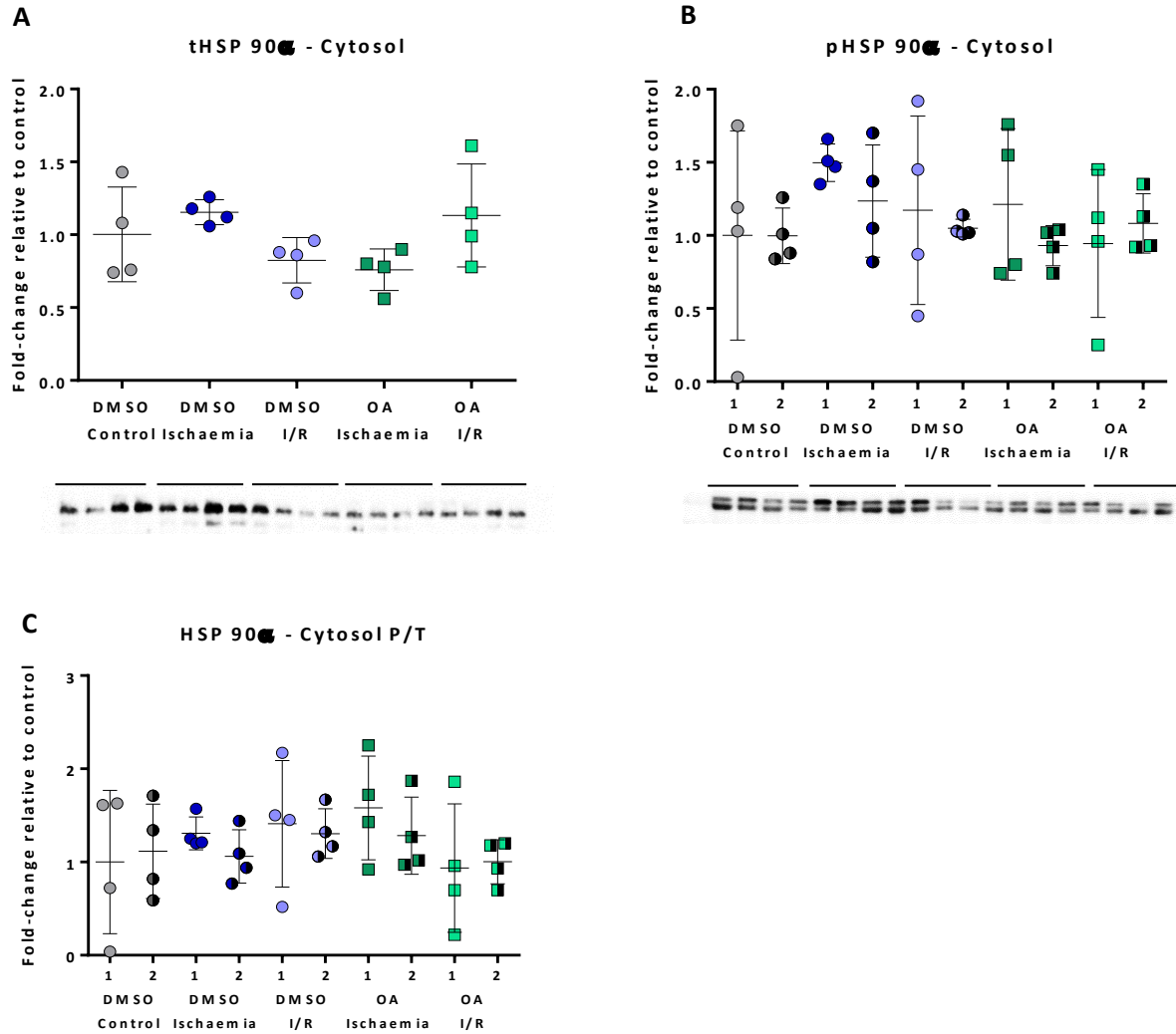


Figure 7.4 - HSP90 α expressed in the cytosolic fraction

Total (A) and phosphorylated HSP90 α expressed in the cytosolic fraction. Analysis of phosphorylated HSP90 α yielded two protein bands, one at 95 kDa (top band; 1) and another at approximately 90 kDa (bottom band; 2). Total protein expression did not differ between cohorts and neither ischaemia or reperfusion, or PP2A inhibition had any effect on phosphorylation (C). $n = 4$

P/T = ratio of phosphorylated to total protein

PKB/Akt was present in the cytosolic fraction (Figure 7.5A), where an increase in phosphorylation was observed during reperfusion, regardless of treatment ($p = 0.0130$ for DMSO; $p = 0.0084$ for OA; Figure 7.5B). The P/T data of the OA-treated I/R cohort was significantly greater when compared to the OA-treated ischaemia cohort ($p = 0.0001$) or compared to its DMSO-treated I/R counterpart ($p = 0.0014$; Figure 7.5C).

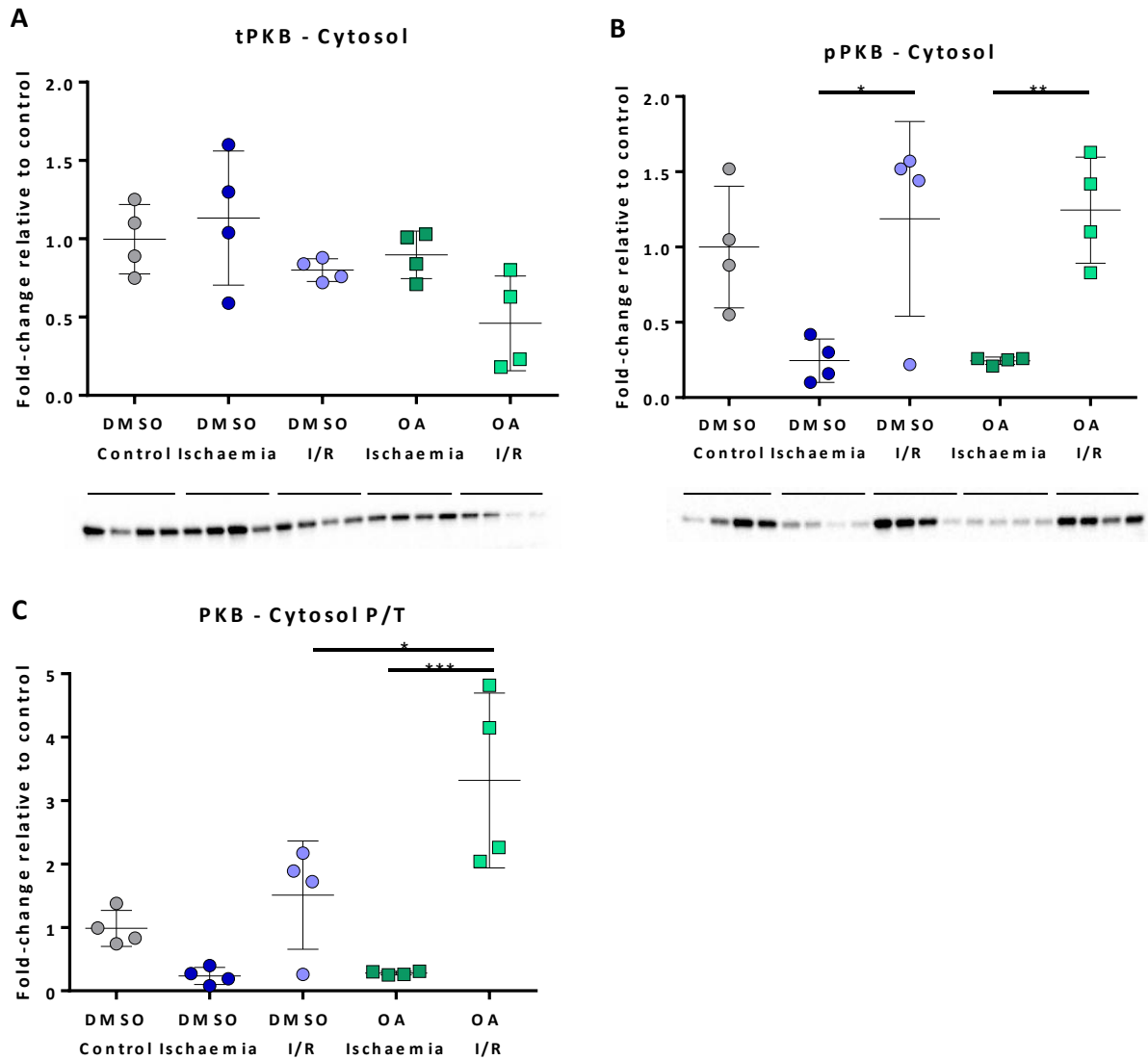


Figure 7.5 - PKB/Akt expressed in the cytosolic fraction

Total (A) and phosphorylated (B) PKB expressed in the cytosolic fraction. Increased phosphorylation was observed in reperfusion, regardless of drug treatment ($p = 0.0130$ for DMSO; $p = 0.0084$ for OA). Increased phosphorylation was reflected in P/T (C), where higher ratios were observed in reperfusion after OA administration when compared to the OA-treated ischaemia cohort ($p = 0.0140$) and the DMSO-treated I/R cohort ($p = 0.0001$). $n = 4$

* $p < 0.05$

** $p < 0.01$

*** $p < 0.001$

P/T = ratio of phosphorylated to total protein

Striatin was present in the cytosol, and neither ischaemia, reperfusion, or PP2A inhibition had any effect on total striatin expression (Figure 7.6). No phosphorylated antibody was commercially available at the time of experimentation.

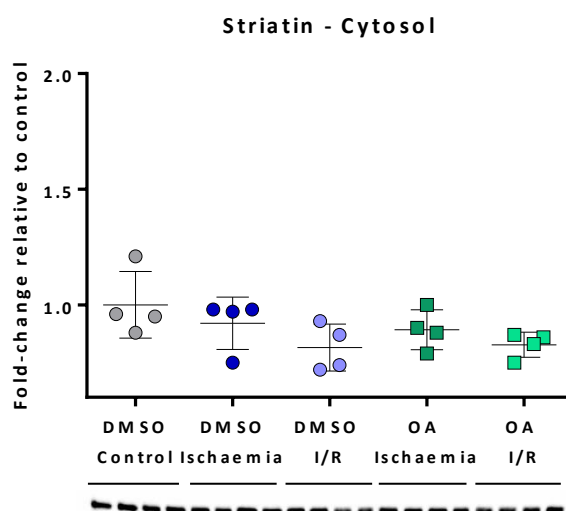


Figure 7.6 - Striatin expressed in the cytosolic fraction

Total striatin present in the cytosolic fraction. Total protein levels did not differ between cohorts and neither ischaemia or reperfusion, nor PP2A inhibition had any effect protein expression. $n = 4$

7.3.3.2 Membrane fraction

Extremely faint bands were detected in the phosphorylated HSP90 α analysis. However, no bands were detected in the total HSP90 α protein analysis (see Addendum C, Figure C.7). The analysis of HSP90 α in the membrane was therefore excluded from this study as the analysis could not be repeated due to time constraints. PKB/Akt was present in the membrane fraction (Figure 7.7A) and no significant differences in absolute phosphorylation was observed (Figure 7.7B). However, an increase in P/T was observed in reperfusion, regardless of drug treatment ($p = 0.0016$ for DMSO; $p = 0.0305$ for OA; Figure 7.7C).

Western blot analysis of striatin in the membrane fraction revealed a strong protein band at ≈ 56 kDa, rather than at 110 kDa (see Addendum C, Figure C.15). It is not known whether this is indeed striatin, a splice variant of striatin, degraded or cleaved striatin, or non-specific antibody binding.

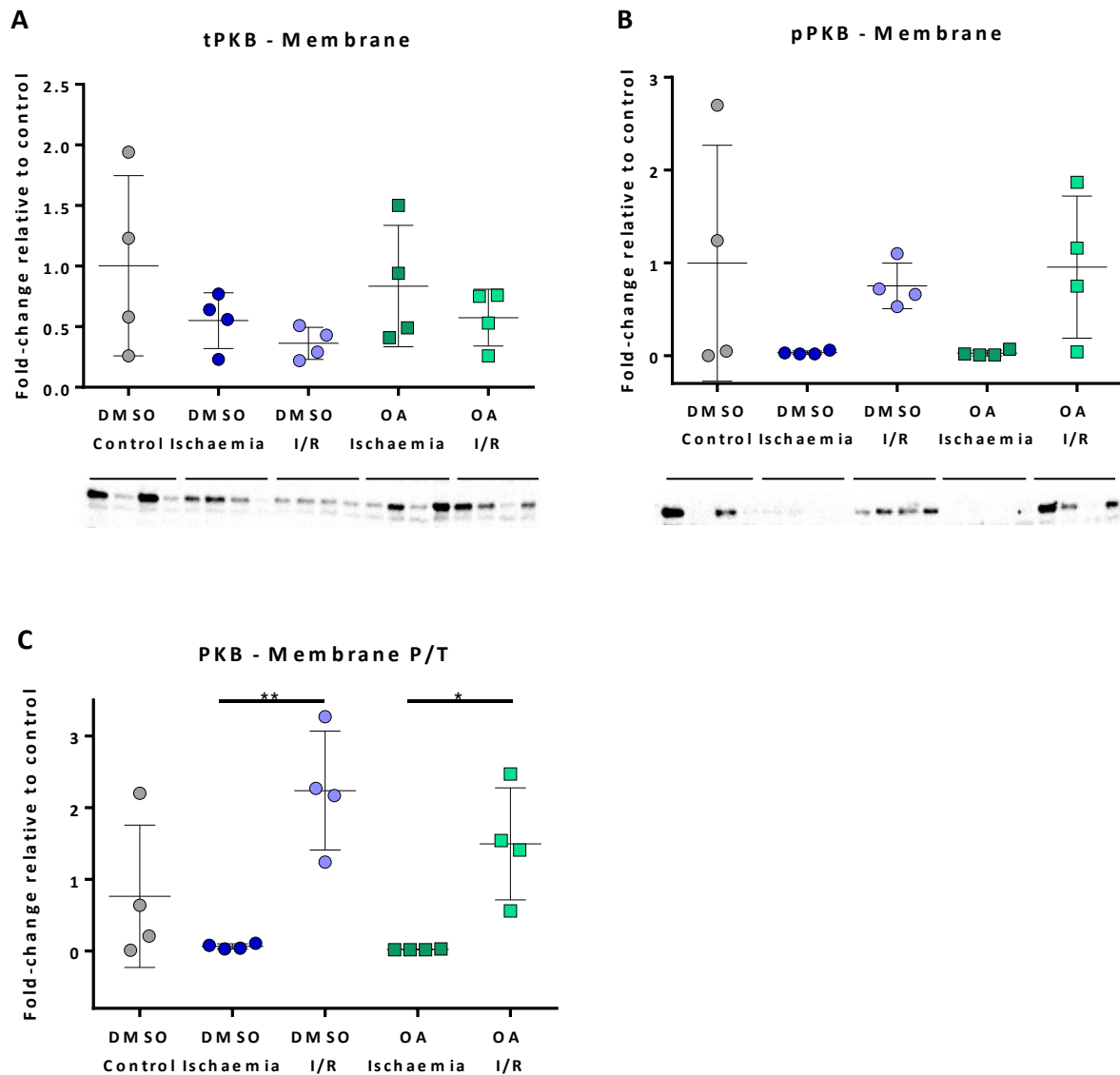


Figure 7.7 - PKB/Akt expressed in the membrane fraction

Total (A) and phosphorylated PKB/Akt (B) expressed in the membrane fraction. No differences in phosphorylation between cohorts were observed. Increased P/T (C) was observed in reperfusion, despite treatment with OA ($p = 0.0016$ for DMSO I/R; $p = 0.0305$ for OA I/R). $n = 4$

* $p < 0.05$

** $p < 0.01$

P/T = ratio of phosphorylated to total protein

7.3.3.3 Nuclear fraction

HSP90 α was present in the nuclear fraction (Figure 7.8A). Although HSP90 α was phosphorylated, no differences in absolute phosphorylation was observed between the cohorts (Figure 7.8B). An increase in P/T was observed in the OA-treated I/R cohort when compared to its DMSO-treated counterpart ($p = 0.0459$; Figure 7.8C).

PKB/Akt was also present in the nuclear fraction (Figure 7.9A). A decrease in phosphorylation of PKB/Akt occurred in the ischaemia and I/R cohorts when compared to control ($p = 0.0115$ and $p = 0.046$, respectively). This ischaemia-associated decrease was rescued by OA administration (Figure 7.9B). This was reflected in both the phosphorylated PKB/Akt and P/T, which was increased in the OA-treated ischaemia cohort when compared to the DMSO-treated ischaemia cohort ($p = 0.0116$; Figure 7.9C).

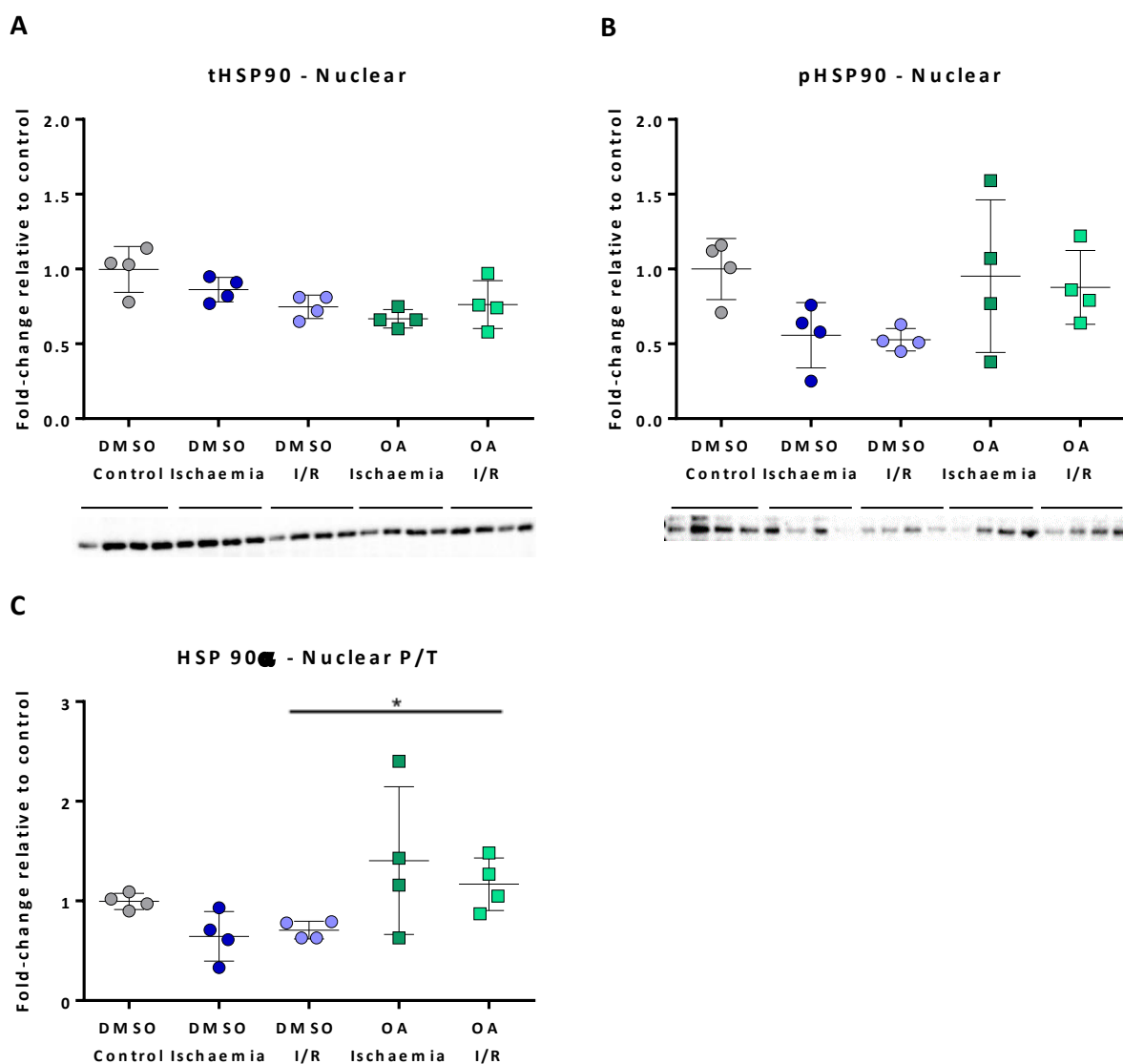


Figure 7.8 - HSP90α expressed in the nuclear fraction

Total (A) and phosphorylated HSP90α expressed in the nuclear fraction. No differences in phosphorylation (B) were observed. An increase in P/T (C) was observed in the OA-treated I/R cohort when compared to its DMSO-treated counterpart ($p = 0.0459$). $n = 4$

* $p < 0.05$

P/T = ratio of phosphorylated to total protein

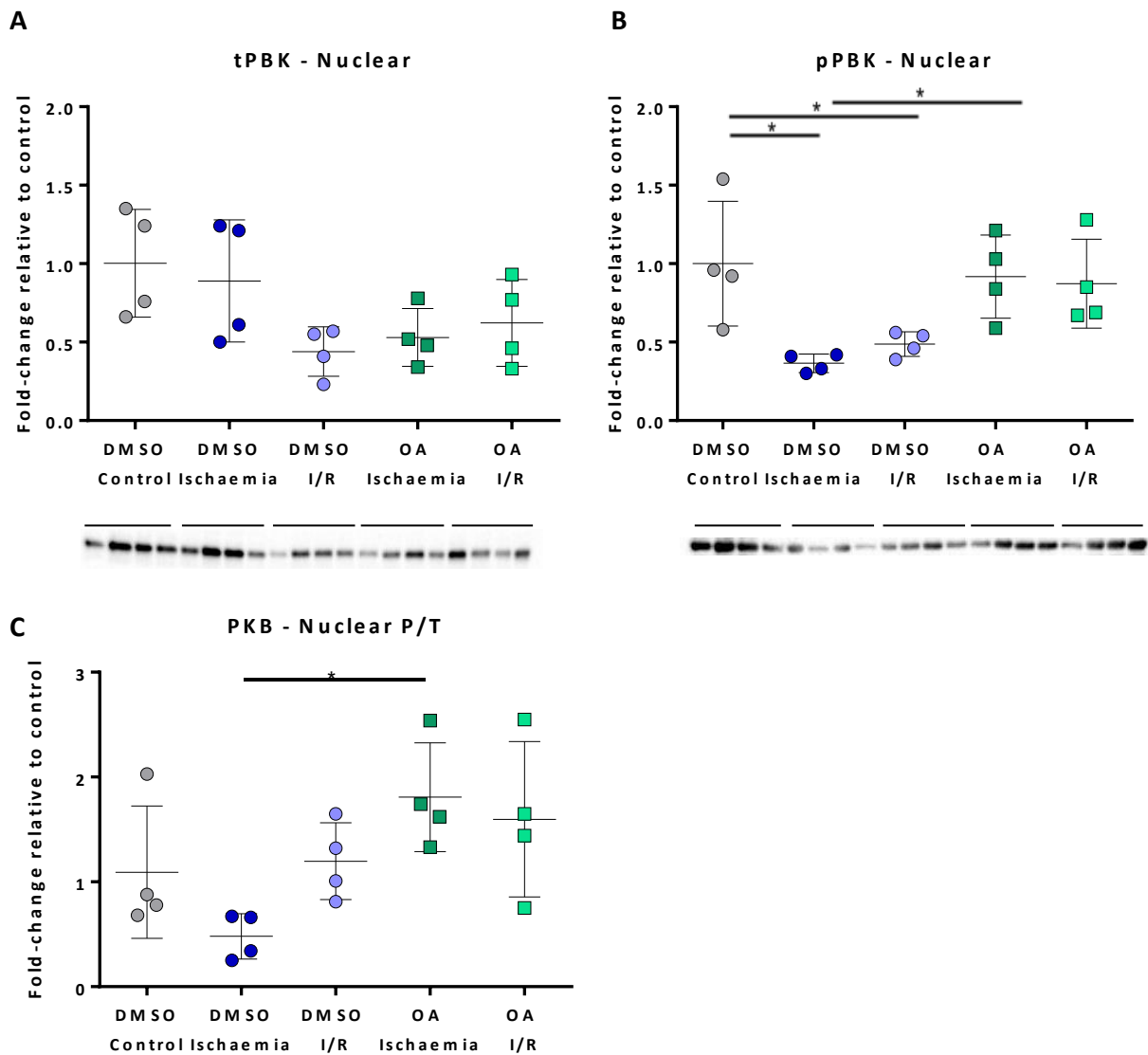


Figure 7.9- PKB/Akt expressed in the nuclear fraction

Total (A) PKB/Akt was expressed in the nuclear fraction. Phosphorylation (B) decreased in the ischaemia and I/R cohorts when compared to control ($p = 0.0115$ and $p = 0.046$, respectively). This was rescued by OA administration. P/T (C) was increased in the OA-treated ischaemia cohort when compared to its DMSO-treated counterpart ($p = 0.0116$). $n = 4$

* $p < 0.05$

P/T = ratio of phosphorylated to total protein

Western blot analysis of striatin in the nuclear fraction revealed protein bands at 110 kDa, as expected (Figure 7.10). Striatin levels were significantly decreased in the DMSO-treated I/R when compared to the DMSO-treated ischaemia cohort ($p = 0.0491$). OA administration prior to I/R increased the amount of striatin in the nuclear fraction after 10 minutes of reperfusion ($p = 0.0119$).

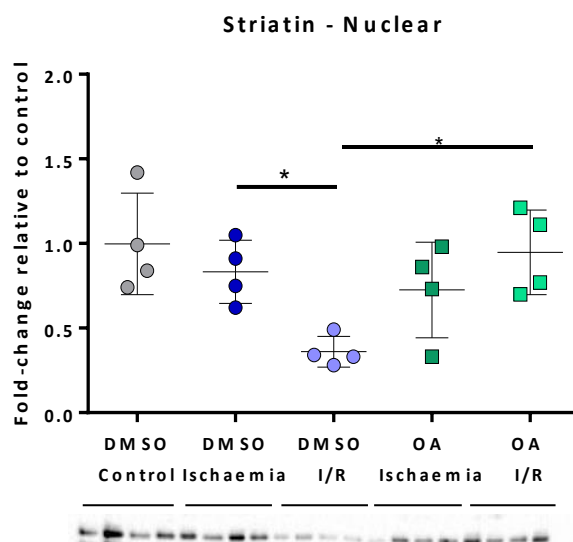


Figure 7.10 - Striatin expressed in the nuclear fraction

Western blot analysis of striatin in the nuclear fraction revealed protein bands at 110 kDa, as expected. Analysis of the band indicated decreased expression of striatin in the DMSO-treated I/R cohort when compared to the DMSO-treated ischaemia cohort ($p = 0.0491$). An increase in striatin expression was observed in the OA-I/R cohort when compared to DMSO I/R ($p = 0.0119$). $n = 4$

* $p < 0.05$

7.4 DISCUSSION

The aim of these experiments was to investigate the effects of PP2A inhibition during myocardial ischaemia and reperfusion on striatin and HSP90 α . This was done to confirm and expand on data generated in the phosphoproteomic part of this work. Therefore, the same perfusion protocol used to generate tissue for phosphoproteomic analysis was employed in this study. In the WCL, PP2A inhibition increased the total amount of HSP90 α during ischaemia and increased the amount of phosphorylated HSP90 α (but not the P/T) during reperfusion. In addition, OA administration increases the total striatin levels during reperfusion (when compared to DMSO-treated I/R). The increase in total striatin and phosphorylated HSP90 α during reperfusion as observed during western blot analysis, correlates with the phosphoproteomic results. The

phosphoproteomic analysis also indicated an increase in phosphorylated striatin, but this could not be investigated in this study due to the lack of available antibody.

Expanding these results, two separate experiments were conducted: co-immunoprecipitation and fractionation. In the co-immunoprecipitation experiments, PP2A was immunoprecipitated from hearts treated with either DMSO (vehicle) or 50 nM OA followed by exposure to ischaemia, or ischaemia and reperfusion. The resulting precipitates were then analysed by western blot to investigate co-precipitation, which would indicate physical interaction with PP2A. How ischaemia and reperfusion, as well as PP2A inhibition during ischaemia and reperfusion, affects the expression and phosphorylation of HSP90 α and striatin were further investigated using western blot analysis of the cytosolic, membrane, and nuclear fractions.

7.4.1 HSP90 α

HSP90 α did not co-precipitate with PP2A, indicating that it may not bind to PP2A, and thus may not be a direct target of PP2A in this setting. Western blot analysis of the WCL showed an increase in phosphorylated HSP90 α during reperfusion when compared to the DMSO-treated cohort (Figure 7.1), confirming the phosphoproteomic data. HSP90 α was present in the cytosol and nucleus and absent in the membrane, which is consistent with literature reports of its intracellular location (Hoter, El-Sabban and Naim, 2018). Analysis of phosphorylated HSP90 α yielded two protein bands in the cytosolic fraction (Figure 7.4), one at 95 kDa (top band; 1) and another at approximately 90 kDa (bottom band; 2). No other bands were detected on the blot, and only one band (at 90 kDa) was present in both the whole cell lysate and nuclear fraction blots. HSP90 α is 90 kDa, indicating that the bottom band was indeed HSP90 α . The top band may represent a population of HSP90 α that is made slightly heavier by various additional post-translational modifications, such as acetylation, tyrosine phosphorylation, or glycosylation (Bio-rad, 2016). Interestingly, this only occurs in the cytoplasm.

Analysis of the WCL indicates that OA administration results in an increase in total HSP90 α during ischaemia and an increase in phosphorylated HSP90 α during reperfusion (Figure 7.1). The increase in phosphorylated observed during reperfusion was reflected in the nuclear fraction, where most HSP90 α was phosphorylated (as reflected by the P/T; Figure 7.8). However, the increase in total protein was not observed in either cytosolic or nuclear fractions. HSP90 α is

known to associated with the plasma membrane (Sidera *et al.*, 2004), which could not be analysed in this study.

Western blot analysis indicates that PP2A inhibition does not influence the phosphorylation of cytosolic HSP90 α (Figure 7.4), despite the increase in phosphorylation during reperfusion observed in the WCL (Figure 7.1). PP2A inhibition prior to ischaemia increased the ratio of phosphorylated HSP90 α (relative to total protein) during reperfusion when compared to the untreated (vehicle containing 0.002% DMSO) I/R cohort in the nuclear fraction (Figure 7.8). HSP90 α has been shown to be phosphorylated in response to double-stranded DNA damage (Quanz *et al.*, 2012), which may explain the abundance of phosphorylated HSP90 α (relative to total protein) in the nucleus.

HSP90 α is upregulated during cellular stress such as ischaemia and I/R (Hoter, El-Sabban and Naim, 2018; Ranek *et al.*, 2018), but this was only seen in our study in ischaemia following OA administration. As the immunoprecipitation experiments suggest that PP2A does not directly modulate HSP90 α activity, the upregulation of total protein in the OA-treated cohort may be an indirect effect of PP2A inhibition, although it is most likely due to the inhibition of inadvertent inhibition of PP5 by OA (Swingle, Ni and Honkanen, 2007).

HSP90 α contains numerous serine, threonine, and tyrosine phosphorylation sites (Hornbeck *et al.*, 2015), and phosphorylation at different sites results in changes to HSP90's specificity (and this is species and tissue specific; Mollapour and Neckers, 2012). The anti-phospho-HSP90 α antibody used in this study recognizes Thr5/Thr7, sites that are phosphorylated by double-stranded DNA protein kinase in response to DNA damage. HSP90 α is phosphorylated at these sites in the cytosol and then accumulates at sites of DNA breaks to form repair foci (Quanz *et al.*, 2012). However, HSP90 α can be phosphorylated at many other sites, and these could not be investigated with the resources at hand.

Administration of OA, but not PP1 or PP2A, disrupts the p60^{V-Src}-HSP90 heterocomplex by promoting hyperphosphorylation of HSP90 in NIH 3T3 cells (Mimnaugh *et al.*, 1995). This would suggest that HSP90 requires dephosphorylation of its threonine residues to properly chaperone p60^{V-Src}, but this is not necessarily true of all HSP90 α -client protein complexes. OA has also been shown to inhibit PP5 (Swingle, Ni and Honkanen, 2007) and therefore, any direct effects of OA administration on HSP90 α observed in this study may likely be due to inhibition of PP5, rather than PP2A. However, PKB/Akt phosphorylation of HSP90 α , specifically in response to stress, is

necessary for HSP90 α 's chaperone activity (Barati *et al.*, 2006). An increase in PKB/Akt phosphorylation during reperfusion was observed in the cytosolic fraction, while an increase in phosphorylated PKB/Akt was observed during ischaemia in the nuclear fraction as a result of OA administration. This may suggest a minor role of PP2A in the indirect regulation of HSP90 α via PKB/Akt regulation, where an increase in phosphorylated PKB/Akt in the nucleus at the end of ischaemia is a precursor for phosphorylated HSP90 α in the nucleus at 10 minutes reperfusion. However, this is yet to be confirmed.

7.4.2 Striatin

Striatin co-precipitated with PP2A, but to varying extents and no trend was observed between cohorts (Figure 7.3A). This was not surprising, as striatin is a regulatory subunit of the PP2A heterotrimer (Castets *et al.*, 1996), and recruits PP2A into STRIPAK complexes (Hwang and Pallas, 2014). Various components that make up STRIPAK complexes (such as PP2A, striatin, striatin-interacting proteins) have been studied in the heart. Due to their presence in cardiac tissue, they have been assumed to form STRIPAK complexes. However, this was only recently confirmed, and a role for cardiac STRIPAK complexes has been suggested. Eden and co-workers (2016) described the role of a STRIPAK complex in cardiomyocyte calcium regulation, and decreased expression of a critical component of the complex, striatin interacting protein 2 (STRIP2, myoscape) in patients with heart failure, which indicates a role in cardiac disease.

Analysis of the WCL showed that OA administration resulted in an increase in striatin during reperfusion (when compared to DMSO-treated cohorts; Figure 7.2), and although this was observed in the nuclear fraction, the increase was not as pronounced as in the WCL (Figure 7.10). Analysis of the WCL produced a blot with many bands, the most prominent of which were located at 110 kDa, and at \approx 56 kDa, but again, only in the DMSO control and DMSO ischaemia cohorts (Figure 7.2). Striatin was present in the cytosolic and nuclear fractions, and its presence in the membrane could not be established as the blot yielded a single band at \approx 56 kDa rather than 110 kDa (see Figure C.13 in Addendum C). This was unexpected, since striatin has been reported to associate with membranes, and thus is expected to be present in the membrane fraction (Moreno, Lane and Pallas, 2001). Analysis of the cytosolic fraction yielded a clean blot with protein bands at 110 kDa with no other bands resulting from non-specific binding (Figure 7.6). Interestingly, analysis of the nuclear fraction produced several protein bands, the first of which is

located at 110 kDa (striatin), some weaker bands between 70 – 110 kDa, and a strong band at \approx 56 kDa that was only in the DMSO control and DMSO ischaemia cohorts (Figure 7.10).

Protein bands that elute at higher-than-expected molecular weights are typically made heavier by various post-translational modifications. Proteins bands that elute at a lower molecular weight could be introduced at various stages in the protocol. First, insufficient protease inhibition can result in degradation of the sample that results in a “smear” as peptides of differing lengths migrate down the gel. Second, isoforms or splice variants of the target protein might exist at different molecular weights. Third, a non-target protein may contain a similar epitope. Fourth, the band may be the results of non-specific binding due to either a high antibody concentration, a poor antibody quality, or insufficient blocking of non-specific sites (Bio-rad, 2016). It is unlikely that protease cleavage is responsible for the unexpected bands observed in this study, as protease inhibitors were used in sample preparation and samples were kept on ice. Additionally, the 56 kDa band was not present in the cytosolic fraction, which yielded a clean blot with one 110 kDa band. Whether striatin contains splice-variants or isoforms has not been reported in literature. The striatin family also includes SG2NA and zinedin, but these proteins have high molecular weights, and unless they have low molecular weight splice variants or isoforms, it is unlikely that they were detected in the analysis. It is not unlikely that the antibody binds a non-target epitope. However, it would be expected to bind to 110 kDa band in the membrane fraction, and not just the 56 kDa band, unless 110 kDa striatin is not present in the membrane fraction, which is contrary to existing literature (Moreno, Lane and Pallas, 2001). As stated, multiple bands that arise on the membrane can result from problems with the antibody. Although this is possible, it is unlikely. Anti-striatin was purchased for this particular set of experiments, which were conducted within three months of antibody arrival. No known non-specific antibody binding is reported by the manufacturer (Prestige[®], Sigma Aldrich), and the blocking of non-specific sites were conducted in the same manner that resulted in clean blots with 110 kDa bands. Although the identity of the 56 kDa band remains unknown, striatin was identified with certainty in the cytosolic and nuclear fractions, as well as the WCL, and these bands were used for quantification. The 56 kDa band was concentrated in the membrane fraction, while also being present in the nucleus, and the WCL.

Analysis of the striatin in the nuclear fraction showed a decrease in expression during I/R in the DMSO-treated cohort when compared to the DMSO-treated ischaemia cohort ($p = 0.0298$; Figure 7.10). This was reversed by OA administration, as an increase in striatin was observed in the OA-treated I/R cohort when compared to its DMSO-treated counterpart.

7.4.3 PKB/Akt

PKB/Akt was co-immunoprecipitated with PP2A in some samples, but this was inconsistent between samples and no conclusion about PP2A's ability to bind PKB/Akt can be drawn from these results (Figure 7.3B). It must be noted that the preparation of the immunoprecipitates took a considerable amount of time, and no phosphatase inhibitors were added to the samples. This may have influenced the binding or dissociation of PKB/Akt from the PP2A antibody/bead complex. Although unlikely, PKB could also have been lost during the washing steps.

Cytosolic PKB/Akt was increased during reperfusion, regardless of drug treatment, but an increase in the ratio of phosphorylated protein to total protein (P/T) was only observed in the OA-treated reperfusion cohort when compared to ischaemia. OA administration also significantly enhanced P/T when compared to the DMSO-treated reperfusion cohort (Figure 7.5). An increase in P/T was again observed in during reperfusion (regardless of drug administration) in the membrane fraction (Figure 7.7). These results are congruent with existing literature that report no phosphorylation of PKB/Akt during ischaemia, but an increase in phosphorylation during reperfusion (Mockridge, Marber and Heads, 2000). Additionally, OA administration prior to I/R has also been reported to enhance PKB/Akt phosphorylation at the onset of reperfusion (Van Vuuren, 2014), which was also observed in this study, specifically in the cytosolic fraction.

Phosphorylation of PKB/Akt decreased in the nuclear fraction not only in response to ischaemia (when compared to control), but also in response to reperfusion (Figure 7.9). This was rescued by OA administration, which significantly increased phosphorylation of PKB/Akt during ischaemia when compared to DMSO-treated ischaemic hearts, but only to levels that were comparable to control hearts that did not undergo ischaemia. This may be an effect of PP2A inhibition, as PKB/Akt is a known substrate of PP2A.

Interestingly, all three proteins investigated present with changes in phosphorylation or total protein expression in the nucleus in response to OA administration. PP2A localizes to the nucleus (Janssens and Goris, 2001) and accumulates in the nucleus during ischaemia, but redistributes to the cytosol during reperfusion (Van Vuuren, 2014). However, how inhibition of PP2A influences its nuclear accumulation and distribution during ischaemia and reperfusion, has not been reported and fell outside the scope of this study.

7.4.4 Conclusion

Western blot analysis of myocardial tissue exposed to OA prior to ischaemia and reperfusion indicate that OA administration resulted in an increase in striatin expression and increase in HSP90 α phosphorylation during reperfusion. This confirmed the data obtained by proteomic analysis. PP2A inhibition also increased the expression of HSP90 α during ischaemia, which is particularly interesting, as immunoprecipitation experiments indicate that PP2A does not have direct contact with HSP90 α . The effects of OA administration on HSP90 α are likely a combination of PP5 inhibition by OA, and the modulation of PKB/Akt (by PP2A inhibition) that has been shown to regulate HSP90 α . PP2A inhibition also increased the expression of striatin during reperfusion, but how (or whether) this contributes to cardioprotection is not known. Striatin co-immunoprecipitated with PP2A, which may indicate the presence of cardiac STRIPAKs, which have been recently identified in the heart. Lastly, PP2A inhibition enhanced the signalling of PKB/Akt, which is cardioprotective.

All three proteins investigated in this study presented with changes in phosphorylation or total protein expression in the nucleus in response to OA administration. It would be interesting to performed simulated ischaemia in a cell line (such as H9c2) studied using fluorescence microscopy to determine whether the observed changes were due to PP2A activity (or inhibition) in the nucleus.

In the next chapter, we will continue to investigate the results of the phosphoproteomic analysis by examining the effects of PP2A inhibition on the expression and activity of the mitochondrial electron transport chain.

CHAPTER EIGHT

THE EFFECT OF PP2A INHIBITION ON OXIDATIVE PHOSPHORYLATION

8.1 RATIONALE

In chapter five it was determined that 50 nM OA administration prior to 20 minutes global ischaemia and 60 minutes reperfusion reduced IFS as well as increased post-ischaemic cardiac output relative to vehicle control, indicating that PP2A inhibition prior to ischaemia was cardioprotective. In chapter six, pathway analysis of phosphoproteomic data indicated that many of the proteins affected by PP2A inhibition during myocardial ischaemia and reperfusion were related to mitochondrial function and oxidative phosphorylation. This is not surprising, as many pro-survival signalling pathways appear to converge onto the mitochondria (Juhaszova *et al.*, 2004) and the integrity of the mitochondria is vital for cell survival (Borutaite *et al.*, 2003).

PP2A is predominantly present in the cytosol and nucleus (Turowski *et al.*, 1995), as well as in the Golgi apparatus (Ito *et al.*, 2003). PP2A has been shown to be localized to the outer mitochondrial membrane in neuronal endothelial cells, but this is due to a specific regulatory subunit, B β 2, that is exclusively expressed in the brain (Merrill, Slupe and Strack, 2013). An older study investigating the mechanism of ceramide-induced apoptosis in HL-60 cells (a human leukaemia cell line) reported the presence of a ceramide-activated and OA-inhibited phosphatase in isolated mitochondria (Ruvolo *et al.*, 1999). In this study, researchers used a radiolabelled substrate that can only be dephosphorylated by PP2A, PP2B or PP2C. However, unlike PP2B and PP2C, PP2A is not dependent on metal cations for its function, and thus exclusion of cations from the phosphatase assay buffer yielded phosphatase activity that, in theory, should be due to PP2A exclusively. The same research group later discovered that B56 α associated with Bcl-2 in the mitochondrial outer membrane, and ceramide promoted the translocation of PP2A to the mitochondrial membrane of HL-60 cells (Ruvolo *et al.*, 2002).

Taken together, activity of a PP2A-like phosphatase has been described in the mitochondria, PP2A has been shown to associate with the outer mitochondrial membrane under certain conditions in HL-60 cells, B56 α is (in part) responsible for this translocation to the mitochondrial membrane, and B56 α is abundantly expressed in cardiac tissue (McCright *et al.*, 1996; Bhasin *et al.*, 2007). In

addition, the results of chapter six indicate that PP2A inhibition modulates the levels and phosphorylation of many mitochondrial proteins. What remains to be determined is whether the results obtained were due to the direct action of mitochondrial PP2A rather than a downstream effect of a signalling pathway that is regulated by PP2A. Thus, the aim of this chapter was to investigate the direct effects of PP2A inhibition on oxidative phosphorylation using isolated mitochondria in a Clarke-type oxygen oxygraph. A phosphatase activity assay was also conducted to describe phosphatase activity in a cardiac mitochondrial preparation. In addition, immunoblotting of mitochondrial subfractionation was performed to determine whether PP2A associates with the mitochondria and whether it is located inside the mitochondria or restricted to the outer mitochondrial membrane.

8.2 METHODS

8.2.1 Mitochondrial isolation

Mitochondrial isolation was conducted according to the method described by Sordahl and colleagues, with minor adaptations (Sordahl *et al.*, 1969). The hearts of four control mice were pooled for isolation of one mitochondrial sample. Enough mitochondria were isolated to run two experiments in tandem, allowing the same mitochondrial sample to be subjected to vehicle (0.004% DMSO) in one chamber and 50 nM OA in the other.

Mice were anaesthetized and their hearts excised as described in chapter two. Upon excision, the hearts were trimmed of excess tissue and atria and placed in ice-cold KE isolation buffer (0.18 M KCl, 0.01 M EDTA, pH 7.4). The tissue was finely minced with scissors and washed in isolation buffer to remove excess blood. Further homogenization was accomplished using a Heidolph Silent Crusher M (2 X 5 seconds at speed 11,500 rpm) followed by centrifugation at 755 x *g* for 10 minutes at 4° C (Sorvall RC6-PLUS, Thermo Scientific). The supernatant containing the cytosolic fraction was transferred to a clean tube and centrifuged at 18,800 x *g* for 10 minutes at 4°C to obtain a mitochondrial pellet. The pellet was then re-suspended in 410 µl ice-cold isolation buffer using a glass-teflon homogenizer and stored on ice until experimentation. 2 µl of this sample was used for protein concentration determination in the Direct Detect® Infrared Spectrometer (Merck Millipore), while the rest was used for oxidative phosphorylation experiments and sub-fractionation.

8.2.2 Mitochondrial oxygen consumption

Immediately after isolation, mitochondria were transferred to a Clarke-type oxygraph (Oxytherm system, Hansatech Instruments) where mitochondrial oxygen consumption was determined using a carbohydrate (glutamate) substrate (Chance and Williams, 1955). A protocol adapted from Blignaut and colleagues was utilized (2019). The chamber containing 650 μ l glutamate buffer (250 mM sucrose, 10 mM TRIS-HCl at pH 7.4, 8.5 mM $K_2HPO_4 \cdot 3H_2O$, 2 mM malate and 5 mM glutamate; adjusted to pH 7.4 with HCl) was allowed to equilibrate to the ambient oxygen levels at 25 °C. 100 μ l isolated mitochondria in KE, as well as 50 nM OA or DMSO, were added to the chamber. Oxygen consumption was recorded at baseline after the addition of mitochondria (State 2) and again after the addition of either 0.004% DMSO or 50 nM OA to ascertain whether DMSO, a known oxygen scavenger, had any effect on oxygen levels within the chamber (State 2 with drug). 459 nmol ADP was added to the chamber to initiate State 3 respiration. Once ADP was depleted and oxygen consumption returned to baseline (State 4), 10x ADP was added to the chamber to ensure the utilization of all oxygen. Once oxygen was depleted, the chamber was sealed for 20 minutes (anoxia), where after the contents were manually re-oxygenated. State 3 was again measured until all the remaining oxygen was consumed. Upon completion of the experiment, the chamber contents were removed and stored at - 80 °C for phosphatase activity assays.

Data were captured with HansaTechPlus software and the values used to calculate the rate of oxygen consumption (nano atoms O/min/mg mitochondria), which was determined after the addition of ADP (State 3), after the depletion of ADP (State 4), and again during State 3 after a 20-minute period of anoxia followed by reoxygenation. The ADP/O (the number of ADP molecules utilized per oxygen atom consumed) was calculated by dividing the number of nano atoms of oxygen used during State 3 by the amount of ADP used during State 3. The rate of oxidative phosphorylation was calculated (nmol ATP produced/min/mg mitochondria during State 3) by multiplying the rate of oxygen consumption with the ADP/O. Lastly, the respiratory control index (RCR), an indication of how well respiration is coupled to phosphorylation, was calculated by dividing the rate of oxygen consumption in State 3 by that of State 4. The amount of ADP (in nmol) used for experimentation was determined by spectrophotometric analysis. 0.02g of ADP was prepared in 5 ml distilled water, and 100 μ l of this was diluted 250x in distilled water. The optical density of this solution was determined using a Helios Ultraviolet spectrophotometer (Unicam), where optical density of ADP is 15.4 at 259 nm.

8.2.3 Phosphatase assay

Samples containing the oxygraph chamber contents were thawed on ice and centrifuged at 5,366 x *g* for 10 min at 4°C (Sigma 1-14K) to obtain the mitochondrial pellet. The pellet was resuspended in a smaller volume of KE buffer, and protein concentration was determined in the Direct Detect® Infrared Spectrometer (Merck Millipore). The samples were then diluted to 2.5 µg/µl. 50 µl of each sample and 50 µl of DiFMUP were added to a 96-well microplate (SPL Life Sciences, Korea). The plates were incubated at 37.5 °C and phosphatase activity was measured by the generation of DIFMU. Fluorescence was measured at 355/460 nm excitation/emission at 10-minute intervals, for 120 minutes. Wells containing only KE and DIFMUP served as blanks.

8.2.4 Mitochondrial sub-fractionation with digitonin

At least 150 µl of fresh mitochondria in KE isolation buffer (from the same isolation used for oxygen consumption experiments) were centrifuged at 5,366 x *g* for 10 min at 4°C (Sigma 1-14K). The supernatant was discarded, and the mitochondrial pellet resuspended in ice-cold mannitol/sucrose buffer (M/S; 70 mM sucrose, 220 mM D-mannitol, 10 mM HEPES, 0.5 M EGTA, adjusted to pH to 7.2 with HCl). To separate the outer mitochondrial membrane (OMM) from the mitoplast (inner mitochondrial membrane and matrix), the protocol described by Blignaut and colleagues was used (2019). 1.2 % digitonin was prepared by boiling 6 mg of digitonin (D141, Sigma-Aldrich) in 0.5 ml of M/S buffer for one minute and allowed to cool on ice. A volume equal to 100 µg mitochondria and an equivalent volume of digitonin solution was added to a tube to yield a final amount of 50 µg mitochondria in 1.2% digitonin solution. This solution was gently stirred at 0° C. During this time, the hypotonicity of the M/S solution causes the mitochondria to swell, and the digitonin permeabilizes the OMM. This facilitates the removal of the OMM from the mitochondria, so that two fractions can be obtained, namely the OMM and swollen mitoplasts. Aliquots were taken from this solution at t = 0 minutes and at t = 20 minutes. Each aliquot was diluted with 10x M/S buffer containing 25 µg/ml BSA to quench the reaction at the time of sampling. The aliquots were then centrifuged at 5,366 x *g* for 10 min at 4°C (Sigma 1-14K) to separate the mitoplast (pellet) from the OMM (supernatant). The supernatant was then further centrifuged at 100,000 x *g* for one hour at 4°C to obtain the OMM fraction. Both the mitoplast and OMM samples were resuspended in 1X SDS buffer (10% glycerol, 50 mM TRIS-HCl pH 6.8, 30 mM β-glycerophosphate, 2.5 mM EGTA, 1 mM SOV, 0.5 mM NaF, 10% SDS) for Western blot analysis.

8.2.5 Western blot analysis

1x lysis buffer and 3x Laemmli buffer were added to the mitoplast and OMM fractions, followed by subsequent boiling for four minutes. 12 µl of each sample were then loaded onto a hand-cast mini gel, and SDS-PAGE and protein transfer proceeded as described in chapter two. The primary antibodies used in this experiment included total VDAC, total SIRT3, total PP2A-A, total PP2A-C, and total Striatin. Additional information on these antibodies can be found in chapter two. Voltage dependent anion channel (VDAC) is an outer mitochondrial membrane channel that is a well-established marker of the OMM (Colombini, 1979), and sirtuin 3 (SIRT3) was used as a mitoplast marker, as it is located in the mitochondrial matrix (Giralt and Villarroya, 2012). A goat anti-rabbit horseradish-peroxidase conjugated secondary antibody (Cell Signalling Technology; cat: 7060S) was utilized to visualize protein bands in the sub-fractions.

Whole cell lysates prepared from hearts perfused with either 0.002% DMSO (vehicle control) or 50 nM OA and exposed to either 20 minutes ischaemia or 20 minutes ischaemia with 10 minutes reperfusion, were also used in western blot analysis. 15 µl of each sample (5 µg/µl; the preparation of which was described in chapter seven) were loaded onto a Criterion™ TGX Stain-Free gel (4-20% acrylamide, Bio-Rad; cat: 5678095) and separated in a Bio-Rad MIDI system (Bio-Rad Laboratories, Inc., USA). The Total OXPHOS Rodent WB Antibody Cocktail (Abcam; cat: ab110413), which contains antibodies against a subunit in each complex, was used to determine the expression of the electron transport chain complexes. An anti-mouse IgG horseradish-peroxidase conjugated secondary antibody (Cell Signalling Technology; cat: 7074) was utilized for the OXPHOS Antibody Cocktail, and all visualization was conducted on the ChemiDoc imaging system as described in chapter two.

8.2.6 Data and statistical analyses

Data were compiled in Microsoft Excel (Microsoft, USA) and analysed in GraphPad© Prism 6.0 (GraphPad Software Inc., San Diego, CA). Data are expressed as mean ± SD, unless otherwise stated. A two-tailed, unpaired Student's T-test was used to compare mitochondrial oxidative capacity of DMSO and OA cohorts. A two-way ANOVA with a Bonferroni *post hoc* test was used to compare phosphatase activity, and a one-way ANOVA was used to compare the pixel intensities of protein bands from the western blot analysis. A p-value equal to or less than 0.05 was considered significant.

8.3 RESULTS

8.3.1 Mitochondrial oxygen consumption

Drug administration had no effect on State 2 respiration, indicating that the amount of DMSO in the chamber did not scavenge detectable amounts of oxygen, and that OA exerted no adverse effects on mitochondria at baseline. 50 nM OA had no effect on the ADP/O, a measure of how efficiently oxygen is utilized during ATP production (Figure 8.1). It also had no effect on the respiratory control index, which compares the rate of oxygen consumption during ADP phosphorylation to the rate of oxygen consumption when ADP is depleted (State 3/State 4).

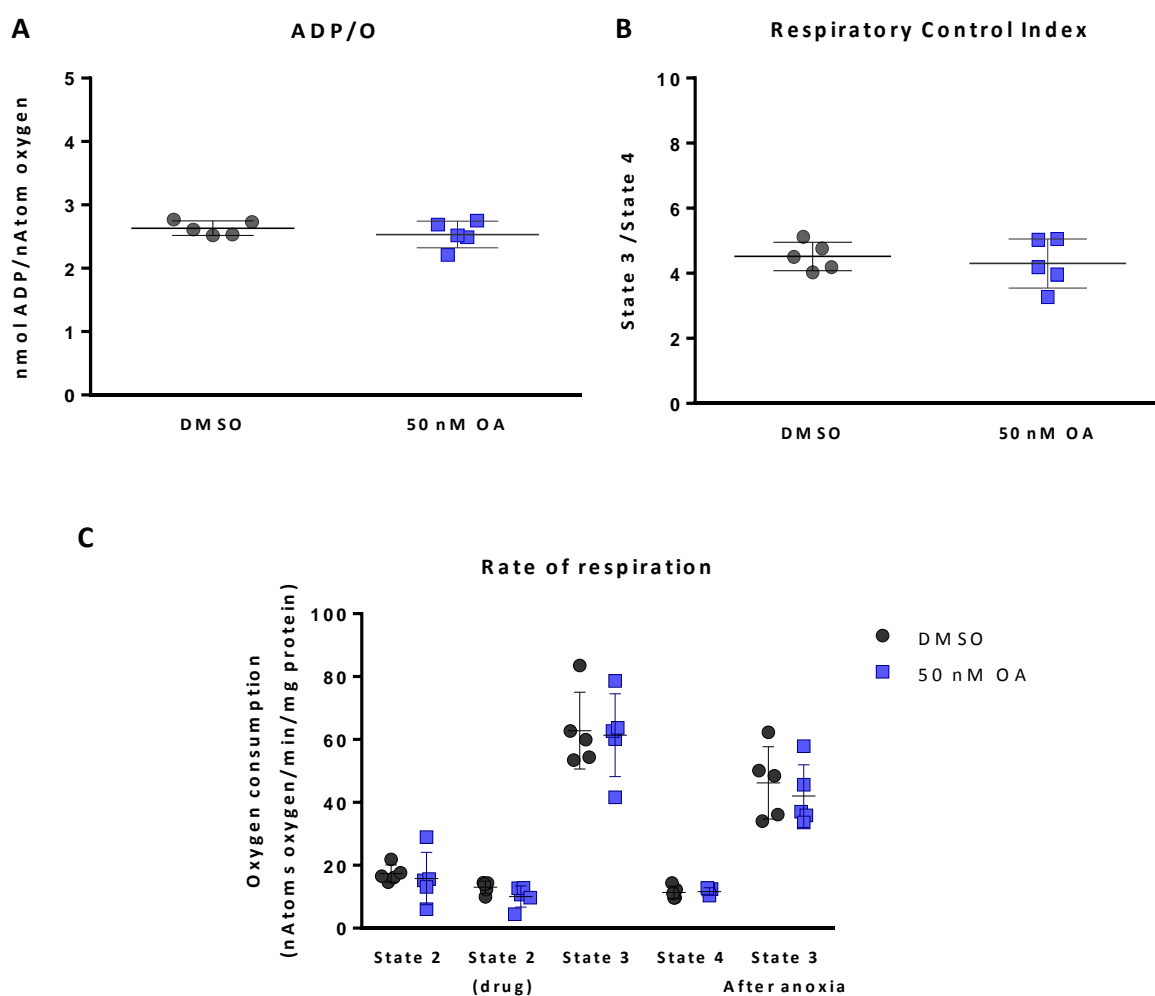


Figure 8.1 - The effects of 50 nM OA on ADP/O, oxidative phosphorylation, and mitochondrial oxygen consumption.

50 nM OA administered directly to mitochondria had no effect on the ADP/O (A), respiratory control index (B), or rate of respiration (C), when compared to DMSO. Data are expressed as mean \pm SD of five separate experiments from tissue pooled from four animals for each experiment.

Lastly, OA had no effect on the percentage recovery after anoxia when compared to DMSO ($17.42 \pm 6.82\%$ vs $21.02 \pm 3.41\%$).

8.3.2 Phosphatase assay

The phosphatase activity assay demonstrated that 50 nM OA administration had no effect on phosphatase activity within the mitochondria (Figure 8.2), although phosphatase activity within the mitochondria was abundant. This supports data generated from the mitochondrial oxidative phosphorylation experiments that demonstrate the failure of 50 nM OA to produce an effect.

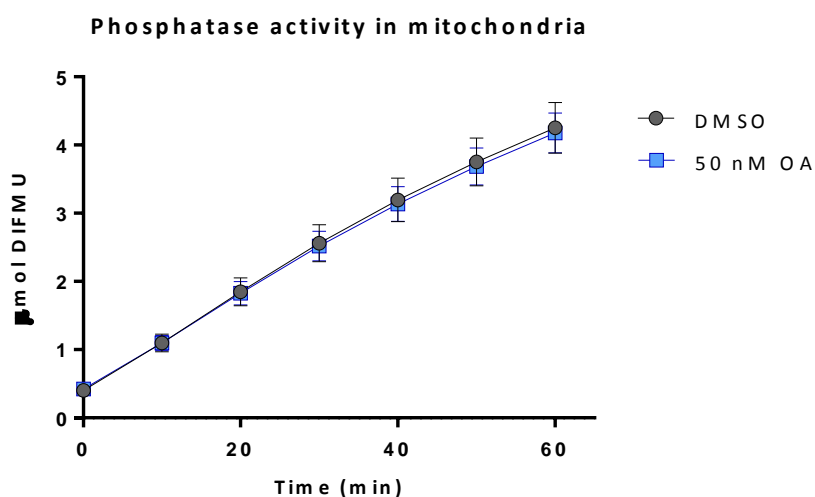


Figure 8.2 - The effect of 50 nM OA on mitochondrial phosphatase activity

50 nM OA administration had no effect on mitochondrial phosphatase activity, indicating that there are possibly no OA-sensitive phosphatases resident in the mitochondria. Data are expressed as mean \pm SD of duplicate wells of samples from five separate experiments.

8.3.3 Western blot analysis

Western blot analysis of the complexes within the mitochondria show no differences in complex expression in the OA-treated cohorts when compared to the DMSO-treated cohorts (Figure 8.3). Interestingly, ischaemia and reperfusion did not affect complex expression.

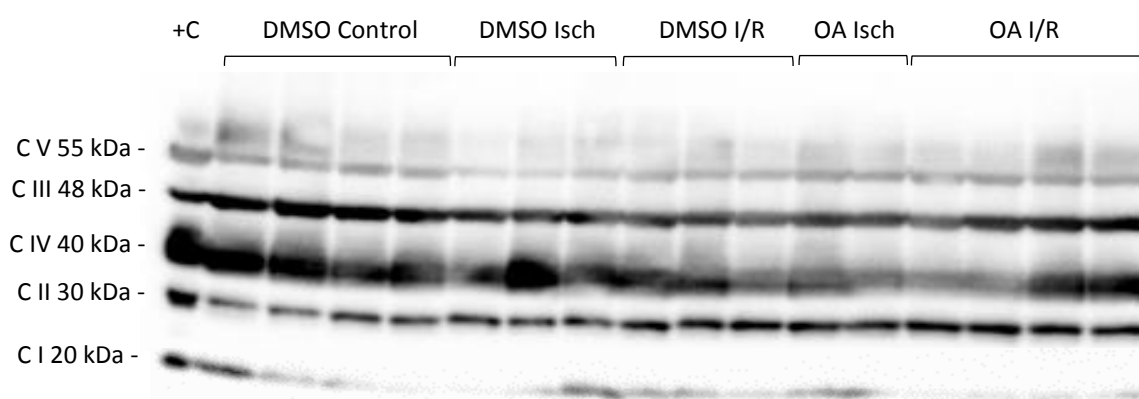
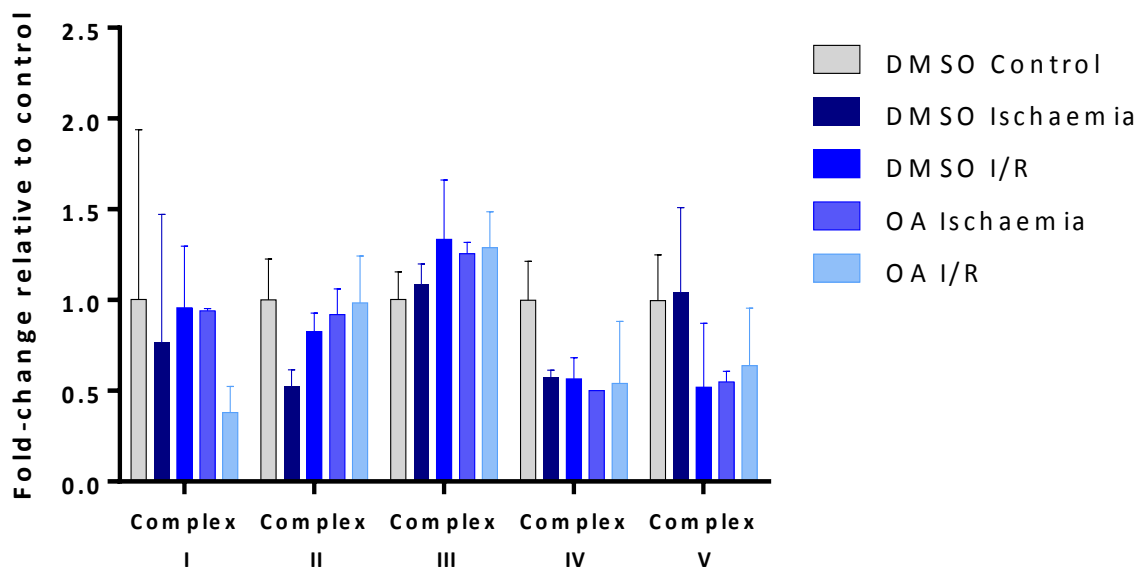


Figure 8.3 - Western blot analysis of mitochondrial complexes in hearts exposed to either DMSO or OA and subjected to ischaemia and/or reperfusion

Western blot analysis of hearts exposed to either DMSO (vehicle) or 50 nM OA and subjected to 20 minutes myocardial ischaemia and 10 minutes reperfusion yielded no differences in complex expression.

+C = positive control

Isch = Ischaemia

I/R = Ischaemia and reperfusion

8.3.4 Mitochondrial sub-fractionation

To separate the OMM from the mitoplast, mitochondria were treated with 1.2% digitonin for either 0 minutes or 20 minutes. At 0 minutes, no separation of the OMM from the mitoplast has taken place. As a result, the mitoplast fraction should theoretically contain intact mitochondria and the OMM fraction should be free of mitochondrial proteins.

VDAC1 is the most abundant protein located on the OMM, and was used as a marker of the OMM (García-Pérez *et al.*, 2011). As expected, VDAC1 was absent in the OMM fraction and present in the mitoplast fraction after 0 minutes digitonin treatment. VDAC1 was also present in both the OMM and mitoplast fractions after 20 minutes digitonin treatment, indicating that the mitoplast fraction still contained a small amount of OMM (n = 3 samples from four hearts; Figure 8.4).

SIRT3 is localized to the inner mitochondrial membrane, cristae, and matrix, and was thus used as a mitoplast marker (Kincaid and Bossy-Wetzel, 2013). SIRT3 was present in the mitoplast fraction at both 0 minutes and 20 minutes digitonin treatment, but was also present in small amounts in the OMM after 20 minutes digitonin treatment. Since the 28 kDa SIRT3 (used in this experiment) is located exclusively in the mitochondria, its presence in the OMM at 20 minutes indicates a small amount of contamination in one of the centrifugation steps.

As stated previously, PP2A is a heterotrimeric protein consisting of a scaffolding (PP2A-A), a regulatory (PP2A-B), and a catalytic (PP2A-C) subunit. All three subunits were included as targets for western blotting. Although PP2A has numerous regulatory subunits, striatin was selected as it was identified by phosphoproteomic analysis to be modulated by PP2A inhibition. For PP2A-A and PP2A-C blots, the whole cell lysate (WCL) control was used as a positive control and allowed to overexpose to determine whether any proteins were located in the mitochondrial fractions. Both PP2A-A and PP2A-C were present in the mitoplast fraction after 0 minutes digitonin treatment. However, neither subunit was present in either the mitoplast or OMM fractions after 20 minutes digitonin treatment. Interestingly, striatin was present in both mitoplast fractions.

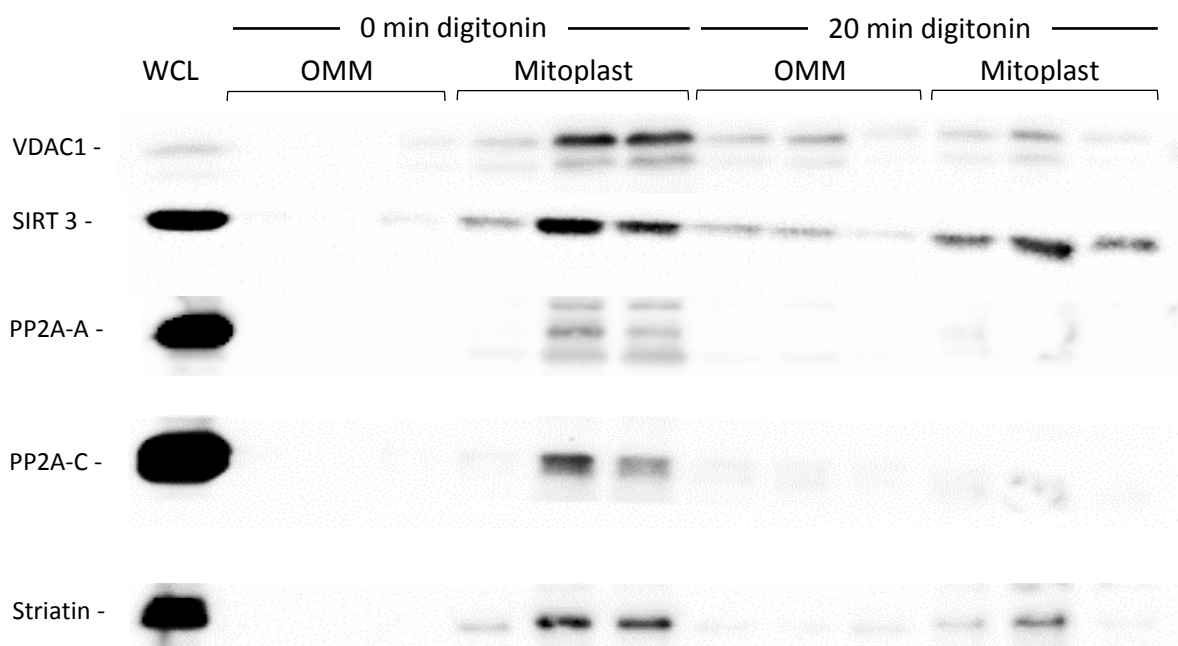


Figure 8.4 - Western blot analysis of the outer mitochondrial membrane and mitoplast fractions obtained after digitonin treatment

VDAC, a marker for the outer mitochondrial membrane (OMM), was present in both the OMM and mitoplast fractions after 20 minutes digitonin treatment, indicating that the mitoplast fraction still contained a small amount of OMM. VDAC was expected to be absent in OMM and present in the mitoplast in the 0-minute digitonin cohort. SIRT3, a marker for the mitochondrial matrix, was present in the mitoplast fraction after 0 minutes and 20 minutes digitonin treatment. The presence of a small amount of SIRT3 in the OMM fraction after 20 minutes digitonin treatment indicated that the OMM fraction was contaminated with mitochondrial matrix proteins. PP2A-A and PP2A-C were found in the mitoplast fraction after 0-minute digitonin treatment, but in neither OMM nor mitoplast fraction after 20-minute digitonin treatment. Striatin is associated with the mitoplast fraction.

8.4 DISCUSSION

In chapter six, it was determined oxidative phosphorylation was a pathway affected by PP2A inhibition. However, it was unclear whether this was the result of PP2A located in the mitochondria or a downstream effect of a signalling pathway that is regulated by PP2A. Thus, the aim of this chapter was to investigate the direct effects of PP2A inhibition on mitochondrial oxidative phosphorylation. In addition, immunoblotting of mitochondrial subfractions was performed to determine whether PP2A associates with the mitochondria and if it does, whether it is located inside the mitochondria or restricted to the outer mitochondrial membrane.

Mitochondria are easy to isolate from heart muscle, simple to use, have established protocols, can be easily manipulated by drug administration, and are ideal for studying mechanisms (Brand and Nicholls, 2011). However, the analysis often requires a relatively large amount of sample and mitochondria are often damaged during the isolation process. In addition, isolated mitochondria lack cellular context (Brand and Nicholls, 2011).

OA (50 nM), when added directly to a mitochondrial preparation, had no effect on the ADP/O, rate of respiration, recovery after anoxia, and particularly the respiratory control index (RCI; Figure 8.1). The RCI (State 3/State 4) is regarded as the most useful measure of the integrity of mitochondrial function, as any change in oxidative phosphorylation will change this value (Morton, Barnes and Zyskowski, 1996; Brand and Nicholls, 2011). Although there is no reference value that would indicate good mitochondrial function and bearing in mind that RCI differs between tissues, a relatively high RCI indicates a high rate of substrate oxidation and ATP turnover, as well as low proton leakage (Brand and Nicholls, 2011). Since the RCI was unaffected by OA administration, it is unlikely that OA itself is directly affecting any aspect of respiration, as was shown by the States 3 and 4 respiration (Figure 8.1). This may also indicate that there are no OA-sensitive phosphatases such as PP2A, PP4, and PP1 (PP1 should be inhibited at the concentration used) located in the mitochondria, or they may be located within the matrix where OA could not penetrate (as OA is extremely hydrophobic and may be trapped in the membrane). The phosphatase activity assay of the isolated mitochondria showed that phosphatase activity was unaffected by OA administration, which supports the observation that OA-sensitive phosphatases are not present in the mitochondria.

In chapter six, it was determined that OA administration increased the abundance of certain subunits in complexes IV, V and I (to a degree). To confirm this, western blot analysis of the complexes was performed using a Rodent OXPHOS antibody cocktail. OA administration had no effect on complex expression during ischaemia or following reperfusion when compared to the DMSO cohorts (Figure 8.3). This was contrary to the results obtained by phosphoproteomic analysis. However, it should be noted that the Rodent OXPHOS antibody cocktail contains a single subunit from each complex, and as reported in chapter six, it appears as if the complexes are not collectively modulated by PP2A inhibition. Rather PP2A inhibition affects certain subunits within a complex, which may not be reflected by the analysis of a different subunit within the complex. Clearly this needs to be further investigated.

To determine whether PP2A is possibly located within the matrix, isolated mitochondria were sub-fractionated into outer mitochondrial membrane (OMM) and mitoplast (inner mitochondrial membrane and matrix) fractions using 1.2% digitonin. Although the mitochondrial fractions were not completely free of contaminants, the sub-fractionation yielded an OMM and mitoplast fraction that were distinctly different enough to investigate the presence of three PP2A subunits – PP2A-A, -C and striatin. The scaffolding (PP2A-A) and catalytic (PP2A-C) subunits were both present in intact mitochondria (0-minute digitonin treatment), but absent from the OMM fraction after digitonin treatment for 20 minutes. Although both scaffolding and catalytic subunits were detected in the mitoplast fraction after 0 minutes digitonin treatment, neither these subunits were detected in the OMM fraction after 20-minute treatment (although the catalytic subunit did show very faint bands). This may indicate that after 20 minutes of digitonin treatment, the membrane proteins and membrane-associated proteins were solubilized. When the samples were centrifuged and separated into the mitoplast (pellet) and the OMM fraction (OMM and proteins in the inter-mitochondrial space), the OMM was centrifuged again to separate the OMM from any proteins contained within the inter-mitochondrial space. As the amount of protein retrieved from the inter-mitochondrial space (supernatant in the final centrifugation step) is not enough for western blot analysis, this was discarded, while the OMM (pellet) was stored. If the membrane bound PP2A was solubilized during digitonin treatment and discarded along with the proteins contained in the inter-mitochondrial space, it would be present in the mitoplast fraction after 0 minutes digitonin treatment, but absent in either fraction after 20 minutes digitonin treatment.

In response to stress, PP2A has been reported to localize to the OMM of neuronal endothelial cells where it induces mitochondrial fragmentation by dephosphorylating dynamin-related protein 1, resulting in apoptosis (Merrill, Slupe and Strack, 2013). In addition, studies in HL-60 cells demonstrated that PP2A is targeted to the OMM by the B56 α subunit that associates with Bcl-2, a process associated with apoptosis (Ruvolo *et al.*, 2002). Although the amount of PP2A identified in the mitochondrial OMM fraction did not show a strong protein band in our study, this may be due to the fact that the tissue used for mitochondrial isolation was free of stressors. A more prominent translocation of PP2A to the OMM may have been observed if hearts were exposed to a stressor, such as I/R injury.

Striatin was detected in both mitoplast fractions, indicating that striatin forms part of the inner mitochondrial membrane or part of the matrix. As stated in the previous chapter, striatin is a

cytoskeletal scaffolding protein that has also been described as a B^{''} regulatory subunit of PP2A. The B^{''} family also contains two other members, S/G₂ nuclear autoantigen (SG2NA) and zinedin; all three of which bind to calmodulin in a Ca²⁺-dependent manner (Castets *et al.*, 2000; Moreno *et al.*, 2000). Striatin has been reported to be localized in the cytosolic and membrane fractions (Nader *et al.*, 2017), but the localization of striatin in the mitochondrial fraction has not been reported to date.

Another B^{''} subunit related to striatin, SG2NA, has been reported to localize DJ-1 (an antioxidant protein) to the mitochondria under conditions of oxidative stress (Tanti and Goswami, 2014). However, whether this localization occurred on the OMM or within the intermembrane space or matrix could not be confirmed, as these experiments were conducted with intact mitochondria. In addition, DJ-1 has been reported to localize to the OMM (Tanti and Goswami, 2014) and interact with complex I in the inner mitochondrial membrane (Niki *et al.*, 2012). As such, its localization within the mitochondria does not clarify whether SG2NA localizes only with the OMM or within the mitochondrial matrix.

The function of striatin in the mitochondria has not been defined and falls outside the scope of this study. It is not clear whether striatin's function in the mitochondria is due to its function as a scaffolding protein or to target PP2A or other proteins into the mitochondria. Striatin targets kinases or other phosphatases in complexes known as STRIPAKs, although no mitochondrial STRIPAKs have been reported to date. Based on the sub-fractionation results, it is unlikely that striatin targets PP2A to the mitochondria, and neither the catalytic nor scaffolding subunit of PP2A was identified in the mitoplast fraction. However, it must be noted that control (unstressed) tissue was used for these experiments while tissue exposed to myocardial I/R injury was used for the phosphoproteomic study. PP2A localization in the inner mitochondrial membrane or matrix has not been confirmed in stressed tissue, but it may be reasonable to assume that PP2A is recruited to the OMM during cellular stress, as currently reported in literature (Ruvolo *et al.*, 1999, 2002).

To summarize, 50 nM OA administered directly to intact mitochondria had no effect on oxidative phosphorylation. A phosphatase assay confirmed no change in mitochondrial phosphatase activity in the OA-treated mitochondria when compared to the DMSO-treated (vehicle) mitochondria. In addition, immunoblotting of mitochondrial sub-fractions confirmed the presence of both the catalytic and scaffolding subunit in intact mitochondria, but not OMM and mitoplast subfractions. PP2A was most likely localized at the OMM (which has been reported in literature before) but solubilized with the digitonin treatment, which may explain the lack of PP2A

in the OMM fraction in this study. Therefore, the effects of PP2A inhibition on oxidative phosphorylation described in chapter six is likely not due to a direct action of PP2A on mitochondrial proteins, but rather the downstream effect of a signalling pathway that is modulated by PP2A. However, the role of PP2A on mitochondria function under conditions of stress is yet to be investigated.

Lastly, this study is the first to demonstrate that striatin is expressed in the mitoplast fraction of mitochondria under basal conditions. The function of mitochondrial striatin is unknown.

8.5 LIMITATIONS

In this study we utilized isolated myocardial mitochondria from control animals that were not exposed to any stress. A more appropriate method would be to isolate mitochondria from hearts that were subjected to ischaemia and reperfusion after 50 nM OA administration, following the same isolated, working heart protocol used in the preparation of the phosphoproteomic samples. However, optimization experiments for the oxygraph experiments confirmed that the small amount of mitochondrial protein isolated from one mouse heart could not be used for accurate measurements in the systems that were available in our laboratory. Hearts from at least two animals needed to be pooled into a single experiment. For mitochondrial bioenergetic experiments, mitochondria need to be viable and therefore cannot be frozen. In addition, mitochondria quickly lose viability and must be used for functional studies immediately after isolation. Thus, pooling mitochondria isolated from two separate perfusion experiments would result in more mitochondrial protein from hearts that have been subjected to ischaemia/reperfusion but contain a large proportion of non-viable mitochondria. For this logistical reason, we did not make use of hearts exposed to treatment and I/R, but rather pooled hearts from four control animals, isolated the mitochondria together, and used this for two experiments run in tandem. Using a different method of analysis that requires less mitochondria, such as the Seahorse XF Analyzer, would have allowed us to use tissue generated from an *ex vivo* perfusion.

8.6 FUTURE WORK

As stated, using a different method of analysis (such as the Seahorse XF Analyzer) would allow us to investigate mitochondrial oxygen consumption in hearts exposed to OA and subjected to ischaemia and reperfusion. A simple phosphatase activity assay using various inhibitors would also give some information regarding the identity of the phosphatase families present in the mitochondria that were responsible for the large phosphatase assay observed in this study.

It would also be interesting to investigate the role of striatin in the mitochondria. It is unlikely that it is acting as a regulatory subunit of PP2A, targeting it to the mitochondria, but whether it is forming STRIPAK complexes, functioning in vesicle trafficking, or has a function not yet described in existing literature, still has to be determined. If striatin is forming STRIPAK complexes within the mitochondria, it may be one of the few (if not the first) reported cases of a STRIPAK complex that does not contain the PP2A AC dimer.

CHAPTER NINE

FINAL CONCLUSION

Since the discovery of ischaemic preconditioning, our understanding of the pathophysiology of ischaemia/reperfusion injury has dramatically increased. Despite this, ischaemic heart disease remains the leading cause of global morbidity and mortality. Historically, the role of protein kinases in I/R injury has been the focus of potential therapeutic targets. However, information regarding the role of phosphatases in I/R injury is lacking and clarifying this role in the cellular response to I/R injury is critical in order to enhance the efficacy of existing cardioprotective interventions or to identify new therapeutic targets.

It is well-established that cardioprotection is associated with phosphorylation and activation of proteins such as PKB/Akt and ERK during early reperfusion. Thus, the hypothesis of this study was that during ischaemia and subsequent reperfusion, PP2A negatively regulates proteins associated with survival signalling and inhibition of PP2A may favour survival. Our aims were to investigate the effects of PP2A inhibition on the outcomes of I/R (using endpoints such as infarct size and functional recovery), to characterize the phosphoproteome of myocardial tissue exposed to I/R in the presence and absence of PP2A inhibition, and to identify proteins that are not known to be substrates of PP2A and also to describe how PP2A inhibition influences their expression and degree of phosphorylation during I/R.

To determine the optimal dose of inhibitor (okadaic acid; OA) that results in PP2A inhibition, the isolated working mouse heart was perfused with either control (Krebs Henseleit buffer), vehicle control (0.13% DMSO) or 10, 50, or 100 nM OA. We determined that 50 nM OA administered *ex vivo* was sufficient to reduce PP2A activity, as measured *in vitro*. We then evaluated the effect of 50 nM OA administration prior to 20 minutes global ischaemia and 60 minutes reperfusion in an isolated perfused mouse heart model. OA effectively reduced infarct size, but it did not exert a major effect on functional recovery during reperfusion. Therefore, PP2A inhibition prior to myocardial ischaemia and reperfusion is cardioprotective, in that it reduces lethal reperfusion injury. However, how PP2A inhibition influences the intracellular processes that result in cell survival without affecting function is not fully understood, and to investigate this we employed a phosphoproteomic approach.

Phosphoproteomic analysis was conducted on hearts exposed to 50 nM OA and subjected to 20 minutes global ischaemia followed by 10 minutes reperfusion. A large amount of data was generated from the analysis of phosphoproteomics during I/R in the presence and absence of PP2A inhibition: 1841 proteins and 684 phosphorylated proteins were identified, of which 898 proteins were differentially expressed and 184 proteins were differentially phosphorylated under conditions of PP2A inhibition. Four phosphosites on titin that have not been previously described were tentatively identified. However, further studies validating this are still required.

Pathway analysis of the proteins affected by OA administration indicated that the major pathways affected were those associated with mitochondrial function and oxidative phosphorylation, regulation of epithelial adherens signalling and remodelling and cytoskeletal signalling. As the number of proteins identified in the analysis was too large for an extensive analysis of individual function, two proteins from the data set were selected for further analysis based on the following criteria: (i) the proteins had to be differentially expressed as well as (ii) undergo a change in phosphorylation in the OA-treated group, and (iii) the phosphorylated protein must have at least a two-fold increased expression. These changes had to be statistically significant since a high degree of certainty was required in the identification of these proteins. 41 proteins fit these criteria and a brief literature search was conducted to determine the function of each protein, whether the proteins had any reported association with PP2A (or possible association with PP2A), as well as any known roles in ischaemia/reperfusion. Striatin and HSP90 α were selected for experimental confirmation and further analysis, and mitochondrial respiration was further investigated.

Western blot analysis confirmed the phosphoproteomic results that PP2A inhibition increased striatin expression and increased phosphorylation of HSP90 α during reperfusion. Striatin, but not HSP90 α coimmunoprecipitated with PP2A, indicating that the increased phosphorylation of HSP90 α was possibly an indirect effect of PP2A inhibition. Striatin is a regulatory subunit of PP2A, but also functions as a scaffold that recruits kinases, other phosphatases, and other proteins into STRIPAK complexes. Therefore, coimmunoprecipitation of striatin may indicate the presence of STRIPAK complexes in the heart. This will require further research, as the presence of STRIPAK complexes in cardiac tissues in the context of calcium handling has only recently been described (Eden *et al.*, 2016).

Pathway analysis identified oxidative phosphorylation as the pathway most-affected by PP2A inhibition. To further investigate this, an *in vitro* approach was used where 50 nM OA was

administered directly to mitochondria for polarographic evaluation of the mitochondrial oxidative phosphorylation process. OA had no direct effect on oxidative phosphorylation, and failure of OA to elicit an effect might indicate that there is no PP2A in mitochondria. A phosphatase assay confirmed a large amount of measurable phosphatase activity within the mitochondria that was not affected by OA administration. Sub-fractionation of the mitochondria confirmed the presence of the AC dimer in intact mitochondria, but not in OMM and mitoplast subfractions. This would indicate that PP2A was most likely localized at the OMM (which has been reported in literature before) but solubilized with the digitonin treatment. This would suggest that the effects observed in the phosphoproteomic analysis are due to an indirect effect of PP2A inhibition, where PP2A modulates a signalling pathway that results in changes to oxidative phosphorylation. As these experiments were conducted in *in vitro* in mitochondria isolated from unstressed tissue, the role of PP2A on mitochondrial function under conditions of stress is yet to be investigated. An interesting result generated in this study is the observation that striatin is present in the mitoplast fraction of mitochondria under basal conditions. The function of mitochondrial striatin is unknown, but future work investigating the function of striatin, both in the mitochondria and in potential STRIPAK complexes in the heart, would certainly yield more insight concerning its role in heart mitochondria.

An unexpected result of this study was the observation that 10 mM SOV administered to immunoprecipitated PP2A resulted in massive inhibition of a serine/threonine phosphatase, which has not been previously described. Consequently, we decided to investigate the effects of SOV on PP2A activity using purified enzymes, cardiac lysates, and the isolated perfusing working heart model. To our knowledge, this study is the first to demonstrate that SOV is a weak, competitive inhibitor of PP2A. SOV administered in a cardiac lysate also reduced PP2A activity after immunoprecipitation (and subsequent washing steps), indicating that SOV either binds tightly to PP2A, or at least reduces PP2A binding to the immunoprecipitation antibody. During the investigation into the impact of SOV on the kinetic parameters of PP2A we observed that PP2A has a low affinity for DIFMUP, the substrate used in the phosphatase activity assay which we employed. DIFMUP is a commercially available substrate that allows for measurement of phosphatase activity, and is arguably the most convenient, uncomplicated, and most sensitive method currently available. However, the results obtained in this study indicate that the kinetics of PP2A's affinity towards this substrate may not effectively mimic PP2A's affinity towards natural substrates. This may influence the reproducibility of results achieved with the DIFMUP substrate when compared to other methods, although this has not been validated.

In conclusion, PP2A negatively regulates protein phosphorylation during ischaemia and subsequent reperfusion, and inhibition of this phosphatase contributes to cardioprotection. This affects a multitude of proteins, some of which are directly regulated by PP2A, while others are downstream targets of signalling pathways modulated by PP2A. Unfortunately, not all samples prepared for phosphoproteomic analysis were analysed. This would have yielded valuable insight into intracellular changes associated with PP2A inhibition, particularly during ischaemia, and the lack of these data is a large limitation in this study. However, the phosphoproteomic analysis of the I/R cohorts generated a large amount of data, which can serve as a platform for future studies on PP2A. Finally, this study is the first to identify striatin in the mitochondria. Further investigation into the role and function of mitochondrial striatin would surely yield interesting results. Cardiac STRIPAKs have also recently been identified, the function of which is largely unknown, warranting further investigation.

This study makes a worthwhile contribution to current knowledge regarding the role of PP2A in the heart. Our approach in the use of phosphoproteomic analysis is, to our knowledge, the first of its kind to investigate the effects of phosphatase inhibition during myocardial I/R. The analysis revealed previously unknown effects of PP2A in the phenomenon of I/R, particularly its indirect effect on oxidative phosphorylation and the discovery of striatin in the mitochondria.

REFERENCES

- A. Khan, S. *et al.* (2006) 'Rapamycin confers preconditioning-like protection against ischemia-reperfusion injury in isolated mouse heart and cardiomyocytes', *Journal of Molecular and Cellular Cardiology*. Academic Press, 41(2), pp. 256–264. doi: 10.1016/j.yjmcc.2006.04.014.
- Aasum, E. *et al.* (2002) 'Cardiac function and metabolism in type 2 diabetic mice after treatment with BM 17.0744, a novel PPAR- α activator', *American Journal of Physiology - Heart and Circulatory Physiology*. American Physiological Society Bethesda, MD, 283(3 52-3), pp. H949–H957. doi: 10.1152/ajpheart.00226.2001.
- Abe, E. *et al.* (2000) 'Structure, expression, and chromosomal localization of the human gene encoding a germinal center-associated nuclear protein (GANP) that associates with MCM3 involved in the initiation of DNA replication.', *Gene*, 255(2), pp. 219–27.
- Adams, J. M. and Cory, S. (2001) 'Life-or-death decisions by the Bcl-2 protein family', *Trends in Biochemical Sciences*. Elsevier, 26(1), pp. 61–66. doi: 10.1016/S0968-0004(00)01740-0.
- Adams, M. G. and Pelter, M. M. (2002) 'Reperfusion arrhythmias.', *American Journal of Critical Care: An Official Publication, American Association of Critical-Care Nurses*. American Association of Critical Care Nurses, 11(3), pp. 273–5.
- Agostinis, P. *et al.* (1996) 'A comparative study of the phosphotyrosyl phosphatase specificity of protein phosphatase type 2A and phosphotyrosyl phosphatase type 1B using phosphopeptides and the phosphoproteins p50/HS1, c-Fgr and Lyn', *European Journal of Biochemistry*, 236(2), pp. 548–557. doi: 10.1111/j.1432-1033.1996.00548.x.
- Ahn, J.-H. *et al.* (2007) 'Protein kinase A activates protein phosphatase 2A by phosphorylation of the B56 subunit', *Proceedings of the National Academy of Sciences*. National Academy of Sciences, 104(8), pp. 2979–2984. doi: 10.1073/pnas.0611532104.
- Ai, X. *et al.* (2005) 'Ca²⁺/calmodulin-dependent protein kinase modulates cardiac ryanodine receptor phosphorylation and sarcoplasmic reticulum Ca²⁺ leak in heart failure', *Circulation Research*. Lippincott Williams & Wilkins, 97(12), pp. 1314–1322. doi: 10.1161/01.RES.0000194329.41863.89.
- Ai, X. and Pogwizd, S. M. (2005) 'Connexin 43 Downregulation and Dephosphorylation in Nonischemic Heart Failure Is Associated With Enhanced Colocalized Protein Phosphatase Type 2A', *Circulation Research*. Lippincott Williams & Wilkins, 96(1), pp. 54–63. doi: 10.1161/01.RES.0000152325.07495.5a.
- Alessi, D. R. *et al.* (1995) 'Inactivation of p42 MAP kinase by protein phosphatase 2A and a protein tyrosine phosphatase, but not CL100, in various cell lines', *Current Biology*. Cell Press, 5(3), pp. 283–295. doi: 10.1016/S0960-9822(95)00059-5.
- Armstrong, S. C. *et al.* (1998) 'Protein phosphatase inhibitors calyculin A and fostriecin protect rabbit cardiomyocytes in late ischemia', *Journal of Molecular and Cellular Cardiology*, 30(1), pp. 61–73. doi: 10.1006/jmcc.1997.0572.

- Arokium, H. *et al.* (2007) 'Substitutions of potentially phosphorylatable serine residues of bax reveal how they may regulate its interaction with mitochondria', *Journal of Biological Chemistry*, 282(48), pp. 35104–35112. doi: 10.1074/jbc.M704891200.
- Arrell, D. K. *et al.* (2006) 'Proteomic analysis of pharmacological preconditioning: Novel protein targets converge to mitochondrial metabolism pathways', *Circulation Research*, 99(7), pp. 706–714. doi: 10.1161/01.RES.0000243995.74395.f8.
- De Baere, I. *et al.* (1999) 'Purification of porcine brain protein phosphatase 2A leucine carboxyl methyltransferase and cloning of the human homologue', *Biochemistry*. American Chemical Society, 38(50), pp. 16539–16547. doi: 10.1021/bi991646a.
- Ballif, B. A. *et al.* (2004) 'Phosphoproteomic analysis of the developing mouse brain', *Molecular and Cellular Proteomics*. American Society for Biochemistry and Molecular Biology, 3(11), pp. 1093–1101. doi: 10.1074/mcp.M400085-MCP200.
- Barati, M. T. *et al.* (2006) 'A proteomic screen identified stress-induced chaperone proteins as targets of Akt phosphorylation in mesangial cells', *Journal of Proteome Research*. NIH Public Access, 5(7), pp. 1636–1646. doi: 10.1021/pr0502469.
- Barford, D., Das, A. K. and Egloff, M. P. (1998) 'The structure and mechanism of protein phosphatases: Insights into catalysis and regulation', *Annual Review of Biophysics and Biomolecular Structure*. Annual Reviews 4139 El Camino Way, P.O. Box 10139, Palo Alto, CA 94303-0139, USA, pp. 133–164. doi: 10.1146/annurev.biophys.27.1.133.
- Barrera-Chimal, J. *et al.* (2014) 'Intra-renal transfection of heat shock protein 90 alpha or beta (Hsp90 or Hsp90) protects against ischemia/reperfusion injury', *Nephrology Dialysis Transplantation*. Narnia, 29(2), pp. 301–312. doi: 10.1093/ndt/gft415.
- Basso, A. D. *et al.* (2002) 'Akt Forms an Intracellular Complex with Heat Shock Protein 90 (Hsp90) and Cdc37 and Is Destabilized by Inhibitors of Hsp90 Function', *Journal of Biological Chemistry*, 277(42), pp. 39858–39866. doi: 10.1074/jbc.M206322200.
- Basu, A. (2006) 'Posttranslational modifications of Bcl2 family members-a potential therapeutic target for human malignancy', *Frontiers in Bioscience*, 11(1), p. 1508. doi: 10.2741/1900.
- Baxter, G. F. (2002) 'The neutrophil as a mediator of myocardial ischemia-reperfusion injury: Time to move on', *Basic Research in Cardiology*, 97(4), pp. 268–275. doi: 10.1007/s00395-002-0366-7.
- Bean, B. P., Nowycky, M. C. and Tsien, R. W. (1984) ' β -Adrenergic modulation of calcium channels in frog ventricular heart cells', *Nature*. Nature Publishing Group, 307(5949), pp. 371–375. doi: 10.1038/307371a0.
- Beavers, D. L. *et al.* (2014) 'Emerging roles of junctophilin-2 in the heart and implications for cardiac diseases', *Cardiovascular Research*. Narnia, 103(2), pp. 198–205. doi: 10.1093/cvr/cvu151.
- Becker, A. C. *et al.* (2010) 'Acute coronary syndromes in treatment-naïve black south africans with human immunodeficiency virus infection', *Journal of Interventional Cardiology*, 23(1), pp. 70–77. doi: 10.1111/j.1540-8183.2009.00520.x.
- Belevych, A. E. *et al.* (2011) 'The relationship between arrhythmogenesis and impaired contractility in heart failure: Role of altered ryanodine receptor function', *Cardiovascular Research*. Narnia, 90(3), pp. 493–502. doi: 10.1093/cvr/cvr025.

- Beltrao, P. *et al.* (2013) 'Evolution and functional cross-talk of protein post-translational modifications', *Molecular Systems Biology*, 9(1), p. n/a-n/a. doi: 10.1002/msb.201304521.
- Benetti, F. J. (1985) 'Direct coronary surgery with saphenous vein bypass without either cardiopulmonary bypass or cardiac arrest.', *The Journal of Cardiovascular Surgery*, 26(3), pp. 217–22.
- Bernardi, P. (2017) 'Mitochondrial Transport of Cations: Channels, Exchangers, and Permeability Transition', *Physiological Reviews*, 79(4), pp. 1127–1155. doi: 10.1152/physrev.1999.79.4.1127.
- Bernardi, P. and Di Lisa, F. (2015) 'The mitochondrial permeability transition pore: Molecular nature and role as a target in cardioprotection', *Journal of Molecular and Cellular Cardiology*. Academic Press, 78, pp. 100–106. doi: 10.1016/j.yjmcc.2014.09.023.
- Bernelot Moens, S. J. *et al.* (2012) 'Rapid Estrogen Receptor Signaling Is Essential for the Protective Effects of Estrogen Against Vascular Injury', *Circulation*, 126(16), pp. 1993–2004. doi: 10.1161/CIRCULATIONAHA.112.124529.
- Betrie, A. H. *et al.* (2017) 'Evidence of a Cardiovascular Function for Microtubule-Associated Protein Tau', *Journal of Alzheimer's Disease*, 56(2), pp. 849–860. doi: 10.3233/JAD-161093.
- Bhasin, N. *et al.* (2007) 'Molecular basis for PP2A regulatory subunit B56 α targeting in cardiomyocytes', *American Journal of Physiology - Heart and Circulatory Physiology*. American Physiological Society, 293(1), pp. H109–H119. doi: 10.1152/ajpheart.00059.2007.
- Bio-rad (2016) 'Western Blot Doctor™ — Protein Band Appearance Problems', pp. 1–5.
- Blaich, A. *et al.* (2010) 'Facilitation of murine cardiac L-type Cav1.2 channel is modulated by Calmodulin kinase II-dependent phosphorylation of S1512 and S1570', *Proceedings of the National Academy of Sciences*, 107(22), pp. 10285–10289. doi: 10.1073/pnas.0914287107.
- Blignaut, M. *et al.* (2019) 'Ataxia-Telangiectasia Mutated is located in cardiac mitochondria and impacts oxidative phosphorylation', *Scientific Reports*. Nature Publishing Group, 9(1), p. 4782. doi: 10.1038/s41598-019-41108-1.
- Bliksøen, M. *et al.* (2015) 'Mitochondrial DNA damage and repair during ischemia-reperfusion injury of the heart', *Journal of Molecular and Cellular Cardiology*. Academic Press, 78, pp. 9–22. doi: 10.1016/j.yjmcc.2014.11.010.
- Bochelen, D., Rudin, M. and Sauter, A. (1999) 'Calcineurin inhibitors FK506 and SDZ ASM 981 alleviate the outcome of focal cerebral ischemic/reperfusion injury', *Journal of Pharmacology and Experimental Therapeutics*, 288(2), pp. 653–659.
- Boengler, K. *et al.* (2005) 'Connexin 43 in cardiomyocyte mitochondria and its increase by ischemic preconditioning', *Cardiovascular Research*, 67(2), pp. 234–244. doi: 10.1016/j.cardiores.2005.04.014.
- Bolli, R. *et al.* (1989) 'Direct evidence that oxygen-derived free radicals contribute to postischemic myocardial dysfunction in the intact dog.', *Proceedings of the National Academy of Sciences of the United States of America*, 86(12), pp. 4695–9.
- Bolli, R. (1992) 'Myocardial "stunning" in man.', *Circulation*, 86(6), pp. 1671–1691. doi: 10.1161/01.CIR.86.6.1671.

- Borutaite, V. *et al.* (2003) 'Inhibition of mitochondrial permeability transition prevents mitochondrial dysfunction, cytochrome c release and apoptosis induced by heart ischemia.', *Journal of Molecular and Cellular Cardiology*, 35(4), pp. 357–66.
- Boulikas, T. (1994) 'Control of DNA replication by protein phosphorylation', *Anticancer Research*, 14(6 B), pp. 2465–2472.
- Bowers, K. C., Allshire, A. P. and Cobbold, P. H. (1992) 'Bioluminescent measurement in single cardiomyocytes of sudden cytosolic ATP depletion coincident with rigor', *Journal of Molecular and Cellular Cardiology*, 24(3), pp. 213–218. doi: 10.1016/0022-2828(92)93159-H.
- Bradford, M. M. (1976) 'A rapid and sensitive method for the quantitation of microgram quantities of protein utilizing the principle of protein-dye binding', *Analytical Biochemistry*. Academic Press, 72(1–2), pp. 248–254. doi: 10.1016/0003-2697(76)90527-3.
- Brand, M. D. and Nicholls, D. G. (2011) 'Assessing mitochondrial dysfunction in cells', *Biochemical Journal*, 435(2), pp. 297–312. doi: 10.1042/BJ20110162.
- Braunwald, E. and Kloner, R. A. (1982) 'The stunned myocardium: Prolonged, postischemic ventricular dysfunction', *Circulation*, 66(6 I), pp. 1146–1149. doi: 10.1161/01.CIR.66.6.1146.
- Braunwald, E. and Kloner, R. A. (1985) 'Myocardial reperfusion: A double-edged sword?', *Journal of Clinical Investigation*. American Society for Clinical Investigation, 76(5), pp. 1713–1719. doi: 10.1172/JCI112160.
- Breitschopf, K. *et al.* (2002) 'Posttranslational Modification of Bcl-2 Facilitates Its Proteasome-Dependent Degradation: Molecular Characterization of the Involved Signaling Pathway', *Molecular and Cellular Biology*, 20(5), pp. 1886–1896. doi: 10.1128/mcb.20.5.1886-1896.2000.
- Brognaard, J. *et al.* (2007) 'PHLPP and a Second Isoform, PHLPP2, Differentially Attenuate the Amplitude of Akt Signaling by Regulating Distinct Akt Isoforms', *Molecular Cell*. Elsevier, 25(6), pp. 917–931. doi: 10.1016/j.molcel.2007.02.017.
- Bryant, J. C., Westphal, R. S. and Wadzinski, B. E. (1999) 'Methylated C-terminal leucine residue of PP2A catalytic subunit is important for binding of regulatory B α subunit.', *The Biochemical Journal*. Portland Press Ltd, 339 (Pt 2(Pt 2), pp. 241–6.
- Budas, G. R. *et al.* (2010) 'Mitochondrial import of PKC ϵ is mediated by HSP90: a role in cardioprotection from ischaemia and reperfusion injury', *Cardiovascular Research*. Narnia, 88(1), pp. 83–92. doi: 10.1093/cvr/cvq154.
- Cadenas, S. (2018) 'Mitochondrial uncoupling, ROS generation and cardioprotection', *Biochimica et Biophysica Acta (BBA) - Bioenergetics*, 1859(9), pp. 940–950. doi: 10.1016/j.bbabi.2018.05.019.
- Castets, F. *et al.* (1996) 'A novel calmodulin-binding protein, belonging to the WD-repeat family, is localized in dendrites of a subset of CNS neurons', *Journal of Cell Biology*. The Rockefeller University Press, 134(4), pp. 1051–1062. doi: 10.1083/jcb.134.4.1051.
- Castets, F. *et al.* (2000) 'Zinedin, SG2NA, and striatin are calmodulin-binding, WD repeat proteins principally expressed in the brain', *Journal of Biological Chemistry*, 275(26), pp. 19970–19977. doi: 10.1074/jbc.M909782199.

- Cayla, X. *et al.* (1990) 'Isolation and Characterization of a Tyrosyl Phosphatase Activator from Rabbit Skeletal Muscle and *Xenopus laevis* Oocytes', *Biochemistry*. American Chemical Society, 29(3), pp. 658–667. doi: 10.1021/bi00455a010.
- Chain, E. B., Mansford, K. R. L. and Opie, L. H. (1969) 'Effects of insulin on the pattern of glucose metabolism in the perfused working and Langendorff heart of normal and insulin-deficient rats', *Biochemical Journal*, 115(3), pp. 537–546. doi: 10.1042/bj1150537.
- Chance, B. and Williams, G. R. (1955) 'RESPIRATORY ENZYMES IN OXIDATIVE PHOSPHORYLATION', *Journal of Biological Chemistry*. American Society for Biochemistry and Molecular Biology, 217(1), pp. 383–394.
- Chang, Y.-T. Y.-W. *et al.* (2013) 'Quantitative Phosphoproteomic Study of Pressure-Overloaded Mouse Heart Reveals Dynamin-Related Protein 1 as a Modulator of Cardiac Hypertrophy', *Molecular & Cellular Proteomics*, 12(11), pp. 3094–3107. doi: 10.1074/mcp.M113.027649.
- Chen, G. Y. and Nuñez, G. (2010) 'Sterile inflammation: sensing and reacting to damage.', *Nature reviews. Immunology*, 10(12), pp. 826–37. doi: 10.1038/nri2873.
- Chen, J., Martin, B. L. and Brautigan, D. L. (1992) 'Regulation of protein serine-threonine phosphatase type-2A by tyrosine phosphorylation', *Science*. American Association for the Advancement of Science, 257(5074), pp. 1261–1264. doi: 10.1126/science.1325671.
- Chernoff, J. *et al.* (1983) 'Characterization of a phosphotyrosyl protein phosphatase activity associated with a phosphoserine protein phosphatase of Mr = 95,000 from bovine heart.', *The Journal of Biological Chemistry*, 258(12), pp. 7852–7.
- Chiang, C.-W. *et al.* (2003) 'Protein Phosphatase 2A Dephosphorylation of Phosphoserine 112 Plays the Gatekeeper Role for BAD-Mediated Apoptosis', *Molecular and Cellular Biology*. American Society for Microbiology (ASM), 23(18), pp. 6350–6362. doi: 10.1128/mcb.23.18.6350-6362.2003.
- Cho, U. S. and Xu, W. (2007) 'Crystal structure of a protein phosphatase 2A heterotrimeric holoenzyme', *Nature*, 445(7123), pp. 53–57. doi: 10.1038/nature05351.
- Choi, J. S. *et al.* (2005) 'Phosphorylation of PTEN and Akt in astrocytes of the rat hippocampus following transient forebrain ischemia', *Cell and Tissue Research*, 319(3), pp. 359–366. doi: 10.1007/s00441-004-1033-0.
- Chung, H. *et al.* (1999) 'Mutation of Tyr307 and Leu309 in the protein phosphatase 2A catalytic subunit favors association with the $\alpha 4$ subunit which promotes dephosphorylation of elongation factor-2', *Biochemistry*. American Chemical Society, 38(32), pp. 10371–10376. doi: 10.1021/bi990902g.
- Cohen, M. V., Yang, X.-M. and Downey, J. M. (1999) 'Smaller infarct after preconditioning does not predict extent of early functional improvement of reperfused heart', *American Journal of Physiology-Heart and Circulatory Physiology*, 277(5), pp. H1754–H1761. doi: 10.1152/ajpheart.1999.277.5.H1754.
- Cohen, M. V. *et al.* (2001) 'Acetylcholine, bradykinin, opioids, and phenylephrine, but not adenosine, trigger preconditioning by generating free radicals and opening mitochondrial K(ATP) channels.', *Circulation Research*, 89(3), pp. 273–8.

- Cohen, P. (2001) 'The role of protein phosphorylation in human health and disease: Delivered on June 30th 2001 at the FEBS meeting in Lisbon', *European Journal of Biochemistry*. John Wiley & Sons, Ltd (10.1111), 268(19), pp. 5001–5010. doi: 10.1046/j.0014-2956.2001.02473.x.
- Cohen, P. (2002) 'The Structure And Regulation Of Protein Phosphatases', *Annual Review of Biochemistry*. Annual Reviews 4139 El Camino Way, P.O. Box 10139, Palo Alto, CA 94303-0139, USA , 58(1), pp. 453–508. doi: 10.1146/annurev.biochem.58.1.453.
- Cohen, P., Klumpp, S. and Schelling, D. L. (1989) 'An improved procedure for identifying and quantitating protein phosphatases in mammalian tissues.', *FEBS letters*, 250(2), pp. 596–600.
- Colombini, M. (1979) 'A candidate for the permeability pathway of the outer mitochondrial membrane.', *Nature*. Nature Publishing Group, 279(5714), pp. 643–645. doi: 10.1038/279643a0.
- Crans, D. C. *et al.* (2004) 'The Chemistry and Biochemistry of Vanadium and the Biological Activities Exerted by Vanadium Compounds'. doi: 10.1021/cr020607t.
- Cundell, M. J. *et al.* (2016) 'A PP2A-B55 recognition signal controls substrate dephosphorylation kinetics during mitotic exit', *Journal of Cell Biology*, 214(5), pp. 539–554. doi: 10.1083/jcb.201606033.
- Das, B. and Mishra, T. . (2013) 'Management of arrhythmias in acute myocardial infarction', *International Journal of Contemporary Medical Research*, 3(5), pp. 1401–1405. doi: 10.1007/BF02953865.
- Datta, S. R. *et al.* (1997) 'Akt phosphorylation of BAD couples survival signals to the cell- intrinsic death machinery', *Cell*, 91(2), pp. 231–241. doi: 10.1016/S0092-8674(00)80405-5.
- Dautzenberger, G, F. M., Muller, D. and Richter, D. (1993) 'Dephosphorylation of phosphorylated atrial natriuretic peptide by protein phosphatase 2A', *European Journal of Biochemistry*, 211(3), pp. 485–490. doi: 10.1111/j.1432-1033.1993.tb17574.x.
- Davare, M. A., Horne, M. C. and Hell, J. W. (2000) 'Protein phosphatase 2a is associated with class c l-type calcium channels (Cav1.2) and Antagonizes channel phosphorylation by cAMP-dependent protein kinase', *Journal of Biological Chemistry*. American Society for Biochemistry and Molecular Biology, 275(50), pp. 39710–39717. doi: 10.1074/jbc.M005462200.
- Debold, E. P., Beck, S. E. and Warshaw, D. M. (2008) 'Effect of low pH on single skeletal muscle myosin mechanics and kinetics', *American Journal of Physiology-Cell Physiology*. American Physiological Society, 295(1), pp. C173–C179. doi: 10.1152/ajpcell.00172.2008.
- Decker, R. S. *et al.* (2005) 'Myosin-Binding Protein C Phosphorylation, Myofibril Structure, and Contractile Function During Low-Flow Ischemia', *Circulation*, 111(7), pp. 906–912. doi: 10.1161/01.CIR.0000155609.95618.75.
- Decker, R. S. *et al.* (2012) 'The dynamic role of cardiac myosin binding protein-C during ischemia', *Journal of Molecular and Cellular Cardiology*, 52(5), pp. 1145–1154. doi: 10.1016/j.yjmcc.2012.01.006.
- Degli Esposti, M. *et al.* (2003) 'Post-translational modification of Bid has differential effects on its susceptibility to cleavage by caspase 8 or caspase 3', *Journal of Biological Chemistry*, 278(18), pp. 15749–15757. doi: 10.1074/jbc.M209208200.

- DeGrande, S. T. *et al.* (2013) 'Molecular mechanisms underlying cardiac protein phosphatase 2A regulation in heart', *Journal of Biological Chemistry*, 288(2), pp. 1032–1046. doi: 10.1074/jbc.M112.426957.
- Dehmer, G. J. and Smith, K. J. (2009) 'Drug-eluting coronary artery stents', *American Family Physician*. Massachusetts Medical Society, 80(11), pp. 254–265. doi: 10.1056/NEJMra1210816.
- Deng, X. *et al.* (1998) 'Reversible phosphorylation of Bcl2 following interleukin 3 or bryostatin 1 is mediated by direct interaction with protein phosphatase 2A.', *The Journal of Biological Chemistry*, 273(51), pp. 34157–63.
- Dondelinger, Y., Vandenabeele, P. and Bertrand, M. J. M. (2016) 'Regulation of RIPK1's cell death function by phosphorylation', *Cell Cycle*, 15(1), pp. 5–6. doi: 10.1080/15384101.2015.1112688.
- Donthi, R. V., Huisamen, B. and Lochner, A. (2000) 'Effect of Vanadate and Insulin on Glucose Transport in Isolated Adult Rat Cardiomyocytes', *Cardiovascular Drugs and Therapy*. Kluwer Academic Publishers, 14(5), pp. 463–470. doi: 10.1023/A:1007876703644.
- Drake, M. *et al.* (1996) 'The immunosuppressant FK506 ameliorates ischaemic damage in the rat brain', *Acta Physiologica Scandinavica*. John Wiley & Sons, Ltd (10.1111), 158(2), pp. 155–159. doi: 10.1046/j.1365-201X.1996.535298000.x.
- DuBell, W. H. *et al.* (2002) 'Effects of PP1/PP2A inhibitor calyculin A on the E-C coupling cascade in murine ventricular myocytes', *American Journal of Physiology - Heart and Circulatory Physiology*. American Physiological Society Bethesda, MD, 282(1 51-1), pp. H38–H48. doi: 10.1152/ajpheart.00536.2001.
- Eden, M. *et al.* (2016) 'Myoscape controls cardiac calcium cycling and contractility via regulation of L-type calcium channel surface expression', *Nature Communications*. Nature Publishing Group, 7(1), p. 11317. doi: 10.1038/ncomms11317.
- Eichhorn, P. J. A., Creighton, M. P. and Bernards, R. (2009) 'Protein phosphatase 2A regulatory subunits and cancer', *Biochimica et Biophysica Acta - Reviews on Cancer*, 1795(1), pp. 1–15. doi: 10.1016/j.bbcan.2008.05.005.
- Eisner, D. A. *et al.* (2017) 'Calcium and Excitation-Contraction Coupling in the Heart', *Circulation Research*. Wolters Kluwer Health, 121(2), pp. 181–195. doi: 10.1161/CIRCRESAHA.117.310230.
- Elaimy, A. L. *et al.* (2016) 'ATM is the primary kinase responsible for phosphorylation of Hsp90α after ionizing radiation.', *Oncotarget*. Impact Journals, LLC, 7(50), pp. 82450–82457. doi: 10.18632/oncotarget.12557.
- Engelman, R. M. (1994) 'Myocardial stunning: a temperature dependent phenomenon.', *Journal of Cardiac Surgery*, 9(3 Suppl), pp. 493–6.
- Espach, Y. (2017) 'An investigation into the importance of the ATM protein in the myocardial pathology associated with insulin resistance and type 2 diabetes'. Stellenbosch : Stellenbosch University.
- Etard, C., Roostalu, U. and Strähle, U. (2008) 'Shuttling of the chaperones Unc45b and Hsp90a between the A band and the Z line of the myofibril', *The Journal of Cell Biology*, 180(6), pp. 1163–1175. doi: 10.1083/jcb.200709128.

- Fabiato, A. (2017) 'Calcium-induced release of calcium from the cardiac sarcoplasmic reticulum', *American Journal of Physiology-Cell Physiology*, 245(1), pp. C1–C14. doi: 10.1152/ajpcell.1983.245.1.c1.
- Fan, L. *et al.* (2016) 'FAM122A, a new endogenous inhibitor of protein phosphatase 2A', *Oncotarget. Impact Journals, LLC*, 7(39), pp. 63887–63900. doi: 10.18632/oncotarget.11698.
- Fan, W. J. *et al.* (2009) 'Dexamethasone-induced cardioprotection: A role for the phosphatase MKP-1?', *Life Sciences*, 84(23–24), pp. 838–846. doi: 10.1016/j.lfs.2009.03.014.
- Fan, W. J. *et al.* (2010) 'Kinases and phosphatases in ischaemic preconditioning: A re-evaluation', *Basic Research in Cardiology*. Springer-Verlag, 105(4), pp. 495–511. doi: 10.1007/s00395-010-0086-3.
- Farrar, W. L. *et al.* (1990) 'Cytokine regulation of protein phosphorylation', *Cytokine*, 2(2), pp. 77–91. doi: 10.1016/1043-4666(90)90001-A.
- Favre, B. *et al.* (1994) 'The catalytic subunit of protein phosphatase 2A is carboxyl-methylated in vivo', *Journal of Biological Chemistry*, 269(23), pp. 16311–16317.
- Fellner, T. *et al.* (2003) 'A novel and essential mechanism determining specificity and activity of protein phosphatase 2A (PP2A) in vivo', *Genes and Development*, 17(17), pp. 2138–2150. doi: 10.1101/gad.259903.
- Fenton, R. A., Dickson, E. W. and Dobson, J. G. (2005) 'Inhibition of phosphatase activity enhances preconditioning and limits cell death in the ischemic/reperfused aged rat heart', *Life Sciences*. Pergamon, 77(26), pp. 3375–3388. doi: 10.1016/j.lfs.2005.05.047.
- Ferdinandy, P. and Schulz, R. (2003) 'Nitric oxide, superoxide, and peroxynitrite in myocardial ischaemia-reperfusion injury and preconditioning', *British Journal of Pharmacology*. Wiley-Blackwell, 138(4), pp. 532–543. doi: 10.1038/sj.bjp.0705080.
- Fishbein, M. C. *et al.* (1981) 'Early phase acute myocardial infarct size quantification: Validation of the triphenyl tetrazolium chloride tissue enzyme staining technique', *American Heart Journal*. Mosby, 101(5), pp. 593–600. doi: 10.1016/0002-8703(81)90226-X.
- Ford, W. R. *et al.* (2001) 'Angiotensin II reduces infarct size and has no effect on post-ischaemic contractile dysfunction in isolated rat hearts', *British Journal of Pharmacology*, 134(1), pp. 38–45. doi: 10.1038/sj.bjp.0704225.
- Fostinis, Y. *et al.* (1992) 'Heat shock protein HSP90 and its association with the cytoskeleton: a morphological study', *Biochemistry and Cell Biology*, 70(9), pp. 779–786. doi: 10.1139/o92-118.
- Fox, J. L. *et al.* (2010) 'Tyrosine dephosphorylation is required for Bak activation in apoptosis', *EMBO Journal*, 29(22), pp. 3853–3868. doi: 10.1038/emboj.2010.244.
- Frangogiannis, N. G. (2012) 'Regulation of the inflammatory response in cardiac repair', *Circulation Research*. Edited by A. Rosenzweig, 110(1), pp. 159–173. doi: 10.1161/CIRCRESAHA.111.243162.
- Franke, W. W. *et al.* (2015) 'Striatins as plaque molecules of zonulae adhaerentes in simple epithelia, of tessellate junctions in stratified epithelia, of cardiac composite junctions and of various size classes of lateral adherens junctions in cultures of epithelia- and carcinoma-derived cells', *Cell and Tissue Research*. Springer Berlin Heidelberg, 359(3), pp. 779–797. doi: 10.1007/s00441-014-2053-z.

- Fujiu, K., Wang, J. and Nagai, R. (2014) 'Cardioprotective function of cardiac macrophages', *Cardiovascular Research*, 102(2), pp. 232–239. doi: 10.1093/cvr/cvu059.
- Fujiwara, N. *et al.* (2016) 'Regulation of beclin 1 protein phosphorylation and autophagy by protein phosphatase 2A (PP2A) and death-associated protein kinase 3 (DAPK3)', *Journal of Biological Chemistry*, 291(20), pp. 10858–10866. doi: 10.1074/jbc.M115.704908.
- Gadicherla, A. K. *et al.* (2012) 'Damage to mitochondrial complex i during cardiac ischemia reperfusion injury is reduced indirectly by anti-anginal drug ranolazine', *Biochimica et Biophysica Acta - Bioenergetics*. NIH Public Access, 1817(3), pp. 419–429. doi: 10.1016/j.bbabi.2011.11.021.
- Gaillard, S. *et al.* (2001) 'Striatin, a calmodulin-dependent scaffolding protein, directly binds caveolin-1', *FEBS Letters*, 508(1), pp. 49–52. doi: 10.1016/S0014-5793(01)03020-4.
- Gao, L. *et al.* (2014) 'Degradation of cardiac myosin light chain kinase by matrix metalloproteinase-2 contributes to myocardial contractile dysfunction during ischemia/reperfusion', *Journal of Molecular and Cellular Cardiology*. Academic Press, 77, pp. 102–112. doi: 10.1016/j.yjmcc.2014.10.004.
- Gao, T., Furnari, F. and Newton, A. C. (2005) 'PHLPP: A phosphatase that directly dephosphorylates Akt, promotes apoptosis, and suppresses tumor growth', *Molecular Cell*. Elsevier, 18(1), pp. 13–24. doi: 10.1016/j.molcel.2005.03.008.
- García-Dorado, D. *et al.* (2014) 'Protection Against Myocardial Ischemia-reperfusion Injury in Clinical Practice', *Revista Española de Cardiología (English Edition)*. Elsevier, 67(5), pp. 394–404. doi: 10.1016/j.rec.2014.01.010.
- García-Pérez, C. *et al.* (2011) 'Alignment of sarcoplasmic reticulum-mitochondrial junctions with mitochondrial contact points', *American Journal of Physiology - Heart and Circulatory Physiology*. American Physiological Society, 301(5), pp. H1907-15. doi: 10.1152/ajpheart.00397.2011.
- García-Rivas, G. D. J. *et al.* (2005) 'Inhibition of the mitochondrial calcium uniporter by the oxo-bridged dinuclear ruthenium amine complex (Ru360) prevents from irreversible injury in postischemic rat heart', *FEBS Journal*, 272(13), pp. 3477–3488. doi: 10.1111/j.1742-4658.2005.04771.x.
- Gardai, S. J. *et al.* (2004) 'Phosphorylation of Bax ser184 by Akt regulates its activity and apoptosis in neutrophils', *Journal of Biological Chemistry*. American Society for Biochemistry and Molecular Biology, 279(20), pp. 21085–21095. doi: 10.1074/jbc.M400063200.
- Garlick, P. B. *et al.* (1987) 'Direct detection of free radicals in the reperfused rat heart using electron spin resonance spectroscopy', *Circulation Research*, 61(5), pp. 757–760. doi: 10.1161/01.RES.61.5.757.
- Garza, A. E. *et al.* (2015) 'Critical Role of Striatin in Blood Pressure and Vascular Responses to Dietary Sodium Intake', *Hypertension*. Lippincott Williams & Wilkins/Hagerstown, MD, 66(3), pp. 674–680. doi: 10.1161/HYPERTENSIONAHA.115.05600.
- Gho, B. C. G. *et al.* (1996) 'Myocardial protection by brief ischemia in noncardiac tissue', *Circulation*. American Heart Association, 94(9), pp. 2193–2200. doi: 10.1161/01.CIR.94.9.2193.
- Gibbs, C. L. (2017) 'Cardiac energetics.', *Physiological Reviews*, 58(1), pp. 174–254. doi: 10.1152/physrev.1978.58.1.174.

- Giorgio, V. *et al.* (2017) 'Ca²⁺ binding to F-ATP synthase β subunit triggers the mitochondrial permeability transition', *EMBO reports*, 18(7), pp. 1065–1076. doi: 10.15252/embr.201643354.
- Giralt, A. and Villarroya, F. (2012) 'SIRT3, a pivotal actor in mitochondrial functions: metabolism, cell death and aging', *Biochemical Journal*, 444(1), pp. 1–10. doi: 10.1042/BJ20120030.
- Goeckeler, Z. M. *et al.* (2000) 'Phosphorylation of myosin light chain kinase by p21-activated kinase PAK2', *Journal of Biological Chemistry*. American Society for Biochemistry and Molecular Biology, 275(24), pp. 18366–18374. doi: 10.1074/jbc.M001339200.
- Gong, X. *et al.* (2010) 'Mechanisms regulating the nuclear translocation of p38 MAP kinase', *Journal of Cellular Biochemistry*, 110(6), pp. 1420–1429. doi: 10.1002/jcb.22675.
- Gordon, J. *et al.* (2011) 'Protein phosphatase 2a (PP2A) binds within the oligomerization domain of striatin and regulates the phosphorylation and activation of the mammalian Ste20-Like kinase Mst3', *BMC Biochemistry*. BioMed Central Ltd, 12(1), p. 54. doi: 10.1186/1471-2091-12-54.
- Gordon, J. A. (1991) 'Use of vanadate as protein-phosphotyrosine phosphatase inhibitor', *Methods in Enzymology*. Academic Press, 201(C), pp. 477–482. doi: 10.1016/0076-6879(91)01043-2.
- Götz, J. *et al.* (1998) 'Delayed embryonic lethality in mice lacking protein phosphatase 2A catalytic subunit α ', *Proceedings of the National Academy of Sciences of the United States of America*, 95(21), pp. 12370–12375. doi: 10.1073/pnas.95.21.12370.
- Goudreault, M. *et al.* (2009) 'A PP2A Phosphatase High Density Interaction Network Identifies a Novel Striatin-interacting Phosphatase and Kinase Complex Linked to the Cerebral Cavernous Malformation 3 (CCM3) Protein', *Molecular & Cellular Proteomics*. American Society for Biochemistry and Molecular Biology, 8(1), pp. 157–171. doi: 10.1074/MCP.M800266-MCP200.
- Govindan, S. *et al.* (2012) 'Pathogenic properties of the N-terminal region of cardiac myosin binding protein-C in vitro', *Journal of Muscle Research and Cell Motility*. Springer Netherlands, 33(1), pp. 17–30. doi: 10.1007/s10974-012-9292-y.
- Griffiths, E. J. *et al.* (1998) 'Mitochondrial calcium transporting pathways during hypoxia and reoxygenation in single rat cardiomyocytes', *Cardiovascular Research*, 39(2), pp. 423–433. doi: 10.1016/S0008-6363(98)00104-7.
- Griffiths, E. J. and Halestrap, A. P. (2015) 'Mitochondrial non-specific pores remain closed during cardiac ischaemia, but open upon reperfusion', *Biochemical Journal*. Portland Press Ltd, 307(1), pp. 93–98. doi: 10.1042/bj3070093.
- Grocott, H. P., Stafford-Smith, M. and Mora-Mangano, C. T. (2018) 'Cardiopulmonary Bypass Management and Organ Protection', in *Kaplan's Essentials of Cardiac Anesthesia for Cardiac Surgery*. Elsevier, pp. 608–663. doi: 10.1016/B978-0-323-49798-5.00025-5.
- Grover, G. J. *et al.* (2004) 'Excessive ATP hydrolysis in ischemic myocardium by mitochondrial F₁F₀-ATPase: effect of selective pharmacological inhibition of mitochondrial ATPase hydrolase activity', *American Journal of Physiology-Heart and Circulatory Physiology*, 287(4), pp. H1747–H1755. doi: 10.1152/ajpheart.01019.2003.
- Grüntzig, A. R., Senning, A. and Siegenthaler, W. E. (1979) 'Nonoperative dilatation of coronary-artery stenosis: percutaneous transluminal coronary angioplasty.', *The New England journal of medicine*, 301(2), pp. 61–8. doi: 10.1056/NEJM197907123010201.

- Gu, X. *et al.* (2010) 'Cardiac functional improvement in rats with myocardial infarction by up-regulating cardiac myosin light chain kinase with neuregulin', *Cardiovascular Research*. Narnia, 88(2), pp. 334–343. doi: 10.1093/cvr/cvq223.
- Guan, K. L. and Dixon, J. E. (1991) 'Evidence for protein-tyrosine-phosphatase catalysis proceeding via a cysteine-phosphate intermediate', *Journal of Biological Chemistry*. American Society for Biochemistry and Molecular Biology, 266(26), pp. 17026–17030.
- Guo, A. *et al.* (2008) 'Signaling networks assembled by oncogenic EGFR and c-Met.', *Proceedings of the National Academy of Sciences of the United States of America*. National Academy of Sciences, 105(2), pp. 692–7. doi: 10.1073/pnas.0707270105.
- Guo, F. *et al.* (2014) 'Structural basis of PP2A activation by PTPA, an ATPdependent activation chaperone', *Cell Research*. Nature Publishing Group, 24(2), pp. 190–203. doi: 10.1038/cr.2013.138.
- Guo, H. and Damuni, Z. (1993) 'Autophosphorylation-activated protein kinase phosphorylates and inactivates protein phosphatase 2A', *Proceedings of the National Academy of Sciences of the United States of America*, 90(6), pp. 2500–2504. doi: 10.1073/pnas.90.6.2500.
- Hagemann, D. and Xiao, R. P. (2002) 'Dual site phospholamban phosphorylation and its physiological relevance in the heart', *Trends in Cardiovascular Medicine*, 12(2), pp. 51–56. doi: 10.1016/S1050-1738(01)00145-1.
- Halestrap, A. P. *et al.* (1998) 'Elucidating the molecular mechanism of the permeability transition pore and its role in reperfusion injury of the heart', *Biochimica et Biophysica Acta - Bioenergetics*, 1366(1–2), pp. 79–94. doi: 10.1016/S0005-2728(98)00122-4.
- Halestrap, A. P. (2009) 'What is the mitochondrial permeability transition pore?', *Journal of Molecular and Cellular Cardiology*. Academic Press, 46(6), pp. 821–831.
- Halestrap, A. P. (2015) 'Calcium-dependent opening of a non-specific pore in the mitochondrial inner membrane is inhibited at pH values below 7. Implications for the protective effect of low pH against chemical and hypoxic cell damage', *Biochemical Journal*, 278(3), pp. 715–719. doi: 10.1042/bj2780715.
- Hall, D. D. *et al.* (2006) 'Binding of protein phosphatase 2A to the L-type calcium channel Ca v1.2 next to Ser1928, its main PKA site, is critical for Ser1928 dephosphorylation', *Biochemistry*, 45(10), pp. 3448–3459. doi: 10.1021/bi051593z.
- Halliwell, B., Lai, E. K. and Mccay, P. B. (1989) 'Marked Reduction of Free Radical Generation and Contractile Dysfunction by Antioxidant Therapy Begun at the Time of Reperfusion', *Circulation research*, 65(3), pp. 607–622.
- Hamdani, N., Krysiak, J., *et al.* (2013) 'Crucial role for Ca²⁺/calmodulin-dependent protein kinase-II in regulating diastolic stress of normal and failing hearts via titin phosphorylation', *Circulation Research*, 112(4), pp. 664–674. doi: 10.1161/CIRCRESAHA.111.300105.
- Hamdani, N., Franssen, C., *et al.* (2013) 'Myocardial titin hypophosphorylation importantly contributes to heart failure with preserved ejection fraction in a rat metabolic risk model', *Circulation: Heart Failure*, 6(6), pp. 1239–1249. doi: 10.1161/CIRCHEARTFAILURE.113.000539.

- Hamdani, N., Herwig, M. and Linke, W. A. (2017) 'Tampering with springs: phosphorylation of titin affecting the mechanical function of cardiomyocytes', *Biophysical Reviews*. Springer, 9(3), pp. 225–237. doi: 10.1007/s12551-017-0263-9.
- Hare, J. M. and Colucci, W. S. (1995) 'Role of nitric oxide in the regulation of myocardial function', *Progress in Cardiovascular Diseases*, 38(2), pp. 155–166. doi: 10.1016/S0033-0620(05)80004-0.
- Hartwig, J. H. *et al.* (1992) 'MARCKS is an actin filament crosslinking protein regulated by protein kinase C and calcium-calmodulin', *Nature*. Nature Publishing Group, 356(6370), pp. 618–622. doi: 10.1038/356618a0.
- Hashimoto, Y. and Soderling, T. R. (1990) 'Phosphorylation of smooth muscle myosin light chain kinase by Ca²⁺/calmodulin-dependent protein kinase II: Comparative study of the phosphorylation sites', *Archives of Biochemistry and Biophysics*, 278(1), pp. 41–45. doi: 10.1016/0003-9861(90)90228-Q.
- Hausenloy, D. *et al.* (2004) 'Transient Mitochondrial Permeability Transition Pore Opening Mediates Preconditioning-Induced Protection', *Circulation*, 109(14), pp. 1714–1717. doi: 10.1161/01.CIR.0000126294.81407.7D.
- Hausenloy, D. J. and Yellon, D. M. (2003) 'The mitochondrial permeability transition pore: Its fundamental role in mediating cell death during ischaemia and reperfusion', *Journal of Molecular and Cellular Cardiology*, 35(4), pp. 339–341. doi: 10.1016/S0022-2828(03)00043-9.
- Hausenloy, D. J. and Yellon, D. M. (2004) 'New directions for protecting the heart against ischaemia-reperfusion injury: Targeting the Reperfusion Injury Salvage Kinase (RISK)-pathway', *Cardiovascular Research*. Oxford University Press, 61(3), pp. 448–460. doi: 10.1016/j.cardiores.2003.09.024.
- Hausenloy, D. J. and Yellon, D. M. (2013) 'Myocardial Ischemia-Reperfusion Injury : a Neglected Therapeutic Target', *Journal of Clinical Investigation*, 123(1), pp. 92–100. doi: 10.1172/JCI62874.92.
- Hawke, T. J. *et al.* (2007) 'Xin, an actin binding protein, is expressed within muscle satellite cells and newly regenerated skeletal muscle fibers', *American Journal of Physiology-Cell Physiology*, 293(5), pp. C1636–C1644. doi: 10.1152/ajpcell.00124.2007.
- Hégarat, N. *et al.* (2014) 'PP2A/B55 and Fcp1 Regulate Greatwall and Ensa Dephosphorylation during Mitotic Exit', *PLoS Genetics*. Edited by G. P. Copenhaver, 10(1), p. e1004004. doi: 10.1371/journal.pgen.1004004.
- Heidkamp, M. C. *et al.* (2007) 'Protein kinase C ϵ -dependent MARCKS phosphorylation in neonatal and adult rat ventricular myocytes', *Journal of Molecular and Cellular Cardiology*. Academic Press, 42(2), pp. 422–431. doi: 10.1016/J.YJMCC.2006.10.017.
- Hein, S. *et al.* (2000) 'The role of the cytoskeleton in heart failure', *Cardiovascular Research*. Narnia, 45(2), pp. 273–278. doi: 10.1016/S0008-6363(99)00268-0.
- Hemmings, B. A. *et al.* (1990) ' α - and β Forms of the 65-kDa Subunit of Protein Phosphatase 2A Have a Similar 39 Amino Acid Repeating Structure', *Biochemistry*. American Chemical Society, 29(13), pp. 3166–3173. doi: 10.1021/bi00465a002.
- Hendrix, P. *et al.* (1993) 'Structure and expression of a 72-kDa regulatory subunit of protein phosphatase 2A. Evidence for different size forms produced by alternative splicing', *Journal of Biological Chemistry*, 268(20), pp. 15267–15276.

- Herzig, S. and Neumann, J. (2000) 'Effects of Serine/Threonine Protein Phosphatases on Ion Channels in Excitable Membranes', *Physiological Reviews*, 80(1), pp. 173–210. doi: 10.1152/physrev.2000.80.1.173.
- Heusch, G. (2013) 'Cardioprotection: Chances and challenges of its translation to the clinic', *The Lancet*, pp. 166–175. doi: 10.1016/S0140-6736(12)60916-7.
- Heusch, G., Boengler, K. and Schulz, R. (2010) 'Editorial: Inhibition of mitochondrial permeability transition pore opening: The holy grail of cardioprotection', *Basic Research in Cardiology*, 12 March, pp. 151–154. doi: 10.1007/s00395-009-0080-9.
- Heyndrickx, G. R. *et al.* (1975) 'Regional myocardial functional and electrophysiological alterations after brief coronary artery occlusion in conscious dogs', *Journal of Clinical Investigation*. American Society for Clinical Investigation, 56(4), pp. 978–985. doi: 10.1172/JCI108178.
- Hidalgo, C. *et al.* (2009) 'PKC phosphorylation of titin's PEVK element: A novel and conserved pathway for modulating myocardial stiffness', *Circulation Research*, 105(7), pp. 631–638. doi: 10.1161/CIRCRESAHA.109.198465.
- Hlobilková, A. *et al.* (2003) 'The mechanism of action of the tumour suppressor gene PTEN.', *Biomedical papers of the Medical Faculty of the University Palacky, Olomouc, Czechoslovakia*, 147(1), pp. 19–25.
- Hochachka, P. W. and Mommsen, T. P. (1983) 'Protons and anaerobiosis.', *Science (New York, N.Y.)*. American Association for the Advancement of Science, 219(4591), pp. 1391–7. doi: 10.1126/SCIENCE.6298937.
- Hoffman, A., Taleski, G. and Sontag, E. (2017) 'The protein serine/threonine phosphatases PP2A, PP1 and calcineurin: A triple threat in the regulation of the neuronal cytoskeleton', *Molecular and Cellular Neuroscience*, 84, pp. 119–131. doi: 10.1016/j.mcn.2017.01.005.
- Højlund, K. *et al.* (2003) 'Proteome analysis reveals phosphorylation of ATP synthase β -subunit in human skeletal muscle and proteins with potential roles in type 2 diabetes', *Journal of Biological Chemistry*. American Society for Biochemistry and Molecular Biology, 278(12), pp. 10436–10442. doi: 10.1074/jbc.M212881200.
- Hombauer, H. *et al.* (2007) 'Generation of active protein phosphatase 2A is coupled to holoenzyme assembly', *PLoS Biology*. Edited by P. Walter, 5(6), pp. 1355–1365. doi: 10.1371/journal.pbio.0050155.
- Hornbeck, P. V. *et al.* (2015) 'PhosphoSitePlus, 2014: Mutations, PTMs and recalibrations', *Nucleic Acids Research*, 43(D1), pp. D512–D520. doi: 10.1093/nar/gku1267.
- Hornberg, J. J. *et al.* (2004) 'Principles behind the multifarious control of signal transduction', *FEBS Journal*, 272(1), pp. 244–258. doi: 10.1111/j.1432-1033.2004.04404.x.
- Hoter, A., El-Sabban, M. E. and Naim, H. Y. (2018) 'The HSP90 family: Structure, regulation, function, and implications in health and disease', *International Journal of Molecular Sciences*. Multidisciplinary Digital Publishing Institute (MDPI). doi: 10.3390/ijms19092560.
- Hu, J. *et al.* (2014) 'Phosphorylation-dependent mitochondrial translocation of MAP4 is an early step in hypoxia-induced apoptosis in cardiomyocytes', *Cell Death & Disease*. Nature Publishing Group, 5(9), pp. e1424–e1424. doi: 10.1038/cddis.2014.369.

- Hua, F. *et al.* (2018) 'DR region of Na⁺ -K⁺ -ATPase is a new target to protect heart against oxidative injury', *Scientific Reports*. Nature Publishing Group, 8(1), p. 13100. doi: 10.1038/s41598-018-31460-z.
- Hudson, B. *et al.* (2011) 'Hyperphosphorylation of mouse cardiac titin contributes to transverse aortic constriction-induced diastolic dysfunction', *Circulation Research*, 109(8), pp. 858–866. doi: 10.1161/CIRCRESAHA.111.246819.
- Hudson, B. D. *et al.* (2010) 'Excision of titin's cardiac PEVK spring element abolishes PKC α -induced increases in myocardial stiffness', *Journal of Molecular and Cellular Cardiology*, 48(5), pp. 972–978. doi: 10.1016/j.yjmcc.2009.12.006.
- Huke, S. and Bers, D. M. (2008) 'Ryanodine receptor phosphorylation at Serine 2030, 2808 and 2814 in rat cardiomyocytes', *Biochemical and Biophysical Research Communications*, 376(1), pp. 80–85. doi: 10.1016/j.bbrc.2008.08.084.
- Huret, J. (2011) 'STRN (striatin, calmodulin binding protein)', *Atlas of Genetics and Cytogenetics in Oncology and Haematology*, 13(4), pp. 293–296. doi: 10.4267/2042/44453.
- Hutchinson, K. R. *et al.* (2015) 'Increased myocardial stiffness due to cardiac titin isoform switching in a mouse model of volume overload limits eccentric remodeling', *Journal of Molecular and Cellular Cardiology*, 79, pp. 104–114. doi: 10.1016/j.yjmcc.2014.10.020.
- Huttlin, E. L. *et al.* (2010) 'A Tissue-Specific Atlas of Mouse Protein Phosphorylation and Expression', *Cell*, 143(7), pp. 1174–1189. doi: 10.1016/j.cell.2010.12.001.
- Huyer, G. *et al.* (1997) 'Mechanism of inhibition of protein-tyrosine phosphatases by vanadate and pervanadate', *Journal of Biological Chemistry*. American Society for Biochemistry and Molecular Biology, 272(2), pp. 843–851. doi: 10.1074/jbc.272.2.843.
- Hwang, J. and Pallas, D. C. (2014) 'STRIPAK complexes: Structure, biological function, and involvement in human diseases', *International Journal of Biochemistry and Cell Biology*. Pergamon, 47(1), pp. 118–148. doi: 10.1016/j.biocel.2013.11.021.
- Ibáñez, B. *et al.* (2015) 'Evolving Therapies for Myocardial Ischemia/Reperfusion Injury', *Journal of the American College of Cardiology*. Elsevier, 65(14), pp. 1454–1471. doi: 10.1016/J.JACC.2015.02.032.
- Ikehara, T. *et al.* (2007) 'Methylation of the C-terminal leucine residue of the PP2A catalytic subunit is unnecessary for the catalytic activity and the binding of regulatory subunit (PR55/B)', *Biochemical and Biophysical Research Communications*, 354(4), pp. 1052–1057. doi: 10.1016/j.bbrc.2007.01.085.
- Inserte, J., Hernando, V. and Garcia-Dorado, D. (2012) 'Contribution of calpains to myocardial ischaemia/reperfusion injury', *Cardiovascular Research*, 96(1), pp. 23–31. doi: 10.1093/cvr/cvs232.
- Ishihara, H. *et al.* (1989) 'Calyculin A and okadaic acid: inhibitors of protein phosphatase activity.', *Biochemical and Biophysical Research Communications*, 159(3), pp. 871–7. doi: 10.1016/0006-291X(89)92189-X.
- Ito, A. *et al.* (2000) 'A truncated isoform of the PP2A B56 subunit promotes cell motility through paxillin phosphorylation', *EMBO Journal*. EMBO Press, 19(4), pp. 562–571. doi: 10.1093/emboj/19.4.562.

- Ito, A. *et al.* (2003) 'Localization of the PP2A B56 γ regulatory subunit at the Golgi complex: Possible role in vesicle transport and migration', *American Journal of Pathology*, 162(2), pp. 479–489. doi: 10.1016/S0002-9440(10)63842-4.
- James, A. M. *et al.* (2016) 'A Unifying Mechanism for Mitochondrial Superoxide Production during Ischemia-Reperfusion Injury', *Cell Metabolism*. Elsevier, 23(2), pp. 254–263. doi: 10.1016/j.cmet.2015.12.009.
- Janssens, V. *et al.* (2003) 'Identification and functional analysis of two Ca²⁺-binding EF-hand motifs in the B'/PR72 subunit of protein phosphatase 2a', *Journal of Biological Chemistry*, 278(12), pp. 10697–10706. doi: 10.1074/jbc.M211717200.
- Janssens, V. and Goris, J. (2001) 'Phosphatases Implicated in Cell Growth and Signalling', *Biochemical Journal*, 353(Pt 3), pp. 417–439.
- Jayaprakash, P. *et al.* (2015) 'Hsp90 α and Hsp90 β together operate a hypoxia and nutrient paucity stress-response mechanism during wound healing', *Journal of Cell Science*. The Company of Biologists Ltd, 128(8), pp. 1475–1480. doi: 10.1242/jcs.166363.
- Jennings, R. B. *et al.* (1960) 'Myocardial necrosis induced by temporary occlusion of a coronary artery in the dog.', *Archives of Pathology*, 70, pp. 68–78.
- Jennings, R. B. (2013) 'Historical perspective on the pathology of myocardial ischemia/reperfusion injury', *Circulation Research*, 113(4), pp. 428–438. doi: 10.1161/CIRCRESAHA.113.300987.
- Jennings, R. B., Reimer, K. A. and Steenbergen, C. (1986) 'Myocardial ischemia revisited. The osmolar load, membrane damage, and reperfusion', *Journal of Molecular and Cellular Cardiology*, 18(8), pp. 769–780. doi: 10.1016/S0022-2828(86)80952-X.
- Jennings, R. B., Reimer, K. A. and Steenbergen, C. (1991) 'Effect of inhibition of the mitochondrial ATPase on net myocardial ATP in total ischemia', *Journal of Molecular and Cellular Cardiology*, 23(12), pp. 1383–1395. doi: 10.1016/0022-2828(91)90185-O.
- Jiang, G. (2007) 'PI 3-kinase and its up- and down-stream modulators as potential targets for the treatment of type II diabetes', *Frontiers in Bioscience*, 7(1–3), p. d903. doi: 10.2741/jiang.
- De Jongh, K. S. *et al.* (1996) 'Specific phosphorylation of a site in the full-length form of the α 1 subunit of the cardiac L-type calcium channel by adenosine 3'-5'-cyclic monophosphate-dependent protein kinase', *Biochemistry*. American Chemical Society, 35(32), pp. 10392–10402. doi: 10.1021/bi953023c.
- Jordens, J. *et al.* (2006) 'The protein phosphatase 2A phosphatase activator is a novel peptidyl-prolyl cis/trans-isomerase', *Journal of Biological Chemistry*, 281(10), pp. 6349–6357. doi: 10.1074/jbc.M507760200.
- Juhaszova, M. *et al.* (2004) 'Glycogen synthase kinase-3 β mediates convergence of protection signalling to inhibit the mitochondrial permeability transition pore', *Journal of Clinical Investigation*. American Society for Clinical Investigation, 113(11), pp. 1535–1549. doi: 10.1172/JCI19906.

- Kaiser, R. A. *et al.* (2004) 'Targeted Inhibition of p38 Mitogen-activated Protein Kinase Antagonizes Cardiac Injury and Cell Death Following Ischemia-Reperfusion in Vivo', *Journal of Biological Chemistry*. American Society for Biochemistry and Molecular Biology, 279(15), pp. 15524–15530. doi: 10.1074/jbc.M313717200.
- Kamibayashi, C. *et al.* (1994) 'Comparison of Heterotrimeric Protein Phosphatase 2A Containing', *Biochemistry*, 269(31), pp. 20139–20148.
- Katayose, Y. *et al.* (2000) 'Protein phosphatase 2A inhibitors, I(PP2A)/1 and I(PP2A)/2, associate with and modify the substrate specificity of protein phosphatase 1', *Journal of Biological Chemistry*. American Society for Biochemistry and Molecular Biology, 275(13), pp. 9209–9214. doi: 10.1074/jbc.275.13.9209.
- Kaur, A. and Westermarck, J. (2016) 'Regulation of protein phosphatase 2A (PP2A) tumor suppressor function by PME-1', *Biochemical Society Transactions*. Portland Press Limited, 44(6), pp. 1683–1693. doi: 10.1042/bst20160161.
- Kaźmierczak-Barańska, J. *et al.* (2015) 'Downregulation of striatin leads to hyperphosphorylation of MAP2, induces depolymerization of microtubules and inhibits proliferation of HEK293T cells', *FEBS Letters*. No longer published by Elsevier, 589(2), pp. 222–230. doi: 10.1016/J.FEBSLET.2014.12.003.
- Keates, A. K. *et al.* (2017) 'Cardiovascular disease in Africa: Epidemiological profile and challenges', *Nature Reviews Cardiology*, 14(5), pp. 273–293. doi: 10.1038/nrcardio.2017.19.
- Khalid, U., Jneid, H. and Denktas, A. E. (2017) 'The relationship between total ischemic time and mortality in patients with STEMI: every second counts', *Cardiovascular Diagnosis and Therapy*. AME Publications, 7(S2), pp. S119–S124. doi: 10.21037/cdt.2017.05.10.
- Kharbanda, S. *et al.* (2000) 'Translocation of SAPK/JNK to mitochondria and interaction with Bcl-x(L) in response to DNA damage', *Journal of Biological Chemistry*, 275(1), pp. 322–327. doi: 10.1074/jbc.275.1.322.
- Khew-Goodall, Y. and Hemmings, B. A. (1988) 'Tissue-specific expression of mRNAs encoding alpha- and beta-catalytic subunits of protein phosphatase 2A.', *FEBS letters*, 238(2), pp. 265–8.
- Kiely, M. and Kiely, P. A. (2015) 'PP2A: The wolf in sheep's clothing?', *Cancers*, 7(2), pp. 648–669. doi: 10.3390/cancers7020648.
- Kim, J.-A. *et al.* (2002) 'Cytoskeleton disruption causes apoptotic degeneration of dentate granule cells in hippocampal slice cultures', *Neuropharmacology*. Pergamon, 42(8), pp. 1109–1118. doi: 10.1016/S0028-3908(02)00052-7.
- Kimura, T. *et al.* (2011) 'Protein phosphatase 2a interacts with the na⁺,k⁺-atpase and modulates its trafficking by inhibition of its association with arrestin', *PLoS ONE*. Edited by D. Holowka. Public Library of Science, 6(12), p. e29269. doi: 10.1371/journal.pone.0029269.
- Kincaid, B. and Bossy-Wetzel, E. (2013) 'Forever young: SIRT3 a shield against mitochondrial meltdown, aging, and neurodegeneration', *Frontiers in Aging Neuroscience*. Frontiers, 5, p. 48. doi: 10.3389/fnagi.2013.00048.
- Kinexus Bioinformatics Corporation (2017) *Kinexus | PhosphoNET*. Available at: <http://www.phosphonet.ca/> (Accessed: 22 April 2019).

- Kirchhefer, U. *et al.* (2014) 'Protein phosphatase 2A is regulated by protein kinase Ca (PKCa)-dependent phosphorylation of its targeting subunit B56 α at Ser⁴¹', *Journal of Biological Chemistry*, 289(1), pp. 163–176. doi: 10.1074/jbc.M113.507996.
- Kloner, R. A., Ganote, C. E. and Jennings, R. B. (1974) 'The "no reflow" phenomenon after temporary coronary occlusion in the dog', *Journal of Clinical Investigation*. American Society for Clinical Investigation, 54(6), pp. 1496–1508. doi: 10.1172/JCI107898.
- Kong, M. *et al.* (2009) ' α 4 Is an Essential Regulator of PP2A Phosphatase Activity', *Molecular Cell*. Elsevier, 36(1), pp. 51–60. doi: 10.1016/j.molcel.2009.09.025.
- Kono, Y. *et al.* (2002) 'MCM3-binding GANP DNA-primase is associated with a novel phosphatase component G5PR', *Genes to Cells*. John Wiley & Sons, Ltd (10.1111), 7(8), pp. 821–834. doi: 10.1046/j.1365-2443.2002.00562.x.
- Kostetskii, I. *et al.* (2005) 'Induced Deletion of the *N-Cadherin* Gene in the Heart Leads to Dissolution of the Intercalated Disc Structure', *Circulation Research*, 96(3), pp. 346–354. doi: 10.1161/01.RES.0000156274.72390.2c.
- Kötter, S. *et al.* (2016) 'Titin-Based Cardiac Myocyte Stiffening Contributes to Early Adaptive Ventricular Remodeling after Myocardial Infarction', *Circulation Research*, 119(9), pp. 1017–1029. doi: 10.1161/CIRCRESAHA.116.309685.
- Kovács, Á. *et al.* (2016) 'Renin overexpression leads to increased titin-based stiffness contributing to diastolic dysfunction in hypertensive mRen2 rats', *American Journal of Physiology - Heart and Circulatory Physiology*. American Physiological Society Bethesda, MD, 310(11), pp. H1671–H1682. doi: 10.1152/ajpheart.00842.2015.
- Krebs, E. G. and Fischer, E. H. (2003) 'The phosphorylase b to a converting enzyme of rabbit skeletal muscle', *Biochimica et Biophysica Acta*. Elsevier, 20, pp. 150–157. doi: 10.1016/0006-3002(56)90273-6.
- Kremmer, E. *et al.* (1997) 'Separation of PP2A core enzyme and holoenzyme with monoclonal antibodies against the regulatory A subunit: abundant expression of both forms in cells.', *Molecular and Cellular Biology*, 17(3), pp. 1692–701. doi: 10.1128/mcb.17.3.1692.
- Krüger, M. *et al.* (2009) 'Protein Kinase G Modulates Human Myocardial Passive Stiffness by Phosphorylation of the Titin Springs', *Circulation Research*, 104(1), pp. 87–94. doi: 10.1161/CIRCRESAHA.108.184408.
- Krysiak, J. *et al.* (2018) 'Protein phosphatase 5 regulates titin phosphorylation and function at a sarcomere-associated mechanosensor complex in cardiomyocytes', *Nature Communications*. Nature Publishing Group, 9(1), p. 262. doi: 10.1038/s41467-017-02483-3.
- Kupatt, C. *et al.* (2004) 'Heat Shock Protein 90 Transfection Reduces Ischemia-Reperfusion-Induced Myocardial Dysfunction via Reciprocal Endothelial NO Synthase Serine 1177 Phosphorylation and Threonine 495 Dephosphorylation', *Arteriosclerosis, Thrombosis, and Vascular Biology*, 24(8), pp. 1435–1441. doi: 10.1161/01.ATV.0000134300.87476.d1.
- Kusuoka, H. *et al.* (1987) 'Pathophysiology and pathogenesis of stunned myocardium. Depressed Ca²⁺ activation of contraction as a consequence of reperfusion-induced cellular calcium overload in ferret hearts.', *Journal of Clinical Investigation*, 79(3), pp. 950–961. doi: 10.1172/JCI112906.

- Lacerda, L. *et al.* (2009) 'Ischaemic postconditioning protects against reperfusion injury via the SAFE pathway', *Cardiovascular Research*, 84(2), pp. 201–208. doi: 10.1093/cvr/cvp274.
- Ladner, C. L. *et al.* (2004) 'Visible fluorescent detection of proteins in polyacrylamide gels without staining', *Analytical Biochemistry*, 326(1), pp. 13–20. doi: 10.1016/j.ab.2003.10.047.
- Lahav-Ariel, L. *et al.* (2019) 'Striatin is a novel modulator of cell adhesion', *The FASEB Journal*. Federation of American Societies for Experimental Biology Bethesda, MD, USA, 33(4), pp. 4729–4740. doi: 10.1096/fj.201801882R.
- Landstrom, A. P. *et al.* (2007) 'Mutations in JPH2-encoded junctophilin-2 associated with hypertrophic cardiomyopathy in humans', *Journal of Molecular and Cellular Cardiology*, 42(6), pp. 1026–1035. doi: 10.1016/j.yjmcc.2007.04.006.
- Lavin, M. F. and Gueven, N. (2006) 'The complexity of p53 stabilization and activation', *Cell Death and Differentiation*, 13(6), pp. 941–950. doi: 10.1038/sj.cdd.4401925.
- Lecuona, E. *et al.* (2006) 'Na,K-ATPase α 1-subunit dephosphorylation by protein phosphatase 2A is necessary for its recruitment to the plasma membrane', *The FASEB Journal*, 20(14), pp. 2618–2620. doi: 10.1096/fj.06-6503fje.
- Lee, J. *et al.* (2002) 'A specific protein carboxyl methyltransferase that demethylates phosphoprotein phosphatase 2A in bovine brain.', *Proceedings of the National Academy of Sciences*. National Academy of Sciences, 99(12), pp. 6043–6047. doi: 10.1073/pnas.93.12.6043.
- Lee, J. and Stock, J. (1993) 'Protein phosphatase 2A catalytic subunit is methyl-esterified at its carboxyl terminus by a novel methyltransferase', *Journal of Biological Chemistry*, 268(26), pp. 19192–19195.
- Lee, T. S. *et al.* (2006) 'Calmodulin kinase II is involved in voltage-dependent facilitation of the L-type Cav1.2 calcium channel: Identification of the phosphorylation sites', *Journal of Biological Chemistry*, 281(35), pp. 25560–25567. doi: 10.1074/jbc.M508661200.
- Leistner, M. *et al.* (2019) 'Ischemia time impacts on respiratory chain functions and Ca²⁺-handling of cardiac subsarcolemmal mitochondria subjected to ischemia reperfusion injury', *Journal of Cardiothoracic Surgery*. BioMed Central, 14(1), p. 92. doi: 10.1186/s13019-019-0911-1.
- Lemasters, J. J. *et al.* (1996) 'The pH paradox in ischemia-reperfusion injury to cardiac myocytes.', *EXS*, pp. 99–114.
- Lemke, T. *et al.* (2008) 'Unchanged β -adrenergic stimulation of cardiac L-type calcium channels in Cav1.2 phosphorylation site S1928A mutant mice', *Journal of Biological Chemistry*, 283(50), pp. 34738–34744. doi: 10.1074/jbc.M804981200.
- Li, J. *et al.* (1997) 'PTEN, a putative protein tyrosine phosphatase gene mutated in human brain, breast, and prostate cancer', *Science*, 275(5308), pp. 1943–1947. doi: 10.1126/science.275.5308.1943.
- Li, L. *et al.* (2018) 'Microtubule associated protein 4 phosphorylation leads to pathological cardiac remodeling in mice', *EBioMedicine*. Elsevier, 37, pp. 221–235. doi: 10.1016/j.ebiom.2018.10.017.
- Li, L. *et al.* (2019) 'Cardiac proteomics reveals the potential mechanism of microtubule associated protein 4 phosphorylation-induced mitochondrial dysfunction', *Burns & Trauma*. BioMed Central, 7(1), p. 8. doi: 10.1186/s41038-019-0146-3.

- Li, T. *et al.* (2012) 'Microcystin-Lr induces ceramide to regulate PP2A and destabilize cytoskeleton in HEK293 cells', *Toxicological Sciences*. Narnia, 128(1), pp. 147–157. doi: 10.1093/toxsci/kfs141.
- Li, T. *et al.* (2017) 'Defective Branched-Chain Amino Acid Catabolism Disrupts Glucose Metabolism and Sensitizes the Heart to Ischemia-Reperfusion Injury', *Cell Metabolism*. Cell Press, 25(2), pp. 374–385. doi: 10.1016/j.cmet.2016.11.005.
- Liem, D. A. (2004) 'The Tyrosine Phosphatase Inhibitor Bis(Maltolato)Oxovanadium Attenuates Myocardial Reperfusion Injury by Opening ATP-Sensitive Potassium Channels', *Journal of Pharmacology and Experimental Therapeutics*, 309(3), pp. 1256–1262. doi: 10.1124/jpet.103.062547.
- Lin, S. S. *et al.* (2006) 'PP2A regulates BCL-2 phosphorylation and proteasome-mediated degradation at the endoplasmic reticulum', *Journal of Biological Chemistry*. American Society for Biochemistry and Molecular Biology, 281(32), pp. 23003–23012. doi: 10.1074/jbc.M602648200.
- Lindsey, M. L. *et al.* (2018) 'Guidelines for experimental models of myocardial ischemia and infarction', *American Journal of Physiology - Heart and Circulatory Physiology*. American Physiological Society, 314(4), pp. H812–H838. doi: 10.1152/ajpheart.00335.2017.
- Linke, W. A. (2008) 'Sense and stretchability: The role of titin and titin-associated proteins in myocardial stress-sensing and mechanical dysfunction', *Cardiovascular Research*. Narnia, pp. 637–648. doi: 10.1016/j.cardiores.2007.03.029.
- Linseman, D. A. (2004) 'Glycogen Synthase Kinase-3 Phosphorylates Bax and Promotes Its Mitochondrial Localization during Neuronal Apoptosis', *Journal of Neuroscience*, 24(44), pp. 9993–10002. doi: 10.1523/jneurosci.2057-04.2004.
- Liu, G. *et al.* (1991) 'Protection against infarction afforded by preconditioning is mediated by A1 adenosine receptors in rabbit heart.', *Circulation*, 81(1), pp. 350–365.
- Lochner, A., Genade, S. and Moolman, J. A. (2003) 'Ischemic preconditioning: Infarct size is a more reliable endpoint than functional recovery', *Basic Research in Cardiology*. Steinkopff-Verlag, 98(5), pp. 337–346. doi: 10.1007/s00395-003-0427-6.
- Long, Q., Yang, K. and Yang, Q. (2015) 'Regulation of mitochondrial ATP synthase in cardiac pathophysiology.', *American Journal of Cardiovascular Disease*. e-Century Publishing Corporation, 5(1), pp. 19–32.
- Longin, S. *et al.* (2004) 'An inactive protein phosphatase 2A population is associated with methylesterase and can be re-activated by the phosphotyrosyl phosphatase activator', *Biochemical Journal*, 380(1), pp. 111–119. doi: 10.1042/bj20031643.
- Longin, S. *et al.* (2007) 'Selection of protein phosphatase 2A regulatory subunits is mediated by the C terminus of the catalytic subunit', *Journal of Biological Chemistry*. American Society for Biochemistry and Molecular Biology, 282(37), pp. 26971–26980. doi: 10.1074/jbc.M704059200.
- Longin, S. *et al.* (2008) 'Spatial control of protein phosphatase 2A (de)methylation', *Experimental Cell Research*. Academic Press, 314(1), pp. 68–81. doi: 10.1016/j.yexcr.2007.07.030.
- Lopaschuk, G. D. *et al.* (2010) 'Myocardial Fatty Acid Metabolism in Health and Disease', *Physiological Reviews*, 90(1), pp. 207–258. doi: 10.1152/physrev.00015.2009.

- Lopaschuk, G. D. (2016) 'Metabolic changes in the acutely ischemic heart', *Heart and Metabolism*, 70(70), pp. 32–35.
- Lu, G. *et al.* (2007) 'A novel mitochondrial matrix serine/threonine protein phosphatase regulates the mitochondria permeability transition pore and is essential for cellular survival and development', *Genes and Development*, 21(7), pp. 784–796. doi: 10.1101/gad.1499107.
- Lu, G. *et al.* (2009) 'Protein phosphatase 2Cm is a critical regulator of branched-chain amino acid catabolism in mice and cultured cells', *Journal of Clinical Investigation*. American Society for Clinical Investigation, 119(6), pp. 1678–1687. doi: 10.1172/JCI38151.
- Lu, G. and Wang, Y. (2008) 'Functional diversity of mammalian type 2C protein phosphatase isoforms: New tales from an old family', *Clinical and Experimental Pharmacology and Physiology*. John Wiley & Sons, Ltd (10.1111), 35(2), pp. 107–112. doi: 10.1111/j.1440-1681.2007.04843.x.
- Lu, Q. *et al.* (2004) 'Striatin assembles a membrane signaling complex necessary for rapid, nongenomic activation of endothelial NO synthase by estrogen receptor α ', *Proceedings of the National Academy of Sciences of the United States of America*, 101(49), pp. 17126–17131. doi: 10.1073/pnas.0407492101.
- Lundby, A. *et al.* (2013) 'In vivo phosphoproteomics analysis reveals the cardiac targets of β -adrenergic receptor signaling', *Science Signaling*, 6(278), pp. rs11–rs11. doi: 10.1126/scisignal.2003506.
- Luo, M. and Anderson, M. E. (2013) 'Mechanisms of altered Ca²⁺ handling in heart failure', *Circulation Research*, 113(6), pp. 690–708. doi: 10.1161/CIRCRESAHA.113.301651.
- Luo, Y. *et al.* (2013) 'PTPA activates protein phosphatase-2A through reducing its phosphorylation at tyrosine-307 with upregulation of protein tyrosine phosphatase 1B', *Biochimica et Biophysica Acta - Molecular Cell Research*. Elsevier, 1833(5), pp. 1235–1243. doi: 10.1016/j.bbamcr.2013.02.005.
- Lüss, H. *et al.* (2000) 'Regional expression of protein phosphatase type 1 and 2A catalytic subunit isoforms in the human heart', *Journal of Molecular and Cellular Cardiology*, 32(12), pp. 2349–2359. doi: 10.1006/jmcc.2000.1265.
- Macdougall, L. K., Jones, L. R. and Cohen, P. (1991) 'Identification of the major protein phosphatases in mammalian cardiac muscle which dephosphorylate phospholamban', *European Journal of Biochemistry*, 196(3), pp. 725–734. doi: 10.1111/j.1432-1033.1991.tb15871.x.
- Mæhre, H. K. *et al.* (2018) 'Protein determination—method matters', *Foods*, 7(1). doi: 10.3390/foods7010005.
- Magenta, A. *et al.* (2008) 'Protein Phosphatase 2A Subunit PR70 Interacts with pRb and Mediates Its Dephosphorylation', *Molecular and Cellular Biology*, 28(2), pp. 873–882. doi: 10.1128/MCB.00480-07.
- Manning, G. *et al.* (2002) 'The protein kinase complement of the human genome.', *Science (New York, N.Y.)*. American Association for the Advancement of Science, 298(5600), pp. 1912–34. doi: 10.1126/science.1075762.
- Marais, E. *et al.* (2005) 'The temporal relationship between p38 MAPK and HSP27 activation in ischaemic and pharmacological preconditioning', *Basic Research in Cardiology*. Steinkopff-Verlag, 100(1), pp. 35–47. doi: 10.1007/s00395-004-0495-7.

- Martin, L. *et al.* (2013) 'Tau protein phosphatases in Alzheimer's disease: The leading role of PP2A', *Ageing Research Reviews*, 12(1), pp. 39–49. doi: 10.1016/j.arr.2012.06.008.
- Martindale, J. J. and Metzger, J. M. (2014) 'Uncoupling of increased cellular oxidative stress and myocardial ischemia reperfusion injury by directed sarcolemma stabilization', *Journal of Molecular and Cellular Cardiology*. Elsevier, 67, pp. 26–37. doi: 10.1016/j.yjmcc.2013.12.008.
- Marx, S. O. *et al.* (2000) 'PKA phosphorylation dissociates FKBP12.6 from the calcium release channel (ryanodine receptor): defective regulation in failing hearts.', *Cell*, 101(4), pp. 365–76.
- Matoshvili, Z. and Kipshidze, N. (2014) 'Management of Reperfusion Arrhythmias', in *Urgent Interventional Therapies*. Chichester, UK: John Wiley & Sons, Ltd, pp. 187–191. doi: 10.1002/9781118504499.ch22.
- Matsubara, T. *et al.* (1995) 'Protective effect of vanadate on oxyradical-induced changes in isolated perfused heart', *Molecular and Cellular Biochemistry*, 153(1–2), pp. 79–85. doi: 10.1007/BF01075921.
- Matsushima, S., Tsutsui, H. and Sadoshima, J. (2014) 'Physiological and pathological functions of NADPH oxidases during myocardial ischemia-reperfusion', *Trends in Cardiovascular Medicine*, 24(5), pp. 202–205. doi: 10.1016/j.tcm.2014.03.003.
- Matsushita, Y. *et al.* (2007) 'Mutation of junctophilin type 2 associated with hypertrophic cardiomyopathy', *Journal of Human Genetics*, 52(6), pp. 543–548. doi: 10.1007/s10038-007-0149-Y.
- Mayer, R. E. *et al.* (1991) 'Structure of the 55-kDa regulatory subunit of protein phosphatase 2A: evidence for a neuronal-specific isoform.', *Biochemistry*, 30(15), pp. 3589–97.
- McCole, D. F. (2013) 'Phosphatase regulation of intercellular junctions', *Tissue Barriers*. Taylor & Francis, p. e26713. doi: 10.4161/tisb.26713.
- McConnell, J. L. *et al.* (2007) 'Identification of a PP2A-interacting protein that functions as a negative regulator of phosphatase activity in the ATM/ATR signaling pathway', *Oncogene*, 26(41), pp. 6021–6030. doi: 10.1038/sj.onc.1210406.
- McConnell, J. L. *et al.* (2010) 'Alpha4 is a ubiquitin-binding protein that regulates protein serine/threonine phosphatase 2A ubiquitination', *Biochemistry*. NIH Public Access, 49(8), pp. 1713–1718. doi: 10.1021/bi901837h.
- McCright, B. *et al.* (1996) 'The B56 family of protein phosphatase 2A (PP2A) regulatory subunits encodes differentiation-induced phosphoproteins that target PP2A to both nucleus and cytoplasm', *Journal of Biological Chemistry*. American Society for Biochemistry and Molecular Biology, 271(36), pp. 22081–22089. doi: 10.1074/jbc.271.36.22081.
- Meng, G. *et al.* (2011) 'Microcystin-LR induces cytoskeleton system reorganization through hyperphosphorylation of tau and HSP27 via PP2A inhibition and subsequent activation of the p38 MAPK signaling pathway in neuroendocrine (PC12) cells', *Toxicology*. Elsevier, 290(2–3), pp. 218–229. doi: 10.1016/J.TOX.2011.09.085.

- Merrill, R. A., Slupe, A. M. and Strack, S. (2013) 'N-terminal phosphorylation of protein phosphatase 2A/B β 2 regulates translocation to mitochondria, dynamin-related protein 1 dephosphorylation, and neuronal survival.', *The FEBS journal*. NIH Public Access, 280(2), pp. 662–73. doi: 10.1111/j.1742-4658.2012.08631.x.
- Mertins, P. *et al.* (2014) 'Ischemia in tumors induces early and sustained phosphorylation changes in stress kinase pathways but does not affect global protein levels', *Molecular and Cellular Proteomics*, 13(7), pp. 1690–1704. doi: 10.1074/mcp.M113.036392.
- Meurs, K. M. *et al.* (2013) 'Association of dilated cardiomyopathy with the striatin mutation genotype in boxer dogs', *Journal of Veterinary Internal Medicine*. John Wiley & Sons, Ltd (10.1111), 27(6), pp. 1437–1440. doi: 10.1111/jvim.12163.
- Mewton, N. *et al.* (2013) 'Postconditioning attenuates no-reflow in STEMI patients', *Basic Research in Cardiology*. Springer Berlin Heidelberg, 108(6), p. 383. doi: 10.1007/s00395-013-0383-8.
- Mimnaugh, E. G. *et al.* (1995) 'Possible Role for Serine/Threonine Phosphorylation in the Regulation of the Heteroprotein Complex between the hsp90 Stress Protein and the pp60v-src Tyrosine Kinase', *Journal of Biological Chemistry*, 270(48), pp. 28654–28659. doi: 10.1074/jbc.270.48.28654.
- Min, J. *et al.* (2013) 'Phosphorylation of β subunit in F₁F₀ ATP synthase is associated with increased iron uptake in iron-overloaded heart mitochondria', *Animal Cells and Systems*. Taylor & Francis, 17(6), pp. 406–412. doi: 10.1080/19768354.2013.867901.
- Minella, A. C. *et al.* (2008) 'Cyclin E phosphorylation regulates cell proliferation in hematopoietic and epithelial lineages in vivo', *Genes and Development*, 22(12), pp. 1677–1689. doi: 10.1101/gad.1650208.
- Miyamoto, S. *et al.* (2010) 'PHLPP-1 negatively regulates Akt activity and survival in the heart', *Circulation Research*. Lippincott Williams & Wilkins Hagerstown, MD, 107(4), pp. 476–484. doi: 10.1161/CIRCRESAHA.109.215020.
- Miyamoto, S., Murphy, A. N. and Brown, J. H. (2008) 'Akt mediates mitochondrial protection in cardiomyocytes through phosphorylation of mitochondrial hexokinase-II', *Cell Death and Differentiation*, 15(3), pp. 521–529. doi: 10.1038/sj.cdd.4402285.
- Mochida, S. *et al.* (2009) 'Regulated activity of PP2A-B55 is crucial for controlling entry into and exit from mitosis in Xenopus egg extracts', *EMBO Journal*, 28(18), pp. 2777–2785. doi: 10.1038/emboj.2009.238.
- Mockridge, J. W., Marber, M. S. and Heads, R. J. (2000) 'Activation of Akt during Simulated Ischemia/Reperfusion in Cardiac Myocytes', *Biochemical and Biophysical Research Communications*, 270(3), pp. 947–952. doi: 10.1006/bbrc.2000.2522.
- Mohamed, B. A. *et al.* (2016) 'Molecular and structural transition mechanisms in long-term volume overload', *European Journal of Heart Failure*, 18(4), pp. 362–371. doi: 10.1002/ejhf.465.
- Mollapour, M. and Neckers, L. (2012) 'Post-translational modifications of Hsp90 and their contributions to chaperone regulation', *Biochimica et Biophysica Acta - Molecular Cell Research*. NIH Public Access, pp. 648–655. doi: 10.1016/j.bbamcr.2011.07.018.

- Moreno, C. S. *et al.* (2000) 'WD40 repeat proteins striatin and S/G(2) nuclear autoantigen are members of a novel family of calmodulin-binding proteins that associate with protein phosphatase 2A.', *The Journal of Biological Chemistry*. NIH Public Access, 275(8), pp. 5257–63.
- Moreno, C. S., Lane, W. S. and Pallas, D. C. (2001) 'A Mammalian Homolog of Yeast MOB1 is Both a Member and a Putative Substrate of Striatin Family-Protein Phosphatase 2A Complexes', *Journal of Biological Chemistry*, 276(26), pp. 24253–24260. doi: 10.1074/jbc.M102398200.
- Morioka, M. *et al.* (1998) 'Serine/Threonine phosphatase activity of calcineurin is inhibited by sodium orthovanadate and dithiothreitol reverses the inhibitory effect', *Biochemical and Biophysical Research Communications*, 253(2), pp. 342–345. doi: 10.1006/bbrc.1998.9783.
- Morishima, I. *et al.* (2000) 'Angiographic no-reflow phenomenon as a predictor of adverse long-term outcome in patients treated with percutaneous transluminal coronary angioplasty for first acute myocardial infarction', *Journal of the American College of Cardiology*. Elsevier, 36(4), pp. 1202–1209. doi: 10.1016/S0735-1097(00)00865-2.
- Morton, J. ., Barnes, M. . and Zyskowski, R. . (1996) 'Respiratory Control Ratio: A Computer Simulation of Oxidative Phosphorylation', *Biochemical Education*, 24(2), pp. 110–111.
- Mourtada-Maarabouni, M. and Williams, G. T. (2008) 'Protein phosphatase 4 regulates apoptosis, proliferation and mutation rate of human cells', *Biochimica et Biophysica Acta - Molecular Cell Research*. Elsevier, 1783(8), pp. 1490–1502. doi: 10.1016/j.bbamcr.2008.03.005.
- Mumby, M. C. *et al.* (1987) 'Cardiac contractile protein phosphatases. Purification of two enzyme forms and their characterization with subunit-specific antibodies.', *Journal of Biological Chemistry*, 262(13), pp. 6257–6265.
- Munton, R. P. *et al.* (2007) 'Qualitative and quantitative analyses of protein phosphorylation in naive and stimulated mouse synaptosomal preparations', *Molecular and Cellular Proteomics*. American Society for Biochemistry and Molecular Biology, 6(2), pp. 283–293. doi: 10.1074/mcp.M600046-MCP200.
- Murata, K., Wu, J. and Brautigan, D. L. (2002) 'B cell receptor-associated protein 4 displays rapamycin-sensitive binding directly to the catalytic subunit of protein phosphatase 2A', *Proceedings of the National Academy of Sciences*, 94(20), pp. 10624–10629. doi: 10.1073/pnas.94.20.10624.
- Murphy, E. and Steenbergen, C. (2008) 'Mechanisms Underlying Acute Protection From Cardiac Ischemia-Reperfusion Injury', *Physiological Reviews*. NIH Public Access, 88(2), pp. 581–609. doi: 10.1152/physrev.00024.2007.
- Murry, C. E., Jennings, R. B. and Reimer, K. A. (1986) 'Preconditioning with ischemia: a delay of lethal cell injury in ischemic myocardium.', *Circulation*, 74(5), pp. 1124–36.
- Nader, M. *et al.* (2017) 'Cardiac striatin interacts with caveolin-3 and calmodulin in a calcium sensitive manner and regulates cardiomyocyte spontaneous contraction rate', *Canadian Journal of Physiology and Pharmacology*, 95(10), pp. 1306–1312. doi: 10.1139/cjpp-2017-0155.
- Naghavi, M. *et al.* (2017) 'Global, regional, and national age-sex specific mortality for 264 causes of death, 1980-2016: A systematic analysis for the Global Burden of Disease Study 2016', *The Lancet*. Elsevier, 390(10100), pp. 1151–1210. doi: 10.1016/S0140-6736(17)32152-9.

- Namboodiripad, A. N. and Jennings, M. L. (2017) 'Permeability characteristics of erythrocyte membrane to okadaic acid and calyculin A', *American Journal of Physiology-Cell Physiology*, 270(2), pp. C449–C456. doi: 10.1152/ajpcell.1996.270.2.c449.
- Neely, J. R. *et al.* (1973) 'Effects of ischemia on function and metabolism of the isolated working rat heart', *American Journal of Physiology*, 225(3), pp. 651–658. doi: 10.1152/ajplegacy.1973.225.3.651.
- Neely, J. R. and Morgan, H. E. (2003) 'Relationship Between Carbohydrate and Lipid Metabolism and the Energy Balance of Heart Muscle', *Annual Review of Physiology*, 36(1), pp. 413–459. doi: 10.1146/annurev.ph.36.030174.002213.
- Niccoli, G. *et al.* (2013) 'Patients with microvascular obstruction after primary percutaneous coronary intervention show a gp91phox (NOX2) mediated persistent oxidative stress after reperfusion', *European Heart Journal: Acute Cardiovascular Care*. SAGE Publications, 2(4), pp. 379–388. doi: 10.1177/2048872613504698.
- Niemi, N. M. and MacKeigan, J. P. (2012) 'Mitochondrial Phosphorylation in Apoptosis: Flipping the Death Switch', *Antioxidants & Redox Signaling*. Mary Ann Liebert, Inc., 19(6), pp. 572–582. doi: 10.1089/ars.2012.4982.
- Niki, T. *et al.* (2012) 'Function of dj-1 in mitochondria', *Yakugaku Zasshi*, 132(10), pp. 1105–1110. doi: 10.1248/yakushi.12-00220-3.
- Nilsson, M. I. *et al.* (2013) 'Xin Is a Marker of Skeletal Muscle Damage Severity in Myopathies', *The American Journal of Pathology*. Elsevier, 183(6), pp. 1703–1709. doi: 10.1016/J.AJP.2013.08.010.
- Noda, K. *et al.* (1993) 'Role of locally formed angiotensin II and bradykinin in the reduction of myocardial infarct size in dogs', *Cardiovascular Research*. Narnia, 27(2), pp. 334–340. doi: 10.1093/cvr/27.2.334.
- Nunbhakdi-Craig, V. *et al.* (2007) 'Expression of protein phosphatase 2A mutants and silencing of the regulatory B α subunit induce a selective loss of acetylated and detyrosinated microtubules', *Journal of Neurochemistry*, 101(4), pp. 959–971. doi: 10.1111/j.1471-4159.2007.04503.x.
- Ogris, E. *et al.* (1999) 'A protein phosphatase methylesterase (PME-1) is one of several novel proteins stably associating with two inactive mutants of protein phosphatase 2A', *Journal of Biological Chemistry*, 274(20), pp. 14382–14391. doi: 10.1074/jbc.274.20.14382.
- Ogris, E., Gibson, D. M. and Pallas, D. C. (1997) 'Protein phosphatase 2A subunit assembly: The catalytic subunit carboxy terminus is important for binding cellular B subunit but not polyomavirus middle tumor antigen', *Oncogene*, 15(8), pp. 911–917. doi: 10.1038/sj.onc.1201259.
- Olsen, J. V. *et al.* (2006) 'Global, In Vivo, and Site-Specific Phosphorylation Dynamics in Signaling Networks', *Cell*, 127(3), pp. 635–648. doi: 10.1016/j.cell.2006.09.026.
- Onen, C. L. (2013) 'Epidemiology of ischaemic heart disease in sub-Saharan Africa : review article', *Cardiovascular Journal Of Africa*. Clinics Cardive Publishing (Pty) Ltd., 24(2), pp. 34–42. doi: 10.5830/CVJA-2012-071.
- Orchard, C. and Brette, F. (2008) 't-tubules and sarcoplasmic reticulum function in cardiac ventricular myocytes', *Cardiovascular Research*, 77(2), pp. 237–244. doi: 10.1093/cvr/cvm002.

- Orchard, C. H. and Kentish, J. C. (2017) 'Effects of changes of pH on the contractile function of cardiac muscle', *American Journal of Physiology-Cell Physiology*, 258(6), pp. C967–C981. doi: 10.1152/ajpcell.1990.258.6.c967.
- Ortega-Gutiérrez, S. *et al.* (2008) 'Targeted disruption of the PME-1 gene causes loss of demethylated PP2A and perinatal lethality in mice', *PLoS ONE*. Edited by N. Gay, 3(7), p. e2486. doi: 10.1371/journal.pone.0002486.
- Orth, K. *et al.* (1996) 'Molecular ordering of apoptotic mammalian CED-3/ICE-like proteases', *Journal of Biological Chemistry*. American Society for Biochemistry and Molecular Biology, 271(35), pp. 20977–20980. doi: 10.1074/jbc.271.35.20977.
- Paradies, G. *et al.* (2004) 'Decrease in Mitochondrial Complex I Activity in Ischemic/Reperfused Rat Heart: Involvement of Reactive Oxygen Species and Cardiolipin', *Circulation Research*, 94(1), pp. 53–59. doi: 10.1161/01.RES.0000109416.56608.64.
- Park, J. L. and Lucchesi, B. R. (1999) 'Mechanisms of myocardial reperfusion injury', in *Annals of Thoracic Surgery*, pp. 1905–1912. doi: 10.1016/S0003-4975(99)01073-5.
- Parks, D. A. and Granger, D. N. (2017) 'Contributions of ischemia and reperfusion to mucosal lesion formation', *American Journal of Physiology-Gastrointestinal and Liver Physiology*, 250(6), pp. G749–G753. doi: 10.1152/ajpgi.1986.250.6.g749.
- Pattingre, S. *et al.* (2005) 'Bcl-2 antiapoptotic proteins inhibit Beclin 1-dependent autophagy', *Cell*, 122(6), pp. 927–939. doi: 10.1016/j.cell.2005.07.002.
- Perkin, J. *et al.* (2015) 'Phosphorylating Titin's Cardiac N2B Element by ERK2 or CaMKII δ Lowers the Single Molecule and Cardiac Muscle Force', *Biophysical Journal*. Cell Press, 109(12), pp. 2592–2601. doi: 10.1016/J.BPJ.2015.11.002.
- Peters, N. S. *et al.* (1993) 'Reduced content of connexin43 gap junctions in ventricular myocardium from hypertrophied and ischemic human hearts.', *Circulation*, 88(3), pp. 864–75. doi: 10.1161/01.cir.88.3.864.
- Petronilli, V. *et al.* (1994) 'Regulation of the permeability transition pore, a voltage-dependent mitochondrial channel inhibited by cyclosporin A', *BBA - Bioenergetics*. Elsevier, 1187(2), pp. 255–259. doi: 10.1016/0005-2728(94)90122-8.
- Pfeffer, M. (1995) 'Ventricular Remodeling After Acute Myocardial Infarction', *Annual Review of Medicine*, 46(1), pp. 455–466. doi: 10.1146/annurev.med.46.1.455.
- Physiol, A. J. *et al.* (2013) 'Bradykinin induces mitochondrial ROS generation via NO , cGMP , PKG , and mitoK ATP channel opening and leads to cardioprotection Bradykinin induces mitochondrial ROS generation via NO , cGMP , PKG , and mitoK ATP channel opening and leads to cardioprotec', *American Journal of Physiology, Heart and Circulatory Physiology*, 36688(September 2003), pp. 468–476. doi: 10.1152/ajpheart.00360.2003.
- Piper, H. M., García-Dorado, D. and Ovize, M. (1998) 'A fresh look at reperfusion injury', *Cardiovascular Research*, pp. 291–300. doi: 10.1016/S0008-6363(98)00033-9.
- Plácido, A. I. *et al.* (2017) 'Phosphatase 2A Inhibition Affects Endoplasmic Reticulum and Mitochondria Homeostasis Via Cytoskeletal Alterations in Brain Endothelial Cells', *Molecular Neurobiology*, 54(1), pp. 154–168. doi: 10.1007/s12035-015-9640-1.

- Pojoga, L. H. *et al.* (2012) 'Activation of the mineralocorticoid receptor increases striatin levels', *American Journal of Hypertension*. NIH Public Access, 25(2), pp. 243–249. doi: 10.1038/ajh.2011.197.
- Polverini, P. J. (2011) 'Role of the macrophage in angiogenesis-dependent diseases', *EXS*, 79, pp. 11–28. doi: 10.1007/978-3-0348-9006-9_2.
- Porter, A. G. and Jänicke, R. U. (1999) 'Emerging roles of caspase-3 in apoptosis', *Cell Death and Differentiation*. Nature Publishing Group, 6(2), pp. 99–104. doi: 10.1038/sj.cdd.4400476.
- Price, N. E. and Mumby, M. C. (2000) 'Effects of regulatory subunits on the kinetics of protein phosphatase 2A.', *Biochemistry*, 39(37), pp. 11312–8.
- Prickett, T. D. and Brautigan, D. L. (2007) 'Cytokine Activation of p38 Mitogen-Activated Protein Kinase and Apoptosis Is Opposed by alpha-4 Targeting of Protein Phosphatase 2A for Site-Specific Dephosphorylation of MEK3', *Molecular and Cellular Biology*, 27(12), pp. 4217–4227. doi: 10.1128/mcb.00067-07.
- Przyklenk, K. *et al.* (1993) 'Regional ischemic "preconditioning" protects remote virgin myocardium from subsequent sustained coronary occlusion.', *Circulation*, 87(3), pp. 893–9. doi: 10.1161/01.cir.87.3.893.
- Puhl, S.-L. and Steffens, S. (2019) 'Neutrophils in Post-myocardial Infarction Inflammation: Damage vs. Resolution?', *Frontiers in Cardiovascular Medicine*. Frontiers, 6, p. 25. doi: 10.3389/fcvm.2019.00025.
- Quanz, M. *et al.* (2012) 'Heat Shock Protein 90α (Hsp90α) Is Phosphorylated in Response to DNA Damage and Accumulates in Repair Foci', *Journal of Biological Chemistry*, 287(12), pp. 8803–8815. doi: 10.1074/jbc.M111.320887.
- Raedschelders, K., Ansley, D. M. and Chen, D. D. Y. (2012) 'The cellular and molecular origin of reactive oxygen species generation during myocardial ischemia and reperfusion', *Pharmacology & Therapeutics*. Pergamon, 133(2), pp. 230–255. doi: 10.1016/J.PHARMTHERA.2011.11.004.
- Ramos, I. T. *et al.* (2018) 'Simultaneous Assessment of Cardiac Inflammation and Extracellular Matrix Remodeling after Myocardial Infarction', *Circulation. Cardiovascular imaging*. Lippincott Williams & Wilkins/Hagerstown, MD, 11(11). doi: 10.1161/CIRCIMAGING.117.007453.
- Ranek, M. J. *et al.* (2018) 'The role of heat shock proteins and co-chaperones in heart failure', *Philosophical Transactions of the Royal Society B: Biological Sciences*. The Royal Society, 373(1738), p. 20160530. doi: 10.1098/rstb.2016.0530.
- El Refaey, M. *et al.* (2019) 'Protein Phosphatase 2A Regulates Cardiac Na⁺ Channels', *Circulation Research*. Lippincott Williams & Wilkins/Hagerstown, MD, 124(5), pp. 737–746. doi: 10.1161/circresaha.118.314350.
- Reimer, K. A. *et al.* (1977) 'The wavefront phenomenon of ischemic cell death. 1. Myocardial infarct size vs duration of coronary occlusion in dogs.', *Circulation*, 56(5), pp. 786–94.
- Reimer, K. A. and Jennings, R. B. (1979) 'The "wavefront phenomenon" of myocardial ischemic cell death. II. Transmural progression of necrosis within the framework of ischemic bed size (myocardium at risk) and collateral flow', *Laboratory Investigation*, 40(6), pp. 633–644.

- Reimer, K. A., Murry, C. E. and Richard, V. J. (1989) 'The role of neutrophils and free radicals in the ischemic-reperfused heart: Why the confusion and controversy?', *Journal of Molecular and Cellular Cardiology*, December, pp. 1225–1239. doi: 10.1016/0022-2828(89)90669-X.
- Reinders, J. *et al.* (2007) 'Profiling phosphoproteins of yeast mitochondria reveals a role of phosphorylation in assembly of the ATP synthase', *Molecular and Cellular Proteomics*. American Society for Biochemistry and Molecular Biology, 6(11), pp. 1896–1906. doi: 10.1074/mcp.M700098-MCP200.
- Rena, G. *et al.* (2015) 'Roles of the forkhead in rhabdomyosarcoma (FKHR) phosphorylation sites in regulating 14-3-3 binding, transactivation and nuclear targeting', *Biochemical Journal*. Portland Press Limited, 354(3), pp. 605–612. doi: 10.1042/bj3540605.
- Richardson, W. J. *et al.* (2015) 'Physiological implications of myocardial scar structure', in *Comprehensive Physiology*. Hoboken, NJ, USA: John Wiley & Sons, Inc., pp. 1877–1909. doi: 10.1002/cphy.c140067.
- Rider, M. H. *et al.* (2009) 'Fulfilling the Krebs and Beavo criteria for studying protein phosphorylation in the era of mass spectrometry-driven kinome research', *Archives of Physiology and Biochemistry*, 115(5), pp. 298–310. doi: 10.3109/13813450903338108.
- Rigor, R. R. *et al.* (2013) 'Myosin Light Chain Kinase Signaling in Endothelial Barrier Dysfunction', *Medicinal Research Reviews*. John Wiley & Sons, Ltd, 33(5), pp. 911–933. doi: 10.1002/med.21270.
- Rodriguez, P., Bhogal, M. S. and Colyer, J. (2003) 'Stoichiometric phosphorylation of cardiac ryanodine receptor on serine 2809 by calmodulin-dependent kinase II and protein kinase A', *Journal of Biological Chemistry*. American Society for Biochemistry and Molecular Biology, 278(40), pp. 38593–38600. doi: 10.1074/jbc.M301180200.
- Roh, J. S. and Sohn, D. H. (2018) 'Damage-Associated Molecular Patterns in Inflammatory Diseases', *Immune Network*. The Korean Association of Immunologists, 18(4), p. e27. doi: 10.4110/in.2018.18.e27.
- Rossello, X. *et al.* (2016) 'Characterization of the Langendorff Perfused Isolated Mouse Heart Model of Global Ischemia-Reperfusion Injury: Impact of Ischemia and Reperfusion Length on Infarct Size and LDH Release', *Journal of Cardiovascular Pharmacology and Therapeutics*. SAGE PublicationsSage CA: Los Angeles, CA, 21(3), pp. 286–295. doi: 10.1177/1074248415604462.
- Rostron, K. A. *et al.* (2017) 'Cardiac dysfunction in mice with reduced striatin expression', *Heart*. BMJ Publishing Group Ltd and British Cardiovascular Society, 103(Suppl 5), p. A115.1-A115. doi: 10.1136/heartjnl-2017-311726.159.
- Ruan, H. *et al.* (2009) 'Inducible and cardiac specific PTEN inactivation protects ischemia/reperfusion injury', *Journal of Molecular and Cellular Cardiology*. Academic Press, 46(2), pp. 193–200. doi: 10.1016/j.yjmcc.2008.10.021.
- Ruknudin, A. M. *et al.* (2007) 'Phosphorylation and other conundrums of Na/Ca exchanger, NCX1', in *Annals of the New York Academy of Sciences*, pp. 103–118. doi: 10.1196/annals.1387.036.
- Ruvolo, P. P. *et al.* (1999) 'Ceramide induces Bcl2 dephosphorylation via a mechanism involving mitochondrial PP2A.', *The Journal of biological chemistry*. American Society for Biochemistry and Molecular Biology, 274(29), pp. 20296–300. doi: 10.1074/jbc.274.29.20296.

- Ruvolo, P. P. *et al.* (2002) 'A functional role for the B56 α -subunit of protein phosphatase 2A in ceramide-mediated regulation of Bcl2 phosphorylation status and function', *Journal of Biological Chemistry*, 277(25), pp. 22847–22852. doi: 10.1074/jbc.M201830200.
- Sadayappan, S. *et al.* (2006) 'Cardiac myosin binding protein C phosphorylation is cardioprotective.', *Proceedings of the National Academy of Sciences of the United States of America*. National Academy of Sciences, 103(45), pp. 16918–23. doi: 10.1073/pnas.0607069103.
- Santoro, M. F. *et al.* (2016) *Regulation of Protein Phosphatase 2A Activity by Caspase-3 during Apoptosis**.
- Sariahmetoglu, M. *et al.* (2012) 'Phosphorylation status of matrix metalloproteinase 2 in myocardial ischaemia - Reperfusion injury', *Heart*, 98(8), pp. 656–662. doi: 10.1136/heartjnl-2011-301250.
- Sato, S., Fujita, N. and Tsuruo, T. (2000) 'Modulation of Akt kinase activity by binding to Hsp90', *Proceedings of the National Academy of Sciences*, 97(20), pp. 10832–10837. doi: 10.1073/pnas.170276797.
- Schmidt, B. Z. and Perlmutter, D. H. (2005) 'Grp78, Grp94, and Grp170 interact with α_1 -antitrypsin mutants that are retained in the endoplasmic reticulum', *American Journal of Physiology-Gastrointestinal and Liver Physiology*, 289(3), pp. G444–G455. doi: 10.1152/ajpgi.00237.2004.
- Schmitz, M. H. A. *et al.* (2010) 'Live-cell imaging RNAi screen identifies PP2A-B55 α and importin- β 21 as key mitotic exit regulators in human cells', *Nature Cell Biology*, 12(9), pp. 886–893. doi: 10.1038/ncb2092.
- Schomig, A. (1990) 'Catecholamines in myocardial ischemia. Systemic and cardiac release.', *Circulation*, 274(3), pp. 13–22.
- Schultz, J. E. *et al.* (2017) 'Evidence for involvement of opioid receptors in ischemic preconditioning in rat hearts', *American Journal of Physiology-Heart and Circulatory Physiology*, 268(5), pp. H2157–H2161. doi: 10.1152/ajpheart.1995.268.5.h2157.
- Schulze, D. H. *et al.* (2003) 'Sodium/calcium exchanger (NCX1) macromolecular complex', *Journal of Biological Chemistry*. American Society for Biochemistry and Molecular Biology, 278(31), pp. 28849–28855. doi: 10.1074/jbc.M300754200.
- Sents, W. *et al.* (2013) 'The biogenesis of active protein phosphatase 2A holoenzymes: A tightly regulated process creating phosphatase specificity', *FEBS Journal*. John Wiley & Sons, Ltd (10.1111), 280(2), pp. 644–661. doi: 10.1111/j.1742-4658.2012.08579.x.
- Sequeira, V. *et al.* (2014) 'The physiological role of cardiac cytoskeleton and its alterations in heart failure', *Biochimica et Biophysica Acta (BBA) - Biomembranes*. Elsevier, 1838(2), pp. 700–722. doi: 10.1016/j.bbmem.2013.07.011.
- Seshacharyulu, P. *et al.* (2013) 'Phosphatase: PP2A structural importance, regulation and its aberrant expression in cancer', *Cancer Letters*, 335(1), pp. 9–18. doi: 10.1016/j.canlet.2013.02.036.
- Shah, A. S. V. *et al.* (2018) 'Global burden of atherosclerotic cardiovascular disease in people living with HIV systematic review and meta-analysis', *Circulation*, 138(11), pp. 1100–1112. doi: 10.1161/CIRCULATIONAHA.117.033369.

- Shimizu, S. *et al.* (2003) 'Protein-tyrosine Phosphatase 1B as New Activator for Hepatic Lipogenesis via Sterol Regulatory Element-binding Protein-1 Gene Expression', *Journal of Biological Chemistry*. American Society for Biochemistry and Molecular Biology, 278(44), pp. 43095–43101. doi: 10.1074/jbc.M306880200.
- Sidebotham, D. and Gillham, M. (2007) 'Hemodynamic Instability and Resuscitation', *Cardiothoracic Critical Care*. Butterworth-Heinemann, pp. 295–315. doi: 10.1016/B978-075067572-7.50023-0.
- Sidera, K. *et al.* (2004) 'Involvement of cell surface HSP90 in cell migration reveals a novel role in the developing nervous system', *Journal of Biological Chemistry*. American Society for Biochemistry and Molecular Biology, 279(44), pp. 45379–45388. doi: 10.1074/jbc.M405486200.
- Siegmund, B. *et al.* (1997) 'Halothane protects cardiomyocytes against reoxygenation-induced hypercontracture.', *Circulation*, 96(12), pp. 4372–9.
- Silberman, G. A. *et al.* (2010) 'Uncoupled cardiac nitric oxide synthase mediates diastolic dysfunction', *Circulation*, 121(4), pp. 519–528. doi: 10.1161/CIRCULATIONAHA.109.883777.
- Sinn, H. W. *et al.* (2002) 'Localization of the novel Xin protein to the adherens junction complex in cardiac and skeletal muscle during development', *Developmental Dynamics*, 225(1), pp. 1–13. doi: 10.1002/dvdy.10131.
- Smetana, J. H. C. and Zanchin, N. I. T. (2007) 'Interaction analysis of the heterotrimer formed by the phosphatase 2A catalytic subunit, $\alpha 4$ and the mammalian ortholog of yeast Tip41 (TIPRL)', *FEBS Journal*, 274(22), pp. 5891–5904. doi: 10.1111/j.1742-4658.2007.06112.x.
- Smoly, I. *et al.* (2017) 'An Asymmetrically Balanced Organization of Kinases versus Phosphatases across Eukaryotes Determines Their Distinct Impacts', *PLoS Computational Biology*, 13(1), pp. 1–21. doi: 10.1371/journal.pcbi.1005221.
- Soderling, T. R. *et al.* (1979) 'Phosphorylation and inactivation of glycogen synthase by phosphorylase kinase.', *Proceedings of the National Academy of Sciences of the United States of America*, 76(6), pp. 2536–40.
- Solenkova, N. V. *et al.* (2005) 'Endogenous adenosine protects preconditioned heart during early minutes of reperfusion by activating Akt', *American Journal of Physiology-Heart and Circulatory Physiology*, 290(1), pp. H441–H449. doi: 10.1152/ajpheart.00589.2005.
- Sontag, E. *et al.* (1993) 'The interaction of SV40 small tumor antigen with protein phosphatase 2A stimulates the map kinase pathway and induces cell proliferation', *Cell*. Cell Press, 75(5), pp. 887–897. doi: 10.1016/0092-8674(93)90533-V.
- Sontag, E. *et al.* (1996) 'Regulation of the phosphorylation state and microtubule-binding activity of tau by protein phosphatase 2A', *Neuron*. Elsevier, 17(6), pp. 1201–1207. doi: 10.1016/S0896-6273(00)80250-0.
- Sontag, E. *et al.* (1999) 'Molecular interactions among protein phosphatase 2A, tau, and microtubules. Implications for the regulation of tau phosphorylation and the development of tauopathies', *Journal of Biological Chemistry*. American Society for Biochemistry and Molecular Biology, 274(36), pp. 25490–25498. doi: 10.1074/jbc.274.36.25490.
- Sontag, J. M. and Sontag, E. (2014) 'Protein phosphatase 2A dysfunction in Alzheimer's disease', *Frontiers in Molecular Neuroscience*, 7(MAR), p. 16. doi: 10.3389/fnmol.2014.00016.

- Sordahl, L. A. *et al.* (1969) 'Some Ultrastructural and Biochemical Characteristics of Tumor Mitochondria Isolated in Albumin-containing Media', *Cancer Research*, 29(11), pp. 2002–2009.
- Soroka, J. *et al.* (2012) 'Conformational Switching of the Molecular Chaperone Hsp90 via Regulated Phosphorylation', *Molecular Cell*. Cell Press, 45(4), pp. 517–528. doi: 10.1016/J.MOLCEL.2011.12.031.
- Sotiropoulos, I. *et al.* (2017) 'Atypical, non-standard functions of the microtubule associated Tau protein', *Acta Neuropathologica Communications*. BioMed Central, 5(1), p. 91. doi: 10.1186/s40478-017-0489-6.
- Stiermaier, T. *et al.* (2013) 'Reperfusion strategies in ST-segment elevation myocardial infarction.', *Minerva medica*, 104(4), pp. 391–411.
- Stokes, M. P. *et al.* (2012) 'PTMScan direct: Identification and quantification of peptides from critical signaling proteins by immunoaffinity enrichment coupled with LC-MS/MS', in *Molecular and Cellular Proteomics*, pp. 187–201. doi: 10.1074/mcp.M111.015883.
- Strack, S. *et al.* (1998) 'Brain protein phosphatase 2A: Developmental regulation and distinct cellular and subcellular localization by B subunits', *Journal of Comparative Neurology*. John Wiley & Sons, Ltd, 392(4), pp. 515–527. doi: 10.1002/(SICI)1096-9861(19980323)392:4<515::AID-CNE8>3.0.CO;2-3.
- Subbarao Sreedhar, A. *et al.* (2004) 'Hsp90 isoforms: functions, expression and clinical importance', *FEBS Letters*. John Wiley & Sons, Ltd, 562(1–3), pp. 11–15. doi: 10.1016/S0014-5793(04)00229-7.
- Suga, H. (2017) 'Ventricular energetics', *Physiological Reviews*, 70(2), pp. 247–277. doi: 10.1152/physrev.1990.70.2.247.
- Sun, X. *et al.* (2014) 'A mitochondrial ATP synthase subunit interacts with TOR signaling to modulate protein homeostasis and lifespan in *Drosophila*', *Cell Reports*. NIH Public Access, 8(6), pp. 1781–1792. doi: 10.1016/j.celrep.2014.08.022.
- Swingle, M., Ni, L. and Honkanen, R. E. (2007) 'Small-molecule inhibitors of ser/thr protein phosphatases: Specificity, use and common forms of abuse', *Methods in Molecular Biology*. NIH Public Access, 365, pp. 23–38. doi: 10.1385/1-59745-267-X:23.
- Tachibana, K. *et al.* (1981) 'Okadaic Acid, a Cytotoxic Polyether from Two Marine Sponges of the Genus *Halichondria*', *Journal of the American Chemical Society*. American Chemical Society, 103(9), pp. 2469–2471. doi: 10.1021/ja00399a082.
- Taegtmeyer, H., Hems, R. and Krebs, H. A. (1980) 'Utilization of energy-providing substrates in the isolated working rat heart', *Biochemical Journal*. Portland Press Ltd, 186(3), pp. 701–711. doi: 10.1042/bj1860701.
- Takada, Y. (2004) 'Cytoprotective Effect of Sodium Orthovanadate on Ischemia/Reperfusion-Induced Injury in the Rat Heart Involves Akt Activation and Inhibition of Fodrin Breakdown and Apoptosis', *Journal of Pharmacology and Experimental Therapeutics*, 311(3), pp. 1249–1255. doi: 10.1124/jpet.104.070839.
- Takeda, S. *et al.* (2003) 'Attenuation of ischemia-reperfusion induced changes in cardiac performance and sarcoplasmic reticulum function by vanadate', *Experimental and Clinical Cardiology*. Pulsus Group, 8(3), pp. 134–138.

- Tanabe, A. *et al.* (2012) 'MARCKS dephosphorylation is involved in bradykinin-induced neurite outgrowth in neuroblastoma SH-SY5Y cells', *Journal of Cellular Physiology*, 227(2), pp. 618–629. doi: 10.1002/jcp.22763.
- Tansey, E. E. *et al.* (2006) 'Reduction and Redistribution of Gap and Adherens Junction Proteins After Ischemia and Reperfusion', *Annals of Thoracic Surgery*. NIH Public Access, 82(4), pp. 1472–1479. doi: 10.1016/j.athoracsur.2006.04.061.
- Tanti, G. K. and Goswami, S. K. (2014) 'SG2NA recruits DJ-1 and Akt into the mitochondria and membrane to protect cells from oxidative damage', *Free Radical Biology and Medicine*, 75, pp. 1–13. doi: 10.1016/j.freeradbiomed.2014.07.009.
- Tanveer, A. *et al.* (1996) 'Involvement of cyclophilin D in the activation of a mitochondrial pore by Ca²⁺ and oxidant stress', *European Journal of Biochemistry*, 238(1), pp. 166–172. doi: 10.1111/j.1432-1033.1996.0166q.x.
- Tatli, E. *et al.* (2013) 'Arrhythmias following Revascularization Procedures in the Course of Acute Myocardial Infarction: Are They Indicators of Reperfusion or Ongoing Ischemia?', *The Scientific World Journal*, 2013, pp. 1–7. doi: 10.1155/2013/160380.
- Tehrani, M. A., Mumby, M. C. and Kamibayashi, C. (1996) 'Identification of a novel protein phosphatase 2A regulatory subunit highly expressed in muscle', *Journal of Biological Chemistry*. American Society for Biochemistry and Molecular Biology, 271(9), pp. 5164–5170. doi: 10.1074/jbc.271.9.5164.
- Terentyev, D. *et al.* (2009) 'MiR-1 overexpression enhances ca²⁺ release and promotes cardiac arrhythmogenesis by targeting pp2a regulatory subunit b56 α and causing camkii-dependent hyperphosphorylation of RyR2', *Circulation Research*. Lippincott Williams & Wilkins, 104(4), pp. 514–521. doi: 10.1161/CIRCRESAHA.108.181651.
- ThermoScientific (2004) *EnzChek[®] Phosphatase Assay Kit (E12020)*, *Biochemical Journal*.
- TIMI Study Group (1985) 'The Thrombolysis in Myocardial Infarction (TIMI) Trial: phase I findings', *New England Journal of Medicine*, 312(14), pp. 932–936. doi: 10.1056/NEJM198504043121437.
- Tobisawa, T. *et al.* (2017) 'Insufficient activation of Akt upon reperfusion because of its novel modification by reduced PP2A-B55 α contributes to enlargement of infarct size by chronic kidney disease', *Basic Research in Cardiology*. Springer Berlin Heidelberg, 112(3), p. 31. doi: 10.1007/s00395-017-0621-6.
- Tobita, T. *et al.* (2017) 'Identification of MYLK3 mutations in familial dilated cardiomyopathy', *Scientific Reports*. Nature Publishing Group, 7(1), p. 17495. doi: 10.1038/s41598-017-17769-1.
- Du Toit, E. F. *et al.* (2007) 'Efficacy of ischaemic preconditioning in the eNOS overexpressed working mouse heart model', *European Journal of Pharmacology*. Elsevier, 556(1–3), pp. 115–120. doi: 10.1016/j.ejphar.2006.11.004.
- Du Toit, E. F. and Opie, L. H. (1994) 'Inhibitors of Ca²⁺ ATPase pump of sarcoplasmic reticulum attenuate reperfusion stunning in isolated rat heart', *Journal of Cardiovascular Pharmacology*, 24(4), pp. 678–684. doi: 10.1097/00005344-199410000-00020.

- Totzeck, A. *et al.* (2008) 'No impact of protein phosphatases on connexin 43 phosphorylation in ischemic preconditioning', *American Journal of Physiology-Heart and Circulatory Physiology*, 295(5), pp. H2106–H2112. doi: 10.1152/ajpheart.00456.2008.
- Toyokuni, S. (1999) 'Reactive oxygen species-induced molecular damage and its application in pathology.', *Pathology international*, 49(2), pp. 91–102.
- Trinidad, J. C. *et al.* (2008) 'Quantitative analysis of synaptic phosphorylation and protein expression', in *Molecular and Cellular Proteomics*. American Society for Biochemistry and Molecular Biology, pp. 684–696. doi: 10.1074/mcp.M700170-MCP200.
- Trockenbacher, A. *et al.* (2001) 'MID1, mutated in Opitz syndrome, encodes an ubiquitin ligase that targets phosphatase 2A for degradation', *Nature Genetics*, 29(3), pp. 287–294. doi: 10.1038/ng762.
- Truong, T. H. and Carroll, K. S. (2013) 'Redox regulation of protein kinases', *Critical Reviews in Biochemistry and Molecular Biology*. John Wiley & Sons, Ltd (10.1111), 48(4), pp. 332–356. doi: 10.3109/10409238.2013.790873.
- Tsiani, E., Abdullah, N. and Fantus, I. G. (1997) 'Insulin-mimetic agents vanadate and pervanadate stimulate glucose but inhibit amino acid uptake', *American Journal of Physiology - Cell Physiology*, 272(1 41-1), pp. C156–C162. doi: 10.1152/ajpcell.1997.272.1.C156.
- Turkbey, E. B. *et al.* (2015) 'Prevalence and correlates of myocardial scar in a US cohort', *JAMA - Journal of the American Medical Association*. American Medical Association, 314(18), pp. 1945–1954. doi: 10.1001/jama.2015.14849.
- Turner, M. S. *et al.* (2004) 'Reversible connexin 43 dephosphorylation during hypoxia and reoxygenation is linked to cellular ATP levels', *Circulation Research*. Lippincott Williams & Wilkins, 95(7), pp. 726–733. doi: 10.1161/01.RES.0000144805.11519.1e.
- Turowski, P. *et al.* (1995) 'Differential methylation and altered conformation of cytoplasmic and nuclear forms of protein phosphatase 2A during cell cycle progression', *Journal of Cell Biology*. Rockefeller University Press, 129(2), pp. 397–410. doi: 10.1083/jcb.129.2.397.
- Turowski, P. *et al.* (2013) 'Vimentin Dephosphorylation by Protein Phosphatase 2A Is Modulated by the Targeting Subunit B55', *Molecular Biology of the Cell*. Edited by T. Hunter, 10(6), pp. 1997–2015. doi: 10.1091/mbc.10.6.1997.
- UNAIDS (2018) *AIDSinfo | UNAIDS*. Available at: <http://aidsinfo.unaids.org/> (Accessed: 22 April 2019).
- Usui, T. *et al.* (1999) 'Protein phosphatase 2A inhibitors, phoslactomycins, effects on the cytoskeleton in NIH/3T3 cells', *Journal of Biochemistry*. Narnia, 125(5), pp. 960–965. doi: 10.1093/oxfordjournals.jbchem.a022375.
- Valls-Lacalle, L. *et al.* (2016) 'Succinate dehydrogenase inhibition with malonate during reperfusion reduces infarct size by preventing mitochondrial permeability transition', *Cardiovascular Research*. Narnia, 109(3), pp. 374–384. doi: 10.1093/cvr/cvv279.
- Valverde, C. A. *et al.* (2010) 'Transient Ca²⁺ depletion of the sarcoplasmic reticulum at the onset of reperfusion', *Cardiovascular Research*. Oxford University Press, 85(4), p. 671. doi: 10.1093/CVR/CVP371.

- Vandenberg, J. I., Metcalfe, J. C. and Grace, A. A. (1993) 'Mechanisms of pHi recovery after global ischemia in the perfused heart', *Circulation Research*, 72(5), pp. 993–1003.
- Vénéreau, E., Ceriotti, C. and Bianchi, M. E. (2015) 'DAMPs from cell death to new life', *Frontiers in Immunology*, 6(AUG), p. 422. doi: 10.3389/fimmu.2015.00422.
- Verma, S. *et al.* (2002) 'Fundamentals of Reperfusion Injury for the Clinical Cardiologist', *Circulation*, 105(20), pp. 2332–2336. doi: 10.1161/01.cir.0000016602.96363.36.
- Villén, J. *et al.* (2007) 'Large-scale phosphorylation analysis of mouse liver', *Proceedings of the National Academy of Sciences of the United States of America*. National Academy of Sciences, 104(5), pp. 1488–1493. doi: 10.1073/pnas.0609836104.
- Vinten-Johansen, J. (2004) 'Involvement of neutrophils in the pathogenesis of lethal myocardial reperfusion injury', *Cardiovascular Research*. Narnia, 61(3), pp. 481–497. doi: 10.1016/j.cardiores.2003.10.011.
- Virdee, K., Parone, P. A. and Tolkovsky, A. M. (2000) 'Phosphorylation of the pro-apoptotic protein BAD on serine 155, a novel site, contributes to cell survival', *Current Biology*, 10(18), pp. 1151–1154. doi: 10.1016/S0960-9822(00)00702-8.
- Voorhoeve, P. M., Hijmans, E. M. and Bernards, R. (1999) 'Functional interaction between a novel protein phosphatase 2A regulatory subunit, PR59, and the retinoblastoma-related p107 protein', *Oncogene*. Nature Publishing Group, 18(2), pp. 515–524. doi: 10.1038/sj.onc.1202316.
- Van Vuuren, D. (2014) *The role of Protein Phosphatase 2A (PP2A) in Myocardial Ischaemia/Reperfusion Injury*. Stellenbosch : Stellenbosch University.
- Wagner, E. *et al.* (2012) 'Stimulated Emission Depletion Live-Cell Super-Resolution Imaging Shows Proliferative Remodeling of T-Tubule Membrane Structures After Myocardial Infarction', *Circulation Research*, 111(4), pp. 402–414. doi: 10.1161/CIRCRESAHA.112.274530.
- Wang, F. *et al.* (2018) 'Protein interactomes of protein phosphatase 2A B55 regulatory subunits reveal B55-mediated regulation of replication protein A under replication stress', *Scientific Reports*. Nature Publishing Group, 8(1), p. 2683. doi: 10.1038/s41598-018-21040-6.
- Wang, Q. *et al.* (2014) 'New insights into the roles of xin repeat-containing proteins in cardiac development, function, and disease', in *International Review of Cell and Molecular Biology*. NIH Public Access, pp. 89–128. doi: 10.1016/B978-0-12-800180-6.00003-7.
- Wanichawan, P. *et al.* (2011) ' Full-length cardiac Na⁺/Ca²⁺ exchanger 1 protein is not phosphorylated by protein kinase A ', *American Journal of Physiology-Cell Physiology*. American Physiological Society, 300(5), pp. C989–C997. doi: 10.1152/ajpcell.00196.2010.
- Wegner, A. M. *et al.* (2007) 'An automated fluorescence-based method for continuous assay of PP2A activity', *Methods in Molecular Biology*. New Jersey: Humana Press, 365, pp. 61–69. doi: 10.1385/1-59745-267-X:61.
- Wehrens, X. H. T. *et al.* (2004) 'UltraRapid Communication Phosphorylation Regulates the Cardiac Ryanodine Receptor', *Circulation Research*. Lippincott Williams & Wilkins, 94(6), pp. e61–70. doi: 10.1161/01.RES.0000125626.33738.E2.

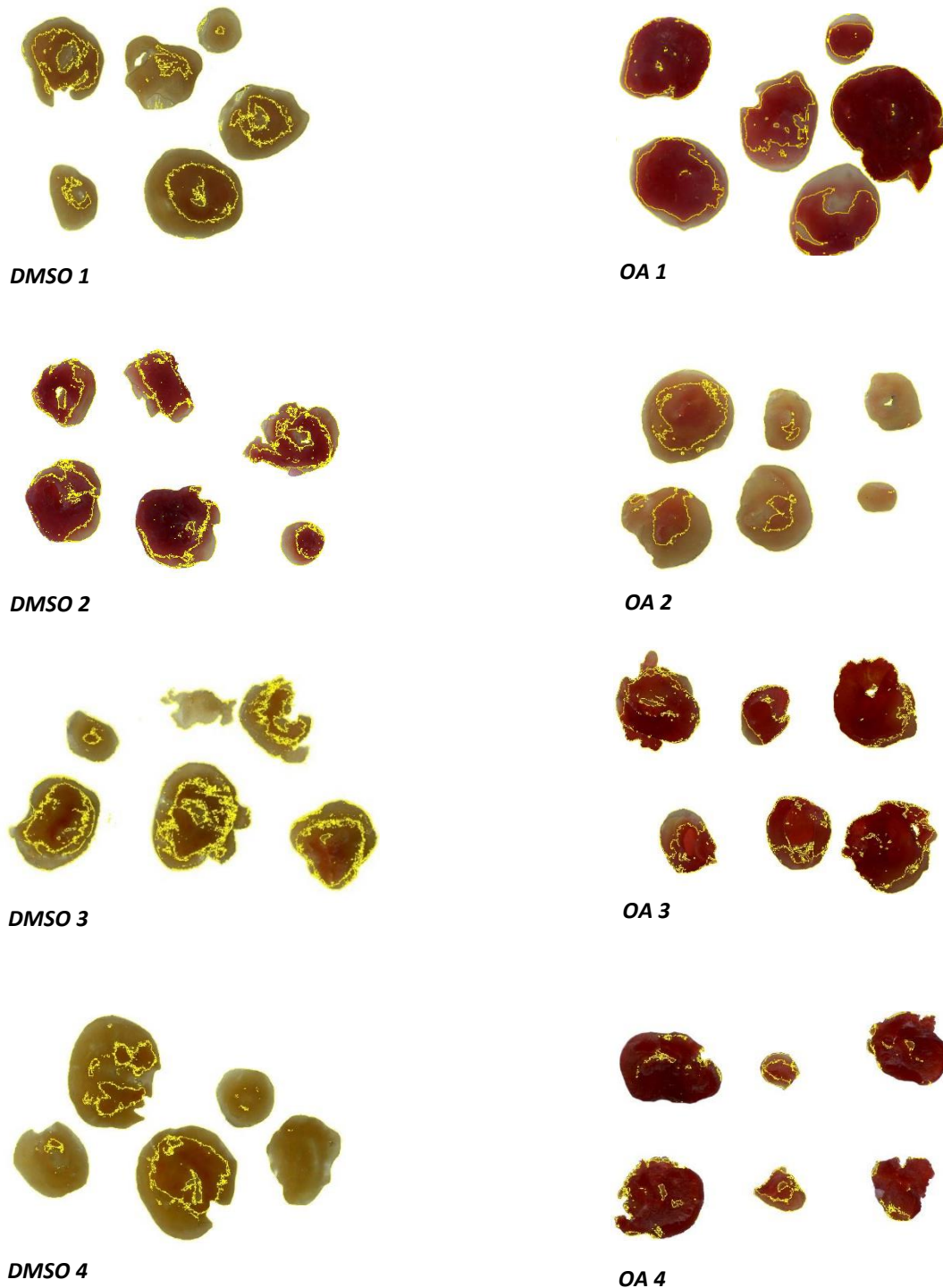
- Weinbrenner, C., Liu, G. S., *et al.* (1998) 'Cyclosporine a limits myocardial infarct size even when administered after onset of ischemia', *Cardiovascular Research*. Narnia, 38(3), pp. 676–684. doi: 10.1016/S0008-6363(98)00064-9.
- Weinbrenner, C., Baines, C. P., *et al.* (1998) 'Fostriecin, an inhibitor of protein phosphatase 2A, limits myocardial infarct size even when administered after onset of ischemia', *Circulation*, 98(9), pp. 899–905. doi: 10.1161/01.CIR.98.9.899.
- Weis, F. *et al.* (2010) 'The 90-kDa Heat Shock Protein Hsp90 Protects Tubulin against Thermal Denaturation', *Journal of Biological Chemistry*, 285(13), pp. 9525–9534. doi: 10.1074/jbc.M109.096586.
- Wen, Y.-A. *et al.* (2013) 'Downregulation of PHLPP Expression Contributes to Hypoxia-Induced Resistance to Chemotherapy in Colon Cancer Cells', *Molecular and Cellular Biology*, 33(22), pp. 4594–4605. doi: 10.1128/MCB.00695-13.
- Wijsekara, N. *et al.* (2005) 'Muscle-Specific Pten Deletion Protects against Insulin Resistance and Diabetes', *Molecular and Cellular Biology*, 25(3), pp. 1135–1145. doi: 10.1128/mcb.25.3.1135-1145.2005.
- Wolvetang, E. J. *et al.* (1994) 'Mitochondrial respiratory chain inhibitors induce apoptosis', *FEBS Letters*, 339(1–2), pp. 40–44. doi: 10.1016/0014-5793(94)80380-3.
- Wong, P. M. *et al.* (2015) 'Regulation of autophagy by coordinated action of mTORC1 and protein phosphatase 2A', *Nature Communications*, 6(1), p. 8048. doi: 10.1038/ncomms9048.
- Woo, J. S. *et al.* (2010) 'S165F mutation of junctophilin 2 affects Ca²⁺ signalling in skeletal muscle', *Biochemical Journal*, 427(1), pp. 125–134. doi: 10.1042/BJ20091225.
- World Health Organization (2018) *Global Health Estimates 2018: Disease burden by Cause, Sex, by Country and Region, 2000-2016.*, World Health Organization.
- Wu, C. G. *et al.* (2017) 'Methylation-regulated decommissioning of multimeric PP2A complexes', *Nature Communications*. Nature Publishing Group, 8(1), p. 2272. doi: 10.1038/s41467-017-02405-3.
- Wu, M. Y. *et al.* (2018) 'Current Mechanistic Concepts in Ischemia and Reperfusion Injury', *Cellular Physiology and Biochemistry*, 46(4), pp. 1650–1667. doi: 10.1159/000489241.
- Xi, L., Hess, M. L. and Kukreja, R. C. (1998) 'Ischemic preconditioning in isolated perfused mouse heart: Reduction in infarct size without improvement of post-ischemic ventricular function', *Molecular and Cellular Biochemistry*. Boston, MA: Springer US, 186(1–2), pp. 69–77. doi: 10.1023/A:1006811128561.
- Xiao, B. *et al.* (2005) 'Characterization of a novel PKA phosphorylation site, serine-2030, reveals no PKA hyperphosphorylation of the cardiac ryanodine receptor in canine heart failure', *Circulation Research*. Lippincott Williams & Wilkins, 96(8), pp. 847–855. doi: 10.1161/01.RES.0000163276.26083.e8.
- Xie, Y. W. and Wolin, M. S. (1996) 'Role of nitric oxide and its interaction with superoxide in the suppression of cardiac muscle mitochondrial respiration. Involvement in response to hypoxia/reoxygenation.', *Circulation*, 94(10), pp. 2580–6.

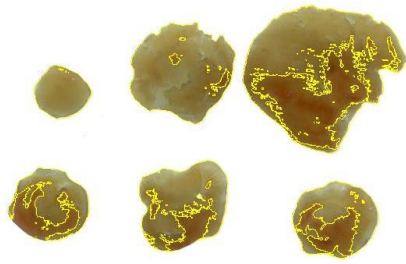
- Xin, M. and Deng, X. (2006) 'Protein phosphatase 2A enhances the proapoptotic function of Bax through dephosphorylation', *Journal of Biological Chemistry*. American Society for Biochemistry and Molecular Biology, 281(27), pp. 18859–18867. doi: 10.1074/jbc.M512543200.
- Xing, Y. *et al.* (2005) 'Protein phosphatase subunit G5PR is needed for inhibition of B cell receptor-induced apoptosis', *The Journal of Experimental Medicine*, 202(5), pp. 707–719. doi: 10.1084/jem.20050637.
- Xing, Y. *et al.* (2008) 'Structural Mechanism of Demethylation and Inactivation of Protein Phosphatase 2A', *Cell*, 133(1), pp. 154–163. doi: 10.1016/j.cell.2008.02.041.
- Xing, Y. *et al.* (2016) 'Mutual inhibition of insulin signaling and PHLPP-1 determines cardioprotective efficiency of Akt in aged heart', *Aging*. Impact Journals, LLC, 8(5), pp. 873–888. doi: 10.18632/aging.100933.
- Xu, Y. *et al.* (2006) 'Structure of the Protein Phosphatase 2A Holoenzyme', *Cell*, 127(6), pp. 1239–1251. doi: 10.1016/j.cell.2006.11.033.
- Yamasaki, R. *et al.* (2002) 'Protein kinase A phosphorylates titin's cardiac-specific N2B domain and reduces passive tension in rat cardiac myocytes', *Circulation Research*, 90(11), pp. 1181–1188. doi: 10.1161/01.RES.0000021115.24712.99.
- Yan, L. *et al.* (2008) 'PP2A regulates the pro-apoptotic activity of FOXO1', *Journal of Biological Chemistry*. American Society for Biochemistry and Molecular Biology, 283(12), pp. 7411–7420. doi: 10.1074/jbc.M708083200.
- Yellon, D. M. and Hausenloy, D. H. (2007) 'Myocardial Reperfusion Injury — NEJM', *The New England Journal of Medicine*, pp. 1121–35. doi: 10.1056/NEJMr071667.
- Yellon, D. M. and Opie, L. H. (2006) 'Postconditioning for protection of the infarcting heart', *Lancet*, 367(9509), pp. 456–458. doi: 10.1016/S0140-6736(06)68157-9.
- Young, J. C., Hoogenraad, N. J. and Hartl, F. U. (2003) 'Molecular chaperones Hsp90 and Hsp70 deliver preproteins to the mitochondrial import receptor Tom70', *Cell*, pp. 41–50. doi: 10.1016/S0092-8674(02)01250-3.
- Yu, J., Boyapati, A. and Rundell, K. (2001) 'Critical role for SV40 small-t antigen in human cell transformation', *Virology*. Academic Press, 290(2), pp. 192–198. doi: 10.1006/viro.2001.1204.
- Zanivan, S. *et al.* (2008) 'Solid tumor proteome and phosphoproteome analysis by high resolution mass spectrometry', *Journal of Proteome Research*. American Chemical Society, 7(12), pp. 5314–5326. doi: 10.1021/pr800599n.
- Zha, J. *et al.* (1996) 'Serine phosphorylation of death agonist BAD in response to survival factor results in binding to 14-3-3 not BCL-X(L)', *Cell*, 87(4), pp. 619–28.
- Zhang, F. X., Pan, W. and Hutchins, J. B. (2002) 'Phosphorylation of F1FO ATPase δ -Subunit Is Regulated by Platelet-Derived Growth Factor in Mouse Cortical Neurons In Vitro', *Journal of Neurochemistry*. John Wiley & Sons, Ltd (10.1111), 65(6), pp. 2812–2815. doi: 10.1046/j.1471-4159.1995.65062812.x.

- Zhang, J. *et al.* (2015) 'A simple and visible colorimetric method through Zr⁴⁺-phosphate coordination for the assay of protein tyrosine phosphatase 1B and screening of its inhibitors', *Analyst*, 140(16), pp. 5716–5723. doi: 10.1039/c5an00970g.
- Zhang, M., Tanaka, T. and Ikura, M. (1995) 'Calcium-induced conformational transition revealed by the solution structure of apo calmodulin', *Nature Structural Biology* 1995 2:9. Nature Publishing Group, 2(9), p. 758. doi: 10.1038/nsb0995-758.
- Zhang, Z. M. *et al.* (2016) 'Race and sex differences in the incidence and prognostic significance of silent myocardial infarction in the Atherosclerosis Risk in Communities (ARIC) study', *Circulation*. Lippincott Williams & Wilkins Hagerstown, MD, 133(22), pp. 2141–2148. doi: 10.1161/CIRCULATIONAHA.115.021177.
- Zhao, Z.-Q. *et al.* (2003) 'Inhibition of myocardial injury by ischemic postconditioning during reperfusion: comparison with ischemic preconditioning.', *American Journal of Physiology. Heart and Circulatory Physiology*, 285(2), pp. 579–588. doi: 10.1152/ajpheart.01064.2002.
- Zhou, H. *et al.* (2017) 'PP2A mediates apoptosis or autophagic cell death in multiple myeloma cell lines', *Oncotarget*. Impact Journals, LLC, 8(46), pp. 80770–80789. doi: 10.18632/oncotarget.20415.
- Zhou, J. *et al.* (2003) 'Characterization of the Aalpha and Abeta subunit isoforms of protein phosphatase 2A: differences in expression, subunit interaction, and evolution', *Biochemical Journal*. Portland Press Ltd, 369(2), pp. 387–398. doi: 10.1042/bj20021244.
- Zhu, T. *et al.* (1997) 'The interconversion of protein phosphatase 2A between PP2A1 and PP2A0 during retinoic acid-induced granulocytic differentiation and a modification on the catalytic subunit in S phase of HL-60 cells.', *Archives of Biochemistry and Biophysics*, 339(1), pp. 210–7.
- Zhu, X. and Zuo, L. (2013) 'Characterization of oxygen radical formation mechanism at early cardiac ischemia', *Cell Death and Disease*. Nature Publishing Group, 4(9), p. e787. doi: 10.1038/cddis.2013.313.
- Zijun Su (2017) *Up-regulation of junctophilin-2 prevents ER stress and apoptosis in hypoxia/reoxygenation-stimulated H9c2 cells*. University of Western Ontario.
- Zolnierowicz, S. *et al.* (1994) 'Diversity in the Regulatory B-Subunits of Protein Phosphatase 2A: Identification of a Novel Isoform Highly Expressed in Brain', *Biochemistry*. American Chemical Society, 33(39), pp. 11858–11867. doi: 10.1021/bi00205a023.
- Zorov, D. B., Juhaszova, M. and Sollott, S. J. (2014) 'Mitochondrial Reactive Oxygen Species (ROS) and ROS-Induced ROS Release', *Physiological Reviews*, 94(3), pp. 909–950. doi: 10.1152/physrev.00026.2013.
- Zuppinger, C., Eppenberger-Eberhardt, M. and Eppenberger, H. M. (2000) 'N-Cadherin: structure, function and importance in the formation of new intercalated disc-like cell contacts in cardiomyocytes.', *Heart Failure Reviews*, 5(3), pp. 251–257. doi: 10.1023/A:1009809520194.

ADDENDUM A – INFARCT SIZE DETERMINATION

Figure A.0.1 - Heart slices of DMSO- or OA-perfused hearts where yellow indicates the demarcation of viable (red) and non-viable (pale) tissue

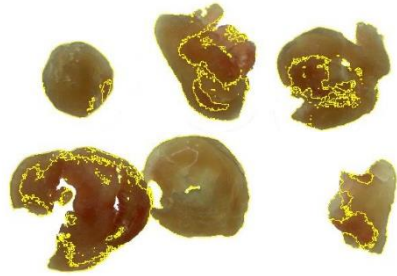




DMSO 5



OA 5



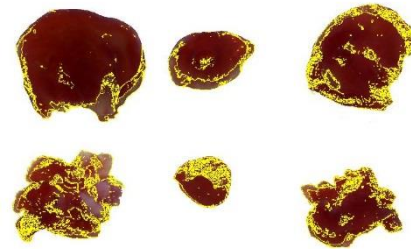
DMSO 6



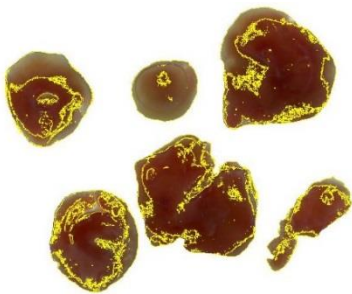
OA 6



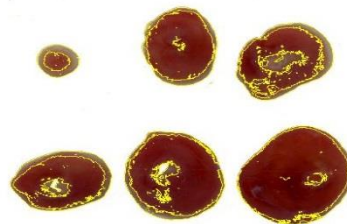
DMSO 7



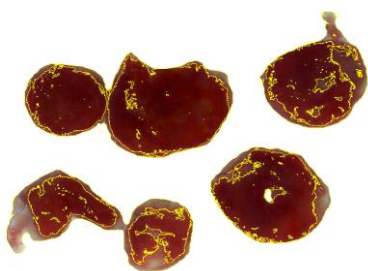
OA 7



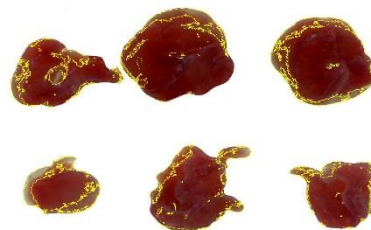
DMSO 8



OA 8



DMSO 9



OA 9

ADDENDUM B –

ADDITIONAL PHOSPHOPROTEOMIC DATA

Table B.1 - List of proteins present in myocardial tissue subjected to ischaemia and reperfusion following 50 nM OA administration. Fold changes (\log_2) and p values are shown for proteins and phosphorylated proteins.

Accession no:	Description	Proteome		Phosphoproteome	
		Fold change	Adj. P-Value	Fold change	Adj. P-Value
Q9ET80	Junctophilin-1	6.64	1.24E-16	1.82	3.88E-04
Q9JJC6	RILP-like protein 1	6.64	1.24E-16	0.95	8.10E-03
Q9CXW2	28S ribosomal protein S22, mitochondrial	6.64	1.24E-16		
Q9D0Y8	39S ribosomal protein L52, mitochondrial	6.64	1.24E-16		
Q9QZB7	Actin-related protein 10	6.64	1.24E-16		
Q9WTL7	Acyl-protein thioesterase 2	6.64	1.24E-16		
Q3UHQ0	AP2-associated protein kinase 1	6.64	1.24E-16		
Q9D0L7	Armadillo repeat-containing protein 10	6.64	1.24E-16		
Q3TCJ1	BRISC complex subunit Abraxas 2	6.64	1.24E-16		
P28651	Carbonic anhydrase-related protein	6.64	1.24E-16		
P31428	Dipeptidase 1	6.64	1.24E-16		
Q99KV1	DnaJ homolog subfamily B member 11	6.64	1.24E-16		
Q8BZ98	Dynamamin-3	6.64	1.24E-16		
Q69ZR2	E3 ubiquitin-protein ligase	6.64	1.24E-16		
Q3UJB9	Enhancer of mRNA-decapping protein 4	6.64	1.24E-16		
Q9Z0N2	Eukaryotic translation initiation factor 2 subunit 3, Y-linked	6.64	1.24E-16		
Q9EPK7	Exportin-7	6.64	1.24E-16		
Q8C8Y0	Glutamyl-tRNA(Gln) amidotransferase subunit C, mitochondrial	6.64	1.24E-16		
Q6PD26	GPI transamidase component PIG-S	6.64	1.24E-16		
Q9CR41	Huntingtin-interacting protein K	6.64	1.24E-16		
Q6P9N1	Hyccin	6.64	1.24E-16		
Q9R000	Integrin beta-1-binding protein 2	6.64	1.24E-16		
Q8C165	N-fatty-acyl-amino acid synthase/hydrolase	6.64	1.24E-16		
Q7TSV4	Phosphoglucomutase-2	6.64	1.24E-16		
Q6Q477	Plasma membrane calcium-transporting ATPase 4	6.64	1.24E-16		
Q8BGV0	Probable asparagine--tRNA ligase, mitochondrial	6.64	1.24E-16		
Q8BXN7	Protein phosphatase 1K, mitochondrial	6.64	1.24E-16		
Q80WQ2	Protein VAC14 homolog	6.64	1.24E-16		
Q9D009	Putative lipoyltransferase 2, mitochondrial	6.64	1.24E-16		
Q00915	Retinol-binding protein 1	6.64	1.24E-16		
P62746	Rho-related GTP-binding protein RhoB	6.64	1.24E-16		
Q64518	Sarcoplasmic/endoplasmic reticulum calcium ATPase 3	6.64	1.24E-16		
Q6NZC7	SEC23-interacting protein	6.64	1.24E-16		
P42230	Signal transducer and activator of transcription 5A	6.64	1.24E-16		

Table B.1 continued

Accession no:	Description	Proteome		Phosphoproteome	
		Fold change	Adj. P-Value	Fold change	Adj. P-Value
Q9WV80	Sorting nexin-1	6.64	1.24E-16		
Q9CU62	Structural maintenance of chromosomes protein 1A	6.64	1.24E-16		
Q8CG47	Structural maintenance of chromosomes protein 4	6.64	1.24E-16		
Q6A028	Switch-associated protein 70	6.64	1.24E-16		
Q91Z38	Tetratricopeptide repeat protein 1	6.64	1.24E-16		
Q9ET30	Transmembrane 9 superfamily member 3	6.64	1.24E-16		
Q9JLH8	Tropomodulin-4	6.64	1.24E-16		
Q9D6F9	Tubulin beta-4A chain	6.64	1.24E-16		
Q8C7R4	Ubiquitin-like modifier-activating enzyme 6	6.64	1.24E-16		
Q922Y1	UBX domain-containing protein 1	6.64	1.24E-16		
Q8BWQ6	UPF0505 protein C16orf62 homolog	6.64	1.24E-16		
P63044	Vesicle-associated membrane protein 2	6.64	1.24E-16		
Q8BVE3	V-type proton ATPase subunit H	6.64	1.24E-16		
Q80Y81	Zinc phosphodiesterase ELAC protein 2	6.64	1.24E-16		
Q9CQJ1	HIG1 domain family member 2A	5.3	0.0001		
Q9JHU9	Inositol-3-phosphate synthase 1	3.98	0.0003		
P36536	GTP-binding protein SAR1a	3.87	1.24E-16		
Q5DTJ9	Myopalladin	3.75	1.24E-16	-0.76	2.46E-02
P61014	Cardiac phospholamban	3.52	3.31E-16	3.52	3.31E-16
Q5SX39	Myosin-4	3.32	1.24E-16	0.50	2.51E-02
Q9D0M5	Dynein light chain 2, cytoplasmic	3.29	1.24E-16		
Q8BK63	Casein kinase I isoform alpha	3.28	0.0143		
Q8JZU0	Nucleoside diphosphate-linked moiety X motif 13	3.28	0.0100		
P85094	Isochorismatase domain-containing protein 2A	3.24	1.24E-16		
Q8K2I3	Dimethylaniline monooxygenase [N-oxide-forming] 2	3.23	0.0115		
P63260	Actin, cytoplasmic 2	3.21	5.42E-11		
Q3TVI8	Pre-B-cell leukemia transcription factor-interacting protein 1	3.09	4.24E-05		
A6H8H2	DENN domain-containing protein 4C	3.07	0.0331		
Q91YX5	Acyl-CoA:lysophosphatidylglycerol acyltransferase	2.98	2.32E-06		
Q61160	FAS-associated death domain protein	2.98	0.0050		
Q91XL9	Oxysterol-binding protein-related protein 1	2.95	0.0022		
O89017	Legumain	2.93	0.0168		
Q7TMB8	Cytoplasmic FMR1-interacting protein 1	2.91	1.94E-05		
Q9CRB8	Mitochondrial fission process protein 1	2.89	1.24E-16		
O35972	39S ribosomal protein L23, mitochondrial	2.87	9.62E-07		
O88967	ATP-dependent zinc metalloprotease	2.84	0.0002		
Q61735	Leukocyte surface antigen CD47	2.84	1.17E-13		
Q8C3X8	Lipase maturation factor 2	2.84	0.0089		
Q8R404	MICOS complex subunit MIC13	2.81	1.24E-16		
Q9CR60	Vesicle transport protein GOT1B	2.81	0.0009		
COHKE1	Histone H2A type 1-B	2.75	5.60E-11		
Q922U2	Keratin, type II cytoskeletal 5	2.71	5.04E-09		

Table B.1 continued

Accession no:	Description	Proteome		Phosphoproteome	
		Fold change	Adj. P-Value	Fold change	Adj. P-Value
Q8CFI5	Probable proline--tRNA ligase, mitochondrial	2.7	0.0252		
Q9CQZ1	Heat shock factor-binding protein 1 LisH domain and HEAT repeat-containing protein	2.65	2.88E-05		
Q148V7	KIAA1468	2.62	0.0001		
Q8BU31	Ras-related protein Rap-2c	2.59	0.0061		
Q6IR34	G-protein-signaling modulator 1 (E3-independent) E2 ubiquitin-conjugating enzyme	2.55	6.81E-09	1.21	5.47E-03
Q6ZPJ3	UBE2O	2.55	0.0053	-6.64	3.31E-16
Q3TBW2	39S ribosomal protein L10, mitochondrial	2.47	1.36E-06		
Q6PHN9	Ras-related protein Rab-35	2.47	0.0001		
Q60770	Syntaxin-binding protein 3	2.47	0.0075		
P60710	Actin, cytoplasmic 1	2.39	2.27E-12	-0.97	1.78E-02
Q8VED5	Keratin, type II cytoskeletal 79	2.39	0.0003		
Q99JB2	Stomatin-like protein 2, mitochondrial	2.35	0.0215		
Q91VH6	Protein MEMO1	2.34	2.26E-07		
Q8BTJ4	Bis(5'-adenosyl)-triphosphatase enpp4	2.33	0.0234		
Q9D883	Splicing factor U2AF 35 kDa subunit	2.32	0.0177		
Q07813	Apoptosis regulator BAX	2.31	1.64E-14		
Q80TL7	Protein MON2 homolog	2.28	0.0349		
P28658	Ataxin-10	2.26	0.0001		
Q8C0C7	Phenylalanine--tRNA ligase alpha subunit	2.26	5.98E-07		
Q8VHY0	Chondroitin sulfate proteoglycan 4	2.25	0.0072		
Q9QZN4	F-box only protein 6	2.25	0.0020		
P62254	Ubiquitin-conjugating enzyme E2	2.22	0.0011		
Q8K3W0	BRISC and BRCA1-A complex member 2	2.21	0.0049		
Q8R1H0	Homeodomain-only protein Mitochondrial import inner membrane translocase subunit TIM16	2.2	0.0004		
Q9CQV1	Transcription factor BTF3	2.2	1.77E-06		
Q64152	Nesprin-2	2.2	7.74E-07		
Q6ZWQ0	Nesprin-2	2.18	2.41E-05		
Q61599	Rho GDP-dissociation inhibitor 2	2.17	0.0003		
P59017	Bcl-2-like protein	2.13	2.66E-06		
Q61532	Mitogen-activated protein kinase 6	2.13	0.0439		
Q99PP7	E3 ubiquitin-protein ligase TRIM33	2.12	0.0246		
P49442	Inositol polyphosphate 1-phosphatase	2.12	0.0001		
Q9CZR2	N-acetylated-alpha-linked acidic dipeptidase 2	2.12	0.0073		
P49722	Proteasome subunit alpha type-2	2.12	0.0001		
P47955	60S acidic ribosomal protein P1	2.1	2.57E-10		
Q9EP89	Serine beta-lactamase-like protein LACTB, mitochondrial	2.09	0.0003		
P97355	Spermine synthase	2.07	1.12E-05		
Q99J36	THUMP domain-containing protein 1 NADH dehydrogenase [ubiquinone] 1 alpha subcomplex subunit 3	2.06	3.36E-08		
Q9CQ91	Calcium-independent phospholipase A2-gamma	2.05	2.21E-09		
Q8K1N1	Astrocytic phosphoprotein PEA-15	2	1.83E-07		

Table B.1 continued

Accession no:	Description	Proteome		Phosphoproteome	
		Fold change	Adj. P-Value	Fold change	Adj. P-Value
Q8K310	Matrin-3	1.99	3.19E-06		
Q9WUM4	Coronin-1C	1.95	0.0052		
Q9Z2A5	Arginyl-tRNA--protein transferase 1	1.93	0.0003		
Q9EPN1	Neurobeachin	1.92	0.0001		
Q8BWZ3	N-alpha-acetyltransferase 25, NatB auxiliary subunit	1.91	0.0203		
P61971	Nuclear transport factor 2	1.91	7.15E-11		
Q8BFZ3	Beta-actin-like protein 2	1.9	7.62E-12		
Q4KML4	Costars family protein ABRACL	1.9	0.0002		
P99028	Cytochrome b-c1 complex subunit 6, mitochondrial	1.9	5.65E-08		
P00397	Cytochrome c oxidase subunit 1	1.88	9.24E-08		
Q64310	Surfeit locus protein 4	1.88	4.66E-05		
Q8VDP6	CDP-diacylglycerol--inositol 3-phosphatidyltransferase	1.86	0.0013		
Q91YP2	Neurolysin, mitochondrial	1.85	0.0045		
P19123	Troponin C, slow skeletal and cardiac muscles	1.85	1.63E-07		
Q8BH53	Cilia- and flagella-associated protein 69	1.84	0.0146		
Q91VW5	Golgin subfamily A member 4	1.83	0.0002		
Q9QVP4	Myosin regulatory light chain 2, atrial isoform	1.83	2.16E-07		
Q60715	Prolyl 4-hydroxylase subunit alpha-1	1.81	0.0123		
P50285	Dimethylaniline monooxygenase [N-oxide-forming] 1	1.78	0.0002		
Q9QZE5	Coatomer subunit gamma-1	1.75	0.0002		
Q80XN0	D-beta-hydroxybutyrate dehydrogenase, mitochondrial	1.75	8.08E-07		
Q9CX60	Protein LBH	1.75	0.0372		
Q8VCF0	Mitochondrial antiviral-signaling protein	1.74	1.78E-05		
P56392	Cytochrome c oxidase subunit 7A1, mitochondrial	1.73	0.0003		
P54310	Hormone-sensitive lipase	1.73	0.0255		
Q7TMY8	E3 ubiquitin-protein ligase HECTD1	1.72	0.0271		
P62267	40S ribosomal protein S23	1.7	0.0001		
P05125	Natriuretic peptides A	1.68	2.79E-06		
O89079	Coatomer subunit epsilon	1.66	0.0007		
P55772	Ectonucleoside triphosphate diphosphohydrolase 1	1.64	0.0004		
P28656	Nucleosome assembly protein 1-like 1	1.63	0.0010		
P51125	Calpastatin	1.6	1.87E-05	0.82	3.12E-02
Q8WUR0	Protein C19orf12 homolog	1.6	0.0051		
P47753	F-actin-capping protein subunit alpha-1	1.57	0.0064		
Q9DCT2	NADH dehydrogenase [ubiquinone] iron-sulfur protein 3, mitochondrial	1.57	1.54E-05		
Q9WV35	C->U-editing enzyme APOBEC-2	1.56	0.0001		
Q9CQ92	Mitochondrial fission 1 protein	1.56	9.98E-08		
P63028	Translationally-controlled tumor protein	1.56	8.34E-06		
Q9DB29	Isoamyl acetate-hydrolyzing esterase 1 homolog	1.55	0.0022		
P61922	4-aminobutyrate aminotransferase, mitochondrial	1.54	0.0271		
P50543	Protein S100-A11	1.54	0.0078		
Q3TW96	UDP-N-acetylhexosamine pyrophosphorylase-like protein 1	1.54	0.0159		

Table B.1 continued

Accession no:	Description	Proteome		Phosphoproteome	
		Fold change	Adj. P-Value	Fold change	Adj. P-Value
Q9DCS3	Enoyl-[acyl-carrier-protein] reductase, mitochondrial	1.53	1.14E-07		
P61164	Alpha-centractin	1.52	5.24E-07		
P39054	Dynamin-2	1.51	0.0001		
P62301	40S ribosomal protein S13	1.5	6.30E-07		
O88587	Catechol O-methyltransferase	1.46	1.14E-06		
Q9DBG7	Signal recognition particle receptor subunit alpha	1.46	0.0345		
P68368	Tubulin alpha-4A chain	1.45	0.0001		
P18826	Phosphorylase b kinase regulatory subunit alpha, skeletal muscle isoform	1.43	0.0251		
Q9D0G0	28S ribosomal protein S30, mitochondrial	1.42	0.0275		
P61924	Coatomer subunit zeta-1	1.42	0.0164		
Q9DBL9	1-acylglycerol-3-phosphate O-acyltransferase ABHD5	1.41	0.0294		
P97370	Sodium/potassium-transporting ATPase subunit beta-3	1.41	0.0044		
Q9D1C8	Vacuolar protein sorting-associated protein 28 homolog	1.41	0.0119		
P09541	Myosin light chain 4	1.39	0.0002		
Q80UY2	E3 ubiquitin-protein ligase HUWE1	1.38	0.0004		
Q922E6	FAST kinase domain-containing protein 2, mitochondrial	1.38	0.0305		
O35658	Complement component 1 Q subcomponent-binding protein, mitochondrial	1.37	0.0003		
O54734	Dolichyl-diphosphooligosaccharide--protein glycosyltransferase 48 kDa subunit	1.37	0.0010		
Q5SSK3	Transcription elongation factor, mitochondrial	1.36	0.0066		
P35585	AP-1 complex subunit mu-1	1.33	0.0466		
Q9D7A8	Armadillo repeat-containing protein 1	1.33	0.0002		
Q9JJZ2	Tubulin alpha-8 chain	1.33	8.84E-06		
O70194	Eukaryotic translation initiation factor 3 subunit D	1.32	0.0021		
Q8BZA9	Fructose-2,6-bisphosphatase TIGAR	1.3	0.0007		
P13541	Myosin-3	1.3	0.0362		
P62631	Elongation factor 1-alpha 2	1.29	0.0007		
Q9CPQ3	Mitochondrial import receptor subunit TOM22 homolog	1.29	3.90E-05		
Q9D0L4	Uncharacterized aarF domain-containing protein kinase 1	1.29	4.81E-05		
P63330	Serine/threonine-protein phosphatase 2A catalytic subunit alpha isoform	1.28	0.0004		
Q7TPR4	Alpha-actinin-1	1.26	0.0017		
Q9CPU4	Microsomal glutathione S-transferase 3	1.26	0.0003		
Q61301	Catenin alpha-2	1.25	0.0324		
Q08857	Platelet glycoprotein 4	1.24	0.0013		
P97493	Thioredoxin, mitochondrial	1.24	0.0032		
P70265	6-phosphofructo-2-kinase/fructose-2,6-bisphosphatase 2	1.23	0.0084		
Q9WVT6	Carbonic anhydrase 14	1.21	0.0303		
Q9DBG6	Dolichyl-diphosphooligosaccharide--protein glycosyltransferase subunit 2	1.21	0.0008		
P55096	ATP-binding cassette sub-family D member 3	1.2	0.0002		
P00405	Cytochrome c oxidase subunit 2	1.2	0.0023		

Table B.1 continued

Accession no:	Description	Proteome		Phosphoproteome	
		Fold change	Adj. P-Value	Fold change	Adj. P-Value
P03893	NADH-ubiquinone oxidoreductase chain 2	1.2	0.0002		
Q8VCA8	Secernin-2	1.19	0.0100		
Q8BJZ4	28S ribosomal protein S35, mitochondrial	1.18	0.0111		
P36536	GTP-binding protein SAR1a	1.17	0.0439		
Q3U7R1	Extended synaptotagmin-1	1.16	0.0311		
Q9Z2D6	Methyl-CpG-binding protein 2	1.16	0.0016		
P70404	Isocitrate dehydrogenase [NAD] subunit gamma 1, mitochondrial	1.15	0.0038		
Q60870	Receptor expression-enhancing protein 5	1.15	0.0031		
Q8VE95	UPF0598 protein C8orf82 homolog	1.13	0.0003		
P34914	Bifunctional epoxide hydrolase 2	1.12	0.0052		
P49138	MAP kinase-activated protein kinase 2	1.12	0.0491		
Q9CPQ8	ATP synthase subunit g, mitochondrial	1.11	0.0059		
P80314	T-complex protein 1 subunit beta	1.11	0.0028		
P62821	Ras-related protein Rab-1A	1.1	0.0062		
P51667	Myosin regulatory light chain 2, ventricular/cardiac muscle isoform	1.09	0.0069	0.64	9.92E-03
Q03265	ATP synthase subunit alpha, mitochondrial	1.09	0.0074		
Q9WVC3	Caveolin-2	1.09	0.0480		
P06801	NADP-dependent malic enzyme	1.08	0.0033		
Q99LC8	Translation initiation factor eIF-2B subunit alpha	1.08	0.0075		
P61982	14-3-3 protein gamma	1.07	0.0087		
P59017	Bcl-2-like protein 13	1.05	0.0061	0.49	2.82E-02
Q14C51	Pentatricopeptide repeat domain-containing protein 3, mitochondrial	1.05	0.0022		
P63268	Actin, gamma-enteric smooth muscle	1.04	0.0117		
Q9CZR8	Elongation factor Ts, mitochondrial	1.03	0.0137		
P23242	Gap junction alpha-1 protein	1.02	0.0143	1.17	1.15E-02
Q9D1A2	Cytosolic non-specific dipeptidase	1.02	0.0005		
Q9CQ65	S-methyl-5'-thioadenosine phosphorylase	1.01	0.0167		
P58771	Tropomyosin alpha-1 chain	1	0.0165		
P62830	60S ribosomal protein L23	0.99	0.0012		
Q9CR68	Cytochrome b-c1 complex subunit Rieske, mitochondrial	0.99	0.0147		
P62880	Guanine nucleotide-binding protein G(I)/G(S)/G(T) subunit beta-2	0.98	0.0011		
Q9D7N3	28S ribosomal protein S9, mitochondrial	0.97	0.0113		
Q80Y14	Glutaredoxin-related protein 5, mitochondrial	0.97	0.0155		
Q1XH17	Tripartite motif-containing protein 72	0.97	0.0229		
P54775	26S proteasome regulatory subunit 6B	0.96	0.0059		
Q9D1X0	Nucleolar protein 3	0.96	0.0016		
Q8BG95	Protein phosphatase 1 regulatory subunit 12B	0.96	0.0481		
O09111	NADH dehydrogenase [ubiquinone] 1 beta subcomplex subunit 11, mitochondrial	0.95	0.0271		
A6H6E2	Multimerin-2	0.94	0.0287		
Q9CR21	Acyl carrier protein, mitochondrial	0.93	0.0331		

Table B.1 continued

Accession no:	Description	Proteome		Phosphoproteome	
		Fold change	Adj. P-Value	Fold change	Adj. P-Value
Q04447	Creatine kinase B-type	0.92	0.0347		
P43023	Cytochrome c oxidase subunit 6A2, mitochondrial	0.92	0.0347		
Q9D0S9	Histidine triad nucleotide-binding protein 2, mitochondrial	0.91	0.0358		
Q9D1G1	Ras-related protein Rab-1B	0.91	0.0031		
O88746	Target of Myb protein 1	0.91	0.0192		
Q8BWM0	Prostaglandin E synthase 2	0.9	0.0134		
O35381	Acidic leucine-rich nuclear phosphoprotein 32 family member A	0.89	0.0071		
P56480	ATP synthase subunit beta, mitochondrial	0.89	0.0434		
O88487	Cytoplasmic dynein 1 intermediate chain 2	0.89	0.0100		
P54797	Transport and Golgi organization 2 homolog	0.89	0.0121		
G5E829	Plasma membrane calcium-transporting ATPase 1	0.88	0.0253		
Q9Z2Q5	39S ribosomal protein L40, mitochondrial	0.86	0.0100		
Q9DCB8	Iron-sulfur cluster assembly 2 homolog, mitochondrial	0.85	0.0115		
Q3UHB1	5'-nucleotidase domain-containing protein 3	0.84	0.0424		
P62806	Histone H4	0.84	0.0225		
P38060	Hydroxymethylglutaryl-CoA lyase, mitochondrial	0.83	0.0197		
O35343	Importin subunit alpha-3	0.82	0.0427		
Q9ES82	Popeye domain-containing protein 2	0.8	0.0263		
Q00519	Xanthine dehydrogenase/oxidase	0.8	0.0137		
P62855	40S ribosomal protein S26	0.79	0.0367		
Q8R0F8	Acylpyruvase FAHD1, mitochondrial	0.79	0.0288		
Q7TMM9	Tubulin beta-2A chain	0.78	0.0401		
P03893	NADH-ubiquinone oxidoreductase chain 2	0.76	0.0125		
Q7TMY8	E3 ubiquitin-protein ligase HUWE1	0.75	0.0148		
P05977	Myosin light chain 1/3, skeletal muscle isoform	0.75	0.0295		
P11531	Dystrophin	0.74	0.0415		
Q6PDI5	Proteasome adapter and scaffold protein ECM29	0.74	0.0409		
Q61234	Alpha-1-syntrophin	0.71	0.0488		
A2APY7	Arginine-hydroxylase NDUFAF5, mitochondrial	0.71	0.0222		
P62751	60S ribosomal protein L23a	0.7	0.0005		
Q9QZ57	Heat shock protein beta-3 OS	0.67	0.0360		
Q01815	Voltage-dependent L-type calcium channel subunit alpha-1	0.67	0.0044		
Q8BL97	Serine/arginine-rich splicing factor 7	0.64	0.0003		
P62082	40S ribosomal protein S7	0.63	0.0373		
Q8K3W2	Leucine-rich repeat-containing protein 10	0.63	0.0174		
P62242	40S ribosomal protein S8	0.62	0.0003		
O08583	THO complex subunit 4	0.61	0.0076		
Q8R4S0	Protein phosphatase 1 regulatory subunit 14C	0.6	0.0060		
P56812	Programmed cell death protein 5	0.58	0.0007		
Q8BSY0	Aspartyl/asparaginyl beta-hydroxylase	0.5	0.0260		
Q8QZS1	3-hydroxyisobutyryl-CoA hydrolase, mitochondrial	0.49	0.0279		

Table B.1 continued

Accession no:	Description	Proteome		Phosphoproteome	
		Fold change	Adj. P-Value	Fold change	Adj. P-Value
P12787	Cytochrome c oxidase subunit 5A, mitochondrial	0.49	0.0203		
Q9DBZ5	Eukaryotic translation initiation factor 3 subunit K	0.49	0.0224		
Q91VK1	Basic leucine zipper and W2 domain-containing protein 2 Protein S100-A1 OS=Mus musculus OX=10090	0.46	0.0380		
P56565	GN=S100a1 PE=1 SV=2	0.46	0.0212		
Q9Z210	Peroxisomal membrane protein 11B	0.41	0.0237		
Q62417	Sorbin and SH3 domain-containing protein 1	0.4	0.0306	0.40	2.53E-02
P61087	Ubiquitin-conjugating enzyme E2	0.36	0.0231		
Q6ZWW3	60S ribosomal protein L10	0.35	0.0360		
P84084	ADP-ribosylation factor 5 Ubiquinol-cytochrome-c reductase complex assembly	0.34	0.0030		
Q9CQY6	factor 2	0.33	0.0299		
P48962	ADP/ATP translocase 1	0.32	0.0479	0.32	4.79E-02
O08715	A-kinase anchor protein 1, mitochondrial	0.32	0.0239		
P50462	Cysteine and glycine-rich protein 3	0.29	0.0030	0.63	2.95E-02
Q99KJ8	Dynactin subunit 2 NADH dehydrogenase [ubiquinone] 1 beta subcomplex subunit 5, mitochondrial OS=Mus musculus OX=10090	0.29	0.0031		
Q9CQH3	GN=Ndufb5 PE=1 SV=1	0.28	0.0230	0.48	4.94E-03
P56135	ATP synthase subunit f, mitochondrial	0.28	0.0089		
Q8BMS4	Ubiquinone biosynthesis O-methyltransferase, mitochondrial	0.26	0.0031		
Q9DCT8	Cysteine-rich protein 2	0.24	0.0173		
P11404	Fatty acid-binding protein, heart	0.23	0.0102	1.08	2.46E-02
Q9JJI8	60S ribosomal protein L38	0.22	0.0069		
Q99NB1	Acetyl-coenzyme A synthetase 2-like, mitochondrial	0.15	0.0330		
Q924X2	Carnitine O-palmitoyltransferase 1, muscle isoform	0.14	0.0336		
Q9D8Y1	Transmembrane protein 126A	0.13	0.0230		
P21107	Tropomyosin alpha-3 chain	0.13	0.0147		
P62897	Cytochrome c, somatic	0.11	0.0039		
P47857	ATP-dependent 6-phosphofructokinase, muscle type	0.07	0.0397		
P19783	Cytochrome c oxidase subunit 4 isoform 1, mitochondrial	-0.07	0.0472		
Q78IK2	Up-regulated during skeletal muscle growth protein 5	-0.08	0.0412		
Q99020	Heterogeneous nuclear ribonucleoprotein A/B NADH dehydrogenase [ubiquinone] 1 beta subcomplex	-0.09	0.0290		
Q9CQZ6	subunit 3 NADH dehydrogenase [ubiquinone] 1 alpha subcomplex	-0.09	0.0005		
Q9D8B4	subunit 11	-0.11	0.0294		
Q62234	Myomesin-1	-0.12	0.0081	-1.41	6.97E-03
P19157	Glutathione S-transferase P 1 NADH dehydrogenase [ubiquinone] 1 alpha subcomplex	-0.12	0.0494		
Q9DC69	subunit 9, mitochondrial	-0.12	0.0184		
Q8CGB6	Tensin-2	-0.13	0.0313		
P48787	Troponin I, cardiac muscle	-0.13	0.0160		
Q9JI91	Alpha-actinin-2	-0.14	0.0224		
Q8BZF8	Phosphoglucosyltransferase-like protein 5	-0.14	0.0139		

Table B.1 continued

Accession no:	Description	Proteome		Phosphoproteome	
		Fold change	Adj. P-Value	Fold change	Adj. P-Value
Q7TMF3	NADH dehydrogenase [ubiquinone] 1 alpha subcomplex subunit 12	-0.15	0.0474		
P62071	Ras-related protein R-Ras2	-0.15	0.0355		
P50752	Troponin T, cardiac muscle	-0.15	0.0346		
Q9CQQ7	ATP synthase F(0) complex subunit B1, mitochondrial	-0.16	0.0113		
Q9CZ13	Cytochrome b-c1 complex subunit 1, mitochondrial	-0.16	0.0208		
Q8BLF1	Neutral cholesterol ester hydrolase 1	-0.16	0.0143		
Q8BWB1	Synaptopodin 2-like protein	-0.16	0.0325		
Q01853	Transitional endoplasmic reticulum ATPase	-0.16	0.0024		
Q8BH59	Calcium-binding mitochondrial carrier protein Aralar1	-0.17	0.0022		
Q8VEK3	Heterogeneous nuclear ribonucleoprotein U	-0.17	0.0377		
P57776	Elongation factor 1-delta	-0.18	0.0035		
P54071	Isocitrate dehydrogenase [NADP], mitochondrial	-0.18	0.0042		
P16125	L-lactate dehydrogenase B chain	-0.19	0.0429	0.91	3.65E-02
P47963	60S ribosomal protein L13	-0.19	0.0386		
Q8CI94	Glycogen phosphorylase, brain form	-0.19	0.0018		
Q9D0F9	Phosphoglucomutase-1	-0.19	0.0465		
Q9JIW9	Ras-related protein Ral-B	-0.19	0.0076		
Q91ZA3	Propionyl-CoA carboxylase alpha chain, mitochondrial	-0.2	0.0229	-1.38	1.91E-02
Q9Z1J3	Cysteine desulfurase, mitochondrial	-0.2	0.0493		
O35459	Delta(3,5)-Delta(2,4)-dienoyl-CoA isomerase, mitochondrial	-0.2	0.0439		
P97443	Histone-lysine N-methyltransferase	-0.2	0.0151		
Q99LY9	NADH dehydrogenase [ubiquinone] iron-sulfur protein 5	-0.2	0.0090		
P97371	Proteasome activator complex subunit 1	-0.2	0.0237		
Q8K0Z7	Translational activator of cytochrome c oxidase 1	-0.2	0.0102		
Q9Z0S1	3'(2'),5'-bisphosphate nucleotidase 1	-0.21	0.0398		
P03930	ATP synthase protein 8	-0.21	0.0043		
Q91VT4	Carbonyl reductase family member 4	-0.21	0.0326		
Q9D2G2	Dihydrolipoyllysine-residue succinyltransferase component of 2-oxoglutarate dehydrogenase complex, mitochondrial	-0.21	0.0442		
Q9CQC7	NADH dehydrogenase [ubiquinone] 1 beta subcomplex subunit 4	-0.21	0.0261		
Q922R8	Protein disulfide-isomerase A6	-0.21	0.0073		
Q64737	Trifunctional purine biosynthetic protein adenosine-3	-0.21	0.0258		
Q9CQ69	Cytochrome b-c1 complex subunit 8	-0.22	0.0016		
P05064	Fructose-bisphosphate aldolase A	-0.22	0.0090		
Q9CQ54	NADH dehydrogenase [ubiquinone] 1 subunit C2	-0.22	0.0017		
P14148	60S ribosomal protein L7	-0.23	0.0227		
Q9CZU6	Citrate synthase, mitochondrial	-0.23	0.0213		
Q9D1L0	Coiled-coil-helix-coiled-coil-helix domain-containing protein 2	-0.23	0.0081		
Q8CAQ8	MICOS complex subunit Mic60	-0.23	0.0142		
Q7TQ48	Sarcalumenin	-0.24	0.0016	3.04	1.28E-06

Table B.1 continued

Accession no:	Description	Proteome		Phosphoproteome	
		Fold change	Adj. P-Value	Fold change	Adj. P-Value
Q8BFP9	[Pyruvate dehydrogenase (acetyl-transferring)] kinase isozyme 1, mitochondrial	-0.24	0.0071		
Q99N94	39S ribosomal protein L9, mitochondrial	-0.24	0.0234		
Q9D7J4	Cytochrome c oxidase assembly protein COX20, mitochondrial	-0.24	0.0079		
Q9DCM2	Glutathione S-transferase kappa 1	-0.24	0.0091		
Q9CQN1	Heat shock protein 75 kDa, mitochondrial	-0.24	0.0048		
Q78IK4	MICOS complex subunit Mic27	-0.24	0.0011		
Q8VEM8	Phosphate carrier protein, mitochondrial	-0.24	0.0003		
Q99PT1	Rho GDP-dissociation inhibitor 1	-0.24	0.0214		
P38647	Stress-70 protein, mitochondrial	-0.24	0.0426		
Q9CXV1	Succinate dehydrogenase [ubiquinone] cytochrome b small subunit, mitochondrial	-0.24	0.0332		
P14131	40S ribosomal protein S16	-0.25	0.0271		
Q99JY9	Actin-related protein 3	-0.25	0.0154		
P47934	Carnitine O-acetyltransferase	-0.25	0.0184		
Q9QYB1	Chloride intracellular channel protein 4	-0.25	0.0080		
Q9R0H0	Peroxisomal acyl-coenzyme A oxidase 1	-0.25	0.0079		
Q8BGH2	Sorting and assembly machinery component 50 homolog	-0.25	0.0175		
Q9D2R6	Cytochrome c oxidase assembly factor 3 homolog, mitochondrial	-0.26	0.0313		
Q9CPU0	Lactoylglutathione lyase	-0.26	0.0421		
Q9CPU2	NADH dehydrogenase [ubiquinone] 1 beta subcomplex subunit 2, mitochondrial	-0.26	0.0290		
Q9WU78	Programmed cell death 6-interacting protein	-0.26	0.0368		
P67778	Prohibitin	-0.26	0.0470		
P52479	Ubiquitin carboxyl-terminal hydrolase 10	-0.26	0.0350		
O88685	26S proteasome regulatory subunit 6A	-0.27	0.0079		
Q9DB77	Cytochrome b-c1 complex subunit 2, mitochondrial	-0.27	3.57E-05		
Q5M8N4	Epimerase family protein SDR39U1	-0.27	0.0010		
P63017	Heat shock cognate 71 kDa protein	-0.27	0.0084		
Q7TPW1	Nexilin	-0.27	0.0225		
Q6P1F6	Serine/threonine-protein phosphatase 2A 55 kDa regulatory subunit B alpha	-0.27	0.0110		
Q9CQA3	Succinate dehydrogenase [ubiquinone] iron-sulfur subunit, mitochondrial	-0.27	0.0203		
Q8R1S0	Ubiquinone biosynthesis monooxygenase COQ6, mitochondrial	-0.27	0.0484		
Q9CQW2	ADP-ribosylation factor-like protein 8B	-0.28	0.0053		
Q9D5T0	ATPase family AAA domain-containing protein 1	-0.28	0.0080		
P42125	Enoyl-CoA delta isomerase 1, mitochondrial	-0.28	0.0024		
P26041	Moesin OS=Mus musculus OX=10090 GN=Msn PE=1 SV=3	-0.28	0.0026		
Q02566	Myosin-6 OS=Mus musculus OX=10090 GN=Myh6 PE=1 SV=2	-0.28	0.0149		
Q02053	Ubiquitin-like modifier-activating enzyme 1	-0.28	0.0016		
Q9DCX2	ATP synthase subunit d, mitochondrial	-0.29	0.0388	6.64	3.31E-16
P19253	60S ribosomal protein L13a	-0.29	0.0143		

Table B.1 continued

Accession no:	Description	Proteome		Phosphoproteome	
		Fold change	Adj. P-Value	Fold change	Adj. P-Value
P21550	Beta-enolase	-0.29	0.0138		
O35855	Branched-chain-amino-acid aminotransferase, mitochondrial	-0.29	0.0234		
Q8BMF4	Dihydrolipoyllysine-residue acetyltransferase component of pyruvate dehydrogenase complex, mitochondrial	-0.29	0.0041		
Q3ULJ0	Glycerol-3-phosphate dehydrogenase 1-like protein	-0.29	0.0009		
Q9WVLO	Maleylacetoacetate isomerase	-0.29	0.0071		
P51660	Peroxisomal multifunctional enzyme type 2	-0.29	0.0023		
Q9D0F3	Protein ERGIC-53	-0.29	0.0131		
P62889	60S ribosomal protein L30	-0.3	0.0075		
Q07076	Annexin A7	-0.3	0.0244		
P62869	Elongin-B	-0.3	0.0091		
Q9Z0N1	Eukaryotic translation initiation factor 2 subunit 3, X-linked	-0.3	0.0178		
Q9R0N0	Galactokinase	-0.3	0.0155		
P35486	Pyruvate dehydrogenase E1 component subunit alpha, somatic form, mitochondrial	-0.31	0.0068	-1.34	1.87E-02
Q9CQV8	14-3-3 protein beta/alpha	-0.31	0.0224		
P0DP26	Calmodulin-1	-0.31	0.0053		
Q9DCZ4	MICOS complex subunit Mic26	-0.31	0.0430		
Q9Z2Z6	Mitochondrial carnitine/acylcarnitine carrier protein	-0.31	0.0084		
Q9JJW5	Myozenin-2	-0.31	0.0010		
Q8K411	Presequence protease, mitochondrial	-0.31	0.0052		
Q91VI7	Ribonuclease inhibitor	-0.31	0.0014		
P09671	Superoxide dismutase [Mn], mitochondrial	-0.31	0.0039		
Q64727	Vinculin	-0.32	0.0402	1.66	1.22E-02
Q9D404	3-oxoacyl-[acyl-carrier-protein] synthase, mitochondrial	-0.32	0.0470		
O54724	Caveolae-associated protein 1	-0.32	0.0094		
Q8CIE6	Coatomer subunit alpha	-0.32	0.0071		
P06151	L-lactate dehydrogenase A chain	-0.32	0.0003		
P46638	Ras-related protein Rab-11B	-0.32	0.0030		
P26638	Serine--tRNA ligase, cytoplasmic	-0.32	0.0222		
P17751	Triosephosphate isomerase	-0.32	0.0402		
Q8VDN2	Sodium/potassium-transporting ATPase subunit alpha-1	-0.33	0.0041	0.57	6.31E-03
Q9CQ62	2,4-dienoyl-CoA reductase, mitochondrial	-0.33	0.0155		
P62852	40S ribosomal protein S25	-0.33	0.0049		
Q9Z0X1	Apoptosis-inducing factor 1, mitochondrial	-0.33	0.0115		
Q9D7X3	Dual specificity protein phosphatase 3	-0.33	0.0034		
P58252	Elongation factor 2	-0.33	0.0336		
P24472	Glutathione S-transferase A4	-0.33	0.0064		
P51859	Hepatoma-derived growth factor	-0.33	0.0014		
P49443	Protein phosphatase 1A	-0.33	0.0453		
Q91V41	Ras-related protein Rab-14	-0.33	0.0151		

Table B.1 continued

Accession no:	Description	Proteome		Phosphoproteome	
		Fold change	Adj. P-Value	Fold change	Adj. P-Value
Q9CZB0	Succinate dehydrogenase cytochrome b560 subunit, mitochondrial	-0.33	0.0045		
Q9D517	1-acyl-sn-glycerol-3-phosphate acyltransferase gamma	-0.34	0.0398		
P97461	40S ribosomal protein S5	-0.34	0.0191		
O35435	Dihydroorotate dehydrogenase (quinone), mitochondrial	-0.34	0.0096		
Q9DBJ1	Phosphoglycerate mutase 1	-0.34	0.0077		
Q921G7	Electron transfer flavoprotein-ubiquinone oxidoreductase, mitochondrial	-0.35	0.0041	0.53	1.39E-03
Q6ZWN5	40S ribosomal protein S9	-0.35	0.0079		
P05202	Aspartate aminotransferase, mitochondrial	-0.35	0.0071		
Q60649	Caseinolytic peptidase B protein homolog	-0.35	0.0377		
Q3UMF0	Cordon-bleu protein-like 1	-0.35	0.0459		
O08749	Dihydrolipoyl dehydrogenase, mitochondrial	-0.35	0.0078		
P62827	GTP-binding nuclear protein Ran	-0.35	0.0130		
Q61699	Heat shock protein 105 kDa	-0.35	0.0059		
Q9JKS4	LIM domain-binding protein 3	-0.35	0.0043		
O35386	Phytanoyl-CoA dioxygenase, peroxisomal	-0.35	0.0452		
Q8VDQ1	Prostaglandin reductase 2	-0.35	0.0035		
Q9ERI6	Retinol dehydrogenase 14	-0.35	0.0215		
P42225	Signal transducer and activator of transcription 1	-0.35	0.0353		
P62141	Serine/threonine-protein phosphatase PP1-beta catalytic subunit	-0.36	0.0068		
Q8BWF0	Succinate-semialdehyde dehydrogenase, mitochondrial	-0.36	0.0005		
P35564	Calnexin	-0.37	0.0225	-0.23	2.32E-02
P11499	Heat shock protein HSP 90-beta	-0.37	0.0008		
Q9Z2X1	Heterogeneous nuclear ribonucleoprotein	-0.37	0.0166		
Q91VM9	Inorganic pyrophosphatase 2, mitochondrial	-0.37	0.0125		
Q62159	Rho-related GTP-binding protein RhoC	-0.37	0.0165		
Q9CY27	Very-long-chain enoyl-CoA reductase	-0.37	0.0290		
Q9R0Q7	Prostaglandin E synthase 3	-0.38	0.0006		
Q9R1P3	Proteasome subunit beta type-2	-0.38	0.0037		
Q99MR9	Protein phosphatase 1 regulatory subunit 3A	-0.38	0.0459		
P68369	Tubulin alpha-1A chain	-0.38	0.0003		
Q9D6Y9	1,4-alpha-glucan-branching enzyme	-0.39	0.0021		
P62192	26S proteasome regulatory subunit 4	-0.39	0.0481		
P54822	Adenylosuccinate lyase	-0.39	0.0017		
O09174	Alpha-methylacyl-CoA racemase	-0.39	0.0011		
Q8R016	Bleomycin hydrolase	-0.39	0.0101		
P63094	Guanine nucleotide-binding protein G(s) subunit alpha isoforms short	-0.39	0.0162		
Q9D6R2	Isocitrate dehydrogenase [NAD] subunit alpha, mitochondrial	-0.39	0.0112		
Q791V5	Mitochondrial carrier homolog 2	-0.39	0.0046		
Q8VDC0	Probable leucine--tRNA ligase, mitochondrial	-0.39	0.0010		
Q99JI4	26S proteasome non-ATPase regulatory subunit 6	-0.4	0.0429		

Table B.1 continued

Accession no:	Description	Proteome		Phosphoproteome	
		Fold change	Adj. P-Value	Fold change	Adj. P-Value
Q8BP67	60S ribosomal protein L24	-0.4	0.0099		
A2A5R2	Brefeldin A-inhibited guanine nucleotide-exchange protein 2	-0.4	0.0416		
P63073	Eukaryotic translation initiation factor 4E	-0.4	0.0056		
P10833	Ras-related protein R-Ras	-0.4	0.0318		
Q62384	Zinc finger protein ZPR1	-0.4	0.0222		
P14152	Malate dehydrogenase, cytoplasmic	-0.41	0.0237	1.87	6.78E-05
Q8K1M6	Dynamin-1-like protein	-0.41	0.0046		
O08709	Peroxiredoxin-6	-0.41	0.0138		
P07901	Heat shock protein HSP 90-alpha	-0.42	0.0008	6.64	3.31E-16
P53986	Monocarboxylate transporter 1	-0.42	0.0038	1.72	2.12E-02
Q91V16	Electron transfer flavoprotein regulatory factor 1	-0.42	0.0081		
P17710	Hexokinase-1	-0.42	0.0469		
Q60714	Long-chain fatty acid transport protein 1	-0.42	0.0333		
Q8BG51	Mitochondrial Rho GTPase 1	-0.42	0.0418		
Q9DC61	Mitochondrial-processing peptidase subunit alpha	-0.42	0.0090		
P47811	Mitogen-activated protein kinase 14	-0.42	0.0234		
Q60932	Voltage-dependent anion-selective channel protein 1	-0.42	0.0021		
P16546	Spectrin alpha chain, non-erythrocytic 1	-0.43	0.0004	-0.37	1.78E-02
O09161	Calsequestrin-2	-0.43	0.0009		
P82347	Delta-sarcoglycan	-0.43	0.0005		
P47757	F-actin-capping protein subunit beta	-0.43	0.0025		
Q922U0	Proteasome subunit alpha type-7	-0.43	0.0023		
P97351	40S ribosomal protein S3a	-0.44	0.0152	-6.64	3.31E-16
P18572	Basigin	-0.44	0.0060		
Q6ZWX6	Eukaryotic translation initiation factor 2 subunit	-0.44	0.0037		
P26443	Glutamate dehydrogenase 1, mitochondrial	-0.44	0.0161		
P14602	Heat shock protein beta-1	-0.44	0.0021		
Q64475	Histone H2B type 1-B	-0.44	0.0164		
P45952	Medium-chain specific acyl-CoA dehydrogenase, mitochondrial	-0.44	0.0003		
Q99JI6	Ras-related protein Rap-1b	-0.44	0.0193		
P61079	Ubiquitin-conjugating enzyme E2 D3	-0.44	0.0039		
Q9D832	DnaJ homolog subfamily B member 4	-0.45	0.0313		
Q8R2G4	Ecto-ADP-ribosyltransferase 3	-0.45	0.0152		
P24369	Peptidyl-prolyl cis-trans isomerase B	-0.45	0.0228		
P60867	40S ribosomal protein S20	-0.46	0.0055		
P60766	Cell division control protein 42 homolog	-0.46	0.0229		
Q9Z0Y1	Dynactin subunit 3	-0.46	0.0355		
P48774	Glutathione S-transferase Mu 5	-0.46	0.0048		
P49813	Tropomodulin-1	-0.46	0.0049		
P50136	2-oxoisovalerate dehydrogenase subunit alpha, mitochondrial	-0.47	0.0050	-1.36	1.59E-02
Q9CY64	Biliverdin reductase A	-0.47	0.0242		

Table B.1 continued

Accession no:	Description	Proteome		Phosphoproteome	
		Fold change	Adj. P-Value	Fold change	Adj. P-Value
Q71RI9	Kynurenine--oxoglutarate transaminase 3	-0.47	0.0131		
O88441	Metaxin-2	-0.47	0.0026		
O55143	Sarcoplasmic/endoplasmic reticulum calcium ATPase 2	-0.47	0.0004		
Q8C8R3	Ankyrin-2	-0.48	0.0041	0.52	3.97E-02
O35643	AP-1 complex subunit beta-1	-0.48	0.0156		
Q9D8N0	Elongation factor 1-gamma	-0.48	0.0001		
P20108	Thioredoxin-dependent peroxide reductase, mitochondrial	-0.48	0.0012		
Q9Z1Q9	Valine--tRNA ligase	-0.48	0.0006		
Q8VBT1	Beta-taxilin	-0.49	0.0069	0.96	9.82E-03
P48771	Cytochrome c oxidase subunit 7A2, mitochondrial	-0.49	0.0077		
Q9D7X8	Gamma-glutamylcyclotransferase	-0.49	0.0430		
Q3ULD5	Methylcrotonoyl-CoA carboxylase beta chain, mitochondrial	-0.49	0.0018		
Q9DCL9	Multifunctional protein ADE2	-0.49	0.0041		
O70250	Phosphoglycerate mutase 2	-0.49	0.0004		
Q3UIZ8	Myosin light chain kinase 3	-0.5	0.0044	6.64	3.31E-16
Q9WVJ2	26S proteasome non-ATPase regulatory subunit 13	-0.5	0.0184		
P62245	40S ribosomal protein S15a	-0.5	0.0062		
P62717	60S ribosomal protein L18a	-0.5	0.0049		
P17182	Alpha-enolase	-0.5	0.0041		
O08529	Calpain-2 catalytic subunit	-0.5	0.0230		
Q9JM76	Actin-related protein 2/3 complex subunit 3	-0.51	0.0322		
Q61553	Fascin	-0.51	0.0293		
P70168	Importin subunit beta-1	-0.51	0.0009		
Q9JLB0	MAGUK p55 subfamily member 6	-0.51	0.0362		
Q9JK42	[Pyruvate dehydrogenase (acetyl-transferring)] kinase isozyme 2, mitochondrial	-0.52	0.0081		
P53026	60S ribosomal protein L10a	-0.52	0.0193		
P49817	Caveolin-1	-0.52	0.0459		
Q9EP69	Phosphatidylinositide phosphatase SAC1	-0.52	0.0023		
P80317	T-complex protein 1 subunit zeta	-0.52	0.0136		
P32883	GTPase Kras	-0.53	0.0041		
Q61035	Histidine--tRNA ligase, cytoplasmic	-0.53	0.0413		
Q9JLZ3	Methylglutaconyl-CoA hydratase, mitochondrial	-0.53	0.0136		
Q922Q1	Mitochondrial amidoxime reducing component 2	-0.53	0.0305		
P99029	Peroxiredoxin-5, mitochondrial	-0.53	0.0203		
Q8CGY6	Protein unc-45 homolog B	-0.53	0.0015		
P63001	Ras-related C3 botulinum toxin substrate 1	-0.53	0.0003		
P53994	Ras-related protein Rab-2A	-0.53	0.0071		
P11983	T-complex protein 1 subunit alpha	-0.53	0.0042		
Q8VHX6	Filamin-C	-0.54	0.0104	-0.73	3.25E-02
P68510	14-3-3 protein beta	-0.54	0.0113		
P14206	40S ribosomal protein SA	-0.54	0.0023		

Table B.1 continued

Accession no:	Description	Proteome		Phosphoproteome	
		Fold change	Adj. P-Value	Fold change	Adj. P-Value
Q8K370	Acyl-CoA dehydrogenase family member 10	-0.54	0.0008		
P28271	Cytoplasmic aconitate hydratase	-0.54	0.0137		
Q9QZF2	Glypican-1	-0.54	0.0116		
Q9EQ20	Methylmalonate-semialdehyde dehydrogenase [acylating], mitochondrial	-0.54	0.0094		
Q61166	Microtubule-associated protein RP/EB family member 1	-0.54	0.0078		
O09061	Proteasome subunit beta type-1	-0.54	0.0344		
Q8R146	Acylamino-acid-releasing enzyme	-0.55	0.0367		
P61202	COP9 signalosome complex subunit 2	-0.55	0.0120		
Q9JKR6	Hypoxia up-regulated protein 1	-0.55	0.0051		
P29758	Ornithine aminotransferase, mitochondrial	-0.55	0.0006		
P53811	Phosphatidylinositol transfer protein beta isoform	-0.55	0.0347		
P80318	T-complex protein 1 subunit gamma	-0.55	0.0020		
Q99KC8	von Willebrand factor A domain-containing protein 5A	-0.55	0.0162		
Q9CXW4	60S ribosomal protein L11	-0.56	0.0030		
P35979	60S ribosomal protein L12	-0.56	0.0004		
Q8K4G5	Actin-binding LIM protein 1	-0.56	0.0398		
Q9CVB6	Actin-related protein 2/3 complex subunit 2	-0.56	0.0048		
Q791T5	Mitochondrial carrier homolog 1	-0.56	0.0023		
P61089	Ubiquitin-conjugating enzyme E2	-0.56	0.0031		
Q60994	Adiponectin	-0.57	0.0377		
Q8CHT0	Delta-1-pyrroline-5-carboxylate dehydrogenase, mitochondrial	-0.57	0.0313		
P04117	Fatty acid-binding protein, adipocyte	-0.57	0.0088		
P08752	Guanine nucleotide-binding protein G(i) subunit alpha-2	-0.57	0.0157		
P0DN34	NADH dehydrogenase [ubiquinone] 1 beta subcomplex subunit 1	-0.57	0.0290		
P10493	Nidogen-1	-0.57	0.0048		
P62908	40S ribosomal protein S3	-0.58	0.0139		
Q8K010	5-oxoprolinase	-0.58	0.0020		
Q63918	Caveolae-associated protein 2	-0.58	0.0001		
Q499X9	Methionine--tRNA ligase, mitochondrial	-0.58	0.0091		
P60335	Poly(rC)-binding protein 1	-0.58	0.0001		
Q8C1B7	Septin-11	-0.58	0.0063		
E9Q9K5	Triadin	-0.58	0.0009		
Q9EQ06	Estradiol 17-beta-dehydrogenase 11	-0.59	0.0424		
O55023	Inositol monophosphatase 1	-0.59	0.0004		
Q8BVI4	Dihydropteridine reductase	-0.6	0.0110		
P62874	Guanine nucleotide-binding protein G(I)/G(S)/G(T) subunit beta-1	-0.6	0.0005		
P97927	Laminin subunit alpha-4	-0.6	0.0459		
O54901	OX-2 membrane glycoprotein	-0.6	0.0005		
Q60854	Serpin B6	-0.6	0.0080		
P14869	60S acidic ribosomal protein P0	-0.61	0.0029		
P05201	Aspartate aminotransferase, cytoplasmic	-0.61	0.0018		

Table B.1 continued

Accession no:	Description	Proteome		Phosphoproteome	
		Fold change	Adj. P-Value	Fold change	Adj. P-Value
Q60972	Histone-binding protein RBBP4	-0.61	0.0081		
P11438	Lysosome-associated membrane glycoprotein 1	-0.62	0.0005		
P97384	Annexin A11	-0.63	0.0076		
Q8CHS7	Dehydrogenase/reductase SDR family member 7C	-0.63	0.0225		
P68040	Receptor of activated protein C kinase 1	-0.63	0.0021		
Q9CQI6	Coactosin-like protein	-0.64	0.0076		
Q8BH64	EH domain-containing protein 2	-0.64	0.0414		
P60229	Eukaryotic translation initiation factor 3 subunit E	-0.64	0.0457		
Q9WTP7	GTP:AMP phosphotransferase AK3, mitochondrial	-0.64	0.0151		
Q64523	Histone H2A type 2-C	-0.64	0.0001		
Q6ZQI3	Malectin	-0.64	0.0103		
O35685	Nuclear migration protein nudC	-0.64	0.0160		
P35700	Peroxiredoxin-1	-0.64	0.0008		
P61750	ADP-ribosylation factor 4	-0.66	0.0007		
P14211	Calreticulin	-0.66	0.0003		
P97742	Carnitine O-palmitoyltransferase 1, liver isoform	-0.66	0.0233		
Q91Z53	Glyoxylate reductase/hydroxypyruvate reductase	-0.66	0.0003		
Q8COM9	Isoaspartyl peptidase/L-asparaginase	-0.66	0.0072		
Q9JHI5	Isovaleryl-CoA dehydrogenase, mitochondrial	-0.66	0.0026		
Q922Q8	Leucine-rich repeat-containing protein 59	-0.66	0.0008		
Q9CPP6	NADH dehydrogenase [ubiquinone] 1 alpha subcomplex subunit 5	-0.66	0.0313		
Q99K51	Plastin-3	-0.66	0.0005		
Q9WUA2	Phenylalanine--tRNA ligase beta subunit	-0.67	0.0093		
Q08481	Platelet endothelial cell adhesion molecule	-0.67	0.0137		
Q9D1D4	Transmembrane emp24 domain-containing protein 10	-0.67	0.0037		
Q9WTI7	Unconventional myosin-Ic	-0.67	0.0004		
E9Q4Z2	Acetyl-CoA carboxylase 2	-0.68	0.0299		
Q9WTR5	Cadherin-13	-0.68	0.0001		
O88456	Calpain small subunit 1	-0.68	0.0006		
O08788	Dynactin subunit 1	-0.68	0.0162		
Q8JZQ9	Eukaryotic translation initiation factor 3 subunit B	-0.68	0.0060		
P03921	NADH-ubiquinone oxidoreductase chain 5	-0.68	0.0038		
P32020	Non-specific lipid-transfer protein	-0.68	0.0006		
Q7TNG8	Probable D-lactate dehydrogenase, mitochondrial	-0.68	0.0041		
P14733	Lamin-B1	-0.69	0.0094		
Q8BJU0	Small glutamine-rich tetratricopeptide repeat-containing protein alpha	-0.69	0.0007		
P97823	Acyl-protein thioesterase 1	-0.7	0.0196		
P97807	Fumarate hydratase, mitochondrial	-0.7	0.0019		
Q61738	Integrin alpha-7	-0.71	0.0003		
P02468	Laminin subunit gamma-1	-0.71	0.0309		
Q9CZP5	Mitochondrial chaperone BCS1	-0.71	0.0042		
P09411	Phosphoglycerate kinase 1	-0.71	0.0148		

Table B.1 continued

Accession no:	Description	Proteome		Phosphoproteome	
		Fold change	Adj. P-Value	Fold change	Adj. P-Value
P97855	Ras GTPase-activating protein-binding protein 1	-0.72	0.0078		
Q9JI75	Ribosyldihyronicotinamide dehydrogenase [quinone]	-0.72	0.0080		
Q9Z1W9	STE20/SPS1-related proline-alanine-rich protein kinase	-0.72	0.0467		
Q8VCW8	Acyl-CoA synthetase family member 2, mitochondrial	-0.73	0.0064		
Q3TEA8	Heterochromatin protein 1-binding protein 3	-0.73	0.0001		
Q9CR24	Nucleoside diphosphate-linked moiety X motif 8	-0.73	0.0030		
Q6P069	Sorcin	-0.73	0.0004		
P10922	Histone H1.0	-0.74	0.0096		
P40124	Adenylyl cyclase-associated protein 1	-0.75	0.0017		
Q8QZR5	Alanine aminotransferase 1	-0.75	0.0222		
Q8VE38	Oxidoreductase NAD-binding domain-containing protein 1	-0.75	0.0245		
Q9ER88	28S ribosomal protein S29	-0.76	0.0350		
Q99L13	3-hydroxyisobutyrate dehydrogenase, mitochondrial	-0.76	0.0217		
Q9Z1N5	Spliceosome RNA helicase Ddx39b	-0.76	0.0372		
Q91ZJ5	UTP--glucose-1-phosphate uridylyltransferase	-0.76	0.0037		
O70310	Glycylpeptide N-tetradecanoyltransferase 1	-0.77	0.0145		
Q62407	Striated muscle-specific serine/threonine-protein kinase	-0.78	0.0395	-6.64	3.31E-16
Q9DCD0	6-phosphogluconate dehydrogenase, decarboxylating	-0.78	0.0255		
Q71LX4	Talin-2	-0.78	0.0066		
P59266	Fat storage-inducing transmembrane protein 2 [Pyruvate dehydrogenase (acetyl-transferring)] kinase	-0.79	0.0313		
O70571	isozyme 4, mitochondrial	-0.8	0.0034		
Q9WTQ5	A-kinase anchor protein 12	-0.8	0.0192		
P97447	Four and a half LIM domains protein 1	-0.8	0.0101		
Q9CQS8	Protein transport protein Sec61 subunit beta	-0.8	0.0078		
P10605	Cathepsin B	-0.81	0.0007		
Q8CAK1	Putative transferase CAF17 homolog, mitochondrial	-0.81	0.0317		
Q9CZY3	Ubiquitin-conjugating enzyme E2 variant 1	-0.81	0.0034		
P62737	Actin, aortic smooth muscle	-0.82	0.0020		
Q9CRD2	ER membrane protein complex subunit 2	-0.82	0.0226		
Q9CQR4	Acyl-coenzyme A thioesterase 13	-0.83	0.0424		
O35887	Calumenin	-0.83	0.0001		
P12815	Programmed cell death protein 6	-0.83	0.0008		
P52196	Thiosulfate sulfurtransferase	-0.83	0.0064		
Q9JKB3	Y-box-binding protein 3	-0.83	0.0402		
O35639	Annexin A3	-0.84	0.0017		
Q60675	Laminin subunit alpha-2	-0.84	0.0023		
P32020	Non-specific lipid-transfer protein	-0.84	0.0454		
Q9R1P4	Proteasome subunit alpha type-1	-0.84	0.0120		
O88851	Putative hydrolase RBBP9	-0.84	0.0313		
Q9Z1Z0	General vesicular transport factor p115	-0.85	0.0021	-6.64	3.31E-16
P47911	60S ribosomal protein L6	-0.85	0.0105		
Q8BT60	Copine-3	-0.85	0.0414		

Table B.1 continued

Accession no:	Description	Proteome		Phosphoproteome	
		Fold change	Adj. P-Value	Fold change	Adj. P-Value
P48722	Heat shock 70 kDa protein 4L	-0.85	0.0350		
P47738	Aldehyde dehydrogenase, mitochondrial	-0.86	0.0008		
Q9D9V3	Ethylmalonyl-CoA decarboxylase	-0.86	0.0480		
Q9JHL1	Na(+)/H(+) exchange regulatory cofactor NHE-RF2	-0.86	0.0142		
P99026	Proteasome subunit beta type-4	-0.86	0.0213		
Q61074	Protein phosphatase 1G	-0.86	0.0076		
Q9WV32	Actin-related protein 2/3 complex subunit 1B	-0.87	0.0093		
Q9WUR9	Adenylate kinase 4, mitochondrial	-0.87	0.0286		
Q9CZX9	ER membrane protein complex subunit 4	-0.87	0.0043		
Q9WTP7	GTP:AMP phosphotransferase AK3, mitochondrial	-0.87	0.0163		
E9Q7G0	Nuclear mitotic apparatus protein 1	-0.87	0.0230		
Q93092	Transaldolase	-0.87	0.0001		
P21279	Guanine nucleotide-binding protein G(q) subunit alpha	-0.88	0.0213		
P70195	Proteasome subunit beta type-7	-0.88	0.0028		
P27659	60S ribosomal protein L3	-0.89	0.0415		
P61804	Dolichyl-diphosphooligosaccharide--protein glycosyltransferase subunit DAD1	-0.89	0.0022		
P10649	Glutathione S-transferase Mu 1	-0.89	0.0015		
P21619	Lamin-B2	-0.89	0.0257		
P0DN34	NADH dehydrogenase [ubiquinone] 1 beta subcomplex subunit 1	-0.89	0.0258		
P63323	40S ribosomal protein S12	-0.9	0.0208		
P19324	Serpin H1	-0.9	0.0076		
P15626	Glutathione S-transferase Mu 2	-0.91	0.0001		
P68134	Actin, alpha skeletal muscle	-0.92	7.71E-06		
Q9CXW3	Calcyclin-binding protein	-0.92	0.0182		
Q61696	Heat shock 70 kDa protein 1A	-0.92	0.0078		
Q9R0P9	Ubiquitin carboxyl-terminal hydrolase isozyme	-0.92	0.0025		
P58774	Tropomyosin beta chain	-0.93	0.0162	-2.90	1.16E-02
Q8CG76	Aflatoxin B1 aldehyde reductase member 2	-0.93	0.0151		
O08795	Glucosidase 2 subunit beta	-0.93	0.0026		
Q9Z0P4	Paralemmin-1	-0.93	0.0021		
O08553	Dihydropyrimidinase-related protein 2	-0.95	2.12E-05	-1.49	2.56E-03
O70433	Four and a half LIM domains protein 2	-0.95	0.0459		
Q9CR09	Ubiquitin-fold modifier-conjugating enzyme 1	-0.95	0.0075		
P68254	14-3-3 protein theta	-0.96	2.12E-05		
Q9D1R9	60S ribosomal protein L34	-0.96	0.0021		
Q99JX3	Golgi reassembly-stacking protein 2	-0.97	0.0021		
Q9D0J8	Parathyrosin	-0.97	4.00E-05		
Q99PL5	Ribosome-binding protein 1	-0.98	0.0001		
Q9WVA4	Transgelin-2	-0.98	0.0106		
Q99KH8	Serine/threonine-protein kinase 24	-0.99	0.0281		
Q9DBP5	UMP-CMP kinase	-0.99	0.0135		
Q9CXR1	Dehydrogenase/reductase SDR family member 7	-1	0.0041		

Table B.1 continued

Accession no:	Description	Proteome		Phosphoproteome	
		Fold change	Adj. P-Value	Fold change	Adj. P-Value
Q02819	Nucleobindin-1 KN motif and ankyrin repeat domain-containing protein	-1	0.0004		
Q8BX02	2	-1.01	0.0156		
P48193	Protein 4.1 NADH dehydrogenase [ubiquinone] 1 alpha subcomplex subunit 2	-1.01	0.0494		
Q9CQ75	Tubulin beta-2B chain	-1.02	0.0071		
Q9CWF2	Alpha-crystallin B chain	-1.02	0.0017		
P23927	Alpha-crystallin B chain	-1.03	0.0052		
Q61335	B-cell receptor-associated protein 31	-1.03	0.0021		
Q9Z1Q2	Protein ABHD16A	-1.03	0.0400		
Q9R0P5	Destrin	-1.04	0.0414		
O70400	PDZ and LIM domain protein 1	-1.04	0.0167		
Q8VBV7	COP9 signalosome complex subunit 8	-1.05	0.0113		
O09131	Glutathione S-transferase omega-1	-1.05	0.0051		
O88844	Isocitrate dehydrogenase [NADP] cytoplasmic Calcium/calmodulin-dependent protein kinase type II subunit alpha	-1.05	0.0129		
P11798	Endoplasmic reticulum resident protein 44	-1.06	0.0250		
Q9D1Q6	Nucleoside diphosphate kinase B	-1.07	2.12E-05		
Q01768	Protein transport protein Sec23A	-1.07	0.0024		
Q01405	Collagen alpha-1(VI) chain Dolichyl-diphosphooligosaccharide--protein glycosyltransferase subunit STT3B	-1.07	0.0185		
Q04857	Desmin	-1.08	0.0020		
Q3TDQ1	NADP-dependent malic enzyme	-1.08	0.0021		
P31001	Cytochrome b5	-1.09	0.0005	-0.36	3.42E-02
P06801	Cytochrome c oxidase subunit 5B, mitochondrial	-1.09	0.0076		
P56395	Fibrillin-1	-1.11	0.0170		
P19536	Protein canopy homolog 2	-1.11	0.0027		
Q61554	EH domain-containing protein 4	-1.11	0.0228		
Q9QXT0	Endoglin	-1.12	0.0019		
Q9EQP2	Synaptic vesicle membrane protein VAT-1 homolog	-1.13	0.0001		
Q63961	Four and a half LIM domains protein 2 Mitochondrial import inner membrane translocase subunit Tim13	-1.14	0.0031		
Q62465	Dehydrogenase/reductase SDR family member 11	-1.14	0.0010		
O70433	Protein RER1	-1.15	0.0018		
P62075	Annexin A4	-1.15	0.0033		
Q3U0B3	Band 4.1-like protein 2	-1.16	0.0018		
Q9CQU3	Caveolae-associated protein 3	-1.16	0.0430		
P97429	Glutathione synthetase	-1.19	0.0038		
O70318	N-acyl-aromatic-L-amino acid amidohydrolase (carboxylate-forming)	-1.19	0.0137		
Q91VJ2	Protein disulfide-isomerase A3	-1.19	0.0048		
P51855	N-acetylated-alpha-linked acidic dipeptidase 2	-1.19	0.0005		
Q91XE4	Peptidyl-prolyl cis-trans isomerase A	-1.19	0.0043		
P27773		-1.21	0.0135		
Q9CZR2		-1.21	0.0029		
P17742					

Table B.1 continued

Accession no:	Description	Proteome		Phosphoproteome	
		Fold change	Adj. P-Value	Fold change	Adj. P-Value
Q9CQF9	Prenylcysteine oxidase	-1.21	0.0333		
P19096	Fatty acid synthase	-1.22	0.0004		
Q8BH95	Enoyl-CoA hydratase, mitochondrial	-1.23	0.0006		
P28653	Biglycan	-1.24	0.0201		
Q9D7G0	Ribose-phosphate pyrophosphokinase 1	-1.24	0.0114		
P01942	Hemoglobin subunit alpha	-1.25	0.0005		
P07356	Annexin A2	-1.26	0.0116	-1.53	2.73E-02
Q9QXS1	Plectin	-1.27	0.0023	-0.85	7.49E-03
P84089	Enhancer of rudimentary homolog	-1.27	0.0066		
P56213	FAD-linked sulfhydryl oxidase ALR	-1.27	0.0152		
P34884	Macrophage migration inhibitory factor	-1.27	0.0001		
Q8BU85	Methionine-R-sulfoxide reductase B3, mitochondrial	-1.28	0.0260		
P37040	NADPH--cytochrome P450 reductase	-1.28	0.0011		
P30115	Glutathione S-transferase A3	-1.31	0.0055		
Q7TSH2	Phosphorylase b kinase regulatory subunit beta	-1.31	0.0231		
P13707	Glycerol-3-phosphate dehydrogenase [NAD(+)], cytoplasmic	-1.35	2.12E-05		
Q8BG05	Heterogeneous nuclear ribonucleoprotein A3	-1.35	0.0323		
Q8BW75	Amine oxidase [flavin-containing] B	-1.36	0.0007		
Q99P72	Reticulon-4	-1.42	0.0001		
Q9QUM9	Proteasome subunit alpha type-6	-1.43	0.0342		
P08003	Protein disulfide-isomerase A4	-1.43	0.0017		
Q9CR57	60S ribosomal protein L14	-1.44	0.0025		
Q9WV92	Band 4.1-like protein 3	-1.47	0.0222		
Q8VCT4	Carboxylesterase 1D	-1.47	0.0002		
P14069	Protein S100-A6	-1.48	0.0024		
P00329	Alcohol dehydrogenase 1	-1.49	0.0007		
P17183	Gamma-enolase	-1.49	0.0020		
Q62188	Dihydropyrimidinase-related protein 3	-1.52	0.0128	-1.05	5.85E-03
Q9JL35	High mobility group nucleosome-binding domain-containing protein 5	-1.52	0.0160		
Q9D855	Cytochrome b-c1 complex subunit 7	-1.54	9.14E-06		
O55022	Membrane-associated progesterone receptor component 1	-1.55	0.0076	-0.73	6.73E-03
O88569	Heterogeneous nuclear ribonucleoproteins A2/B1	-1.58	0.0008		
Q8R1V4	Transmembrane emp24 domain-containing protein 4	-1.6	0.0043		
P15508	Spectrin beta chain, erythrocytic	-1.62	0.0160		
P15864	Histone H1.2	-1.63	0.0001	-0.59	3.26E-02
P43277	Histone H1.3	-1.66	0.0001	-1.23	5.69E-03
P15105	Glutamine synthetase	-1.67	0.0013		
P43276	Histone H1.5	-1.72	0.0001		
P46460	Vesicle-fusing ATPase	-1.72	0.0036		
P43274	Histone H1.4	-1.76	0.0005	-0.96	6.41E-03
P48678	Prelamin-A/C	-1.79	0.0024		

Table B.1 continued

Accession no:	Description	Proteome		Phosphoproteome	
		Fold change	Adj. P-Value	Fold change	Adj. P-Value
P07724	Serum albumin	-1.8	0.0152		
P20152	Vimentin	-1.81	0.0001	-1.31	2.27E-03
P40142	Transketolase	-1.85	0.0004		
Q64471	Glutathione S-transferase theta-1	-1.9	0.0016		
Q9WVH9	Fibulin-5	-1.96	2.66E-05		
P52503	NADH dehydrogenase [ubiquinone] iron-sulfur protein 6, mitochondrial	-1.97	5.91E-10		
Q06890	Clusterin	-1.99	0.0005		
Q3UPL0	Protein transport protein Sec31A	-1.99	0.0013		
P43275	Histone H1.1	-2.01	0.0057		
P59114	mRNA (2'-O-methyladenosine-N(6)-)-methyltransferase	-2.03	0.0364		
O70423	Membrane primary amine oxidase	-2.06	7.71E-06		
P24549	Retinal dehydrogenase 1	-2.1	0.0031		
Q8K3K7	1-acyl-sn-glycerol-3-phosphate acyltransferase beta	-2.14	0.0050		
P28654	Decorin	-2.15	0.0024		
Q9CR98	Protein FAM136A	-2.26	2.26E-07		
Q91XV3	Brain acid soluble protein 1	-2.37	0.0125		
P05977	Myosin light chain 1/3, skeletal muscle isoform	-2.38	3.64E-05		
O55026	Ectonucleoside triphosphate diphosphohydrolase 2	-2.44	0.0085		
Q9CRY7	Lysophospholipase D GDPD1	-2.5	0.0020		
P46412	Glutathione peroxidase 3	-2.56	0.0050		
P51885	Lumican	-2.58	0.0048		
P01942	Hemoglobin subunit alpha	-2.59	0.0022		
Q05920	Pyruvate carboxylase, mitochondrial	-2.59	7.71E-06		
P40936	Indolethylamine N-methyltransferase	-2.61	0.0048		
P08074	Carbonyl reductase [NADPH] 2	-2.63	0.0011		
Q9QYC0	Alpha-adducin	-2.64	0.0099	-1.03	5.88E-03
P02088	Hemoglobin subunit beta-1	-2.82	3.59E-05		
Q9CZS1	Aldehyde dehydrogenase X, mitochondrial	-2.89	0.0192		
Q9JK53	Prolargin	-3.03	0.0020		
P18872	Guanine nucleotide-binding protein G(o) subunit alpha Prostacyclin synthase OS=Mus musculus OX=10090	-3.04	0.0036		
O35074	GN=Ptgis PE=1 SV=1	-3.61	0.0017		
P16015	Carbonic anhydrase 3	-3.64	1.24E-16		
Q9JIY5	Serine protease HTRA2, mitochondrial	-4.28	0.0219		
P97467	Peptidyl-glycine alpha-amidating monooxygenase	-5.38	0.0175	-5.58	4.94E-03
P19096	Fatty acid synthase	-5.93	0.0001		
O55106	Striatin	-6.64	1.24E-16	6.64	3.31E-16
Q8CON2	Glycerol-3-phosphate acyltransferase 3	-6.64	1.24E-16	1.25	4.72E-02
Q99K28	ADP-ribosylation factor GTPase-activating protein 2	-6.64	1.24E-16		
Q9D0J4	ADP-ribosylation factor-like protein 2	-6.64	1.24E-16		
O88533	Aromatic-L-amino-acid decarboxylase	-6.64	1.24E-16		
Q8K268	ATP-binding cassette sub-family F member 3	-6.64	1.24E-16		
O88738	Baculoviral IAP repeat-containing protein 6	-6.64	1.24E-16		

Table B.1 continued

Accession no:	Description	Proteome		Phosphoproteome	
		Fold change	Adj. P-Value	Fold change	Adj. P-Value
Q9CQC6	Basic leucine zipper and W2 domain-containing protein 1	-6.64	1.24E-16		
P53996	Cellular nucleic acid-binding protein	-6.64	1.24E-16		
Q8K2Q5	Coiled-coil-helix-coiled-coil-helix domain-containing protein 7	-6.64	1.24E-16		
Q9D4H1	Exocyst complex component 2	-6.64	1.24E-16		
Q91WJ8	Far upstream element-binding protein 1	-6.64	1.24E-16		
P27601	Guanine nucleotide-binding protein subunit alpha-13	-6.64	1.24E-16		
Q921F4	Heterogeneous nuclear ribonucleoprotein L-like	-6.64	1.24E-16		
Q60766	Immunity-related GTPase family M protein 1	-6.64	1.24E-16		
Q8VI75	Importin-4	-6.64	1.24E-16		
Q91YE6	Importin-9	-6.64	1.24E-16		
P24547	Inosine-5'-monophosphate dehydrogenase 2	-6.64	1.24E-16		
P43406	Integrin alpha-V	-6.64	1.24E-16		
P0DOV1	Interferon-activable protein 205-B	-6.64	1.24E-16		
A6BLY7	Keratin, type I cytoskeletal 28	-6.64	1.24E-16		
O88447	Kinesin light chain 1	-6.64	1.24E-16		
Q61292	Laminin subunit beta-2	-6.64	1.24E-16		
Q9JHQ5	Leucine zipper transcription factor-like protein 1	-6.64	1.24E-16		
Q9D1G5	Leucine-rich repeat-containing protein 57	-6.64	1.24E-16		
P16675	Lysosomal protective protein	-6.64	1.24E-16		
Q78J03	Methionine-R-sulfoxide reductase B2, mitochondrial	-6.64	1.24E-16		
Q8C052	Microtubule-associated protein 1S	-6.64	1.24E-16		
Q9CYG7	Mitochondrial import receptor subunit TOM34	-6.64	1.24E-16		
Q5FW52	Muscular LMNA-interacting protein	-6.64	1.24E-16		
P09541	Myosin light chain 4	-6.64	3.38E-03		
Q9CWS0	N(G),N(G)-dimethylarginine dimethylaminohydrolase 1	-6.64	1.24E-16		
Q8CI95	Oxysterol-binding protein-related protein 11	-6.64	1.24E-16		
Q8VI36	Paxillin	-6.64	1.24E-16		
Q99KR7	Peptidyl-prolyl cis-trans isomerase F, mitochondrial	-6.64	1.24E-16		
Q9EPL9	Peroxisomal acyl-coenzyme A oxidase 3	-6.64	1.24E-16		
Q9ROA0	Peroxisomal membrane protein PEX14	-6.64	1.24E-16		
Q501J6	Probable ATP-dependent RNA helicase DDX17	-6.64	1.24E-16		
Q8C167	Prolyl endopeptidase-like	-6.64	1.24E-16		
P20444	Protein kinase C alpha type	-6.64	1.24E-16		
Q80X73	Protein pelota homolog	-6.64	1.24E-16		
B2RY56	RNA-binding protein 25	-6.64	1.24E-16		
Q8BIJ7	RUN and FYVE domain-containing protein 1	-6.64	1.24E-16		
Q9WTM5	RuvB-like 2	-6.64	1.24E-16		
Q7TT50	Serine/threonine-protein kinase MRCK beta	-6.64	1.24E-16		
Q8CIN4	Serine/threonine-protein kinase PAK 2	-6.64	1.24E-16		
Q7TSI3	Serine/threonine-protein phosphatase 6 regulatory subunit 1	-6.64	1.24E-16		
Q99J77	Sialic acid synthase	-6.64	1.24E-16		

Table B.1 continued

Accession no:	Description	Proteome		Phosphoproteome	
		Fold change	Adj. P-Value	Fold change	Adj. P-Value
Q9JIV9	Sodium channel protein type 5 subunit alpha	-6.64	1.24E-16		
P70302	Stromal interaction molecule 1	-6.64	1.24E-16		
Q9R1T2	SUMO-activating enzyme subunit 1	-6.64	1.24E-16		
P63280	SUMO-conjugating enzyme UBC9	-6.64	1.24E-16		
O08599	Syntaxin-binding protein 1	-6.64	1.24E-16		
Q66JZ4	T-cell activation inhibitor, mitochondrial	-6.64	1.24E-16		
Q8K1H7	T-complex protein 11-like protein 2	-6.64	1.24E-16		
Q9Z0U1	Tight junction protein ZO-2	-6.64	1.24E-16		
Q8K2L8	Trafficking protein particle complex subunit 12	-6.64	1.24E-16		
P37804	Transgelin	-6.64	1.24E-16		
Q8JZU2	Tricarboxylate transport protein, mitochondrial	-6.64	1.24E-16		
Q3UJD6	Ubiquitin carboxyl-terminal hydrolase 19	-6.64	1.24E-16		
P35123	Ubiquitin carboxyl-terminal hydrolase 4	-6.64	1.24E-16		
Q6A4J8	Ubiquitin carboxyl-terminal hydrolase 7	-6.64	1.24E-16		
P97390	Vacuolar protein sorting-associated protein 45	-6.64	1.24E-16		
Q9ERF3	WD repeat-containing protein 61	-6.64	1.24E-16		
P45481	CREB-binding protein			6.64	3.31E-16
P27546	Microtubule-associated protein 4			6.64	3.31E-16
P26645	Myristoylated alanine-rich C-kinase substrate			6.64	3.31E-16
O09130	NFATC2-interacting protein			6.64	3.31E-16
Q3UQS8	RNA-binding protein 20			6.64	3.31E-16
Q8CHW4	Translation initiation factor eIF-2B subunit epsilon			6.64	3.31E-16
O70373	Xin actin-binding repeat-containing protein 1			6.64	3.31E-16
O70468	Myosin-binding protein C, cardiac-type			3.36	3.31E-16
O88492	Perilipin-4			2.48	7.32E-04
Q99MS7	EH domain-binding protein 1-like protein 1			2.44	8.01E-04
A2ASS6	Titin			2.27	1.43E-03
Q9ET78	Junctophilin-2			2.16	1.25E-06
Q3UIL6	Pleckstrin homology domain-containing family A member 7			2.16	1.96E-03
P10637	Microtubule-associated protein tau			2.12	9.61E-07
Q4QQM4	Tumor protein p53-inducible protein 11			2.02	7.15E-04
A2AJI0	MAP7 domain-containing protein 1			1.95	3.46E-02
P97450	ATP synthase-coupling factor 6, mitochondrial			1.92	2.15E-02
Q148W8	Inactive dual specificity phosphatase 27			1.91	1.25E-02
Q9Z1E4	Glycogen [starch] synthase, muscle			1.79	5.80E-04
Q8K019	Bcl-2-associated transcription factor 1			1.77	1.83E-02
Q9QYG0	Protein NDRG2			1.76	2.28E-04
E9Q401	Ryanodine receptor 2			1.72	4.78E-02
Q920Q8	Influenza virus NS1A-binding protein homolog			1.64	4.72E-02
Q61584	Fragile X mental retardation syndrome-related protein 1			1.47	3.50E-02
Q6P4T2	U5 small nuclear ribonucleoprotein 200 kDa helicase			1.45	1.42E-02
Q9JMH9	Unconventional myosin-XVIIIa			1.28	1.27E-02

Table B.1 continued

Accession no:	Description	Proteome		Phosphoproteome	
		Fold change	Adj. P-Value	Fold change	Adj. P-Value
Q8CIB5	Fermitin family homolog 2			1.21	3.81E-02
Q3UM45	Protein phosphatase 1 regulatory subunit 7			1.19	3.34E-02
P54103	DnaJ homolog subfamily C member 2			1.06	3.77E-02
P09542	Myosin light chain 3			1.05	8.82E-04
Q9D6W8	BLOC-1-related complex subunit 6			1.03	4.94E-03
Q99NH0	Ankyrin repeat domain-containing protein 17			0.89	2.32E-02
A2AMM0	Caveolae-associated protein 4			0.84	4.12E-03
P63024	Vesicle-associated membrane protein 3			0.84	4.79E-02
E9Q6P5	Tetratricopeptide repeat protein 7B			0.80	4.44E-02
Q8BVZ1	Perilipin-5			0.76	5.39E-03
Q4VA53	Sister chromatid cohesion protein PDS5 homolog			0.76	1.94E-02
Q8CC27	Voltage-dependent L-type calcium channel subunit beta-2			0.70	3.75E-02
Q64337	Sequestosome-1			0.69	3.21E-02
Q6NVE8	WD repeat-containing protein 44			0.68	2.46E-02
P51174	Long-chain specific acyl-CoA dehydrogenase, mitochondrial			0.66	5.89E-03
P70670	Nascent polypeptide-associated complex subunit alpha, muscle-specific form			0.64	5.85E-03
Q9Z2F7	BCL2/adenovirus E1B 19 kDa protein-interacting protein 3-like			0.60	3.25E-02
Q6PD31	Trafficking kinesin-binding protein 1			0.60	1.08E-02
Q3TGW2	Endonuclease/exonuclease/phosphatase family domain-containing protein 1			0.58	1.15E-02
D3YXK2	Scaffold attachment factor B1			0.58	1.04E-02
Q6A0A2	La-related protein 4B			0.57	4.94E-03
Q8BMS1	Trifunctional enzyme subunit alpha, mitochondrial			0.55	1.56E-02
Q60953	Protein PML			0.54	3.85E-02
P63038	60 kDa heat shock protein, mitochondrial			0.52	2.19E-03
P62960	Nuclease-sensitive element-binding protein 1			0.51	3.43E-02
Q9JHU2	Palmdelphin			0.50	8.65E-03
Q9D2N4	Dystrobrevin alpha			0.47	2.08E-03
Q9ET54	Palladin			0.47	1.15E-02
P62259	14-3-3 protein epsilon			0.46	1.40E-02
Q02566	Myosin-6			0.44	5.47E-03
A3KGS3	Ral GTPase-activating protein subunit alpha-2			0.42	4.85E-02
Q80XU3	Nuclear ubiquitous casein and cyclin-dependent kinase substrate 1			0.41	2.92E-03
Q9DCL8	Protein phosphatase inhibitor 2			0.41	4.79E-02
P62754	40S ribosomal protein S6			0.40	4.16E-02
O35129	Prohibitin			0.40	4.79E-02
G5E870	E3 ubiquitin-protein ligase TRIP12			0.39	3.43E-02
Q6P8J7	Creatine kinase S-type, mitochondrial			0.37	3.42E-02
Q2NL51	Glycogen synthase kinase-3 alpha			0.35	2.43E-02
O35892	Nuclear autoantigen Sp-100			0.34	8.65E-03
O70251	Elongation factor 1-beta			0.33	2.46E-02

Table B.1 continued

Accession no:	Description	Proteome		Phosphoproteome	
		Fold change	Adj. P-Value	Fold change	Adj. P-Value
Q8R3Q2	Serine/threonine-protein phosphatase 6 regulatory subunit 2			0.30	2.82E-02
Q07113	Cation-independent mannose-6-phosphate receptor			0.29	3.73E-02
Q9D824	Pre-mRNA			0.29	2.66E-03
P26231	Catenin alpha-1			0.27	2.53E-02
Q9ESN9	C-Jun-amino-terminal kinase-interacting protein 3			0.27	2.19E-02
O54940	BCL2/adenovirus E1B protein-interacting protein 2			0.25	1.22E-02
Q8BP27	Swi5-dependent recombination DNA repair protein 1			-0.21	1.13E-02
Q8BR65	Sin3 histone deacetylase corepressor complex component			-0.29	2.60E-02
Q8C0E3	E3 ubiquitin-protein ligase TRIM47			-0.39	2.70E-02
Q9QYB5	Gamma-adducin			-0.43	6.17E-04
Q6PDN3	Myosin light chain kinase, smooth muscle			-0.52	2.03E-02
P70663	SPARC-like protein 1			-0.52	5.88E-03
D3YZP9	Coiled-coil domain-containing protein 6			-0.63	4.13E-02
Q8CI12	Smoothelin-like protein 2			-0.75	3.20E-02
P04247	Myoglobin			-0.90	1.42E-02
Q60949	TBC1 domain family member 1			-0.91	1.80E-02
Q64449	C-type mannose receptor 2			-0.92	2.60E-02
Q8R149	BUD13 homolog			-0.93	3.65E-02
P70414	Sodium/calcium exchanger 1			-0.99	4.94E-03
P70441	Na(+)/H(+) exchange regulatory cofactor NHE-RF1			-1.05	8.35E-03
Q62261	Spectrin beta chain, non-erythrocytic			-1.07	9.27E-04
Q70IV5	Synemin			-1.15	2.92E-03
Q922J3	CAP-Gly domain-containing linker protein 1			-1.22	4.34E-02
Q6AW69	Cingulin-like protein 1			-1.28	1.88E-02
Q8K4L3	Supervillin			-1.32	4.36E-02
Q80TH2	Erbin			-1.38	9.47E-03
Q8BWG8	Beta-arrestin-1			-1.46	9.87E-04
Q4ACU6	SH3 and multiple ankyrin repeat domains protein 3			-1.46	3.96E-02
Q91V09	WD repeat-containing protein 13			-1.53	3.46E-02
Q03517	Secretogranin-2			-1.76	7.66E-03
P47713	Cytosolic phospholipase A2			-1.80	4.94E-03
Q3UYI5	Ral guanine nucleotide dissociation stimulator-like 3			-1.88	1.06E-02
Q9QYB8	Beta-adducin			-2.02	1.26E-03
P35831	Tyrosine-protein phosphatase non-receptor type 12			-2.06	2.64E-06
P63250	G protein-activated inward rectifier potassium channel 1			-2.32	2.14E-02
Q62059	Versican core protein			-2.47	5.85E-03
P14873	Microtubule-associated protein 1B			-2.56	5.39E-03
Q9CSN1	SNW domain-containing protein 1			-2.78	1.54E-02
P08553	Neurofilament medium polypeptide			-4.68	7.14E-04
Q5SWU9	Acetyl-CoA carboxylase 1			-5.23	4.66E-04
P19246	Neurofilament heavy polypeptide			-5.40	1.34E-02
Q9ES28	Rho guanine nucleotide exchange factor 7			-6.64	3.31E-16

Table B.1 continued

Accession no:	Description	Proteome		Phosphoproteome	
		Fold change	Adj. P-Value	Fold change	Adj. P-Value
Q8BVL3	Sorting nexin-17			-6.64	3.31E-16
P39447	Tight junction protein ZO-1			-6.64	3.31E-16

Table B.2 - List of canonical pathways most affected by PP2A inhibition during myocardial ischaemia and reperfusion that have a p value ≤ 0.05 .

Pathway	Phosphoproteome -log ₁₀ (p value)	Proteome -log ₁₀ (p value)
Mitochondrial Dysfunction	1.140281231	9.667922501
Oxidative Phosphorylation	0.608218592	9.801534589
Remodelling of Epithelial Adherens Junctions	1.860202724	8.032253443
Epithelial Adherens Junction Signalling	1.239705689	7.848072841
Actin Cytoskeleton Signalling	2.508917338	4.713349345
Sirtuin Signalling Pathway	0.273295226	6.721259114
ILK Signalling	1.8403215	4.845527476
RhoGDI Signalling	1.114441513	5.349191846
Protein Kinase A Signalling	4.123247768	1.290643555
Tight Junction Signalling	1.158098162	4.179963079
Integrin Signalling	2.605713135	2.615938382
Paxillin Signalling	2.44008395	2.572449884
Caveolar-mediated Endocytosis Signalling	0	4.833010544
RhoA Signalling	1.387320033	3.128033132
Cellular Effects of Sildenafil (Viagra)	0	4.388416167
Calcium Signalling	1.002541798	3.382251841
VEGF Signalling	1.48917652	2.789388108
Sertoli Cell-Sertoli Cell Junction Signalling	1.085553637	3.182978133
Regulation of Actin-based Motility by Rho Signalling by Rho Family GTPases	0.858944115	3.192080093
Protein Ubiquitination Pathway	1.505389492	2.503212439
Hypoxia Signalling in the Cardiovascular System	3.013255479	0.948677196
Valine Degradation I	1.341371785	2.587442673
Gap Junction Signalling	0.390140826	3.472789711
Alanine Degradation I	0	3.61438926
Tec Kinase Signalling	0	3.452766949
CDP-diacylglycerol Biosynthesis I	1.219719576	2.222932982
CXCR4 Signalling	0	3.432528324
Calcium Transport I	0	3.379716065
Mechanisms of Viral Exit from Host Cells	0	3.37130929
Phosphatidylglycerol Biosynthesis II (Non-plastidic)	1.186051236	2.124141606
Triacylglycerol Biosynthesis	0.949156454	2.245383517
FAK Signalling	1.518967047	1.610822627
Agrin Interactions at Neuromuscular Junction	0.752487883	2.195892578
PAK Signalling	0.615203866	2.17424962
NRF2-mediated Oxidative Stress Response	0.393466836	2.378482463
14-3-3-mediated Signalling	0.523636508	2.236432811
Cardiac Hypertrophy Signalling	0.890199765	1.859872346
Breast Cancer Regulation by Stathmin1	0.985138147	1.741041473
Phagosome Maturation	0	2.636119036
D-myo-inositol (3,4,5,6)-tetrakisphosphate Biosynthesis	2.209435864	0.40797901
D-myo-inositol (1,4,5,6)-Tetrakisphosphate Biosynthesis	2.209435864	0.40797901
Insulin Receptor Signalling	2.184748228	0.394194519

Table B.2 continued

Pathway	Phosphoproteome -log₁₀ (p value)	Proteome -log₁₀ (p value)
Agranulocyte Adhesion and Diapedesis	0	2.465656719
3-phosphoinositide Degradation	2.098766007	0.347789147
D-myo-inositol-5-phosphate Metabolism	2.069133585	0.332390551
IL-8 Signalling	0	2.322417056
Phospholipase C Signalling	0.88150375	1.415826489
3-phosphoinositide Biosynthesis	1.817134146	0.41567939
Leucine Degradation I	0	2.089584042
Ketogenesis	0	1.997150322
Branched-chain keto acid Dehydrogenase Complex	1.986885275	0
Methylmalonyl Pathway	1.986885275	0
Neuregulin Signalling	1.607765939	0.36370874
Superpathway of Inositol Phosphate Compounds	1.634392792	0.297174987
EIF2 Signalling	0.350451521	1.574103541
2-oxobutanoate Degradation I	1.890526605	0
Axonal Guidance Signalling	0	1.880592452
Fatty Acid Oxidation I	0	1.873450161
CDK5 Signalling	1.518967047	0.310051887
Regulation of eIF4 and p70S6K Signalling	0.461676242	1.365668111
Death Receptor Signalling	0	1.81503801
Glycogen Biosynthesis II (from UDP-D-Glucose)	1.811896485	0
Cdc42 Signalling	0.453212138	1.323393656
Urate Biosynthesis/Inosine 5'-phosphate Degradation	0	1.77166185
Glycogen Degradation II	0	1.77166185
Leukotriene Biosynthesis	0	1.77166185
Thrombin Signalling	0	1.752117743
Androgen Signalling	1.309566972	0.442233566
Acetyl-CoA Biosynthesis I (Pyruvate Dehydrogenase Complex)	1.745500604	0
Aspartate Degradation II	1.745500604	0
Nitric Oxide Signalling in the Cardiovascular System	1.460565263	0.276705715
Leukocyte Extravasation Signalling	0.374126075	1.315980507
Huntington's Disease Signalling	0.320037642	1.364138595
p38 MAPK Signalling	1.413089552	0.250804762
Glycogen Degradation III	0	1.651466719
tRNA Charging	0	1.642632145
G12/13 Signalling	0	1.628930775
Hepatic Fibrosis / Hepatic Stellate Cell Activation	0	1.554693669
PPAR Signalling	1.550029097	0
Prostate Cancer Signalling	1.534332948	0
S-methyl-5'-thioadenosine Degradation II	0	1.508924561
Spermine Biosynthesis	0	1.508924561
L-DOPA Degradation	0	1.508924561
Palmitate Biosynthesis I (Animals)	0	1.508924561
Fatty Acid Biosynthesis Initiation II	0	1.508924561

Table B.2 continued

Pathway	Phosphoproteome -log₁₀ (p value)	Proteome -log₁₀ (p value)
Methylglyoxal Degradation III	0	1.457387757
Virus Entry via Endocytic Pathways	0	1.449549201
Cardiomyocyte Differentiation via BMP Receptors	0	1.416047305
HIF1α Signalling	1.387320033	0
Synaptic Long-Term Potentiation	1.374780002	0
mTOR Signalling	0	1.352750146
PI3K/AKT Signalling	1.344377883	0
4-aminobutyrate Degradation I	0	1.336217796
Oxidized GTP and dGTP Detoxification	0	1.336217796
Ubiquinol-10 Biosynthesis (Eukaryotic)	1.318438988	0

ADDENDUM C – ADDITIONAL WESTERN BLOT IMAGES

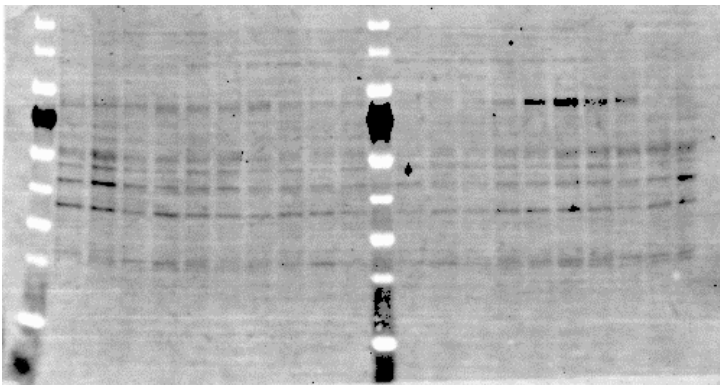


Figure C.1 - Total protein loaded onto membrane for anti-striatin (110 kDa) on immunoprecipitated PP2A samples

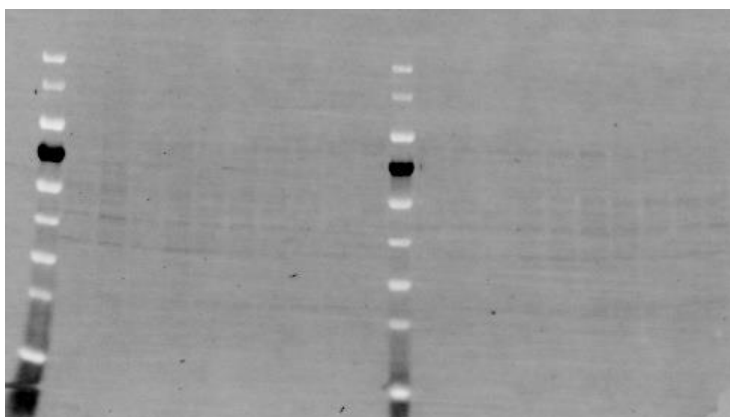


Figure C.2 - Total protein loaded onto membrane for anti-HSP90α (90 kDa) and anti-PKB/Akt (55 kDa) on immunoprecipitated PP2A samples

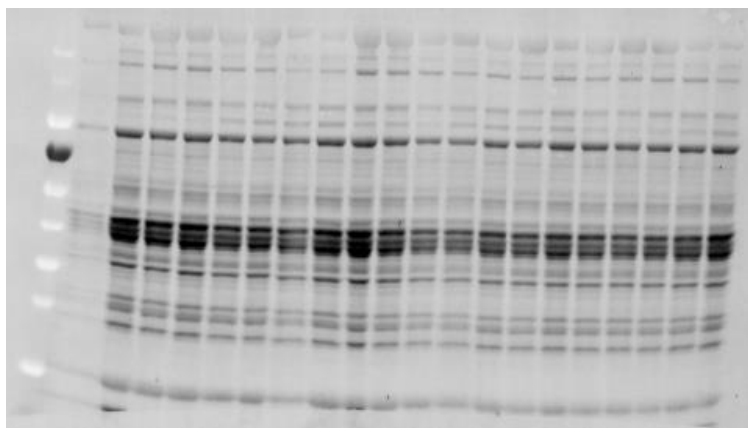


Figure C.3 - Total protein loaded onto membrane for anti-phospho-HSP90α (90 kDa) and anti-phospho-PKB/Akt (55 kDa) for the cytosolic fraction

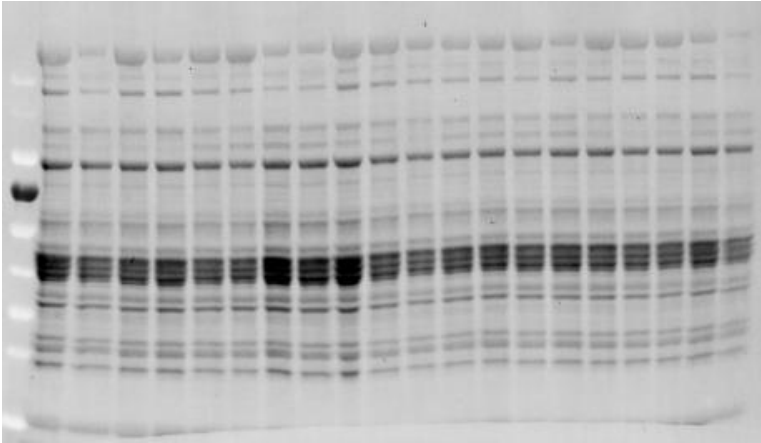


Figure C.5 - Total protein loaded onto membrane for anti-HSP90 α (90 kDa) and anti-PKB/Akt (55 kDa) for the cytosolic fraction

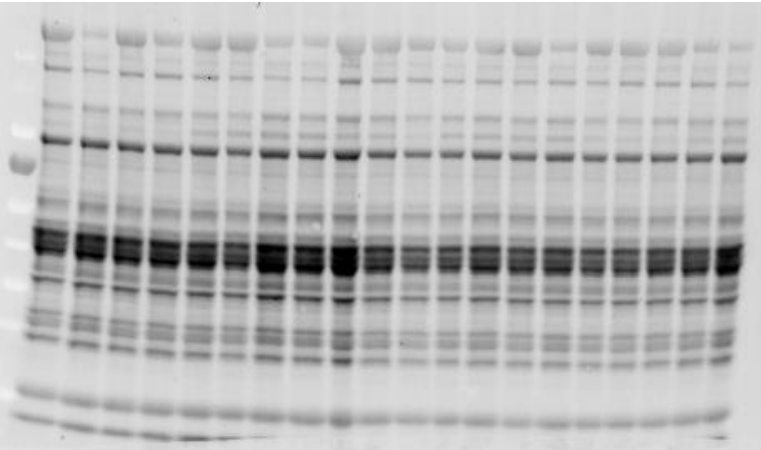


Figure C.4 - Total protein loaded onto membrane for anti-striatin (110 kDa) for the cytosolic fraction

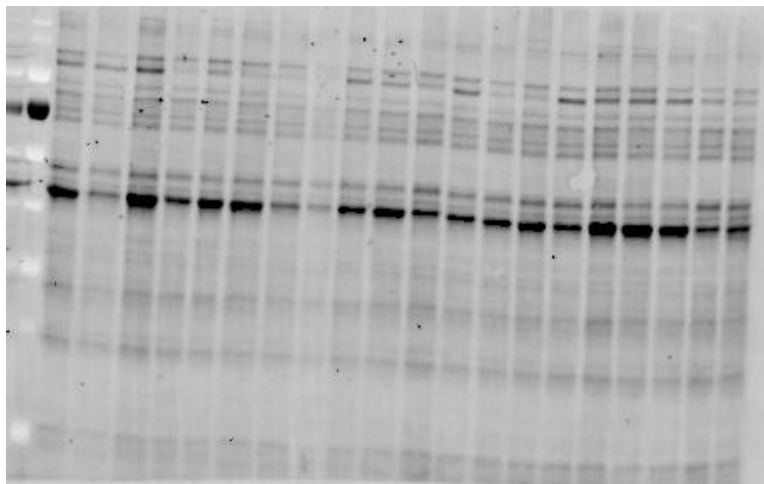


Figure C.6 - Total protein loaded onto membrane for anti-phospho-HSP90 α (90 kDa) and anti-phospho-PKB/Akt (55 kDa) for the membrane fraction

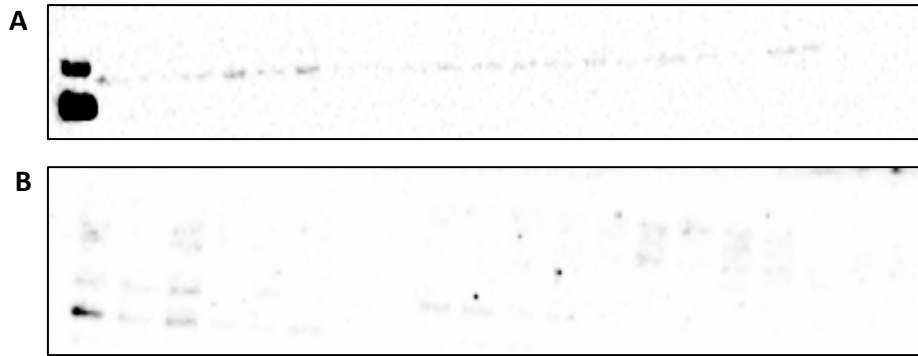


Figure C.7 - Phospho (A) and total (B) HSP90 α (90 kDa) blot analysis

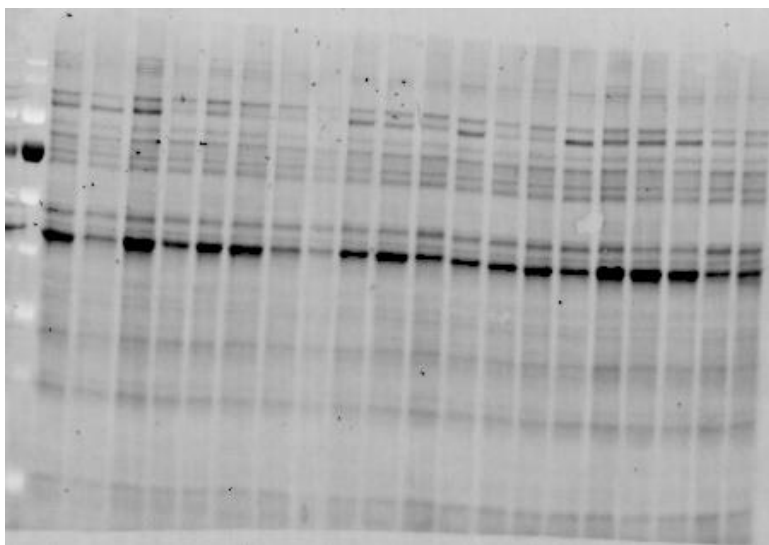


Figure C.8 - Total protein loaded onto membrane for anti-HSP90 α (90 kDa) and anti-PKB/Akt (55 kDa) for the membrane fraction

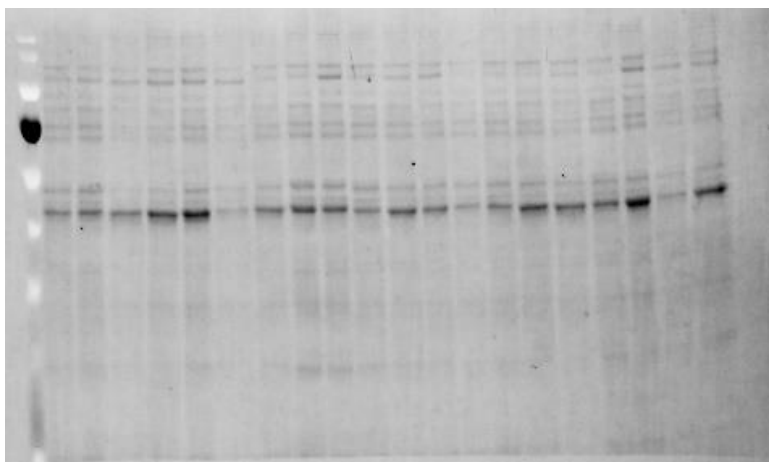


Figure C.9 - Total protein loaded onto membrane for anti-striatin (110 kDa) for the membrane fraction

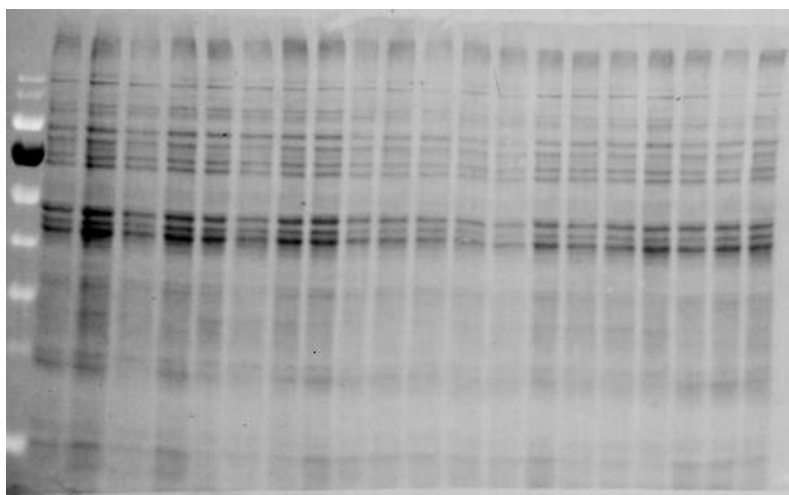


Figure C.12 - Total protein loaded onto membrane for anti-HSP90 α (90 kDa) and anti-PKB/Akt (55 kDa) for the nuclear fraction

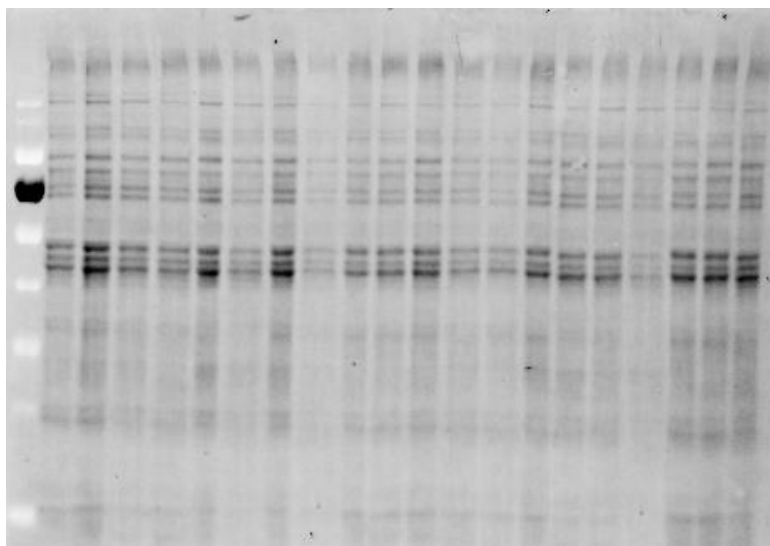


Figure C.11 - Total protein loaded onto membrane for anti-phospho-HSP90 α (90 kDa) and anti-phospho-PKB/Akt (55 kDa) for the nuclear fraction

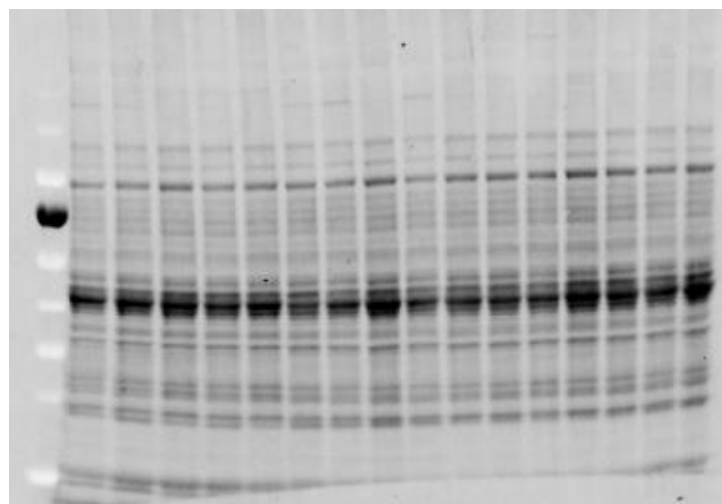


Figure C.10 - Total protein loaded onto membrane for anti-HSP90 α (90 kDa) and anti-PKB/Akt (55 kDa) for the WCL

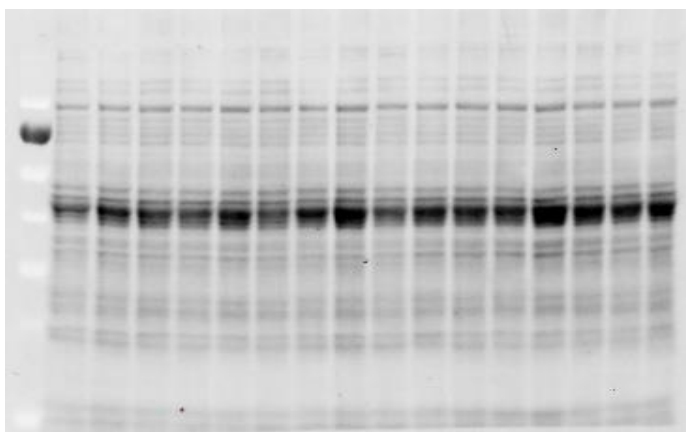


Figure C.14 - Total protein loaded onto membrane for anti-phospho-HSP90α (90 kDa) and anti-phospho-PKB/Akt (55 kDa) for the WCL

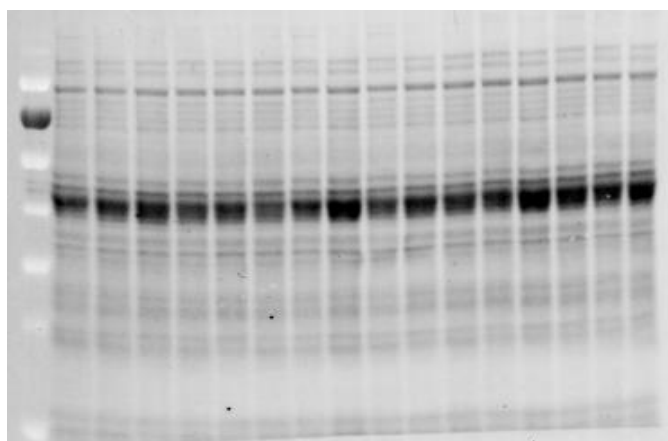


Figure C.13 - Total protein loaded onto membrane for anti-striatin (110 kDa) for the WCL

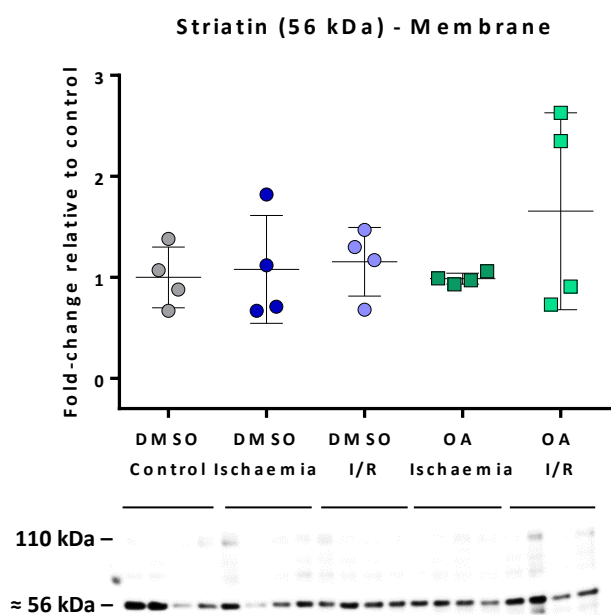


Figure C.15 – Blot for striatin in the membrane fraction